



science & innovation

Department:  
Science and Innovation  
REPUBLIC OF SOUTH AFRICA



National  
Research  
Foundation



agriculture,  
forestry & fisheries

Department:  
Agriculture, Forestry and Fisheries  
REPUBLIC OF SOUTH AFRICA

# SCALE Cruise Report



# SCALE

Southern Ocean seasonal Experiment

Winter Cruise: 18th July 2019 - 12th August 2019

Spring Cruise: 12th October 2019 - 20th November 2019

Compiled by Thomas Ryan-Keogh

# Contents

Chief Scientists	4
Team Leaders	4
Affiliations	6
Cruise Highlights	8
SCALE Media	11
Winter Cruise Narrative	18
Spring Cruise Narrative	21
Cruise Track	24
Winter Cruise	24
Spring Cruise	25
Cruise Station List and Activities	26
General Overview	32
Scientific Reporting	37
<b>1. TEAM BIRDS</b>	37
<b>2. TEAM CO<sub>2</sub></b>	46
<b>3. TEAM DMS</b>	61
<b>4. TEAM FLUX</b>	72
<b>5. TEAM GLIDER</b>	87
<b>6. TEAM MICROBIOME</b>	112
<b>7. TEAM NATM &amp; NOCE</b>	124
<b>8. TEAM OCE</b>	148
<b>9. TEAM PLANKTON</b>	152
<b>10. TEAM PLASTICS</b>	164
<b>11. TEAM PRODUCTION</b>	168
<b>12. TEAM SAWS</b>	196
<b>13. TEAM SEAICE</b>	210
<b>14. TEAM SEALS</b>	264
<b>15. TEAM TRACEX &amp; IRON</b>	266
<b>16. TEAM VIBRATION</b>	280

<b>17. TEAM WAVE</b>	301
<b>18. TEAM WHALES</b>	311
Washup Notes	326
Winter Cruise	326
Spring Cruise	328
Cruise Participants	329
Winter Cruise	329
Spring Cruise	335

## Chief Scientists

Winter Cruise Chief Scientist: A/Prof Marcello Vichi<sup>1</sup>  
 Winter Cruise Co-Chief Scientist: Dr Sandy Thomalla<sup>2</sup>

Spring Cruise Chief Scientist: Dr Thomas Ryan-Keogh<sup>2</sup>  
 Spring Cruise Co-Chief Scientist: A/Prof Marcello Vichi<sup>1</sup>

## Contact Details:

*marcello.vichi@uct.ac.za*

*tryankeogh@csir.co.za*

*sthomalla@csir.co.za*

## Team Leaders

TEAM	Principal Investigator	Winter Cruise Team Leader	Spring Cruise Team Leader	Funding Information
BIRDS	Azwianewi Makhado <sup>3</sup>	Vincent Ward <sup>3</sup>	Derek Engelbrecht <sup>3</sup>	Department of Environmental Affairs: Oceans and Coasts
CO2	Pedro Monteiro <sup>2</sup>	Warren Joubert <sup>4</sup>	Mutshushu Tsanwani <sup>3</sup>	NRF-SANAP 110727
DMS	Tom Bell <sup>5</sup> , Christa Marandino <sup>6</sup> , Dennis Booge <sup>6</sup>	Dennis Booge <sup>6</sup>	George Manville <sup>5</sup>	NE/R007586/1 (NERC, UK); BMBF Fund (Germany); State Oceanic Administration Fund (China)
FLUXES	Clare Eayrs <sup>7</sup>	n/a	Clare Eayrs <sup>7</sup>	G1204 (NYU Abu Dhabi Research Institute)
GLIDER	Sarah Nicholson <sup>2</sup> , Sebastiaan Swart <sup>8</sup>	Louise Biddle <sup>8</sup> , Josh Huysamen <sup>9</sup>	Louise Biddle <sup>8</sup> , Josh Huysamen <sup>9</sup>	NRF-SANAP 110736
IRON	Thato Mtshali <sup>2</sup>	Thato Mtshali <sup>2</sup>	Thato Mtshali <sup>2</sup>	NRF-SANAP 110721; PROTEA

				116648; FSTR18041832231 (LabexMer, France)
MICROBIOME	Thulani Makhalanyane <sup>10</sup>	Jarishma Gokul <sup>10</sup>	Jarishma Gokul <sup>10</sup>	NRF-SANAP 110717
NATM	Katye Altieri <sup>11</sup>	Kurt Spence <sup>11</sup>	Kurt Spence <sup>11</sup>	NRF-SANAP 110732
NOCE	Sarah Fawcett <sup>11</sup>	Raquel Flynn <sup>11</sup>	Raquel Flynn <sup>11</sup>	NRF-SANAP 105539; NRF-SANAP 110735; UCT VC Future Leaders Fund; 185113 (NSF, US); 1850925 (NSF, US)
OCE	Shared Services	Tahlia Henry <sup>11</sup>	Thomas Ryan-Keogh <sup>2</sup>	n/a
PLANKTON	David Walker <sup>12</sup>	David Walker <sup>12</sup>	Simone Louw <sup>12</sup>	n/a
PLASTICS	Peter Ryan <sup>13</sup>	Vonica Perold <sup>13</sup>	Eleanor Weidemann <sup>13</sup>	ACE Foundation and Ferring Pharmaceuticals (Switzerland)
PRODUCTIO N	Sandy Thomalla <sup>2</sup>	Thomas Ryan-Keogh <sup>2</sup>	Thomas Ryan-Keogh <sup>2</sup>	NRF-SANAP 110729
SAWS	Marc de Vos <sup>4</sup>	Marc de Vos <sup>4</sup>	Mardene de Villiers <sup>4</sup>	South African Weather Service
SEAICE	Marcello Vichi <sup>1,11</sup> , Sebastian Skatulla <sup>1,21</sup> , Keith MacHutchon <sup>21</sup> , Tokoloho Rampai <sup>1,22</sup>	Sebastian Skatulla <sup>1,21</sup>	Justin Peard <sup>14</sup> , Riesna Audh <sup>1,11</sup>	NRF-SANAP 118745 NRF-STINT 112632 NRF-ESSRP 118598 International Whales & Climate Research Program
SEALS	Mia Wege <sup>15</sup>	n/a	Marthan Bester <sup>15</sup>	

TRACEX	Alekandra Roychoudhury <sup>16</sup> , Susanne Fietz <sup>16</sup>	Susanne Fietz <sup>16</sup>	Jan-Lucas Menzel <sup>16</sup>	NRF-SANAP 110731; NRF-SANAP 110715; CPRR160415162166
VIBRATION	Annie Bekker <sup>17</sup>	Armand van Zuydam <sup>17</sup>	Martinique Engelbrecht <sup>17</sup>	NRF-SANAP 110737
WAVE	Alessandro Toffoli <sup>18</sup>	Alessandro Toffoli <sup>18</sup>	Alberto Alberello <sup>18,19</sup>	ACE Foundation and Ferring Pharmaceuticals (Switzerland); AAS project 4434 (Australian Antarctic Science Program); CRC-P53991 (Cooperative Research Centres Projects, Australia)
WHALES	Ken Findlay <sup>20</sup>	n/a	Elisa Seyboth <sup>20</sup>	International Whales & Climate Research Program

## Affiliations

1. Marine Research Institute, University of Cape Town
2. Southern Ocean Carbon and Climate Observatory, CSIR
3. Department of Environmental Affairs
4. South African Weather Service
5. Plymouth Marine Laboratory, UK
6. GEOMAR Helmholtz Centre for Ocean Research Kiel, Germany
7. New York University Abu Dhabi, UAE
8. University of Gothenburg, Sweden
9. Sea Technology Services
10. Department of Biochemistry, Genetics and Microbiology, University of Pretoria
11. Department of Oceanography, University of Cape Town
12. Department of Conservation and Marine Sciences, Cape Peninsula University of Technology
13. Fitzpatrick Institute of African Ornithology, University of Cape Town
14. Department of Electrical Engineering, University of Cape Town
15. Mammal Research Institute, Department of Zoology and Entomology, University of Pretoria
16. Department of Earth Sciences, Stellenbosch University

17. Department of Mechanical and Mechatronic Engineering, Stellenbosch University
18. Department of Infrastructure Engineering, The University of Melbourne
19. School of Mathematical Sciences, University of Adelaide
20. Centre for Sustainable Oceans, Faculty of Applied Sciences, Cape Peninsula University of Technology
21. Department of Civil Engineering, University of Cape Town
22. Department of Chemical Engineering, University of Cape Town

## Cruise Highlights

- *The first fully integrated South African cruise program spanning atmosphere, sea ice and ocean measurements across the full seasonal cycle using a combination of ships and robotics platforms (buoyancy gliders, wavegliders, buoys).*
- *A comprehensive interdisciplinary study of the less explored seasons in the Southern Ocean, from polar cyclones and atmospheric fluxes to ice drift, mechanical properties and small-scale ocean physics, from birds and marine mammals to the microbial ecosystem.*
- *High sampling resolution of ocean and sea ice biogeochemistry, trace metals and primary production across both winter and spring.*
- *For the first time the Good Hope line was sampled in spring.*



SCALE Winter Cruise Chief Scientist and Team Leaders



SCALE Spring Cruise Chief Scientist and Team Leaders.



SCALE Winter Cruise group photo.



SCALE Spring Cruise group photo.

## SCALE in the Media and pictures

Website: [www.scale.org.za](http://www.scale.org.za)

Twitter: @SCALExperiment

Selection of media articles on the winter and spring cruise:

<http://blogs.sun.ac.za/sanap/tag/scale-winter-cruise/>

<https://www.news.uct.ac.za/article/-2019-07-15-polar-cyclones-antarctic-sea-ice-and-a-cruise-to-understand-it-all>

[https://www.uni-due.de/sea\\_ice/winter\\_cruise\\_2019\\_report.php](https://www.uni-due.de/sea_ice/winter_cruise_2019_report.php)

[http://marine.weathersa.co.za/News/news-article-scale\\_winter\\_cruise\\_2019.html](http://marine.weathersa.co.za/News/news-article-scale_winter_cruise_2019.html)

<https://www.sanap.ac.za/spring-cruise-2019-onboard-the-s-a-agulhas-ii>

<https://www.dailymaverick.co.za/article/2019-08-05-sa-scientists-gather-cold-facts-about-global-warming/>

<https://eos.org/editors-vox/antarctic-seasonal-sea-ice-melts-faster-than-it-grows>

<https://www.fishingindustrynewssa.com/2019/10/18/sa-agulhas-ii-exploring-students-return-home/>

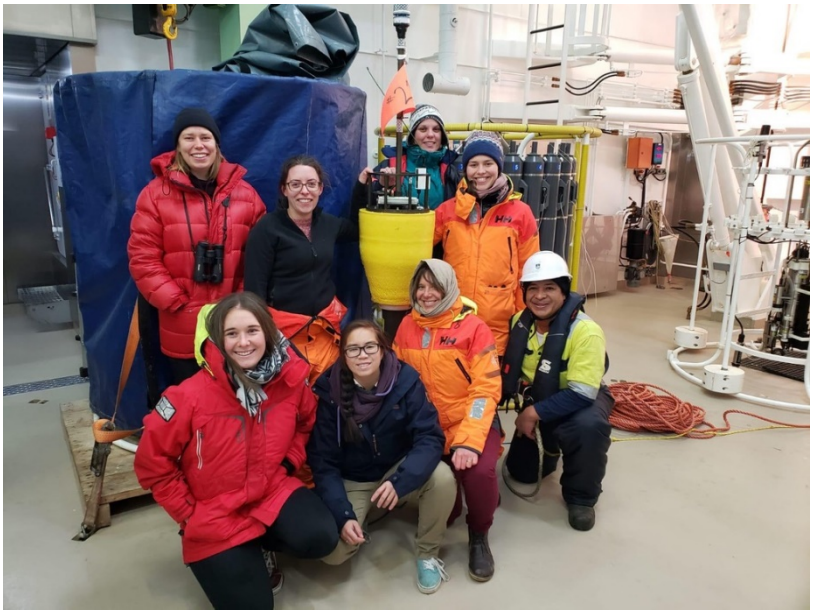
[https://www.environment.gov.za/event/deptactivity/saagulhas2\\_opendayprogramme2019](https://www.environment.gov.za/event/deptactivity/saagulhas2_opendayprogramme2019)

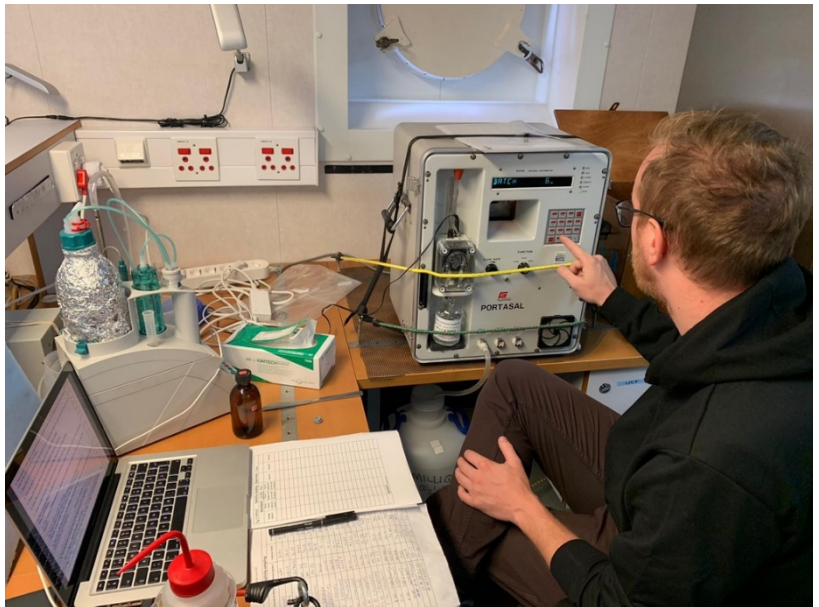
[http://www.science.uct.ac.za/sites/default/files/image\\_tool/images/26/news/Science%20Matters%20final%202019.pdf](http://www.science.uct.ac.za/sites/default/files/image_tool/images/26/news/Science%20Matters%20final%202019.pdf)

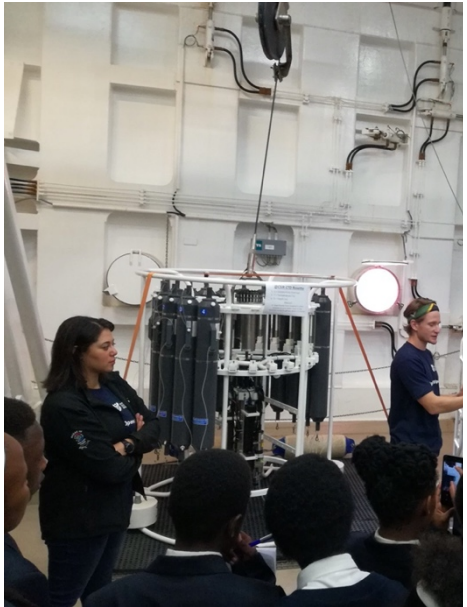
<https://southernoceanfe.wordpress.com/tag/sa-agulhas-ii/>

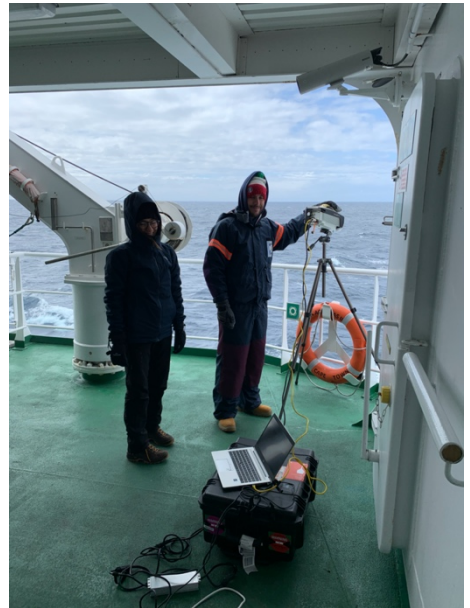
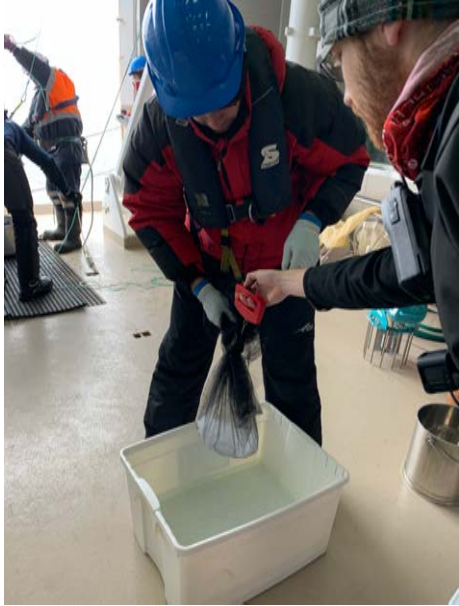
The following collection of images from the winter and spring cruise epitomizes the interdisciplinary, multi-cultural and student-oriented nature of the SCALE programme.

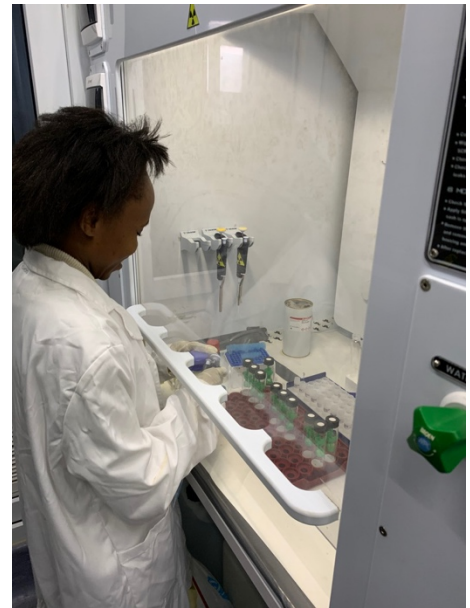












## Winter Cruise Narrative

The first SCALE cruise departed on the 18<sup>th</sup> July. The loading operations started on Monday the 15<sup>th</sup> and completed successfully in the morning of the day of departure. The pre-departure operations were handled by the land Chief Scientist Dr Sandy Thomalla from CSIR-SOCCO. Assistance on behalf of the ship custodian was provided by Mrs Kusi Ngxabani from DEA and Mr Robert Hales and Mr Jawahir Nandha from AMSOL. A/Prof Marcello Vichi was the CS on board. The science program was distributed among 17 teams, for a total of 92 passengers plus the ship doctor and one human dummy recording ship vibrations, for a total of 94 occupied berths out of the total 100 available. The full list of the winter cruise passengers including their demographic information, nationality and role on board is available at the end of the report. A few days before departure the ship custodian requested the presence of the SA Agulhas II to an open day planned in East London in the first week of August 2019. The initial work plan was maintained, although it was clear that any bad weather would have resulted in the cancellation of some operations. This was communicated to all the PIs and team leaders before departure.

Six container labs were loaded on Deck 3, the largest number since the ship was delivered in 2012. Three labs were dedicated to trace metal measurements, one to general chemistry, one for sub-zero ice processing and one was dedicated to C14 radioactive measurements. Dr Ryan-Keogh was the responsible for the radio-hazard operations. A few issues with the connectivity of the containers to the ship safety system delayed the departure by a few hours until the late afternoon. The ship left the quayside after immigration procedures at 18:45 on the 18<sup>th</sup> July.

The navigation proceeded at an average of 13 kn until the first station dedicated to the soaking of the GoFlo. During the night, the ship slowed down to 6 nm to deploy the metal-clean towfish. The system was not fully functional because the device bounced on the keel at times. One part was broken, and the device was retrieved from the water for repairs and not redeployed until the final leg when the ship was back to calmer waters. Intakes for underway pumps were opened and operational after a few hours. Underway measurements continued in open waters throughout the whole cruise. Station VOY-038-SOAK was delayed of 2 hours due to high swell and completed successfully thereafter. On average, the ship maintained a speed between 12 and 13 kn throughout the southbound leg until reaching the ice.

Station SAZ was reached in the morning of the 21<sup>st</sup>, with high sea and wind. Conditions were safe enough for the deployment of the first SOCCO glider, which was successful although characterized by a risky release of the mechanism while the aft frame was hit by a large wave. The glider started the communications and initiated the first descent. CTD operations were cancelled due to the high swell and a new SAZ2 station was established at 45°S for the GoFlo and Niskin CTDs. The new station was reached at 2200 and all activities completed. One major issue was the speed of the CTD winch, that was 20 to 30% slower than during the last 2017 cruise when the Kevlar cable was used.

This required a re-planning of the schedule which was notified to the team leaders. This issue linked to the reduction of the initial ship time due to the open day in East London resulted in the final cancellation of 4 stations out of the original plan.

The navigation continued for 2 days to reach the next station PUZ (600 nm away). An iceberg was intercepted on the 23<sup>rd</sup> and the radar wavelength was adjusted for ice navigation. The passage of a storm slowed down the navigation and station PUZ started in the morning of the 24<sup>th</sup>. Surface water temperature started to be consistently below 1°C from this station onward. After a successful glider deployment, we had to interrupt the calibration CTD due to a malfunctioning sent by the glider (glider cast is available, but no bottle fired). Search operations started and the glider was sighted floating in the vicinity. The recovery was done using the pancake lifting net, which unfortunately damaged one of the sensors due to the large mesh. The glider was not redeployed. The next stations were part of a zonal transect to capture the horizontal dispersal of deep plumes. All stations were successful (double dip of the metal-clean rosette due to issues with the frozen water pump in the CTD), including the deployment of another glider, the sailbuoy and a SWIFT buoy. The buoy unfortunately reported malfunctioning after a few hours. It was spotted 5 nm NE from the station during the night thanks to the radio beacon and the flashlight and decided to be recovered after station GT1E. All station operations and the recovery of the SWIFT were successful, and the ship headed for the sea ice.

Ice observation shifts started, and the first floes were observed in the early afternoon of the 26<sup>th</sup>. A detailed narrative of the MIZ stations and operations is given in the SEAICE team chapter. The sequence of deployments was carefully designed to minimize the impact to the sea ice environment and preserve the conditions. Sea ice features were rapidly varying and large expanses of consolidated ice were only found at the latitude of MIZ3. The long MIZ3 station was the first experience of full-scale sea ice fieldwork completely organized in South Africa. All operations were successful, but unfortunately one member of the coring team experienced frostbites (details are given in the specific chapter and in the wash-up, meeting minutes at the end of the report). This incident was carefully analysed and led to a redesign of the operations for the spring cruise. The many successful stations done during spring confirmed the quality of the new protocols. The pancake lifting on the northward bound leg and the recovery of the other SWIFT buoy were examples of prowess by the ship crew and the scientists involved. All the MIZ stations were completed, although the operations were scattered over multiple cluster stations instead of the initially planned 3 stations in order to find the most appropriate and safe ice conditions.

The ship left the ice in the afternoon of the 28<sup>th</sup> and headed towards the GT2 transect. GT2W was cancelled due to weather and course issues. GT2 was also suspended due to rough conditions. The presence of a SAWS forecaster on board and the prompt support of the weather and ice team allowed to take advantage of a wind gap for a few hours, to complete the station. GT2E was also cancelled due to rough conditions

and ship stability. GT3 was completed successfully on the 31<sup>st</sup> July and the weather finally allowed the neuston net sampling. Time constraints and the need to escape the stormy conditions led to the cancellation of GT4. The next 3 (GT5, 6 and 7) stations were successful, although sudden wind increases often prevented to carry out the bongo and neuston nets operations. On the 4<sup>th</sup> August the ship experienced malfunctioning at the 4<sup>th</sup> generator, which slowed down navigation for about one day. The mandatory ETA to East London, in combination with the revised operation time for CTD casts, required the cancellation of station GT9. The last station GT10 was completed at midday of the 5<sup>th</sup> August, although reduced to the GoFlo and plankton net only to save time.

The SA Agulhas II arrived in port at East London in the afternoon of the 7<sup>th</sup> August, in perfect time for the open day. The SCALE scientists contributed to the event organized by DEA with a display of the advanced scientific equipment used during the cruise to the school classes for the dedicated open day on the 8<sup>th</sup>. SCALE participants were involved as ushers and escorted the members of the public that visited the ship on the 9<sup>th</sup>. Custom clearance was done in East London; the Chief Scientist disembarked the ship, together with the majority of the international participants and other South African scientists. CS on the return trip to Cape Town was Ms Tahlia Henry.

## Spring Cruise Narrative

The departure of the cruise, originally planned for 10<sup>th</sup> October 2019, was delayed due to containers setting off the ships fire alarm system. Once the necessary repairs were completed the ship departed from Cape Town on the 12<sup>th</sup> October 2019 after completion of all passenger procedures. The first station was planned at approximately 36S, to conduct the preparative Geotraces station (soaking, reference and testing of the GoFlo bottles), to deploy the trace metal clean towfish and to deploy the neuston net. The next few days were primarily focused on sailing towards the SAZ station, with underway measurements and other observational activities taking place. Opportunistic neuston net deployments were planned but bad weather prevented any such operations and the trace metal clean towfish also had to be retrieved.

The bad weather continued on the 15<sup>th</sup> October which meant all activities planned for the SAZ station had to be cancelled. The planned recovery of the Sailbuoy (Team Gliders) was additionally not successful due to the instrument failing to send further GPS co-ordinates. A search and rescue pattern were conducted but failed to spot the Sailbuoy, but the sailbuoy ended upon continuing on its trajectory to Cape Town and was recovered in the West Coast National Park in December. On the 16<sup>th</sup> October some good weather allowed a secondary SAZ station to be planned, were 2 x Geotraces CTD casts, 1 x Niskin CTD cast, 2 x bongo nets and 1 x neuston net were successfully deployed. The next station on the 17<sup>th</sup> October 2019 saw the successful deployment of both SOCCO Wavegliders, a neuston net deployment and the redeployment of the trace metal clean fish. The ship continued to steam towards our final open ocean station during the southward leg which we arrive at on the afternoon of the 19<sup>th</sup> October. This station had the full complement of deployments, bongo nets, Geotraces CTD cast, Niskin CTD cast, Buoyancy Glider deployment, neuston nets and marine snowcatcher deployments. The good weather additionally allowed the underway CTD (UCTD) to be tested and for the vibration team to conduct the first of the ship maneuver tests.

From here we began to enter the marginal ice zone and begin the ice leg of the cruise, with the first station MIZ0a on the 20<sup>th</sup> October 2019 seeing the full deployment of instruments including bongo nets, Geotraces CTD cast, Niskin CTD cast, neuston nets and 2 x Buoyancy Glider deployments. Before entering the ice, a UCTD survey was performed in tandem with ship maneuvers ending on the 22<sup>nd</sup> October where the first frazil and pancake ice samples were collected. The ship remained outside of the pack ice for the night of the 22<sup>nd</sup> so that the transition from the ice edge into the ice pack could be documented by the teams after sunrise. The ship sailed into the ice reaching the MIZ1 station at 07:30 where the first SWIFT buoy was deployed alongside shallow (500 m) Geotraces and Niskin CTD casts and marine snowcatcher deployments. From here we moved deeper into the ice arriving at MIZ2 (59.5S) at 03:00 on the 24<sup>th</sup> October 2019 for the deployment of the atmospheric mast and ice mass balance buoy, along with the first

deployment of the sea ice team to collect ice cores. The schedule of operations was set for all ice operations to occur from sunrise onwards with any shipboard activities to take place after ice operations had finished.

The planned deployment of the atmospheric mast was for 24 hours so the ship steamed slightly north to 59S to MIZ3 where ice coring, bongo nets, Geotraces CTD cast, Niskin CTD cast and marine snowcatchers were deployed. The MIZ3 station was completed at lunchtime on the 25<sup>th</sup> October, so the ship sailed south again to MIZ2 recovering the atmospheric mast in the afternoon. The next day (26<sup>th</sup> October 2019) of steaming through the ice was dedicated to a seal census, with opportunistic tagging if a Ross Seal was spotted, with additional vibration maneuvers planned. We arrived at MIZ4 where a safety survey of the seaice was performed and found that it was too thin for any coring operations to occur, so the operations moved onto the bongo net deployments and the Geotraces and Niskin CTD casts. Arrival at MIZ5 on the 28<sup>th</sup> October also found the ice conditions to not be suitable for any ice operations, so the station proceeded as planned for shipboard operations including the deployment of the atmospheric mast sensors attached to the ice gondola from the forward crane.

With the cancellation of coring operations likely to continue a change of plan was enacted where the seaice team leader would conduct visual observations from sunrise and select the location of the next station, MIZ6. A suitable location was found, and a safety assessment was conducted at 06:30 29<sup>th</sup> October 2019 with coring operations commencing at 09:00 with shipboard operations commencing in the afternoon. A similar approach was conducted for MIZ7 on the 30<sup>th</sup> October with same order of operations. The 31<sup>st</sup> October was used for a seal census, with opportunistic tagging and ship's maneuvers. The arrival at MIZ8 found the ice conditions to be less consolidated so the ice operations were switched to pancake and frazil ice collection, with shipboard operations. The 2<sup>nd</sup> November was used as a seal census day allowing the scientists and crews to enjoy watching the Rugby World Cup final and enjoy a braai in the ice. The last ice station MIZ9 was conducted on the 3<sup>rd</sup> November, however high winds meant that there was cancellation of activities.

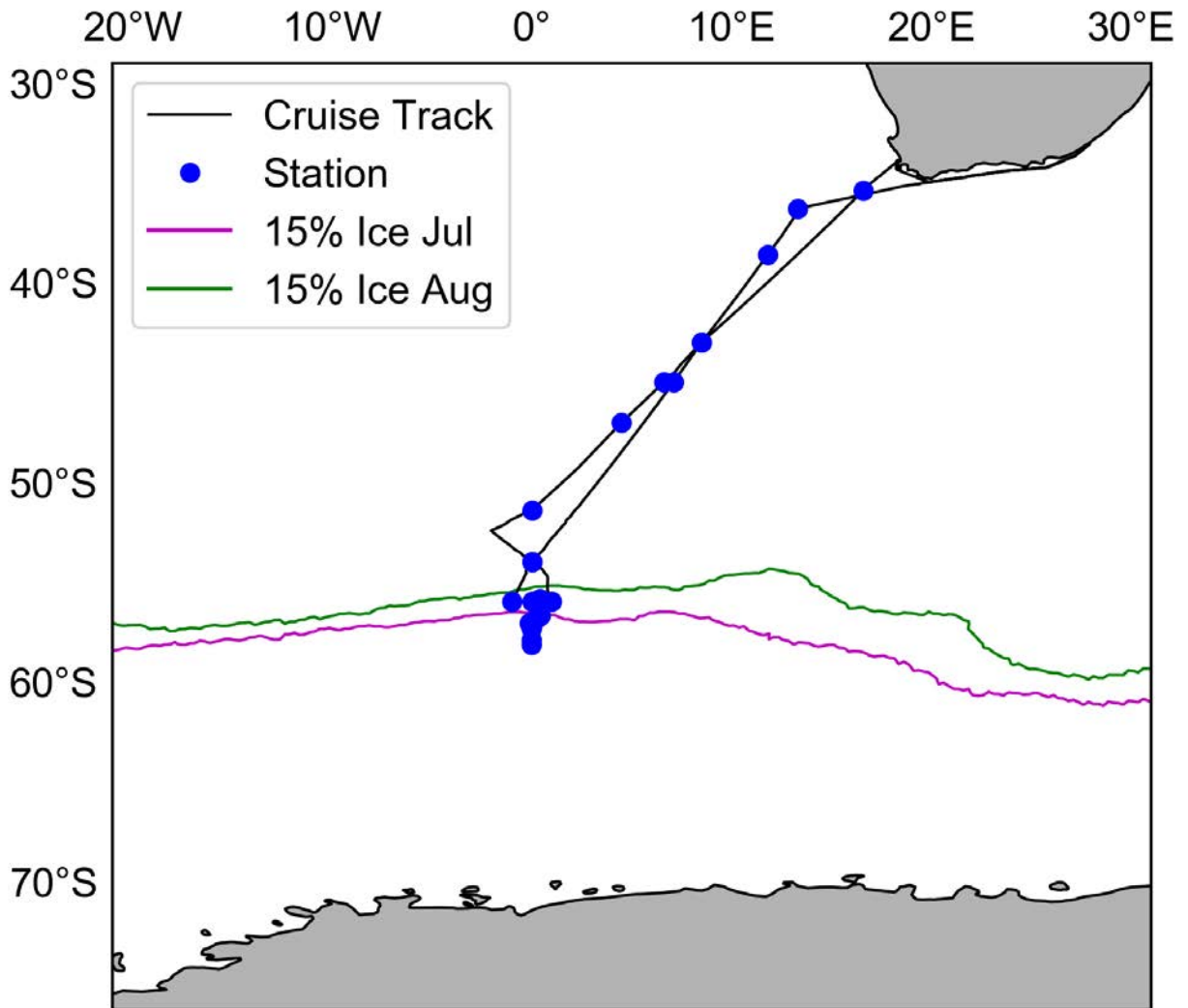
From here the ship exited the ice to the first station of the Whale Survey leg at 57.5S 24.0E where shipboard activities included 2 x Geotraces CTD casts, 1 x Niskin CTD cast, and the first deployment of the McLane pumps. Departing from the station the trace metal clean towfish was deployed with instructions to keep the ship in open waters as it sailed west. This was not possible due to constantly changing ice conditions and weather systems breaking up the pack ice. The result of this was damage to the boom used for the towfish deployment so it was recovered. However, these ice conditions meant that the seaice team had another opportunity to collect frazil ice samples on the 4<sup>th</sup> November. On the 6<sup>th</sup> November at 00:30 we reached WS2 at 55.5S 12.0E where bongo nets, Geotraces CTD and Niskin CTD were deployed. Before finally reaching the last station of the Whale Survey on the night of the 6<sup>th</sup>. From here the ship recovered the

Swift buoys on the 7<sup>th</sup> November, which had been deployed earlier in the cruise at the MIZ stations.

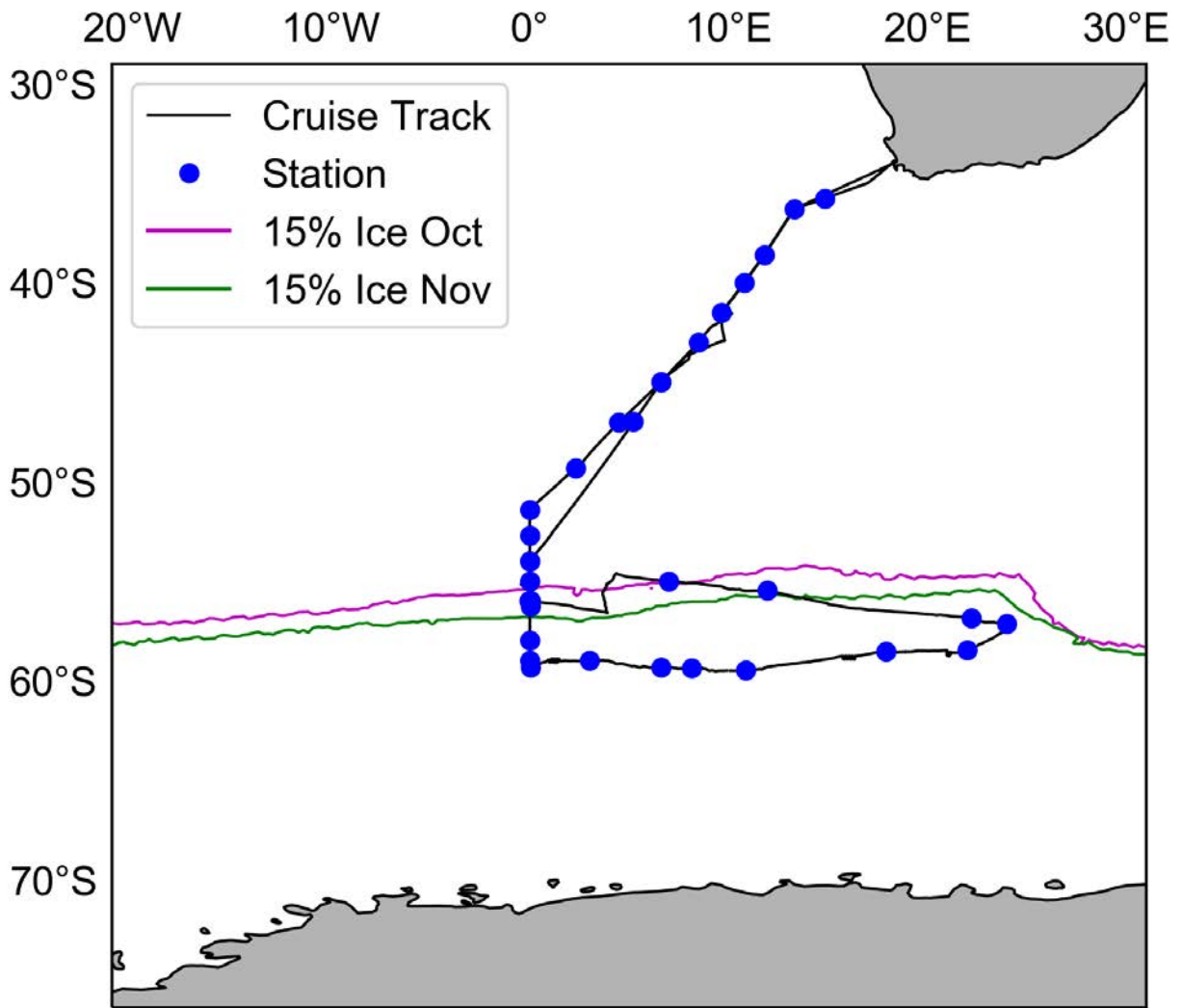
The ship then began the final leg sailing North along the GoodHope line to conduct the 12 GT stations. Between GT1 and GT5 the stations were carried out successfully with only a few net deployments cancelled when the winds were too high. A major weather system with 55 knots winds was due to impact the GT6 station on the 13<sup>th</sup> November, so the decision was made to sail north to GT7 and then sail back to GT6 arriving on the 15<sup>th</sup> November. From GT6 the ship sailed to recover the Wavegliders, which had been deployed on the Southward leg. WG052 was successfully recovered on the afternoon of the 15<sup>th</sup> November, however WG027 had sailed too far off the GoodHope line to be recovered during this cruise. The ship then sailed towards GT7B continuing the planned stations, however additional neuston net stations were added to accommodate the failed deployments at earlier stations due to adverse weather conditions. The GT10 station was successfully completed on the 18<sup>th</sup> November, with the last science activities, including the deployment of the trace metal clean towfish, completed on the afternoon of the 19<sup>th</sup> November. The ship arrived in Cape Town on the evening of the 19<sup>th</sup> November with all passengers disembarking on the 20<sup>th</sup> following the customs clearance.

# Cruise Track

## Winter Cruise



Spring Cruise



## Cruise Station List and Activities

Table 1: SCALE Winter Cruise station list and activities.

Voyage	Ship Station	Grid Number	Date & Time	Latitude	Longitude	Activities
38	AM01092	VOY-038-SOAK	2019-07-19 09:34	-35.3841	16.6134	Soaking of GEOTRACES GoFlo
38	AM01093	VOY-038-SAZ	2019-07-21 08:46	-43.00057	8.49862	Deployment of SOCCO buoyancy glider
38	AM01094	VOY-038-SAZ2	2019-07-21 23:11	-45.00095	7.0858	Go-Flo CTD to bottom for mesocosm experiment, phytoplankton net and bongo net to 200 m (twice)
38	AM01095	VOY-038-PUZ	2019-07-24 08:00	-54.00017	0.01123	Vibration test with stern against waves, deployment of SOCCO buoyancy glider, calibration CTD cancelled due to glider malfunctioning. CTD Profile available but bottle fired just to check lashes SAWS SVP deployment while moving Glider recovery
38	AM01096	VOY-038-GT1W	2019-07-24 23:03	-56.00005	-0.9995	Go-Flo CTD to bottom Aft deck winch: McLane pumps (2 depths)
38	AM01097	VOY-038-GT1	2019-07-25 09:48	-56.0012	0.00185	Phytoplankton net and bongo net to 200 m (twice), deployment of ROAM-MIZ No. 1 Buoyancy gliders, No. 1 Sailbuoy, No. 1 SWIFT buoy (#20 by hand), Go-Flo CTD to bottom, McLane pumps (200 and 1000 m), Niskin CTD to 1500 m, marine-snow catcher (10 m below MLD)
38	AM01098	VOY-038-GT1E	2019-07-26 01:21	-55.99927	1.00423	Go-Flo CTD to bottom, McLane pumps (2 depths)
38		VOY-038-SWIFT	2019-07-26 10:15	-55.86	0.397	SWIFT#20 recovery for malfunctioning
38	AM01099	VOY-038-MIZ1A	2019-07-26 16:00	-57.00007	-0.00313	Bongo net (twice to 200 m), Frazil ice sampler (ship off dp to preserve frazil ice), mini Go-Flo (500 m), marine-snow catcher (10 below mixed layer depth), Niskin (500 m), SWIFT #20 by hand, hoist for SHARC buoy SB01 deployment and zoo-vacuum

38		VOY-038-MIZ1B	2019-07-27 00:01	-57.05867	-0.10695	polar i-SVP deployment
38		VOY-038-MIZ1C	2019-07-27 01:19	-57.11898	-0.0055	Deployment of SWIFT#21 by hand
38		VOY-038-MIZ3A	2019-07-27 10:38	-58.13783	-0.00442	1 Sea Ice Mass Balance Buoy (SIMB) loaded on foredeck from cargo hold. Pre-assembled by science team. 1 gondola or hoist on one crane and 1 hoist on the other for carrying material. The second hoist is for service to bring cores and people back and forth 5 scientists overboard on ice
38		VOY-038-MIZ3B	2019-07-27 17:09	-57.91745	-0.01735	Hoist for polar i-SVP
38	AM01100	VOY-038-MIZ2A	2019-07-27 21:24	-57.34503	-0.0028	Frazil ice sampler (ship off dp to preserve frazil ice), Bongo net (twice to 200 m), mini Go-Flo (500 m), marine-snow catcher (10 m below mixed layer depth), Niskin (500 m), hoist for SHARC SB02 deployment (2 people)
38		VOY-038-MIZ2B	2019-07-28 05:10	-57.16542	0.00522	hoist for polar i-SVP3 deployment (3 people), hoist for zoo-vacuum (2 people)
38		VOY-038-MIZ1D	2019-07-28 09:15	-56.80178	0.30262	Recovery of SWIFT#21 Crane on heli deck: Pancake lift collection
38	AM01105	VOY-038-MIZ1E	2019-07-28 14:02	-56.67417	0.44872	Recovery of SWIFT#20 Plankton winch: Frazil ice sampler (ship off dp to preserve frazil ice) miniGo-Flo to 500 m Vibration manoeuvres: Stern crossing ice and zigzag 10 to 30 degrees for 1 hour going north. Only partially completed
38	AM01107	VOY-038-GT2	2019-07-29 15:45	-54.00088	0.00123	Go-Flo CTD to bottom, 1 marine-snow catchers (10 m BELOW MLD), phytoplankton net and bongo net to 200 m (twice), Niskin CTD to 1500 m

38	AM01108	VOY-038-GT3	2019-07-31 03:11	-51.40167	0.00115	Go-Flo CTD to bottom, Niskin CTD to 1500 m, phytoplankton net and bongo net to 200 m, Neuston net tow @ 2 kn deployed on starboard side; Bulk water sample (40 L) using a rope and bucket
38	AM01109	VOY-038-GT5	2019-08-01 12:53	-46.9999	4.4989	Go-Flo CTD to bottom, 1 marine-snow catchers (10 m BELOW MLD), phytoplankton net and bongo net to 200 m (twice), Niskin CTD to 1500 m, Neuston net tow @ 2 kn deployed on starboard side; Bulk water sample (40 L) using a rope and bucket
38	AM01110	VOY-038-GT6	2019-08-02 08:33	-45.00012	6.59983	Go-Flo CTD to bottom, 1 marine-snow catchers (10 m BELOW MLD), phytoplankton net and bongo net to 200 m (twice), Niskin CTD to 1500 m, Neuston net tow @ 2 kn deployed on starboard side; Bulk water sample (40 L) using a rope and bucket Vibration manoeuvres
38	AM01111	VOY-038-GT7	2019-08-03 03:34	-43.00008	8.50035	Go-Flo CTD to bottom, McLane pump (2 depths), Niskin CTD to 1500 m, phytoplankton net and bongo net to 200 m (twice)
38	AM01112	VOY-038-GT9	2019-08-04 09:18	-38.59913	11.80077	Niskin CTD to 1500 m, McLane pump (2 depths), Go-Flo CTD to bottom
38	AM01113	VOY-038-GT10	2019-08-05 03:59	-36.29938	13.30187	Go-Flo CTD to bottom

Table 2: SCALE Spring Cruise station list and activities.

Voyage	Ship Station	Grid Number	Date & Time	Latitude	Longitude	Activities
40	AM01115	VOY-040-SOAK	13/10/2019 08:18	-35.76973	14.85912	CTD GoFlo (500m), Neuston Net, TM Fish deployment
40	AM01116	VOY-040-SAZ2	16/10/2019 10:54	-45.00015	6.60005	CTD GoFlo (50m), CTD Niskin (1000m), CTD GoFlo (4200m), Bongo Net x 2, Neuston Net
40	AM01117	VOY-040-PFZ	17/10/2019 09:23	-46.99075	5.22762	WaveGlider 027 - Deploy, WaveGlider 052 - Deploy, Neuston Net, TM Fish deployment
40	AM01118	VOY-040-PUZ	19/10/2019 03:36	-54.0002	0.00078	Bongo Net x 2, CTD GoFlo (2300m), CTD Niskin (1000m), Neuston Net, Buoyancy Glider - Deploy, MSC x 2, Vibration Manoeuvres
40	AM01119	VOY-040-MIZ0A	20/10/2019 00:55	-55.00112	0.00048	Bongo Net x 2, CTD GoFlo (1500m), CTD Niskin (1000m), Glider Deploy x 2, Neuston Net
40	AM01120	VOY-040-MIZ0B	22/10/2019 09:30	-55.99768	0.03855	UCTD, Vibration Manoeuvres
40	AM01121	VOY-040-MIZ0C	22/10/2019 14:21	-56.25907	0.04062	Frazil and pancake ice collection
40	AM01122	VOY-040-MIZ1B	23/10/2019 07:19	-57.98233	0.00812	SWIFT Buoy Deployment, CTD GoFlo (500m), CTD Niskin (500m), MSC x 2
40	AM01123	VOY-040-MIZ2	24/10/2019 12:35	-59.3248	0.06662	Coring, IMB, Atmospheric Mast Deployment, CTD GoFlo (500m), CTD Niskin (500m), Bongo Net x2
40	AM01124	VOY-040-MIZ3	24/10/2019 19:45	-58.98332	0.01188	Coring, Bongo Net x 2, CTD GoFlo (500m), CTD Niskin (500m)
40	AM01125	VOY-040-MIZ4	27/10/2019 03:04	-59.00072	3.01717	Bongo Net x 2, CTD GoFlo (500m), CTD Niskin (500m)
40	AM01126	VOY-040-MIZ5	28/10/2019 11:32	-59.33905	6.6162	Coring, Bongo Net x 2, CTD GoFlo (500m), CTD Niskin (500m), MSC x 2, Gondola Measurements
40	AM01127	VOY-040-MIZ6	29/10/2019 12:31	-59.3645	8.15892	Coring, Bongo Net x 1, CTD GoFlo (500m), CTD Niskin (500m)
40	AM01128	VOY-040-MIZ7	30/10/2019 11:26	-59.47255	10.88933	Coring, Bongo Net x 2, CTD GoFlo (500m), CTD Niskin (500m), Gondola Measurements
40	AM01129	VOY-040-MIZ8	01/11/2019 13:16	-58.5488	17.93818	Frazil and pancake ice collection, CTD GoFlo (500m), CTD Niskin (500m), Bongo Net x 2, Gondola Measurements

40	AM01130	VOY-040-MIZ9	03/11/2019 11:33	-58.44913	21.99735	Frazil and pancake ice collection, CTD GoFlo (500m), CTD Niskin (500m)
40	AM01131	VOY-040-WS1	03/11/2019 23:08	-57.15082	23.9956	CTD GoFlo (100m), CTD Niskin (1000m), CTD GoFlo (2000m), McLane Pump
40	AM01132	VOY-040-FRZ	04/11/2019 12:03	-56.84353	22.21852	Frazil ice collection
40	AM01133	VOY-040-WS2	05/11/2019 23:32	-55.44447	11.96473	CTD GoFlo (2000m), CTD Niskin (1000m), Bongo Net x 2
40	AM01134	VOY-040-WS3	06/11/2019 21:13	-55.00078	6.99712	CTD GoFlo (2000m), CTD Niskin (1000m)
40	AM01135	VOY-040-GT1	08/11/2019 15:50	-55.99467	-0.00682	CTD GoFlo (2000m), CTD Niskin (500m), MSC x 2
40	AM01136	VOY-040-GT2	09/11/2019 09:57	-54.00018	-0.00035	Bongo Net x 2, CTD Niskin (300m), CTD GoFlo (2000m), Niskin CTD (2400m), McLane Pump
40	AM01137	VOY-040-GT2B	10/11/2019 03:54	-52.70103	-0.00018	Bongo Net x 2, CTD Niskin (300m), CTD GoFlo (2000m), CTD Niskin (2600m), Neuston Net x2
40	AM01138	VOY-040-GT3	10/11/2019 16:59	-51.3996	0.00072	Bongo Net x 2, CTD Niskin (300m), CTD GoFlo (2000m), CTD Niskin (2600m), Neuston Net x2, McLane Pump, MSC x 2
40	AM01139	VOY-040-GT4	11/11/2019 13:18	-49.3017	2.30265	Bongo Net x 2, CTD Niskin (300m), CTD GoFlo (2000m), CTD Niskin (2600m), Neuston Net x2, McLane Pump
40	AM01140	VOY-040-GT5	12/11/2019 12:18	-47.0006	4.49988	Bongo Net x 1, CTD Niskin (300m), CTD GoFlo (1000m), CTD Niskin (3800m), Neuston Net, McLane Pump, MSC x 2
40	AM01141	VOY-040-GT7	13/11/2019 17:09	-43.00007	8.50007	Bongo Net x 2, CTD Niskin (300m), CTD GoFlo (2000m), CTD Niskin (3800m), Neuston Net x2, McLane Pump, MSC x 2
40	AM01142	VOY-040-GT6	14/11/2019 15:24	-44.99932	6.60022	Bongo Net x 2, CTD Niskin (300m), CTD GoFlo (2000m), CTD Niskin (4300m), Neuston Net x2, McLane Pump
40	AM01143	VOY-040-GT7B	15/11/2019 21:42	-41.50027	9.65755	Bongo Net x 2, CTD Niskin (300m), CTD GoFlo (2000m), CTD Niskin (4500m), Neuston Net x2, McLane Pump

40	AM01144	VOY-040-GT8	16/11/2019 14:45	-40.00048	10.80165	CTD Niskin (300m), CTD GoFlo (2000m), CTD Niskin (4700m), Neuston Net x2, McLane Pump
40	AM01145	VOY-040-GT9	17/11/2019 05:19	-38.6026	11.79955	CTD Niskin (300m), CTD GoFlo (2000m), CTD Niskin (5000m), Neuston Net x2, McLane Pump, MSC x 2
40	AM01146	VOY-040-GT10	18/11/2019 01:49	-36.29947	13.30282	CTD Niskin (300m), CTD GoFlo (2000m), CTD Niskin (4800m), Neuston Net x2, McLane Pump, Vibration Manoeuvres, TM Fish Deployment

## General Overview

The seasonal cycle couples the physical mechanisms of climate forcing to ecosystem response in production, diversity and carbon export (Monteiro et al., 2011; Thomalla et al., 2011), making it an important mode of variability to understand. There are almost no high-resolution biogeochemical data sets in the SO, making it hard to address the problem of model biases: firstly, to identify them and secondly, to characterize their associated mechanisms so that we may improve model projections. There is also very limited knowledge on how the seasonal cycle of oceanic features is linked to the massive seasonality of Antarctic sea ice. In March and April 2017 the extent of Antarctic sea ice reached the lowest minima in existing records (Turner et al., 2017), raising concerns on the anticipated response to anthropogenic warming. The detection of the anthropogenic signal is difficult due to the large internal variability of SO sea ice. The way sea ice would respond to atmospheric and oceanic changes is largely related to the smaller scale physical and mechanical properties and how they evolve with time.

South African science builds on its comparative geographical advantage to strengthen its contribution to long-term and experimental observations towards a greater understanding of the role of fine scale dynamics in shaping the phasing and magnitude of the SO seasonal cycle through novel integrated ship (process study), robotics and biologging experiments. The SCALE cruises exploited its vessel-based operations to data-driven digital assets and contributed to sparse full-scale data on ship responses in the SO, Marginal Ice Zone (MIZ) and Antarctic ice.

The hypothesis is that changes in the seasonal - synoptic modes of variability are a more sensitive indicator of decadal variability and long-term trends than changes in the magnitude of annual means.

### Key research goals:

1. Advance our understanding of the climate sensitivity of the SO through a better understanding of seasonal cycle dynamics of physics, biogeochemistry, and ecology at the sea ice interface and in the upper 1000 m.
2. Observe decadal changes in the ocean interior.
3. Develop digital assets to capitalize on data.
4. An interdisciplinary and international post graduate student training, advanced skills development and observational technology innovation platform.

SCALE focused on the seasonal characteristics of the air-sea ice-ocean interface and upper 1000 m and the long-term (quasi-decadal) change in storage in the ocean interior (100 - 5000 m). The objective in the upper ocean is to compare, through a series of well-considered experiments, the seasonal and storm-linked synoptic variability in sea ice characteristics, mixed layer physics, productivity and CO<sub>2</sub> between zones of varying net uptake and outgassing. The objective in the ocean interior is to investigate changes to carbon, geotraces and heat content relative to a comparable section completed in 2008 (Tanhua et al., 2016). SCALE achieved this through a unique 8-month (July 2019 - February 2020) integrated research platform in the SE Atlantic sector of the SO, which

combines a decadal-scale ship-based basin transect (the Good Hope Line) with seasonal-scale glider and marine mammal data-logger observations of physics, biogeochemistry and ecology of the Subantarctic Zone (SAZ), the Polar Upwelling Zone (PUZ) and the Marginal Ice Zone (MIZ). The data collected will also contribute to the global decadal basin scale observations coordinated by GO-SHIP and GEOTRACES. SCALE comprised of six integrated scientific themes that span a broad range of disciplines and address the strengths of the South African SO community:

1. Air-Sea-Ice Fluxes and Physical Drivers – Seasonal Cycle
2. Ocean Storage – Decadal Variability
3. Biological Carbon Pump (BCP) – Seasonal variability and Process Studies
4. Marine predators - Ecology and Oceanography sampling
5. Sea-ice Dynamics and Rheology - Experimental and Computational Studies
6. Digital Technology - Sensor to Service Solutions for Polar Engineering

### **Air-Sea-Ice Fluxes and Physical Drivers**

The exchange of gases, aerosols, heat and momentum is a key factor influencing long-term climate variability and trends. These fluxes are critical to understanding the links between carbon and climate, aerosols and albedo and the influence of terrestrial particles on ocean biogeochemistry. The SO is characterized by strong seasonality, varying degrees of sea-ice cover and drifts (Vichi et al., 2019), variable and high wind speeds, large temperature ranges, and dramatic meso- and submesoscale variability, rendering it a challenging and dynamic environment to accurately measure these air-sea-ice fluxes (Monteiro et al., 2015; Gregor et al., 2018). The research challenge is to make the links from the driving scales, primarily synoptic and seasonal, to climate feedback decadal scales.

### **Key Research Objectives:**

- What are the spatial and seasonal fluxes of particles, gases, CO<sub>2</sub> and heat between the ocean, atmosphere and ice?
- How does ocean physics determine the synoptic and seasonal evolution of these fluxes?
- How do mesoscale gradients across different zones link with atmospheric forcing to modulate these fluxes?
- How does the passage of a storm reconfigure upper-ocean physics? How does this impact vary seasonally, regionally (i.e., between the SAZ, PUZ and MIZ stations) and what are implications for CO<sub>2</sub> and Primary Production?
- What is the role of severe atmospheric events on the MIZ physical and biogeochemical processes and are they represented sufficiently in atmospheric reanalyses?
- Can we provide a better description of sea-ice dynamics in the MIZ by including more accurate treatments of the physical and mechanical properties of sea ice?
- How does atmospheric chemistry modulate the composition and bioavailability of these fluxes?
- How might these links evolve to influence the long-term role of the SO in regional and global climate?
- What is the natural oxidative capacity of the atmosphere in the SO?

## **Decadal Changes in Ocean Interior**

The Meridional Overturning Circulation (MOC) is a global reaching system of surface and deep ocean currents. It is the primary mechanism for the transport and storage of heat, carbon, salt, freshwater and nutrients, including iron, between ocean basins; connecting the surface ocean and atmosphere with the huge reservoir of the deep sea (Tanhua et al, 2016; Tagliabue et al., 2012).

### **Key Research Objectives:**

- **CO<sub>2</sub> storage in ocean interior:**

1. What are the decadal trends in CO<sub>2</sub> storage in Mode, Intermediate, Deep and Bottom Waters?
2. How much of the storage is linked to the BCP and uptake of anthropogenic CO<sub>2</sub>?

- **Heat Storage:**

1. What are the decadal trends in heat (and freshwater) storage in Mode, Intermediate, Deep and Bottom Waters?
2. How do these changes impact large scale circulation patterns in the Antarctic Circumpolar Current (ACC) and interlinked branches of the MOC?

- **Geotraces: Trace Elements and Isotopes:**

1. How does chemical speciation of trace metals affect uptake and regeneration?
2. How do particle dynamics affect uptake and removal?
3. What are the depth scales for trace element regeneration and what is their sensitivity to environmental variables.
4. How best can we constrain hydrodynamics and water masses, regional and global circulation patterns along with other tracers (eg. Nd isotopes).

## **Biological Carbon Pump**

Changes in climate are likely to affect the composition, abundance, and productivity of phytoplankton in the SO, with feedbacks that threaten the ecosystem services they provide, namely sustaining biodiversity, fueling the food web and fisheries, and mediating global climate through an altered efficiency of the biological carbon pump (BCP) (Moline et al., 2004). Our broad aim is to characterise the drivers of the SO BCP and quantify the transformation processes that constrain its strength and efficiency. In addition, we seek an improved understanding of the response of the BCP to physical, chemical, and biological drivers that vary with time (daily, episodically, seasonally) and space (regional, mesoscale, submesoscale) (e.g. Thomalla et al, 2011).

### **Key Research Objectives:**

- Quantify the biomass and characterize the composition and diversity of bacteria, phytoplankton and zooplankton communities on diurnal, seasonal and spatial scales, and elucidate on the drivers of their variability.
- Determine the co-limiting effects of micronutrient, macronutrient, light (bottom-up) and grazing (top-down) controls on the rates of biogeochemical transformations (e.g. growth rates, net primary production, export production), and understand how these shape community compositions.

- Compare the physiological requirements of the phytoplankton community to the stoichiometry of the (macro and micro) nutrient supply.
- Characterize the export flux (composition, particle size, settling rates) and quantify its strength and efficiency.

### **Ecology of seabirds and marine mammals**

The SO is subject to strong frontal (meso to sub-mesoscale) activity due to the instabilities of the Antarctic Circumpolar Current. Nutrient pulses associated with frontal dynamics have the ability to propagate throughout the food chain from lower trophic levels (phytoplankton) to top predators (e.g. seabirds and marine mammals). In response, marine predators often employ a range of foraging strategies that target key environmental features (e.g. Arthur et al. 2016; Abrahms et al. 2018). In addition, extreme synchronous breeding patterns of high-latitude marine predators make them susceptible to environmental forcing, such that small fluctuations in the seasonal cycle could have detrimental effects of their success. The position of higher-order predators within the food web (e.g. sea birds and Ross seals) can therefore make them bio-indicators of environmental change (reference?). Most marine predator studies occur during the short Antarctic summer field season with fundamental knowledge of marine predator movements, foraging and breeding behaviour during winter and spring months still lacking.

Through the deployment of biologging devices, marine predators can in addition act as remote oceanographic samplers of ice-covered seas that are inaccessible to ships and gliders in winter (Fedak 2004, 2013).

### **Key Research Objectives**

- How do large-scale lateral gradients (along the Goodhope line) in the physical environment constrain top predator foraging habitats?
- Do regions of overlapping strong fine-scale dynamics with high densities in storm track distributions coincide with top-predator foraging hotspots?
- Ascertain seasonal fluctuations in the spatial distribution and density of seabird species at sea.
- To understand seasonal variability in the link between physical structures (e.g. large-scale fronts, eddies and plankton distribution) and their influence on Ross seal (*Ommatophoca rossii*) foraging behaviour.
- As an ancillary objective, any oceanographic and isotopic data collected can be used for any of the other Scientific Themes where deemed needed.

### **Sea-ice Dynamics and Rheology - Experimental and Computational Studies**

The mechanical, physical and biogeochemical properties of sea ice are key to understand its mediating influence on the atmosphere and the ocean. These properties, however, are still largely unknown for the MIZ in the SO, and particularly for the pancake ice region whose features are more difficult to be observed from space. Of particular importance are the purely mechanical material behaviour of ice governed by its elasticity, viscosity and strength in response to metocean conditions, the structural and multiphasic texture and

composition of sea ice and the permeability of its porous structure controlling brine, gas and nutrient contents. The collective knowledge of the aforementioned characteristics will allow us to better constrain remote sensing observations and simulate the seasonal variability of sea ice and its impact on ocean-atmosphere interaction in numerical models. Additionally, knowledge of the encountered ice conditions provide insight into the expected operational profiles for vessels required to work in such environments.

**Key Research Objectives:**

- Improved definition of the extent, structure and seasonal variability of the SO MIZ
- Quantify the MIZ role as a dynamical mediator of momentum and heat transfer and biogeochemical buffer for the upper ocean
- Quantify the responses of pancake ice to wind and swell and development of larger scale parameterizations
- Multiphase modelling of the sea ice freezing process, pore structure evolution and the resulting brine and biogeochemical dynamics
- Computational fluid dynamics modelling of the sea ice rheology in the MIZ and fracture mechanics

**Digital technology solutions for polar engineering**

SCALE experiments will be supported through ship-based operations on the SA Agulhas II polar supply and research vessel. Insight into the operational conditions faced by this modern, first-in-class ship provides vital data which can advance the scientific basis for ice-going vessels in the SO. This ship has been the subject of full-scale engineering measurements since 2012 (Bekker et al., 2018), whereby approximately 200 measurement channels provide information on ship-based human comfort, structural dynamics of the hull and propulsion systems and wave slamming. It is proposed to advance the existing infrastructure and advanced data analytics to explore digital twin technology. A digital twin is a digital representation of the state and behavior of a unique, real asset or process in (almost) real time (Erikstad, 2017) within its operational context. Operational data from SCALE voyages will be combined with data-driven simulation models to evaluate real-time decision aiding, monitoring and information systems to the benefit of ship operations, research and industrial development. Furthermore, the concept of a “ship as a sensor” will be explored whereby the vessel itself could be used to infer environmental observations.

**Key Research Objectives:**

1. Assess ship responses and human comfort as a result of wave slamming and ice.
2. Evaluate the potential of the “ship as a sensor” to predict ice and wave conditions from automated ship-based measurements.
3. Define a baseline for healthy structural responses towards a framework for smart, efficient ship operations to increase useful vessel life.

To prototype “sensor-to-service” applications of ship data for stakeholders including the marine industry, vessel owners, ship-based research and education.

## Scientific Reporting

### 1. TEAM BIRDS

#### 1.1. Winter Cruise

##### 1.1.1. Aim

The aim of the survey was to atlas the winter seabird species distribution and relative abundance in the African sector of the South Atlantic and Southern Ocean as part of the annual seabird survey.

##### 1.1.2. Introduction and methodology

All observations were made aboard the SA Agulhas II during the 2019 winter SCALE cruise (18<sup>th</sup> July to 12<sup>th</sup> August 2019). The approximate course followed is presented in Figure 1.1. The actual observation period was from the 18<sup>th</sup> July to 7 August, and 10-11 August. No observations were made while the vessel was moored in East London Harbour as part of a public exhibition (8-9 August). Observations were conducted during daylight hours with good visibility when the ship was in motion along a transect gradient. Sightings were conducted from Deck 10, in the forward 180 of the vessel out to 300m. No observations were made during sampling stops or during vessel manoeuvre testing. No seabirds reconsidered to be ship followers were recorded. Additionally, birds were recorded as in-flight or sitting on the water at the time of the sighting. All observations were logged on smart phones using the BirdLasser application (written by Lejint).

##### 1.1.3. Results

###### 1.1.3.1. Full protocol sightings

A total of 2935 active observations with a sighting of 40 seabird species. Several groups of unidentified seabirds, mainly prions were also recorded. A total of 6892 individual birds were counted (see Table 1.1).

###### 1.1.3.2. Incidental sightings

Three seabirds were found aboard the ship. Two live South Georgian Diving Petrels *Pelecanoides georgicus* were found on the aft-deck during night operations on 2 August at -45.00, 6.59E and 3 August at -47.000S 8.30E. Both were subsequently released back to sea. These records are important as they fall outside of the publish range of the species. A Kerguelen Petrel *Aphrodroma brevirostris* was found alive on the helideck, ringed and released on 31 July. A King Penguin *Aptenodytes patagonicus* was seen next to the ship while on station at -43.00, 8.49E on 21 July 2019. This record also constitutes

an out-of-range record. A Northern Royal Albatross was recorded while on station on 3 August.

#### **1.1.4. Noticeable issues with BirdLasser**

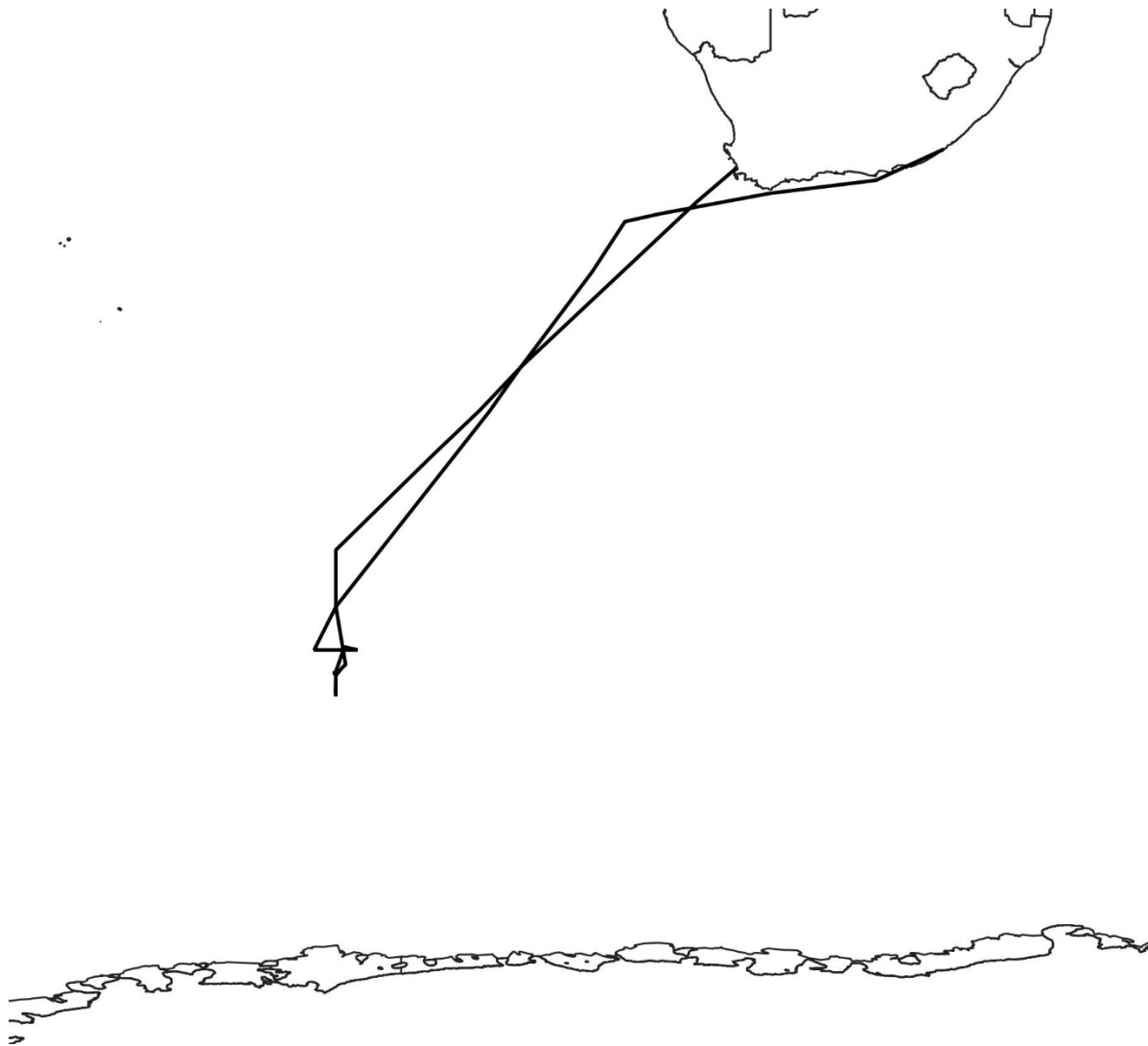
- There should be non-flying option for penguins. Additionally, it would be nice to have additional quick options for porpoising, etc.
- When in cold weather, the app is not glove friendly. In particular some icons are very small and closely spaced.
- There is a noticeable slowdown of the processing speed of digital devices as data is collected. We had to either park the card, and start a new one, or use separate phones for morning and afternoon sessions. We recommend that two cards are opened per day.
- No unknown prion options. It would be ideal to have “confidence” options/boxes for hard to identify species.
- There is no easy way to change the observation range if visibility distance changes.

**Table 1.1:** Summary of seabird species observed during the 2019 winter Scale cruise (18 July-12 August 2019). The observation summary consists the number of observations with the total of birds in parantheses.

Common name	Observations	Notes
<b>Macaroni Penguin</b> <i>Eudyptes chrysolophus</i>	11 (51)	
<b>Gentoo Penguin</b> <i>Pygoscelis papua</i>	1 (6)	
<b>Chinstrap Penguin</b> <i>Pygoscelis antarcticus</i>	36 (181)	
<b>Adelie Penguin</b> <i>Pygoscelis adeliae</i>	9 (25)	
<b>King Penguin</b> <i>Aptenodytes patagonicus</i>	-	Incidental observation
<b>African Penguin</b> <i>Spheniscus demersus</i>	2 (2)	
<b>Unidentified penguins</b>	2 (5)	
<b>Northern Royal Albatross</b> <i>Diomedea sanfordi</i>	-	Incidental observation
<b>Southern Royal Albatross</b> <i>Diomedea epomophora</i>	1 (1)	
<b>Wandering Albatross</b> <i>Diomedea exulans</i>	16 (20)	
<b>Indian Yellow-nosed Albatross</b> <i>Thalassarche carteri</i>	24 (28)	
<b>Shy Albatross</b> <i>Thalassarche cauta</i>	151 (183)	
<b>Black-browed Albatross</b> <i>Thalassarche melanophris</i>	71 (78)	
<b>Grey-headed Albatross</b> <i>Thalassarche chrysostoma</i>	57 (65)	
<b>Sooty Albatross</b> <i>Phoebetria fusca</i>	16 (17)	
<b>Light-mantled Albatross</b> <i>Phoebetria palpebrata</i>	4 (4)	
<b>Unidentified albatrosses</b>	3 (8)	
<b>Northern Giant Petrel</b> <i>Macronectes halli</i>	6 (6)	
<b>Southern Giant Petrel</b> <i>Macronectes giganteus</i>	42 (42)	
<b>Unidentified Giant Petrel</b>	3 (3)	
<b>Cape Petrel</b> <i>Daption capense</i>	56 (97)	
<b>Southern Fulmar</b> <i>Fulmarus glacialisoides</i>	72 (79)	
<b>Antarctic Petrel</b> <i>Thalassoica Antarctica</i>	66 (69)	
<b>Snow Petrel</b> <i>Pagodroma nivea</i>	86 (109)	

<b>White-headed Petrel</b> <i>Pterodroma lessonii</i>	124 (155)	
<b>Soft-plumaged Petrel</b> <i>Pterodroma mollis</i>	181 (210)	
<b>Atlantic Petrel</b> <i>Pterodroma incerta</i>	22 (22)	
<b>Great-winged Petrel</b> <i>Pterodroma macroptera</i>	104 (118)	
<b>Kerguelen Petrel</b> <i>Aphrodroma brevirostris</i>	67 (68)	
<b>Fairy Prion</b> <i>Pachyptila turtur</i>	1 (1)	
<b>Slender-billed Prion</b> <i>Pachyptila belcheri</i>	24 (41)	
<b>Antarctic Prion</b> <i>Pachyptila desolata</i>	368 (585)	
<b>Broad-billed prion complex</b> <i>P. vittata/macgillivrayi</i>	15 (55)	
<b>Unidentified prions</b>	33 (53)	
<b>Blue Petrel</b> <i>Halobaena caerulea</i>	191 (207)	
<b>Grey Petrel</b> <i>Procelleria cinerea</i>	4 (4)	
<b>White-chinned Petrel</b> <i>Procelleria aequinoctialis</i>	164 (253)	
<b>Sooty Shearwater</b> <i>Ardenna grisea</i>	114 (1382)	
<b>Subantarctic Shearwater</b> <i>Puffinus elegans</i>	23 (32)	
<b>Common Diving Petrel</b> <i>Pelecanoides urinatrix</i>	24 (27)	
<b>South Georgian Diving Petrel</b> <i>Pelecanoides georgicus</i>	-	Incidental observations
<b>Cape Gannet</b> <i>Morus capensis</i>	672 (2488)	
<b>Cape Cormorant</b> <i>Phalacrocorax capensis</i>	11 (34)	
<b>Brown Skua</b> <i>Stercorarius antarcticus</i>	17 (19)	
<b>Greater Crested Tern</b> <i>Thalasseus bergii</i>	37 (55)	
<b>Arctic Tern</b> <i>Sterna paradisaea</i>	2 (2)	
<b>Little Tern</b> <i>Sternula albifrons</i>	1 (1)	

Figure 1.1. Course taken by the SA Agulhas on the 2019 winter SCALE cruise



### **1.1.5. Acknowledgments**

We would like to acknowledge the crew of the SA Agulhas II, Chief Scientist onboard Marcello Vichi and Chief Scientist on land Sandy Thomalla, the Department of Environment, Forestry and Fisheries for making the berth space available, and Andrew de Blocq of BirdLife South Africa for the opportunity of a lifetime.

## **1.2. Spring Cruise**

### **1.2.1. Introduction**

A seabird survey was conducted to record the spring seabird species distribution and relative abundance in the African sector of the South Atlantic and Southern Ocean as part of the annual seabird survey. This forms part of a long-term project to map the distribution and density of seabirds in this region to better inform marine biodiversity management in the Southern Ocean.

### **1.2.2. Methodology**

All observations were made aboard the SA Agulhas II during the 2019 SCALE Spring Cruise (11<sup>th</sup> October to 19<sup>th</sup> November 2019). Observations were only made while the ship was sailing and following the official cruise course. No observations related to atlasing were made while the vessel was stationary, during the seal censuses, vessel manoeuvre testing, or when the vessel veered off from the official cruise course for any reason, e.g. avoiding bad weather, collecting wave gliders etc. In addition to the standard seabird survey, a ship-board census of penguin species (Adélie, Emperor, and Chinstrap Penguins) residing in the marginal sea ice zone of the Lazarev Sea was performed along the same north-south transect lines across the ice gradient as followed during the cruise's seal census. All Adélie and Emperor Penguins encountered were photographed and aged according to criteria in field guides. Reliable aging of Chinstrap Penguins is not possible from a distance.

Observations were conducted during daylight hours when visibility was good and the ship was sailing along a transect. Sightings were conducted from Deck 10, in the forward 180° of the vessel to a distance of 300 m. On a few occasions, e.g. excessive glare, the angle of view was reduced to 90°. Care was taken to avoid counting ship-followers. At each shift change-over, the 'new' observer was briefed about ship-followers. Additionally, birds were recorded as in-flight or sitting on the water at the time of the sighting. Several of the smaller species, notably the prions and storm petrels, are notoriously difficult to identify in flight. When specific identification could not be confirmed, the sighting was logged as Unidentified with a note of the group, e.g. prion, storm petrel, etc.

Where possible, all observations were logged on smart phones using the BirdLasser application (Lejint 2018). When this wasn't possible, all sightings were recorded in a notebook with the time, and later reconciled with the ship's data logger.

### **1.2.3. Results**

#### **Full protocol sightings (Figs. 1.2.1 and 1.2.2)**

A total of 49 species were recorded during the Scale Spring Cruise. Unidentified species included a juvenile penguin, storm petrels and prions. A summary of the number of encounters per species recorded during the Scale Spring Cruise is presented in Fig. 1.1. A total of 1132 observations of seabirds were recorded, representing 2913 birds (Fig. 3). On occasion it was not possible to reliably identify some species to species level, e.g. storm petrels, prions and terns, but these are indicated as such in Figs. 1.1 and 1.2.

#### **Incidental sightings**

Chinstrap Penguin:

Small groups visited the ship at 54.00745°S, 0.01105°E on 19 October 2019 and also at 58.44368°S, 21.99602°E on 3 November 2019.

King Penguin:

i) Several individuals visited the ship while stationary at 47.96165°S, 4.5602°E on 17 October 2019.

ii) A single King Penguin briefly visited the ship while stationary at 47.00022°S, 4.50008°E on 12 November 2019.

Macaroni Penguin:

Three were seen next to the ship while on station at 49.2969°S, 2.36967°E on 11 November 2019.

Southern Rockhopper Penguin:

Four birds foraged around the ship while at station 44.99972°S, 6.60582°E on 16 October 2019.

We noted that in the open sea, penguins tend to arrive within the first hour after the ship became stationary. This could be a useful time to log incidental records of penguins present in the area.

#### **1.2.4. Discussion**

The SCALE Spring Cruise represented the first visit to the Antarctic sea ice in the Lazarev Sea during spring. It therefore provided valuable baseline data for future surveys of this kind, and also improved our current knowledge of seasonal seabird distribution and abundance in the Southern Ocean.

The penguin census data will be analysed and submitted to a peer-reviewed journal for consideration for publication.

#### **1.2.5. Acknowledgements**

We express our gratitude to the officers and crew of the MV SA Agulhas II for their assistance and support of the research objectives. Chief Scientist, Tommy Ryan-Keogh, for his professional conduct and meticulous planning of all science-based activities. The Department of Environment, Forestry and Fisheries for making the berth space available and Birdlife South Africa, in particular Mr Andrew De Blocq, for giving us the opportunity to contribute to this amazing project.

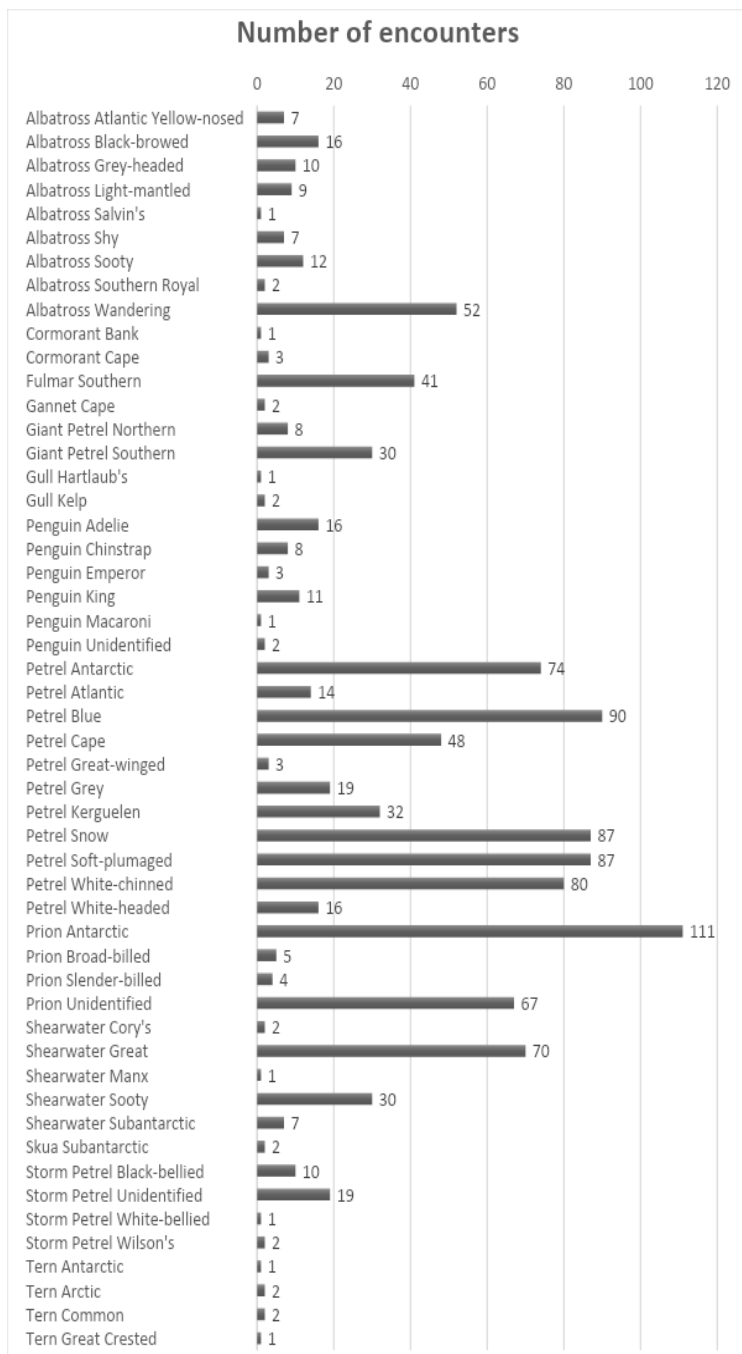


**Fig. 1.2.1.** Number of encounters of seabird species during the Scale Spring Cruise to the Antarctic sea ice from 11 October to 19 November 2019.

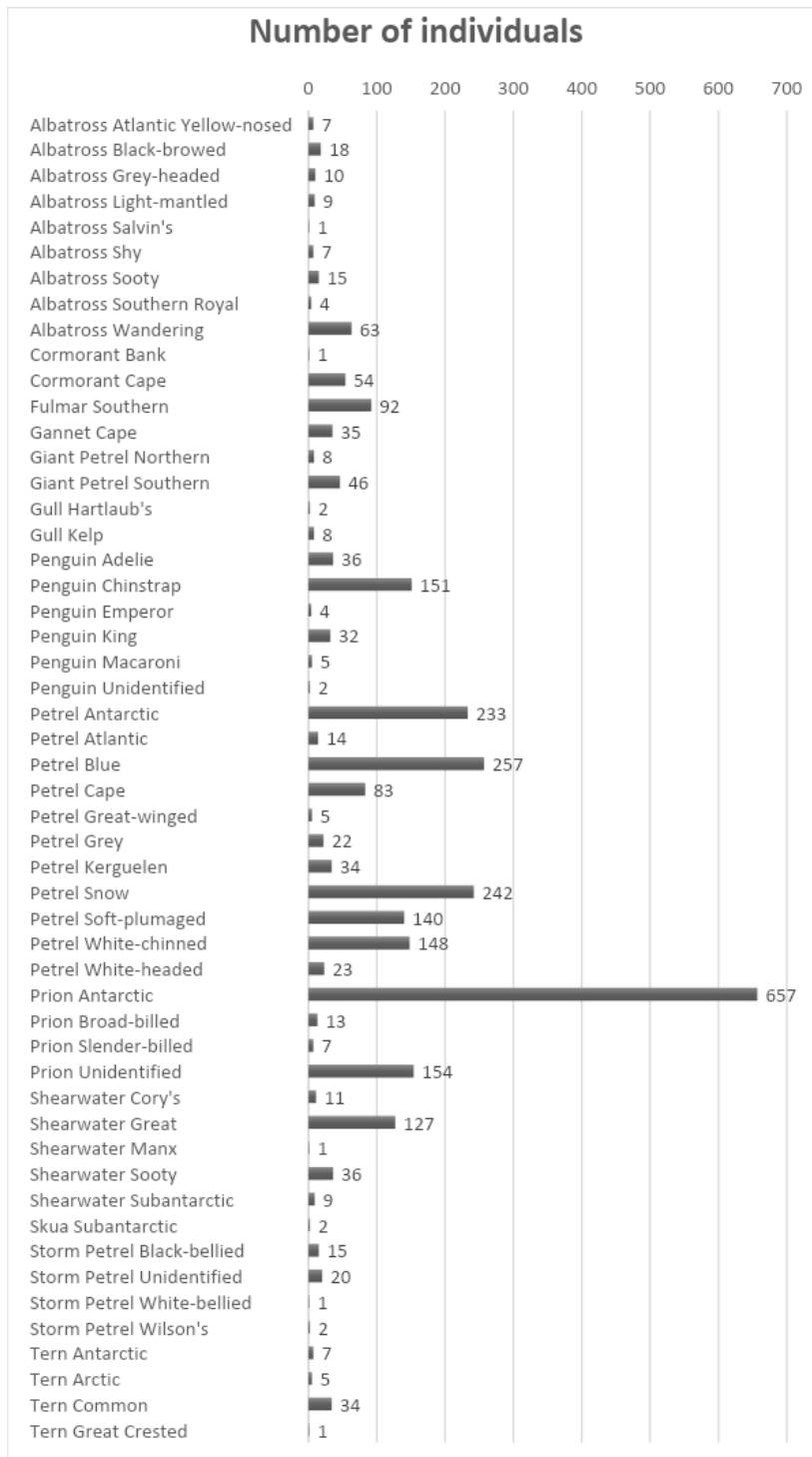


**Fig. 1.2.2.** Number of individuals per seabird species recorded during the Scale Spring Cruise to the Antarctic sea ice from 11 October to 19 November 2019.

## 2. TEAM CO<sub>2</sub>

### 2.1. Winter Cruise

#### 2.1.1. Continuous CO<sub>2</sub> Observations

The four parameters of the carbonate system were measured during the voyage. Underway surface observations of continuous surface pCO<sub>2</sub> (equilibrator based), and individual bottle samples of surface Dissolved Inorganic Carbon (DIC), Total Alkalinity (AT) and pH were collected from the ship's underway seawater supply during the voyage. The following description provides details of the measurements and preliminary results obtained during the voyage. SST and Salinity observations along the sampling track, along with the mean frontal positions observed from absolute dynamic topography are indicated in Fig 2.1.1.

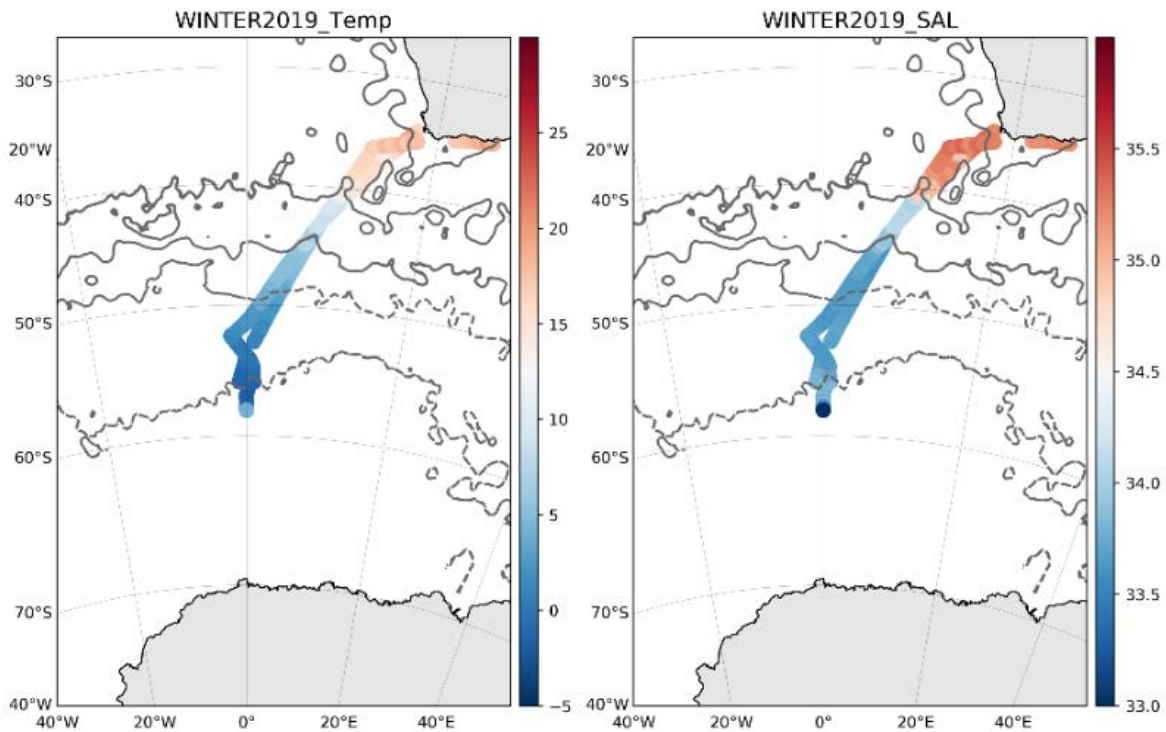


Figure 2.1.1 shows the temperature and salinity collected during the voyage, along with the mean absolute dynamic topography indicated frontal positions (STF, SAF, PF and SBdy from north to south).

#### 2.1.2. Continuous pCO<sub>2</sub>

The gradient between the atmosphere and ocean represents the thermodynamic potential for gas exchange of CO<sub>2</sub> across the air-sea interface. When the concentration is higher in the ocean, gas would tend to reach equilibrium through efflux to the atmosphere and vice versa. Partial pressure of CO<sub>2</sub> in the seawater were measured using an infrared gas analyser after equilibration in a spray chamber (manufactured by General

Oceanics), as described in Pierrot et.al., 2009. The instrument was calibrated using 4 reference gases, certified against reference standards traceable to NOAA central calibration laboratory. The instrument was sequenced to cycle between reference standards, atmospheric air, and seawater roughly every 4 hours. Data was logged through a computer interface using propriety LABVIEW software, which also controlled the mechanical operation of the instrument. Fluctuations in equilibrator pressure were observed throughout the cruise. The instrument was monitored regularly to ensure water flow, gas flow, and pressure levels were within an appropriate range.

Figure 2.1.2 shows the atmospheric pressure and raw  $x\text{CO}_2$  measured along the transect. It shows a distinct some variability ranging between undersaturated  $x\text{CO}_2 \sim 390\text{uatm}$  the Subtropical Region in the north (north of the STF) to supersaturated  $x\text{CO}_2 (> 440\text{uatm})$  in the Antarctic Zone southward of the Polar Front. These are the raw uncalibrated output from the instrument and still has to be processed for screening and calibration using the reference gases, as well as the correction for atmospheric pressure and the non-ideal gas behaviour of  $\text{CO}_2$ . Furthermore, the measurements will be compared to the previous observations of  $\text{pCO}_2$  in the region during previous campaigns.

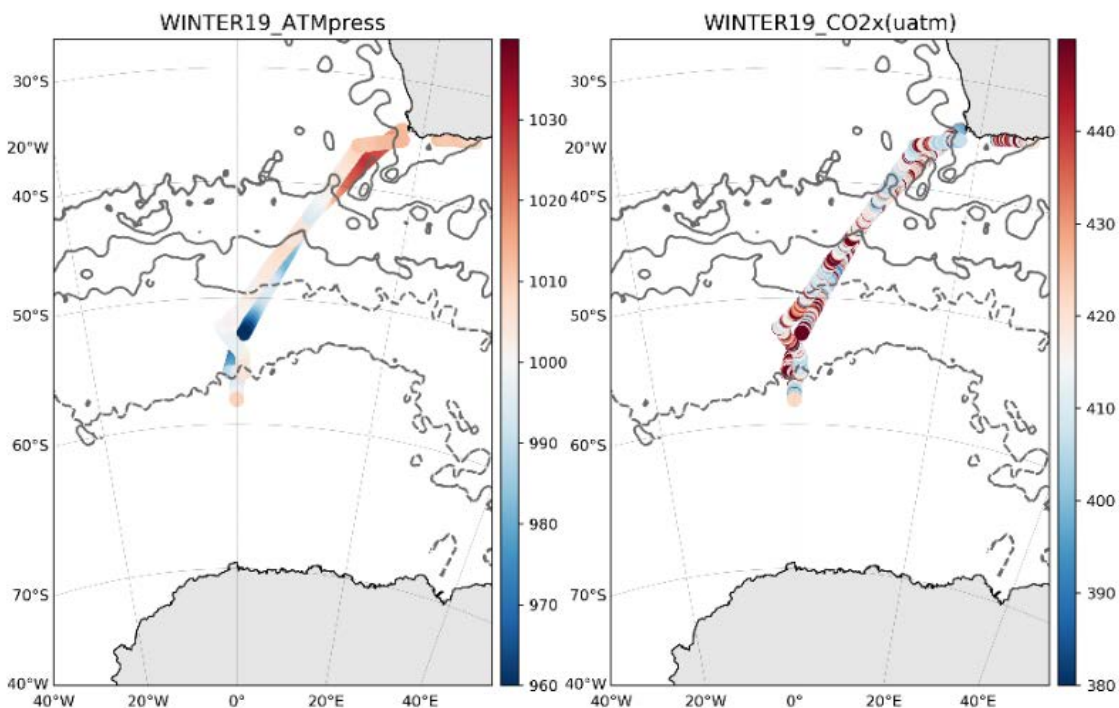


Figure 2.1.2. Raw  $x\text{CO}_2$  ( $\mu\text{atm}$ ) measured continuously along the transect and atmospheric pressure from the ships weather data.

### 2.1.3. Dissolved Inorganic Carbon and Total Alkalinity

Total dissolved inorganic carbon and total alkalinity samples were collected from the wet biology lab, from the same underway water supply where the TSG water is sampled. Intake temperature, salinity and atmospheric pressure were recorded at each point underway samples were collected.

CTD samples were collected from 12 – 13 depths with increased resolution in shallower depths. Samples collected for ship based analysis were stored in 500mL bottles (identical to CRM bottles as supplied by A. Dickson) with 120 $\mu$ L of concentrated HgCl<sub>2</sub> (Mercuric Chloride) to prevent any further biological modification of the sample. The 500mL samples were analysed on board using Marianda's VINDTA 3C (Versatile Instrument for the Determination of Titration Alkalinity). The VINDTA determines total alkalinity by potentiometric titration and also coloumetrically measures CO<sub>2</sub> from the same sample. Accuracy of the VINDTA was determined by running a Dickson's CRM's before and after each batch. Consistency in reproducibility of CRM's was sometimes difficult to achieve for entire batches, in particular for DIC which showed an increase between CRMs at the beginning and end of each batch of roughly 20 samples. The precision of the analysis was tested by replicating 10 samples for DIC and TA collected from the same CTD. The precision for DIC and AT was XX umol/kg and XX umol/kg respectively, prior to adjustment for the correct acid concentration and pipette volumes. This is expected to improve after these corrections are applied to the data.

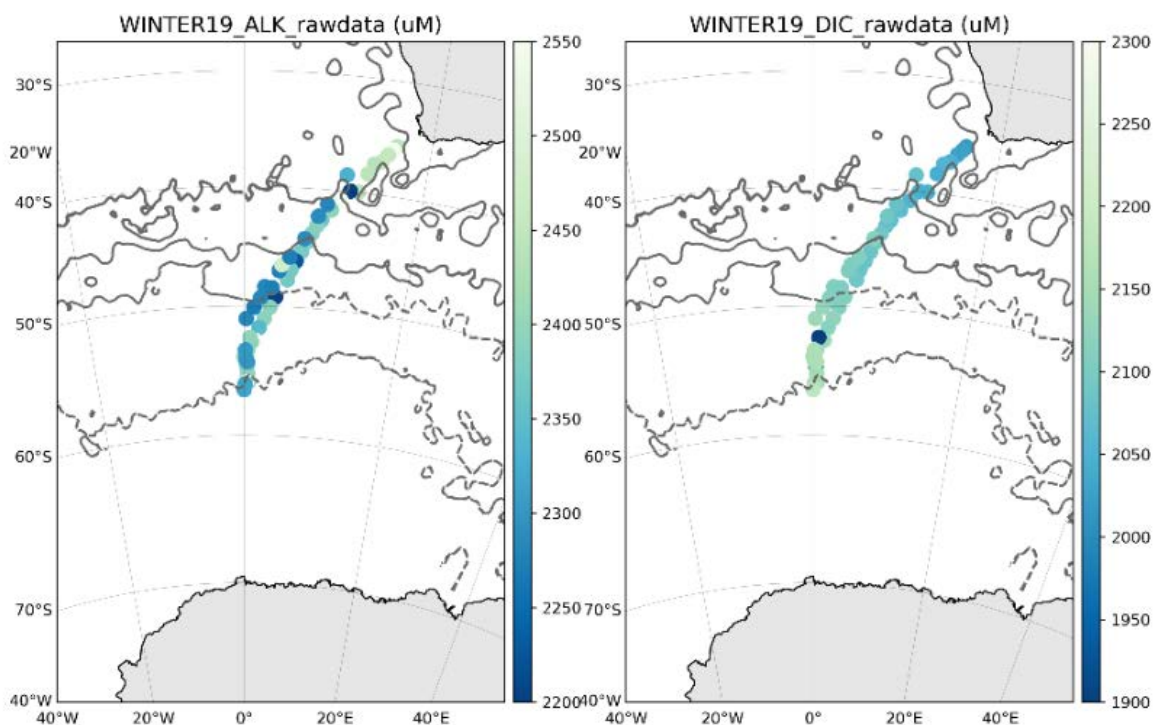


Figure 2.1.3. Shows the raw Dissolved Inorganic Carbon (umol/kg) and Total Alkalinity (umol/kg) along the transect. Correction for certified reference materials, nutrient concentrations and pipette volumes, are yet to be applied to the raw data presented here. Surface DIC Showed a north to south increase from ~ 2060 umol/kg to greater than 2200 umol/kg southward of the Polar Front. TA Showed variability in the surface.

DIC in the northern section of the transect shows depletion of DIC in the surface, potentially related to biological drawdown of DIC, a more homogenous DIC profile is observed in the southern portion potentially related to upwelling south of the PF. This data, after the necessary calibrations, will be further interpreted in conjunction with the nutrient and hydrographic data collected during the cruise.

#### 2.1.4. High precision pH

High precision pH measurements were conducted on underway surface water (Fig 4) as well as subsurface profiles at all the sampling stations using the portable UV visible spectrophotometer (Ocean Optics USB 4000). The pH measurements were based on the addition of a pH-sensitive indicator dye m-cresol purple (mCP) to a water sample (Clayton and Byrne, 1993) with precision < 0.003 pH units. Within the pH-range of seawater the dye changes its color from deep red to purple. The background absorbance (blank) of the water sample is recorded, and then the absorbance after addition of 5  $\mu\text{L}$  and 10  $\mu\text{L}$  of the mCP are also taken at three different wavelengths (434 nm, 578 nm and 730 nm). The pH is determined from a standard mathematical expression using the absorbance values.

The raw pH results collected from samples (Fig. 2.1.4) ranged between 7.727 and 8.069. Upon closer inspection it appears that some drift in measurements occurred during the beginning and end of the cruise. Certified reference materials from Dickson were analysed on a daily basis during the cruise and will be utilised to adjust the raw output presented here. At this stage it is unclear what caused the instrument drift.

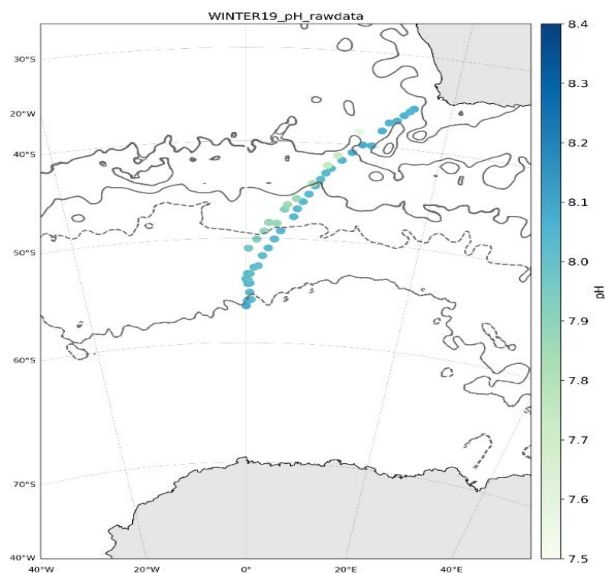


Figure 2.1.4. High resolution pH observations collected from underway seawater during Winter 2019 SCALE campaign, along with the frontal positions using satellite dynamic topography.

Water column profiles of DIC, Alkalinity and pH were also collected at all the process stations along the sampling transect.

### 2.1.5. Continuous N<sub>2</sub>O observations

Nitrous Oxide (N<sub>2</sub>O) were measured continuously in the atmosphere along the cruise transect (Fig. 2.1.5) using a Picarro Cavity Ring Down Spectroscope (Model G5131i), capable of site-specific and bulk measurements of  $\delta^{15}\text{N}$  and  $\delta^{18}\text{O}$  isotopes. The sample inlet was installed on the walkway outside of the bridge (on the front of the bridge to minimise contamination from the ships smokestacks), and pressure tested to ensure leak free conditions. The instrument N<sub>2</sub>O concentrations was calibrated using certified reference gases traceable to the NOAA central calibration laboratory. Some instrument installation problems were encountered during the first few days of the voyages, which was only resolved after feedback from the manufacturer.

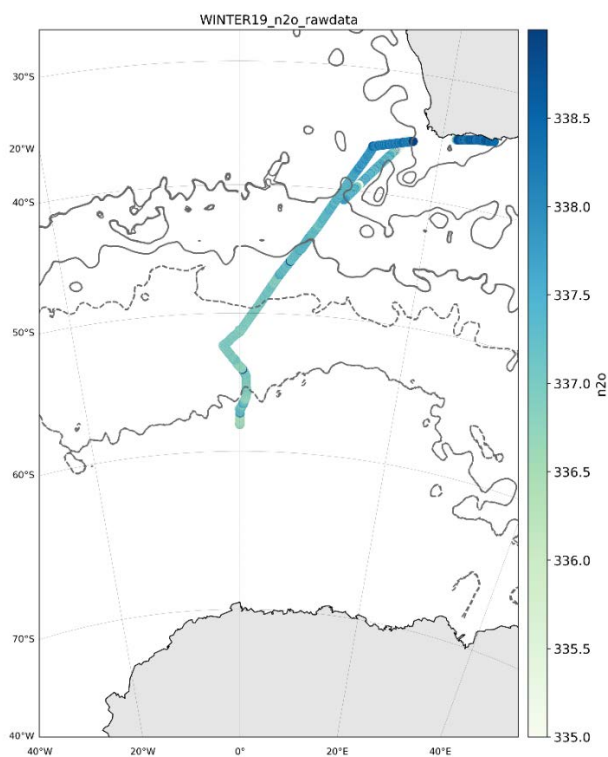


Figure 2.1.5. Atmospheric N<sub>2</sub>O concentrations (raw instrument output) along the sampling transect. Frontal positions are shown using satellite dynamic topography.

### 2.1.6. Appendix:

Table containing sampling information of carbonate (DIC/AT/pH) parameters along the sampling transect during SCALE2019\_winter.

<b><i>bottleID</i></b>	<b><i>lat</i></b>	<b><i>lon</i></b>	<b><i>salt</i></b>	<b><i>temp</i></b>
SCL1	-35.67	16.33	35.35	19.30
SCL2	-36.00	15.99	35.33	17.28
SCL3	-36.47	15.50	35.37	17.98
SCL4	-37.12	14.90	35.20	15.28
SCL5	-37.40	14.15	34.89	13.32
SCL6	-38.31	13.58	35.25	15.72
SCL7	-39.95	12.76	35.20	15.20
SCL8	-39.95	11.85	34.91	14.25
SCL9	-40.82	10.91	34.59	13.82
SCL10	-41.71	9.94	34.09	11.20
SCL11	-42.63	8.91	34.09	8.91
SCL12	-43.14	8.40	34.11	8.52
SCL13	-43.80	7.93	33.96	7.05
SCL14	-44.53	7.42	33.89	6.63
SCL15	-45.40	6.80	33.64	5.48
SCL16	-46.20	6.22	33.62	5.48
SCL17	-46.95	5.66	33.62	5.28

SCL18	-47.77	5.31	33.60	4.92
SCL19	-49.23	3.92	33.67	3.48
SCL20	-50.07	3.26	33.67	2.97
SCL21	-50.97	2.58	33.67	2.34
SCL22	-51.73	1.93	33.72	1.90
SCL23	-52.74	1.43	33.72	1.68
SCL24	-52.88	0.94	33.69	0.92
SCL25	-53.51	0.46	33.67	0.24
SCL26	-54.00	0.01	33.67	-0.20
SCL27	-54.15	0.09	33.66	-0.03
SCL28	-54.47	0.23	33.66	-0.50
SCL29	-55.31	0.45	33.77	-1.25
SCL30	-56.00	0.60	33.76	-0.89
SCL31	-56.00	0.60	33.78	-1.10
SCL32	-56.00	0.29	33.83	-1.40
SCL34	-56.13	0.16	33.81	0.96
SCL35	-56.59	0.00	33.89	-1.67
SCL36	-54.43	0.46	33.69	-0.65

SCL37	-54.16	0.25	33.69	-0.22
SCL39	-53.50	0.17	33.67	-0.04
SCL40	-51.01	0.27	33.66	4.50
SCL41	-50.10	1.22	33.65	2.45
SCL42	-49.29	2.07	33.64	4.16
SCL43	-48.40	2.55	33.65	4.14
SCL44	-48.47	3.46	33.68	4.75
SCL45	-47.04	4.26	33.70	5.18
SCL46	-46.55	4.55	33.74	5.21
SCL47	-45.88	5.47	33.69	5.21
SCL48	-44.28	7.11	33.95	1.55
SCL49	-42.32	8.52	34.11	8.91
SCL50	-41.24	9.44	34.00	9.95
SCL51	-38.59	11.32	34.98	13.94

## **2.2. Spring Cruise**

### **2.2.1. Continuous and CTD-Rosette CO<sub>2</sub> Observations**

The CO<sub>2</sub> group focused on measurements of dissolved inorganic carbon (DIC), total alkalinity (AT) and surface seawater partial pressure of carbon dioxide (pCO<sub>2</sub>) during this voyage. This report gives a summary of sample collection, measurements carried out and preliminary results of unprocessed data obtained on-board.

### **2.2.2. Continuous pCO<sub>2</sub> measurements**

Sea surface pCO<sub>2</sub> measurements were carried out using a General Oceanics underway pCO<sub>2</sub> system with a Licor-LI7000 Infra-red gas detector (Pierrot D., et al, 2009). The underway pCO<sub>2</sub> system was calibrated using 4 reference gases (0 ppm, 284.22 ppm, 399.15 ppm, 429.92 ppm), certified against reference standards traceable to NOAA central calibration laboratory. The instrument was sequenced to cycle between reference standards, atmospheric air, and seawater approximately every 4 hours. Data was logged through a computer interface using proprietary LABVIEW software, which is also controlled by the mechanical operation of the instrument. Measurements were carried out from Cape Town to the marginal ice zone in the Southern Ocean and back to Cape Town.

The two figures below show preliminary results of raw CO<sub>2</sub>x, intake temperature and salinity of the southward leg (Figure 2.2.1) and the northward leg (Figure 2.2.2). The intake temperature and salinity data were obtained from the TSG. Unprocessed data shows that the pCO<sub>2</sub> during the southward transect was higher than on the northward transect. The pCO<sub>2</sub> values during the northward leg ranged from 399-523 μatm whereas values falling between 379 – 1547 μatm were observed during the southward leg. The water content fluctuated between 0 and 14 μm/m throughout the voyage.

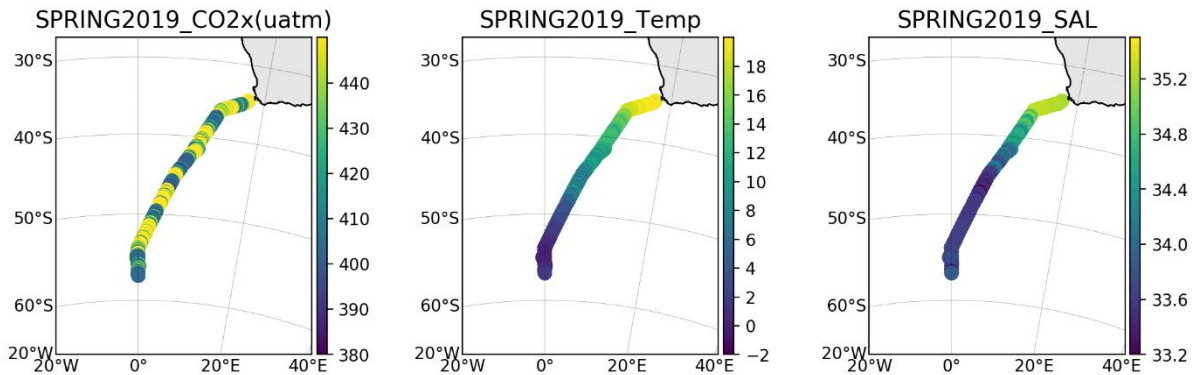


Figure 2.1.1. Preliminary pCO<sub>2</sub> (raw CO<sub>2</sub>x) data from Cape Town to the marginal ice zone.

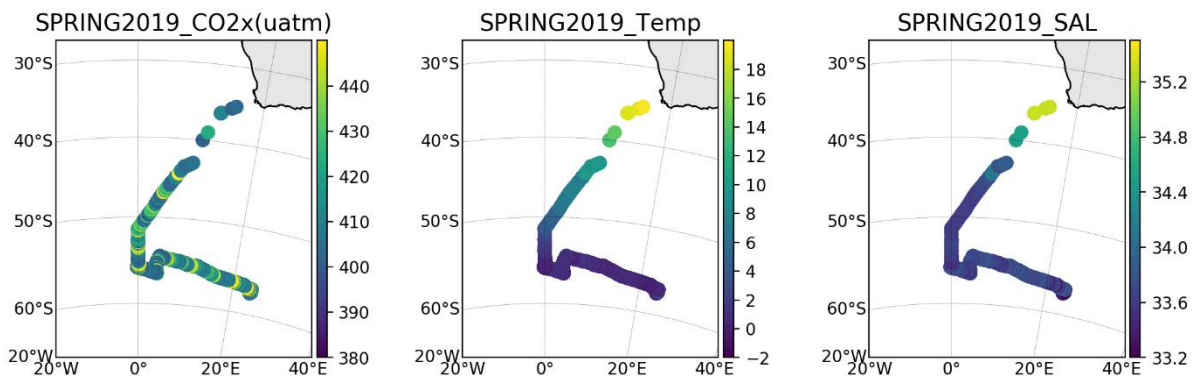


Figure 2.2.2. Preliminary pCO<sub>2</sub> (raw CO<sub>2</sub>x) data from marginal ice zone to Cape Town.

### 2.2.3. Dissolved inorganic carbon (DIC) and total alkalinity (AT) measurements

DIC/AT samples were collected from the underway surface seawater supply in the wet bio-lab where the TSG is placed every four hours. Samples were also collected from CTD stations; SAZ 2, PUZ, the marginal ice zone (MIZ) transect, whale transect (WS) and the Good Hope (GT) transect. The CTD was deployed to a maximum depth of 500 m on the MIZ transect, to a depth of 1000 m on SAZ 2/PUZ/WS and to the bottom of the ocean on the GT transect. A total of 71 underway DIC/AT samples and a total of 458 samples were collected from the CTD niskin bottles. Samples were collected in a 500 ml bottle and spiked with 120  $\mu\text{L}$  of concentrated  $\text{HgCl}_2$  (Mercuric Chloride) to prevent any further biological modification of the sample. The DIC/AT samples were analysed on board using Marianda's VINDTA 3C (Versatile Instrument for the Determination of Titration Alkalinity). The VINDTA determines total alkalinity by potentiometric titration and also colorimetrically measures  $\text{CO}_2$  from the same sample.

### 2.2.4. Underway DIC/AT

Preliminary results for underway samples show that the DIC increases southwards from 2035  $\mu\text{mol/kg}$  to 2193  $\mu\text{mol/kg}$ . As shown in Figure 2.2.3, high DIC values were observed at the marginal ice zone. The AT ranged from 2201  $\mu\text{mol/kg}$  and 2327  $\mu\text{mol/kg}$  with low AT values were between latitude 40°S and 53°S.

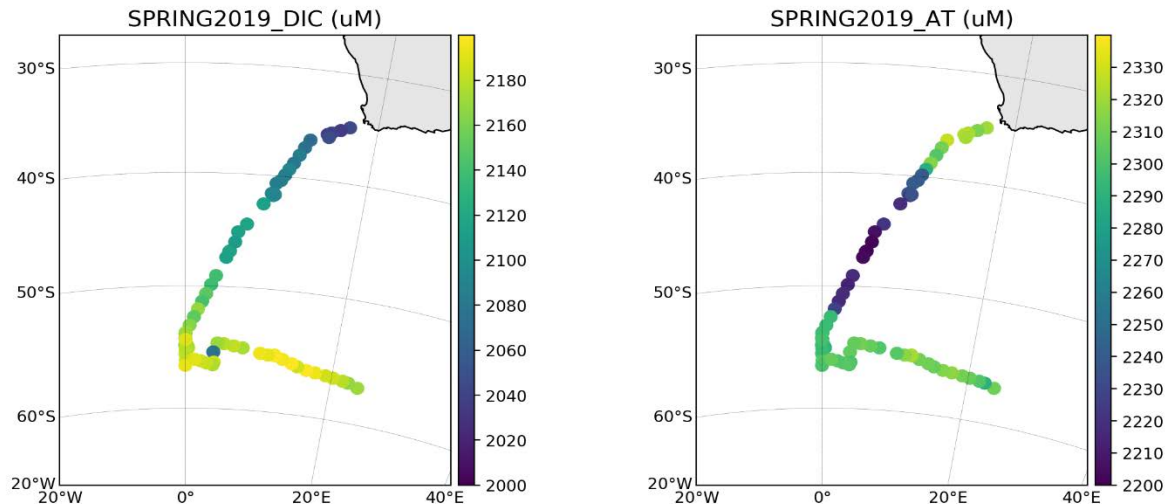


Figure 2.2.3. Shows the raw Dissolved Inorganic Carbon ( $\mu\text{mol/kg}$ ) and Total Alkalinity ( $\mu\text{mol/kg}$ ) of surface water samples collected underway along the ship's track.

### 2.2.5. DIC/AT from CTD samples

#### Marginal ice zone transect (MIZ)

Figure 2.2.4 shows preliminary results of the DIC and AT on the MIZ transect. The results show that both DIC and AT on the marginal ice zone increased with depth. DIC falling between 2177  $\mu\text{mol/kg}$  and 2220  $\mu\text{mol/kg}$  was found between the surface and 100 m depth. DIC values between 100 m to 500 m depth ranged from 2220  $\mu\text{mol/kg}$  to 2730

$\mu\text{mol/kg}$ . AT also increased with depth. The AT above 100 m ranged from 2294 to 2330  $\mu\text{mol/kg}$ . The AT ranged between 2330 to 2361  $\mu\text{mol/kg}$  between 100 m and 500 m depth.

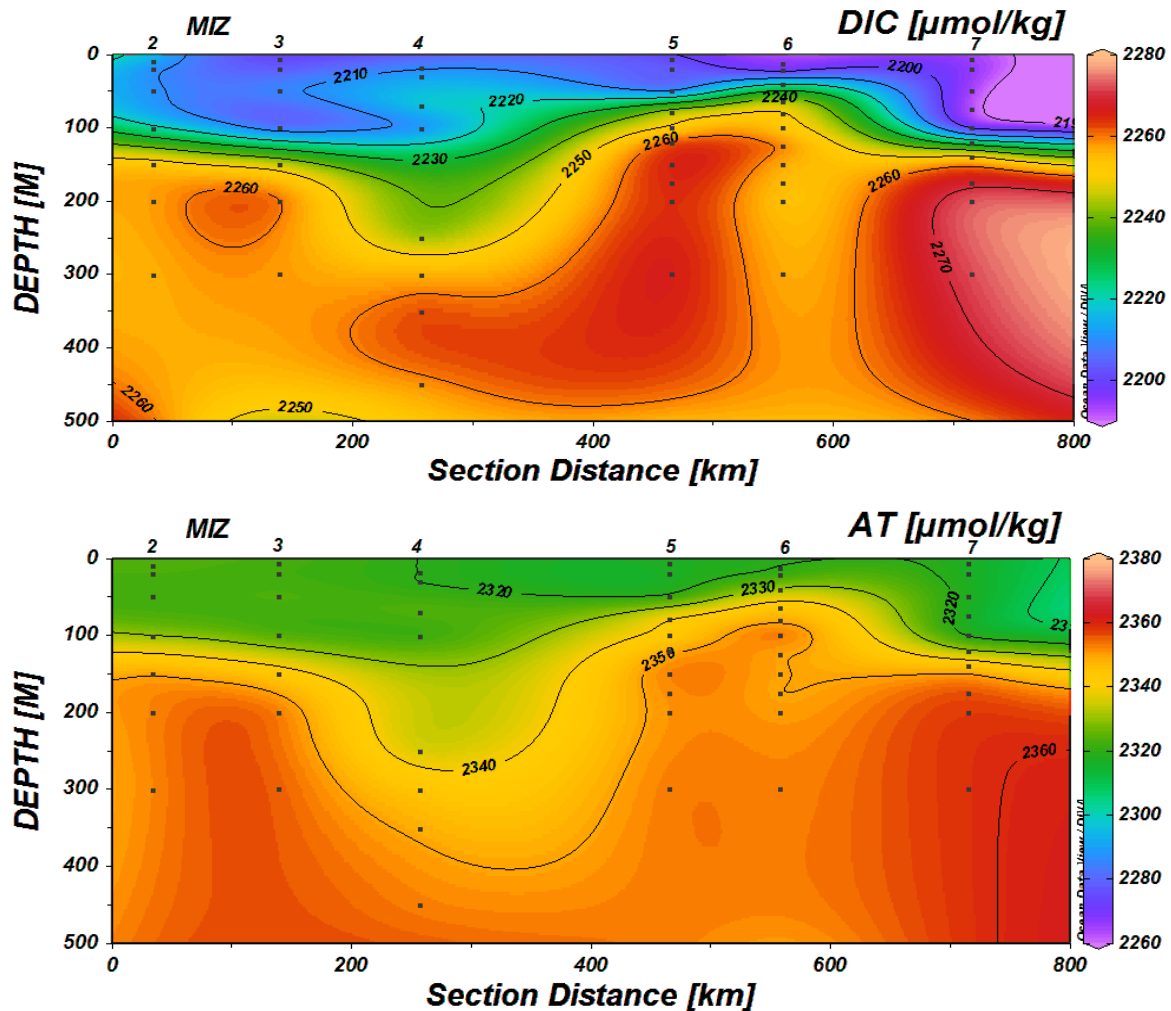


Figure 2.2.4. DIC/AT on the marginal ice zone transect.

### 2.2.6. GoodHope Transect

DIC/AT samples on the GT transect were collected from all 24 CTD bottles immediately after oxygen was sampled. Preliminary results show that DIC ranged from 2079 to 2263  $\mu\text{mol/kg}$ . High values were found below 100m meters in the marginal ice zone. The high DIC observed in the marginal ice zone extended to 100 m below surface to the bottom of the ocean. A layer of high DIC extended northwards from the marginal ice zone between 1000 m and 2000 m. The extension of high DIC from the marginal ice zone was also observed in the bottom layer. AT decreased with depth from surface to the bottom layer with values ranging from 2263 to 2371  $\mu\text{mol/kg}$ .

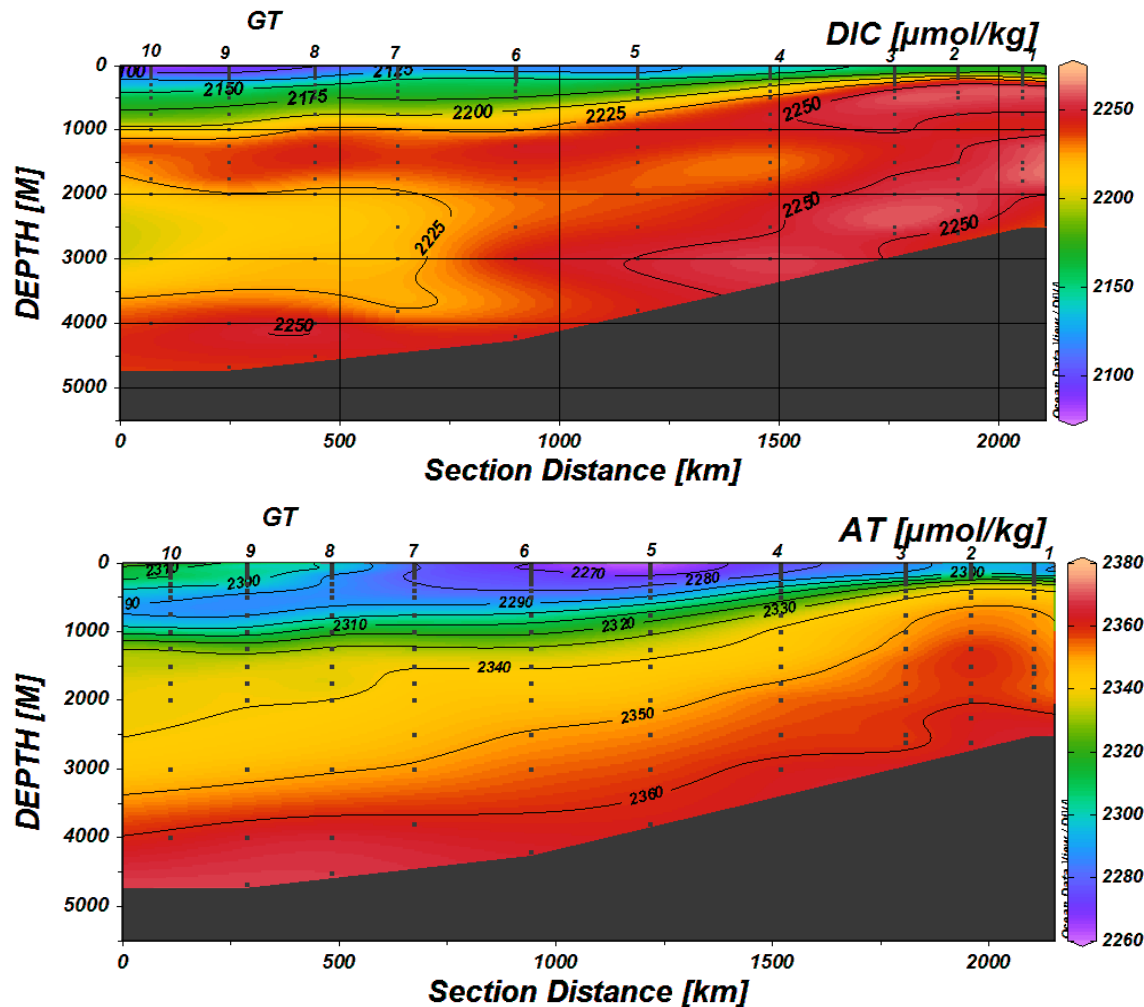


Figure 2.2.5. GT transect DIC and AT.

### 2.2.7. Accuracy

Accuracy of the VINDTA was determined by running a Dickson's CRMs before and after each batch of about 20 samples. CRMs batch number 159 and 183 were used during this voyage. A factor derived from the CRMs given values and measured values will be used to correct the DIC and AT values obtained.

### 2.2.8. Precision

The precision (Table 2.2.1) was checked by taking 8 samples from the same CTD niskin bottle closed at 10 m depth. Preliminary results show that the standard deviation for DIC and AT was  $\pm 3.07 \mu\text{mol/kg}$  and  $\pm 0.57 \mu\text{mol/kg}$ , respectively. A highly impressive precision for AT was achieved. The precision for DIC may be improved to fall within  $\pm 2 \mu\text{mol/kg}$  when further data processing is performed. DIC and AT of 12 underway samples (Table 3) collected for the calibration of the Wave Glider gave a standard deviation that falls within  $\pm 2 \mu\text{mol/kg}$  for both DIC and AT.

CTD samples at 10m depth						
Date	Type	bottle	Lat.	Long.	CT	AT
2019-11-09	CTD	CTD20191109171	-54	0	2134,01	2293,15
2019-11-09	CTD	CTD20191109172	-54	0	2137,21	2292,99
2019-11-09	CTD	CTD20191109173	-54	0	2141,37	2291,58
2019-11-09	CTD	CTD20191109174	-54	0	2137,41	2292,7
2019-11-09	CTD	CTD20191109175	-54	0	2144,06	2292,73
2019-11-09	CTD	CTD20191109176	-54	0	2140,67	2292,86
2019-11-09	CTD	CTD20191109177	-54	0	2137,86	2293,5
2019-11-09	CTD	CTD20191109178	-54	0	2139,1	2292,38
				<b>Average</b>	2138,96	2292,74
				<b>STDev</b>	3,07	0,57

Table 2.2.1. Repeated measurements of seawater samples taken from the same niskin bottle for assessing precision.

### 2.2.9. Bacterial respiration on underway pCO<sub>2</sub> measurements

CO<sub>2</sub> measurements from surface seawater line may be impacted by oxygen removal due to respiration. Underway seawater lines on research vessels may have oxygen deficits up to 2% when compared to CTD niskin bottles (Jarunek et al., 2010). To assess the effects of respiration on our underway pCO<sub>2</sub> measurements, 8 DIC/AT samples collected from the same niskin bottle closed at 10 m depth were compared with samples collected from the underway seawater supply. This was achieved by keeping the CTD at 10 m for half a minute and take 4 samples from the underway seawater supply before the niskin CTD bottle was closed and 4 more samples immediately after the bottle was closed. Table 1 shows that the difference underway samples and CTD samples was 1.7 µmol/kg and 0.86 µmol/kg for DIC and AT respectively. These differences between the two show that respiration may have contributed about 1.7 µmol/kg of DIC to our underway pCO<sub>2</sub> measurements.

Samples from the underway pCO <sub>2</sub> system laboratory						
Date	Type	bottle	Lat.	Long.	DIC (µM)	AT (µM)
2019-11-09	Underway	pCO220191109163	-54	0	2135,01	2294,05
2019-11-09	Underway	pCO220191109164	-54	0	2139,71	2294,64
2019-11-09	Underway	pCO220191109165	-54	0	2142,41	2293,18
2019-11-09	Underway	pCO220191109166	-54	0	2147,53	2294,71
2019-11-09	Underway	pCO220191109167	-54	0	2138,54	2293,91
2019-11-09	Underway	pCO220191109168	-54	0	2141,89	2292,78
2019-11-09	Underway	pCO220191109169	-54	0	2138,33	2292,95
2019-11-09	Underway	pCO220191109170	-54	0	2141,84	2292,58
				<b>Average</b>	2140,66	2293,60
				<b>STDev</b>	3,70	0,84

CTD samples at 10m depth						
Date	Type	bottle	Lat.	Long.	CT	AT
2019-11-09	CTD	CTD20191109171	-54	0	2134,01	2293,15
2019-11-09	CTD	CTD20191109172	-54	0	2137,21	2292,99
2019-11-09	CTD	CTD20191109173	-54	0	2141,37	2291,58
2019-11-09	CTD	CTD20191109174	-54	0	2137,41	2292,7
2019-11-09	CTD	CTD20191109175	-54	0	2144,06	2292,73
2019-11-09	CTD	CTD20191109176	-54	0	2140,67	2292,86
2019-11-09	CTD	CTD20191109177	-54	0	2137,86	2293,5
2019-11-09	CTD	CTD20191109178	-54	0	2139,1	2292,38
				<b>Average</b>	2138,96	2292,74
				<b>STDev</b>	3,07	0,57

Table 2.2.2. Comparison of the CTD samples taken at 10m depth and from the underway pCO<sub>2</sub> system laboratory.

### 2.2.10. Wave glider calibration samples

A Wave Glider with a pCO<sub>2</sub> sensor was deployed during this voyage at latitude 47 °S. DIC/AT samples were collected from the underway seawater supply in the bio-lab where the TSG is placed from the calibration of the pCO<sub>2</sub> sensor. The vessel made two circles around the glider. Six samples were collected when the vessel was making a small circle around the glider and six more samples when the vessel was making a bigger circle around the glider. An average of 2089,21 µmol/kg and 2255,92 µmol/kg was obtained for DIC and AT, respectively. The precision was 1,86 µmol/kg and 1,10 µmol/kg for DIC and AT, respectively.

Date	Cycle	Sample	Lat.	Long.	DIC (uM)	AT (uM)
2019-10-17	Small	WG_S17102019WG1	-46,98	5,19	2087,18	2255,36
2019-10-18	Small	WG_S17102019WG23	-46,98	5,19	2086,66	2254,08
2019-10-19	Small	WG_S17102019WG24	-46,98	5,19	2090,84	2255,68
2019-10-20	Small	WG_S17102019WG25	-46,98	5,19	2091,3	2256,66
2019-10-21	Small	WG_S17102019WG26	-46,98	5,2	2087,69	2257
2019-10-22	Small	WG_S17102019WG27	-46,98	5,21	2088,26	2256,68
2019-10-23	Big	WG_B17102019WG28	-46,99	5,29	2091,46	2256,76
2019-10-24	Big	WG_B17102019WG29	-46,99	5,29	2088,44	2257,46
2019-10-25	Big	WG_B17102019WG30	-46,99	5,28	2087,78	2255,09
2019-10-26	Big	WG_B17102019WG31	-46,99	5,28	2091,22	2254,71
2019-10-29	Big	WG_B17102019WG34	-46,99	5,29	2091,39	2256,79
2019-10-30	Big	WG_B17102019WG2	-46,99	5,29	2088,27	2254,74
				<b>Average</b>	2089,21	2255,92
				<b>STDev</b>	1,86	1,10

Table 2.2.3. DIC/AT samples from the underway seawater supply for calibration of the Wave glider.

Date	Station		Lat.	Long.	Max depth (m)	Sounding (m)
2019-10-16	SAZ-2	AM01116	45° 00.009'S	6° 36.002'E	1000	4288.51
2019-10-19	PUZ		54° 00.205'S	00° 00.187'E	1000	2396.93
2019-10-20	MIZ0a	AM01119	55° 00.067'S	00° 00.027'E	1000	1724.0
2019-10-23	MIZ1b	AM01122	57° 54.384'S	00° 00.793'E	500	4104.96
2019-10-24	MIZ2	AM01123	59° 18.654'S	00° 05.187'E	500	5156.35
2019-10-24	MIZ3	AM01124	58° 58.532'S	00° 01.329'E	500	4217.0
2019-10-27	MIZ4	AM01125	59° 00.005'S	03° 01.056'E	500	5321.79
2019-10-28	MIZ5	AM01126	59° 17.147'S	06° 36.520'E	500	5208.58
2019-10-29	MIZ6	AM01127	59° 20.2231'S	08° 10.705'E	500	?
2019-10-30	MIZ7	AM01128	59° 28.366'S	10° 53.272'E	500	?
2019-11-01	MIZ8	AM01129	58° 32.908'S	17° 56.344'E	500	5091.77
2019-11-03	MIZ9	AM01130	58° 26.114'S	21° 59.522'E	500	5171.52
2019-11-04	WS1	AM01131	51° 09.097'S	23° 59.685'E	1000	4249.0
2019-11-06	WS2	AM01133	55° 26.668'S	11° 57.884'E	1000	4831.0
2019-11-06	WS3	AM01134	55° 00.048'S	06° 59.828'E	1000	2890.64
2019-11-08	GT 01	AM01135	55° 54.658'S	00° 11.064'E	500	3159.78
2019-11-09	GT02	AM01136	54° 00.011'S	00° 00.021'E	2399	2523.0
2019-11-10	GT02b	AM01137	52° 42.060'S	00° 00.015'E	2605	2702.57
2019-11-10	GT03	AM01138	51° 23.981'S	00° 00.034'E	2606	2689.5
2019-11-11	GT04	AM01139	49° 18.102'S	002° 18.159'E	3800	3943.60
2019-11-12	GT05	AM01140	47° 00.016'S	04° 30.002'E	3800	3955.97
2019-11-13	GT06	AM01141	42° 59.917'S	08° 30.470'E	3804	3921.18
2019-11-14	GT07	AM01142	44° 59.533'S	06° 36.419'E	4200	4272.0
2019-11-16	GT07b	AM01143	41° 30.705'S	09° 37.761'E	4509	4621.06
2019-11-16	GT08	AM01144	40° 00.029'S	10° 48.099'E	4678	4739.14
2019-11-17	GT09	AM01145	38° 36.156'S	011° 47.973'E	5001	5110.53
2019-11-18	GT10	AM01146	36° 18.028'S	13° 17.984'E	4667	4832.0

Table 2.2.4. CTD stations where DIC/AT samples were taken.

### 2.2.11. References

Pierrot, D., Neil, Sullivan, C. K., Castle, R., Wanninkhof, R., Luger, H., Johannessen, T., Olsen, A., Feely R. A., Cosca, C. E., Recommendations for autonomous underway pCO<sub>2</sub> measuring systems and data-reduction routines. *Deep Sea-Res.*, 56(2009), pp. 512-522.

Juranek, L. W., Hamme, R. C., Kaiser, J., Wanninkhof, R., and Quay, P. D.: Evidence of O<sub>2</sub> consumption in underway seawater lines: Implications for air-sea O<sub>2</sub> and CO<sub>2</sub> fluxes, *Geophys. Res. Lett.*, 37, L01601, doi:10.1029/2009GL040423, 2010.

### 3. TEAM DMS

#### 3.1. Winter Cruise

##### 3.1.1. Objective

The goal of this study is to evaluate oceanic trace gas concentrations during winter time in the highly undersampled Southern Ocean and find a direct link between biogenic trace gas emissions of dimethyl sulfide (DMS) as well as isoprene and aerosols. In this respect, the Southern Ocean is especially interesting, as it can serve as a natural laboratory to study the connection between naturally produced marine trace gases and aerosol effects, as the influence of anthropogenic produced aerosol precursors is comparably small. On the other hand, the Southern Ocean is predicted to be strongly influenced by climate change (IPCC, 2013) and thus provides a potential setting for feedback mechanisms between trace gases and climate effects. Furthermore, model studies predict high emissions of DMS and isoprene in the Southern Ocean (Lana et al., 2011, Booge et al., 2016), however, the data feeding these models is very sparse in this region. In order to increase the certainty of the surface ocean DMS measurements over a large temperature and concentration gradient, measurements using two different system setups were made of this study. Additionally, this study investigates the DMS production of carbonyl sulfide (OCS) and should validate if the Southern Ocean serves as an OCS hotspot also during winter time (Lennartz et al., 2017).

##### 3.1.2. Methods

An overview of all measured compounds and instrumentation is given in Table 3.1.1.

Aerosol sampler: Daily integrated aerosol measurements (e.g. methanesulfonic acid (MSA), non-sea-salt sulfate (nss-SO<sub>4</sub><sup>2-</sup>) using glass fiber filters and a high-volume bulk sampler (Model M241, University of Miami) were performed from the ship's monkey bridge. A total of 18 sample filters were collected during the cruise. The detailed sampling and measurement methods can be found in Zhang et al. (2015). The analysis of the 18 daily integrated filter samples will be done within the next weeks in the TIO laboratory using a Dionex ICS-2500 ion chromatograph (IC).

LGR OCS Analyzer: Continuous measurements for OCS/CO<sub>2</sub>/CO were carried out in the air (air inlet in front of the bridge) and in the surface water using the ship's underway pump. The one hourly time interval was set to 50 min of water measurements and 10 min of air measurements.

TOF-MS system: Continuous DMS measurements in the air and in the surface water using the ship's underway pump were performed using a home-made purge and trap sampler coupled with a time of flight mass spectrometer system. The seawater and air supply were continuously introduced into the sampler unit and subsampled every 10 min. Throughout the cruise the limit of detection of DMS in seawater and air was found to be

70 pmol L<sup>-1</sup> and 32 pptv, respectively. The detailed method is described in Zhang et al. (2019).

**GC-MS system:** Hourly discrete seawater samples were taken from the ship's underway pump and concentrations of DMS, isoprene and carbonyl sulfide (CS<sub>2</sub>) were measured using a gas chromatograph-mass spectrometer (GC-MS). Measurement technique is described in detail in Booge et al. (2018). Additionally, samples for dimethylsulfoniopropionate (DMSP), the precursor of DMS, and dimethyl sulfoxide (DMSO) the oxidation product of DMS were taken every 2 hours and will be analysed in the GEOMAR based laboratories using the GC-MS. Additionally, samples for all mentioned compounds were also taken during 9 CTD stations (see Table 3.1.2).

Additional seawater from the ship's underway pump, as well as from 9 different CTD stations (Table 3.1.2), was taken for analysis of chromophoric/fluorescent dissolved organic matter (C/FDOM) on a two to four-hourly basis. Filtered samples were kept at ~4°C and the analysis for CDOM and FDOM will be done in the GEOMAR based laboratories after the cruise using a UV-VIS double-beam spectrophotometer and a 3D-EEM fluorescence spectrophotometer, respectively.

Table 3.1.1: Overview of measured compounds and analytical techniques.

Instrumentation		Compounds
Dionex ICS-2500 IC		MSA, nss-SO <sub>4</sub> <sup>2-</sup>
LGR OCS Analyzer		OCS <sub>air</sub> , OCS <sub>water</sub>
TOF-MS		DMS <sub>air</sub> , DMS <sub>water</sub>
GC-MS		DMS <sub>water</sub> , isoprene <sub>water</sub> , CS <sub>2water</sub> , DMSP/O <sub>water</sub>
UV-VIS spectrophotometer	double-beam	CDOM
3D-EEM spectrophotometer	fluorescence	FDOM

Table 3.1.2: Overview of measured compounds (DMS, DMSP/O, isoprene, CS<sub>2</sub>, C/FDOM) from different CTD stations and depths.

Station	Depth [m]								
	5	20	50	75	90	100	125	150	300
GT1		X	X	X	X		X	X	X
MIZ1A (MIZ1s)	X	X	X	X		X	X	X	
MIZ2A		X	X	X		X	X	X	
GT2		X	X	X		X	X	X	X
GT3		X	X	X		X	X	X	X
GT5	X	X	X	X		X	X	X	X
GT6	X	X	X	X		X	X	X	X
GT7		X	X	X		X	X	X	X
GT9	X	X	X	X		X	X	X	X

### 3.1.3. Preliminary results

First preliminary results of the measured trace gases in the surface ocean show a decreasing concentration gradient with decreasing temperature and increasing latitude. Concentrations were almost close to zero within the marginal ice zone. DMS mean surface concentrations were  $0.7 \pm 0.5 \text{ nmol L}^{-1}$  with highest concentrations measured in the coastal region between Cape Town and East London with up to  $4 \text{ nmol L}^{-1}$  (Fig. 3.1.1b). Isoprene and  $\text{CS}_2$  seawater concentrations showed also highest values in the coastal area similar to DMS with values up to  $40 \text{ pmol L}^{-1}$  and  $60 \text{ pmol L}^{-1}$  for isoprene and  $\text{CS}_2$  (Fig. 3.2), respectively. The atmospheric DMS distribution was slightly different to the seawater distribution not showing the extensive increase in the coastal area. The mean air mixing ratio was  $25 \pm 19 \text{ pptv}$  and showed significant variations over the whole cruise track in the Southern Ocean (Fig. 3.1.1a). Preliminary results show that oceanic DMS concentrations derived by the intercalibration between discrete GC-MS and continuous TOF-MS measurements are in very good agreement.

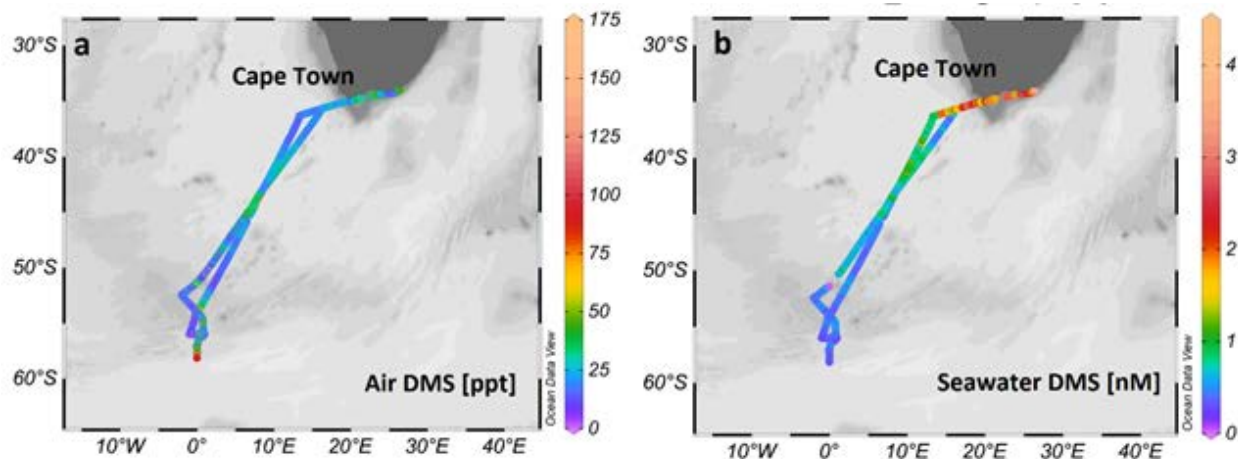


Figure 3.1.1: Distribution of DMS air mixing ratio (a) and DMS seawater concentrations (b) along the cruise track during winter cruise of SCALE.

Atmospheric OCS data are mostly within the expected range (400-500 ppt) and seawater OCS is significantly supersaturated at lower latitudes (mainly beginning of the cruise and in coastal areas) due to photoproduction in the ocean. At higher latitudes OCS is only slightly or not supersaturated as photoproduction is close to zero during winter times in the Southern Ocean (Fig. 3.1.2).

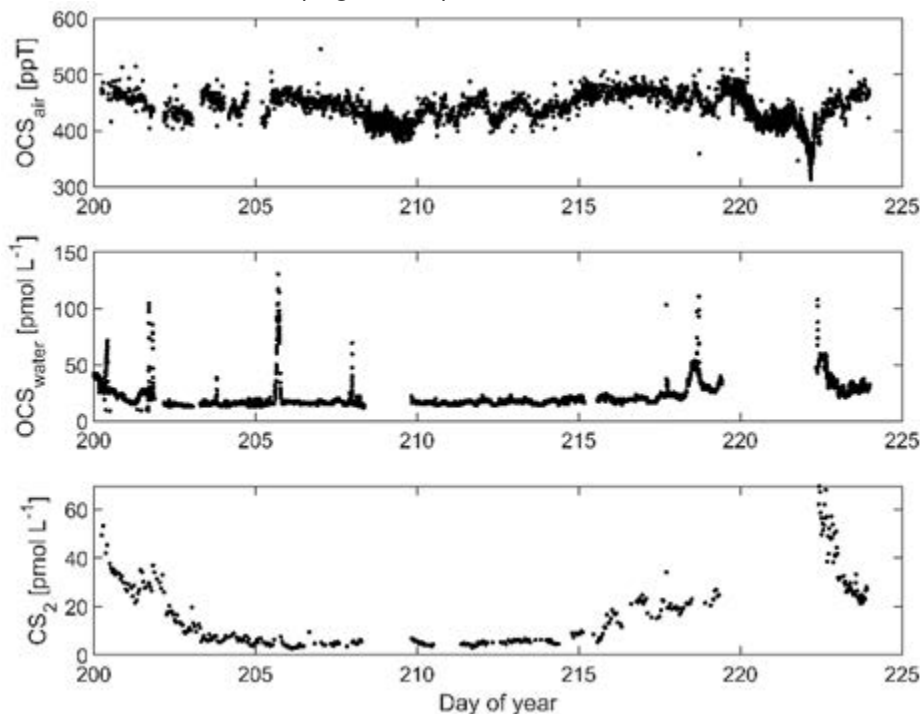


Figure 3.1.2: Distribution of OCS air mixing ratio (top), OCS seawater concentration (middle) and  $CS_2$  seawater concentration (bottom) over day of year during winter cruise of SCALE.

After finalisation of sample analysis and data work up, this data set will be an important contribution of winter data (first ever reported winter time data for oceanic isoprene measurements in the Southern Ocean) in order to understand biogenic trace gas cycling and will serve as crucial model input data for the Southern Ocean.

### 3.1.4. References

Booge, D., Marandino, C. A., Schlundt, C., Palmer, P. I., Schlundt, M., Atlas, E. L., Bracher, A., Saltzman, E. S. und Wallace, D. W. R. (2016) *Can simple models predict large scale surface ocean isoprene concentrations?* Open Access Atmospheric Chemistry and Physics, 16. pp. 11807-11821.

Booge D., C. Schlundt, A. Bracher, S. Endres, B. Zäncker, and C. Marandino (2018) *Marine isoprene production and consumption in the mixed layer of the surface ocean – a field study over two oceanic regions.* Biogeosciences (BG), 15. pp. 649-667.

IPCC, 2013: *Climate Change 2013: The Physical Science Basis. Contribution of Working Group I to the Fifth Assessment Report of the Intergovernmental Panel on Climate Change* [Stocker, T.F., D. Qin, G.-K. Plattner, M. Tignor, S.K. Allen, J. Boschung, A. Nauels, Y. Xia, V. Bex and P.M. Midgley (eds.)]. Cambridge University Press, Cambridge, United Kingdom and New York, NY, USA, 1535 pp, doi:10.1017/CBO9781107415324.

Lana, A., T. Bell, R. Simó, S. M. Vallina, J. Ballabrera-Poy, A. Kettle, J. Dachs, L. Bopp, E. Saltzman, and J. Stefels (2011), *An updated climatology of surface dimethylsulfide concentrations and emission fluxes in the global ocean*, Global Biogeochemical Cycles, 25, GB1004.

Lennartz, S. T., C. A. Marandino, M. von Hobe, P. Cortes, B. Quack, R. Simo, D. Booge, et al., *Direct Oceanic Emissions Unlikely to Account for the Missing Source of Atmospheric Carbonyl Sulfide.*, Atmos. Chem. Phys. 17, no. 1 (2017): 385-402.

Zhang, M., L. Chen, G. Xu, Q. Lin, and M. Liang (2015), *Linking phytoplankton activity in polynya and sulfur aerosols at Zhongshan station, East Antarctica*, Journal of the Atmospheric Sciences, edited, pp. 4629-4642.

Zhang, M., W. Gao, J. Yan, Y. Wu, C. A. Marandino, K. Park, L. Chen, Q. Lin, G. Tan, and M. Pan (2019), *An integrated sampler for shipboard underway measurement of dimethyl sulfide in surface seawater and air*, Atmospheric Environment, 209, 86-91.

## 3.2. Spring Cruise

### 3.2.1. Key objectives

To understand and quantify the production of aerosols derived from marine biogenic trace gas emissions in the Southern Ocean.

### 3.2.2. Operational setup

The mini Atmospheric Pressure Chemical Ionisation Mass Spectrometer (API-CIMS) measurement system, herein 'mini-CIMS' (Saltzman et al., 2009) is a relatively new system that achieves a detection limit of 0.1 nM, whilst providing a compact machine setup solution that can run continuously for long-periods at sea and has near-autonomous operation.

A new segmented flow coil equilibrator (SFCE) setup has been developed to extract DMS from seawater, which includes new techniques and a variety of those that have previously been applied (Blomquist et al., 2017; Saltzman et al., 2009; Wohl et al., 2019; Xie et al., 2001). Important features of the new SFCE are the relatively high flow rates it can achieve (both water and air at  $\geq 200 \text{ mL min}^{-1}$ ), and that equilibrium between water and air is not required due to the introduction of an isotopically-labelled d3-DMS liquid standard in the water flow prior to equilibration.

When in full operation, the coupled segmented flow coil equilibrator (SFCE) and mini-CIMS system is almost completely automated (including flow rates, valve switching, and data logging) and runs continuously. The automated system was paused every 12 hours to change the working standard.

### **3.2.2.1. New segmented flow coil equilibrator (SFCE)**

The SFCE (shown in Fig. 3.2.1) is almost entirely made from Perfluoroalkoxy (PFA) tubing and fittings. PFA is chemically unreactive and suffers minimal adsorptive loss. On the spring cruise The SFCE utilised seawater directly from the ship's underway water pumping system, coupled with synthetic air introduced from a compressed gas source (zero air generator & compressor). Issues were experienced with underway system pressure, and thus flow rate, due to heavy usage by a number of teams onboard. Despite being potentially problematic, this pressure fluctuation did not interfere with the integrity of continuous DMS measurement. Water from the underway system was used to continually over-fill a 500 mL sampling bottle, from which water was then extracted at  $200 \text{ mL min}^{-1}$  into the SFCE using a peristaltic pump. Discrete samples (5 L seawater containers or ice/snow bags) were extracted using the peristaltic pump in exactly the same way.

For seawater (discrete & continuous underway) sampling, an internal liquid working standard containing ethanol and isotopically-labelled deuterated DMS (d3-DMS) is continuously injected into the seawater flow via syringe pump at a fixed flow rate, to deliver a known concentration (set at 4.08 nM) of d3-DMS. DMS ( $\text{CH}_3\text{SCH}_3$ ) has a molecular mass of 62 atomic mass units (amu) before ionisation, and 63 amu afterwards, due to the gaining of a proton. Deuterated DMS ( $\text{CD}_3\text{SCH}_3$ ) has a molecular mass of 65 and 66 amu, before and after ionisation. The difference in molecular mass is key to distinguishing between the isotopic and non-isotopic DMS signals which is ultimately needed to later calculate the ambient seawater DMS concentration. Ice and snow samples were injected with a fixed volume of working standard prior to melting, to ensure the comparability of any losses in DMS and d3-DMS during the melting process. For these ice and snow samples, use of the working standard syringe pump was therefore not required.

In the equilibrator, the seawater flow containing both DMS and d3-DMS is met at a T-section with a flow of synthetic air, mass flow controlled at 400 mL min<sup>-1</sup>. The downstream flow naturally forms distinct segments of air and water. The segmented flow presents a large surface area for the exchange of gas and there is sufficient time for the almost-complete equilibration while it passes through the 5 m coil of PFA tubing. The introduction of an isotopically labelled liquid standard at a known concentration means that complete equilibration of DMS and d3-DMS is not required. The ratio of DMS to d3-DMS is used to calculate the seawater DMS concentration, based on the average blank-corrected mass spectrometer ion current (A) signals recorded at mass/charge (m/z) ratio 63 and 66, for protonated DMS (S<sub>63</sub>) and d3-DMS (S<sub>66</sub>), respectively, as follows

$$\text{DMS}_{\text{sw}} = \frac{S_{63}}{S_{66}} \cdot \frac{F_{\text{std}}}{F_{\text{sw}}} \cdot C_{\text{std}} \quad (1)$$

where F<sub>std</sub> = d3-DMS liquid standard syringe pump flow rate (mL min<sup>-1</sup>), F<sub>sw</sub> = seawater flow rate (mL min<sup>-1</sup>) and C<sub>std</sub> = d3-DMS liquid standard concentration (nM) (Bell et al., 2013).

After passing through the equilibrator, the segmented flow is separated at a 12.7 mm ID vertical T-section which allows the water to drain downwards and fill a S-shaped sump section, and the sample gas to fill the remaining head space and flow up toward the mass spectrometer. A valve restricting water drainage maintains back-pressure on the S-shaped water sump, which prevents sample air escaping with the water, or lab air compromising the system via the drain/sump. Before entering the mini-CIMS, sample air is passed through a Nafion dryer to remove the majority of the water vapour and increase analytical sensitivity to DMS.

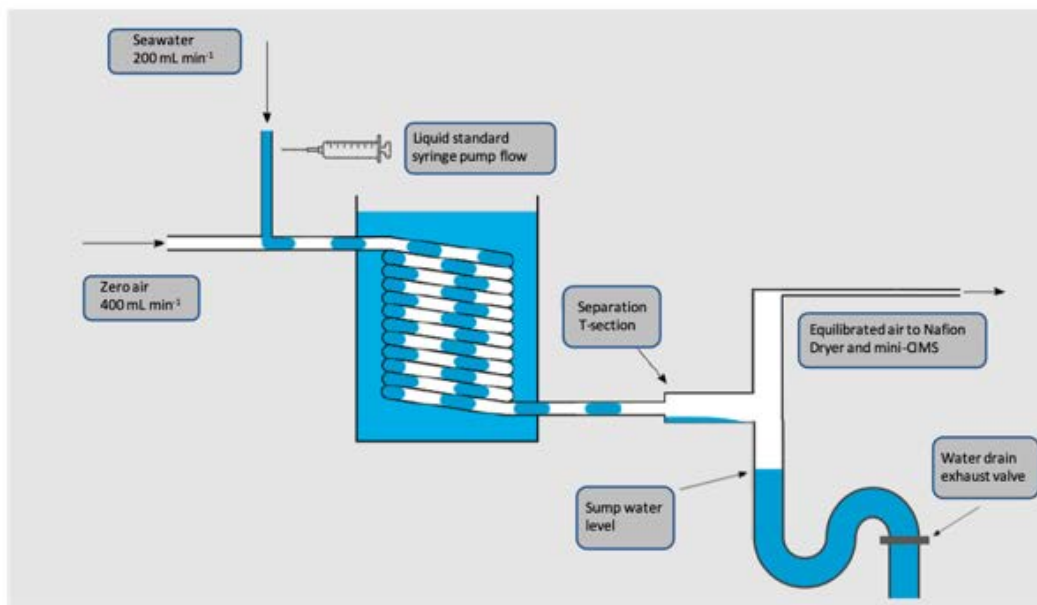
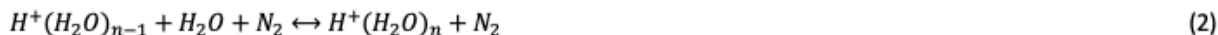


Fig. 1 – Modified & simplified schematic of a segmented flow coil equilibrator (SCFE) used by Wohl et al. (2019)

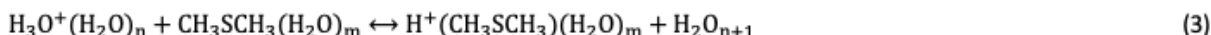
### 3.2.2.2. Mini-CIMS

Once DMS is equilibrated from the seawater supply into a synthetic air stream, this air stream enters the mini-CIMS and is passed through a glass-lined steel tube wrapped in

a  $^{63}\text{Ni}$  foil and a heating coil controlled by a thermocouple-PID temperature controller. Chemical ionisation by the  $^{63}\text{Ni}$  beta particles leads to the formation of protonated water ions and ion clusters,  $(\text{H}_2\text{O})_n\text{H}^+$ , which are simultaneously energised and de-clustered by heating to  $\sim 300^\circ\text{C}$ .



The shift in equilibrium charge distribution to favour lower-order water clusters (i.e.  $n = 0, 1, 2$ ) with lower proton affinities is achieved through heating, and this increases the availability of  $\text{H}^+$  for the ionisation of DMS ( $\text{CH}_3\text{SCH}_3$ ). DMS is ionised via proton transfer from Hydronium ion ( $\text{H}_3\text{O}^+$ ) and its hydrates, where  $n$  and  $m$  indicate the number of water molecules, given by



After passing through the heated radioactive source region at atmospheric pressure (1 atm = 760 Torr), the sample gas is drawn through a small orifice (250  $\mu\text{m}$  diameter) into a low pressure ( $\sim 1$  Torr) region. Water vapour clusters are broken up via collision and charge is transferred to the DMS molecules. The charged ions are steered through a series of increasingly negatively charged foil lenses and focussed into an even lower pressure region ( $\sim 10^{-5}$  Torr). In the low-pressure chamber, ions are electrostatically steered and mass filtered by the mass spectrometer quadrupoles and detected by an electron multiplier.

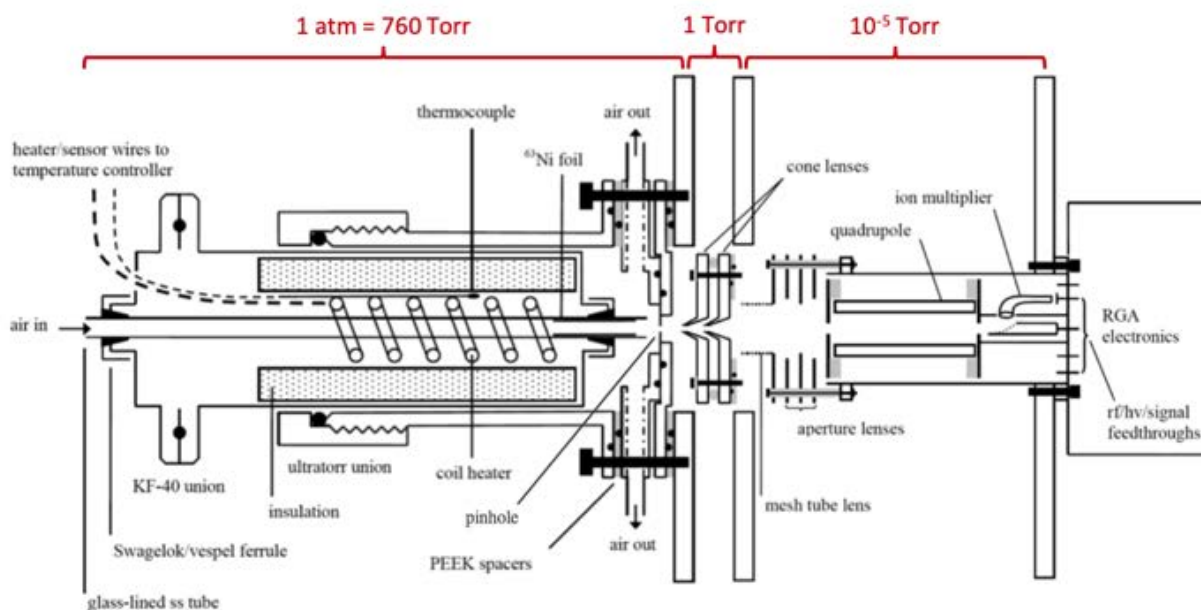


Fig. 2 – Modified schematic of the  $^{63}\text{Ni}$  ion source region, collision chamber and high vacuum region with quadrupole mass spectrometer and ion multiplier in the mini-CIMS instrument used by Saltzman et al. (2009). N.B. This is not exactly the same as the mini-CIMS used at the PML, but provides a conceptual visualisation of the process involved CIMS operation. The division of sections (in red) indicates the pressure regions in the PML mini-CIMS, which differs from the instrument used by Saltzman et al. (2009).

### 3.2.3. Data collection

During the SCALE spring cruise, both discrete and high-resolution continuous underway seawater DMS measurements were made, using the SFCE and mini-CIMS system. Table 1 provides a full overview of all stations and depths at which discrete samples of sub-surface water were collected from CTD niskin bottle casts. Ten ice core samples and three snow samples were also collected across six stations and were analysed for DMS using a new novel vacuum-sealed bagging and melting technique. Continuous underway sampling was operational between 18/10/19 and 18/11/19. Continuous samples were not collected when the underway system was switched off when ice density became too high (22/10/19 to 03/11/19). During this period, only discrete samples were collected and measured (see Table 3.2.1).

**Table 3.2.1.** Summary of discrete samples collected and processed for DMS and DMSP analysis during the SCALE Spring cruise 2019. Each 'Y' green box indicates a depth at which 6 L seawater was sampled from niskins. Blue boxes indicate how many ice core and/or snow samples were collected. Grey box outline indicates the period during which the underway system was switched off.

DATE	STATION	ICE / SNOW	5 (m)	10 (m)	20 (m)	40 (m)	50 (m)	60 (m)	75 (m)	80 (m)	100 (m)	125 (m)	150 (m)	160 (m)	175 (m)	200 (m)	250 (m)	300 (m)
16/10	SAZ2		Y		Y		Y		Y									
19/10	PUZ		Y		Y		Y		Y				Y					Y
20/10	MIZ0a		Y		Y		Y		Y				Y					Y
23/10	MIZ1b				Y		Y		Y									
24/10	MIZ2	x2 ice			Y		Y		Y									
24/10	MIZ3	x1 ice	Y		Y		Y		Y							Y		
27/10	MIZ4		Y				Y		Y		Y				Y	Y		
28/10	MIZ5		Y				Y			Y	Y				Y	Y		
29/10	MIZ6	x3 ice	Y			Y				Y	Y		Y			Y		
30/10	MIZ7	x1 ice x3 snow	Y		Y		Y		Y		Y				Y	Y		
01/11	MIZ8	x1 ice	Y				Y		Y		Y				Y	Y		
03/11	MIZ9	x2 ice	Y				Y		Y		Y				Y	Y		
04/11	WS1		Y				Y		Y		Y				Y		Y	
06/11	WS2		Y				Y		Y		Y				Y		Y	
07/11	WS3		Y				Y		Y		Y				Y		Y	
09/11	GT1		Y				Y		Y		Y	Y			Y			
09/11	GT2		Y	Y	Y			Y			Y	Y	Y		Y			
10/11	GT2b		Y	Y	Y			Y			Y	Y	Y		Y			
10/11	GT3		Y	Y	Y			Y			Y	Y	Y		Y			
11/11	GT4		Y	Y	Y			Y			Y	Y	Y		Y			
12/11	GT5		Y	Y	Y			Y			Y	Y	Y		Y			
14/11	GT7		Y	Y	Y			Y			Y	Y		Y	Y			
15/11	GT6		Y	Y	Y			Y			Y	Y		Y	Y			
16/11	GT7b		Y	Y	Y			Y			Y	Y		Y	Y			
17/11	GT8		Y	Y	Y			Y			Y	Y	Y		Y			
17/11	GT9		Y	Y	Y			Y			Y	Y	Y		Y			
18/11	GT10		Y	Y	Y			Y			Y	Y	Y		Y			

### 3.2.4. Results

Results are not available yet as data is currently being processed at the University of Exeter & PML.

### 3.2.5. Acknowledgements

We thank Chief Scientists Tommy Ryan-Keogh, Marcello Vichi and Sandy Thomalla for their hard work in co-ordinating and executing such a successful SCALE spring cruise. Thanks also to the ice team for accommodating and facilitating last-minute requests from us at the MIZ stations, to all other teams for their enthusiasm and co-operation both in and out of the labs throughout the cruise, and to the captain and all crew of the S.A. Agulhas II for their hard work in ensuring a safe and productive journey.

### 3.2.6. References

Bell, T.G., De Bruyn, W., Miller, S.D., Ward, B., Christensen, K., Saltzman, E.S., 2013. Air-sea dimethylsulfide (DMS) gas transfer in the North Atlantic: Evidence for limited interfacial gas exchange at high wind speed. *Atmos. Chem. Phys.* 13, 11073–11087. <https://doi.org/10.5194/acp-13-11073-2013>

Blomquist, B.W., Brumer, S.E., Fairall, C.W., Huebert, B.J., Zappa, C.J., Brooks, I.M., Yang, M., Bariteau, L., Prytherch, J., Hare, J.E., Czerski, H., Matei, A., Pascal, R.W., 2017. Wind Speed and Sea State Dependencies of Air-Sea Gas Transfer: Results From the High Wind Speed Gas Exchange Study (HiWinGS). *J. Geophys. Res. Ocean.* 122, 8034–8062. <https://doi.org/10.1002/2017JC013181>

Saltzman, E.S., De Bruyn, W.J., Lawler, M.J., Marandino, C.A., McCormick, C.A., 2009. A chemical ionization mass spectrometer for continuous underway shipboard analysis of dimethylsulfide in near-surface seawater. *Ocean Sci.* 5, 537–546. <https://doi.org/10.5194/os-5-537-2009>

Webb, E.K., Pearman, G.I., Leuning, R., 1980. Correction of flux measurements for density effects due to heat and water vapour transfer. *Q. J. R. Meteorol. Soc.* 106, 85–100. <https://doi.org/10.1002/qj.49710644707>

Wohl, C., Capelle, D., Jones, A., Sturges, W.T., Nightingale, P.D., Else, B.G.T., Yang, M., 2019. Segmented flow coil equilibrator coupled to a Proton Transfer Reaction Mass Spectrometer for measurements of a broad range of Volatile Organic Compounds in seawater. *Ocean Sci. Discuss.* 1–37. <https://doi.org/10.5194/os-2019-5>

Xie, H., Zafiriou, O.C., Wang, W., Taylor, C.D., 2001. A simple automated continuous-flow-equilibration method for measuring carbon monoxide in seawater. *Environ. Sci. Technol.* 35, 1475–1480. <https://doi.org/10.1021/es001656v>

## **4. TEAM FLUX**

### **4.1. Background**

Antarctic sea ice grows from a minimum of less than 5 million square kilometres in February to a maximum of over 17 million square kilometres in September (Parkinson 2019). This extensive seasonal cycle in surface cover has a strong influence on the dynamics and thermodynamics of the atmosphere and ocean. Sea ice cover reduces outgoing longwave radiation and convective heat exchange and also reflects incoming shortwave radiation. In winter, it acts as an effective insulator between the cold atmosphere and the relatively warm ocean, hindering sensible heat fluxes and forming an effective barrier to evaporation and turbulent heat loss, which decreases with increasing ice thickness. Most of the Antarctic sea ice cover is seasonal, but in regions of multiyear ice, the thermal differences are much smaller in summer. Radiative and turbulent fluxes to snow and ice surfaces play a role in phase changes and small changes in the surface energy balance have been shown to effect modelled sea ice thickness (Bitz and Lipscomb 1999). In the marginal ice zone, thin ice and open water regions can significantly influence the overall rate of heat exchange between the atmosphere and the ocean.

Air-sea fluxes determine how properties, such as momentum, heat, freshwater, and gases, exchange between the atmosphere and the ocean (e.g., Bourassa et al. 2013). Thermal stratification of the atmospheric boundary layer (ABL) over sea ice varies in space and time depending on ice thickness, open water regions, the diurnal cycle of solar radiation, seasonal and synoptic-scale changes in the weather conditions. The temporal and spatial distribution of thermal stratification of the ABL in the Southern Ocean is not well known but is thought to be less thermally stratified than the Arctic due to the katabatic winds that advect cold air over sea ice and thinner, lower concentration sea ice.

There is sparse temporal and spatial coverage of sea ice flux observations in the Southern Ocean (Swart et al. 2019) and there are almost none from autumn or winter months, or in regions impacted by sea ice cover. Quantitative knowledge on the radiative and turbulent surface fluxes over Antarctic sea ice is still very limited and improving the coverage of turbulent and radiative fluxes measurements in the ice-covered regions of the Southern Ocean has been identified as a priority for Antarctic research (Kennicutt et al. 2019).

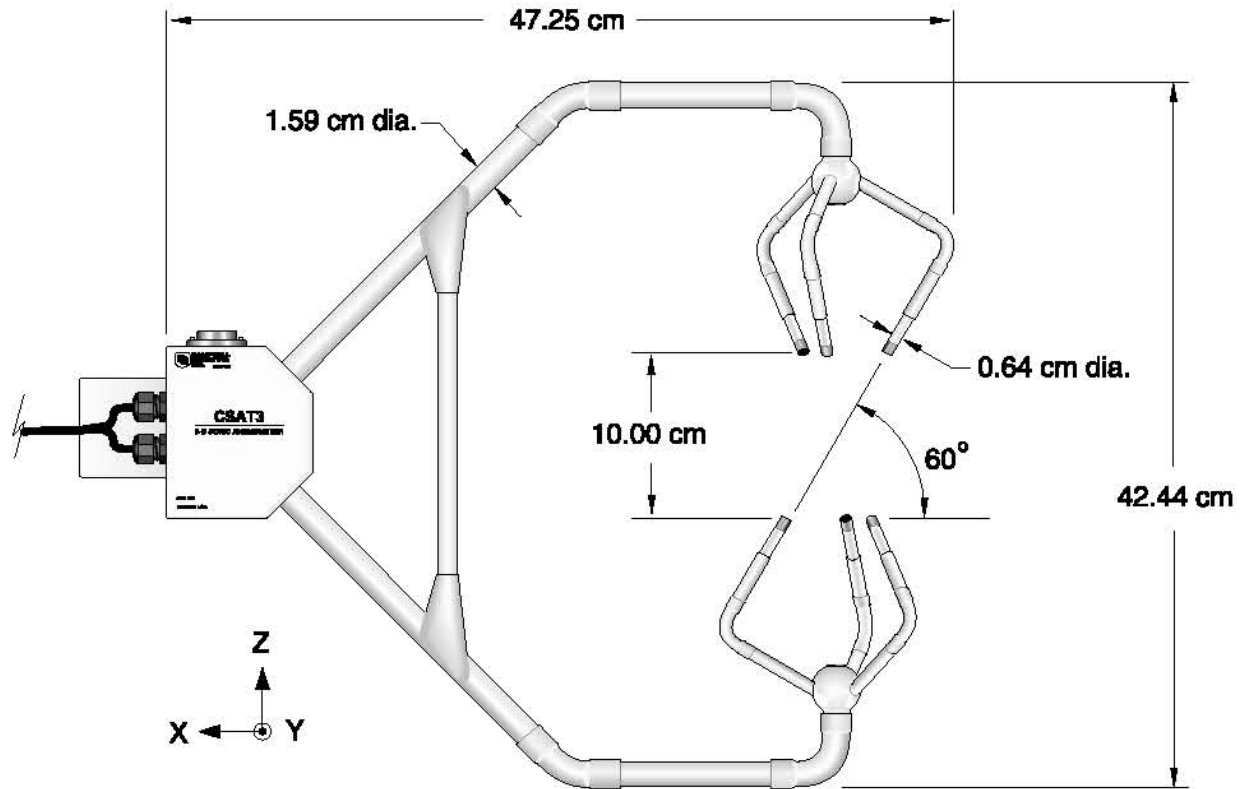
Our aim was to measure the turbulent and radiative fluxes over Antarctic marginal sea ice at the start of the melting season in early spring using a CSAT3D anemometer, a KH20 Hygrometer, and a CNR4 radiometer. We also experimented with a Novalynx evaporation gauge and pan to measure evaporative fluxes.

### **4.2. Methods**

#### **4.2.1. Turbulent and radiative fluxes**

We used the Campbell Scientific CSAT 3D Sonic Anemometer (Figure 4.1) to make eddy-covariance measurements of the orthogonal wind components ( $u_x$ ,  $u_y$ ,  $u_z$ ) and the speed of sound ( $c$ ). Three pairs of non-orthogonally oriented transducers each transmit and receive an ultrasonic signal. The distance between transducers is known (Figure 4.1) and

the time of flight is directly related to the wind speed along the sonic transducer axis. The speed of sound is directly related to the air density, which is related to ambient temperature and, to a lesser extent, humidity. Momentum flux is calculated from fluctuations in the turbulent horizontal and vertical wind from the average. Sensible and latent heat can be calculated by finding the covariance between the vertical wind and scalars. The FW05 thermistor was not working (issue still to be determined but we believe there is a problem either with the cable or the connection) so we could not directly measure sensible heat flux. Instead we will calculate sensible heat flux from the sonic temperature corrected for the effects of water vapour.



Anemometer Head

Figure 4.1: CSAT3 3D Anemometer

The Campbell Scientific KH20 krypton hygrometer (Figure 4.2) measures rapid fluctuations in atmospheric water vapour. Note that it does not measure absolute concentrations. A krypton lamp emits two absorption lines: a major line at 123.58 nm and a minor line at 116.49 nm. As the light travels through air, both lines are absorbed by water vapour, and a small amount of the minor line is absorbed by oxygen. The Lambert-Beer law relates the absorption of light to the material through which the light is travelling and by measuring the light intensity before and after passing through the material we can obtain the water vapour density. The hygrometer needs calibrating on our return to confirm the path length and the absorption coefficient of water vapour.

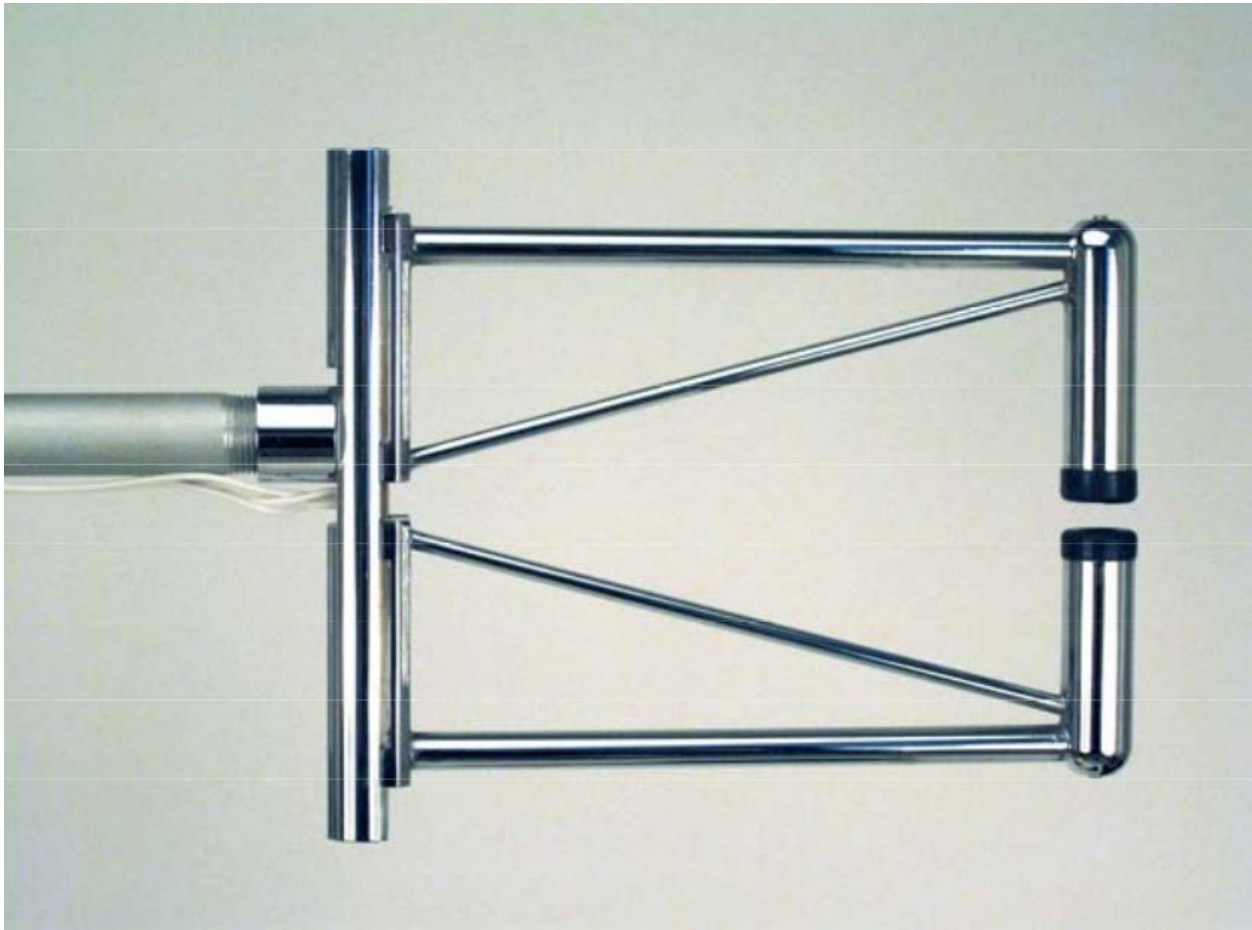


Figure 4.2: KH20 Krypton Hygrometer

The Kipp & Zonen CNR4 Net Radiometer (Figure 4.3) consists of an upward and downward facing pyranometer pair that measures short-wave radiation, and an upward and downward facing pyrgeometer pair that measures long-wave far infrared radiation. The upper long-wave detector has a meniscus dome to ensure that water droplets roll off easily while improving the field of view to nearly 180°, compared with 150° for a flat window.



Figure 4.3 CNR4 Radiometer

We installed the instruments on a mast on a consolidated floe (24-hour deployment) and took measurements over different ice types at 2 m, 5 m, and 10 m at three stations (MIZ5, MIZ7, MIZ8) in the Marginal Ice Zone (1.5-hour deployments).

Table 4.1: Flux measurement stations in the marginal ice zone

Station	Location
MIZ2 (mast)	59.5°S, 0°E
MIZ5	59.3°S, 6.4°E
MIZ7	59.5°S, 10.8°E
MIZ8	59.5°S, 12°E

#### 4.2.2. Mast Deployment: MIZ2

We set up the mast at MIZ2 (59.5°S, 0°E), a consolidated ice flow in the Marginal Ice Zone in the Eastern Weddell Sea, at approximately 07:00 GMT on 24 October. Ice thickness was ~ 80–90 cm and snow thickness was ~ 5–7 cm. The 3D anemometer, krypton hygrometer and radiometer were secured to the mast at a height of ~ 2 m. We assembled the mast with all the instruments in the helicopter hangar (Figure 4.4(a)) and then used the ship’s crane to lift the mast onto the ice. A CR3000 data logger recorded the measurements at 10 Hz. Battery power was supplied to the data logger and instruments by a 12V DC power supply. We deployed by cradle to finish securing the mast (Figure 4.4(b)). We attached guy ropes to help stabilise the mast from movement by the wind, levelled the radiometer and the anemometer, and measured the negative x-axis of the anemometer (118°). Figure 4.4(c) shows the fully assembled mast with snow added to the base to reduce any reflection effects. About four hours after deployment, the ship moved away from the mast location. We analysed the data from this time to avoid interference from the presence of the ship. The mast was retrieved at 15:00 GMT on 25th October (Figure 4.4(d) and 4.4(e)).

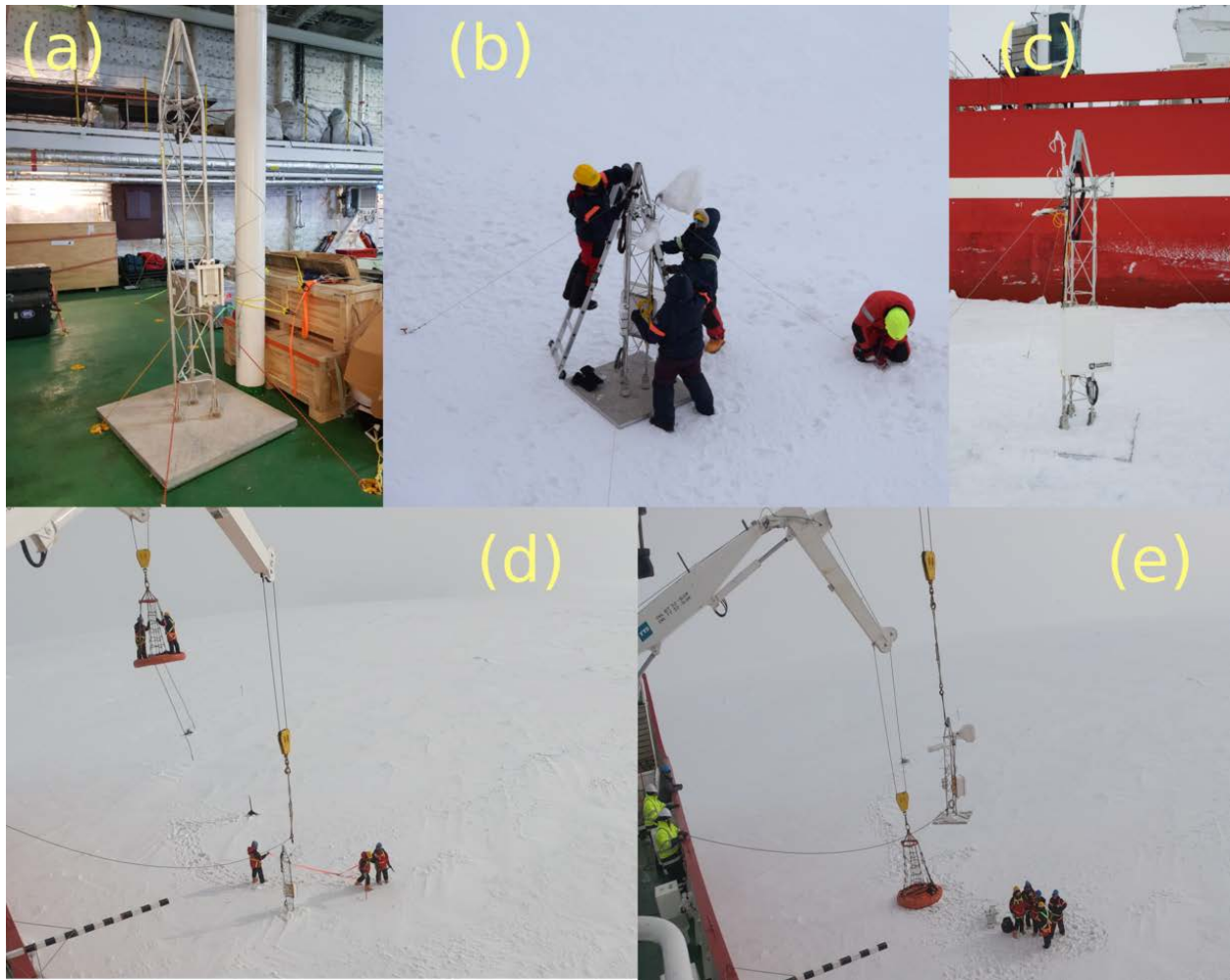


Figure 4.4: (a) the mast was assembled in the helicopter hangar, (b) levelling the instruments and securing the mast, (c) fully-assembled mast, (d) mast retrieval, (e) mast being lifted back onto the ship

#### 4.2.3. Profile Experiments: MIZ5/MIZ7/MIZ8

Sea ice cover consists of ice floes of varying thickness, typically covered by snow, and is broken by cracks, leads and polynyas. Ice conditions are controlled by a close interaction of dynamic and thermodynamic processes, and the configuration of sea ice significantly influences variations of the atmospheric and oceanic circulation at all time and space scales. There can be large variability at local scales, particularly along sea ice margins and leads. We made measurements at approximately 2 m, 5 m and 10 m above sea ice at three different stations in order to assess the variability in fluxes over different ice types. The 2 m height was approximate by the bosun and then 3 m of cable was taken in to get to the 5 m height, and then a further 5 m of cable was taken in to get to 10 m. At MIZ5 we attached the 3D anemometer, krypton hygrometer and radiometer to the gondola (Figure 4.5). This was not a satisfactory set up: the instruments were too close to the gondola and it took too long to put together in the cold on the deck. For MIZ7 and MIZ8 we attached the instruments to the mast instead (Figure 4.6).

#### 4.2.4. Evaporative fluxes

The 255-100 Novalynx analogue output evaporation gauge (Figure 4.7) determines evaporation rate by measuring the changing water level in an evaporation pan, which is connected to the gauge with a steel pipe. The evaporation gauge consists of a chain-mounted float and counterweight that turns a sprocket attached to a 1000  $\Omega$  potentiometer. A datalogger (we used a Campbell Scientific CR6) provides a precision excitation and the gauge produces a DC voltage that changes proportionally to the change in water depth of the evaporation pan.



Figure 4.5: Instruments were cable tied to poles across the gondola and then lowered by crane.



Figure 4.6: At MIZ7 and MIZ8 the instruments were attached to the mast.

While in the marginal ice zone, we deployed the pan and gauge on the helicopter deck between pancake lifting operations (in order that we could use the deck space).

### **4.3. Preliminary Results**

#### **4.3.1. Radiative fluxes**

All fluxes are defined positive upward. Upward (or downward) fluxes are defined to be positive (or negative). The radiometer data were registered at 20 Hz and the results are shown as 5-minute means. Radiative fluxes vary with cloud cover and aerosol amount and characteristics. Apart from ship observations at the time of deployment and recovery we do not have information on cloud cover for the duration of the mast deployment. Downwelling longwave radiation is controlled largely by cloud cover (tends to be high at high latitudes), cloud base height (tends to be low at high latitudes) and water vapour concentration (tends to be small at high latitudes). Upwelling longwave radiation depends on surface skin temperature, which differs widely between ice and open water regions. Small changes in shortwave reflectivity (albedo) and longwave emissivity can alter the energy budget sufficiently to cause substantial growth or melting of ice.



Figure 4.7: Novalynx analogue output evaporation gauge and evaporation pan.

#### 4.3.2. Mast deployment: MIZ2

Figure 4.8 shows the timeseries of incoming and outgoing shortwave radiation. There is a clear diurnal cycle in the incoming and reflected solar radiation. The values for the afternoon of 24 October are slightly lower than the values for the morning of 25 October. The maximum incoming shortwave radiation exceeded  $700 \text{ W m}^{-2}$ . Most of the incoming radiation was reflected by the snow surface. It appears that something went wrong towards the end of the deployment (note the drop and the spikiness in the last couple of hours of the timeseries in Figure 4.8). We do not yet have an explanation for this, but when we recovered the instruments, we noticed that the data logger panel that the radiometer was connected to had come loose.

There are two temperature measurements, one from the radiometer, and the other from the data logger. The data logger was stored inside a protective box and the temperature responds more slowly (Figure 4.9). The air temperature is well-correlated with the shortwave radiation ( $r=0.9$ ). 1 Footprint estimation will be calculated later

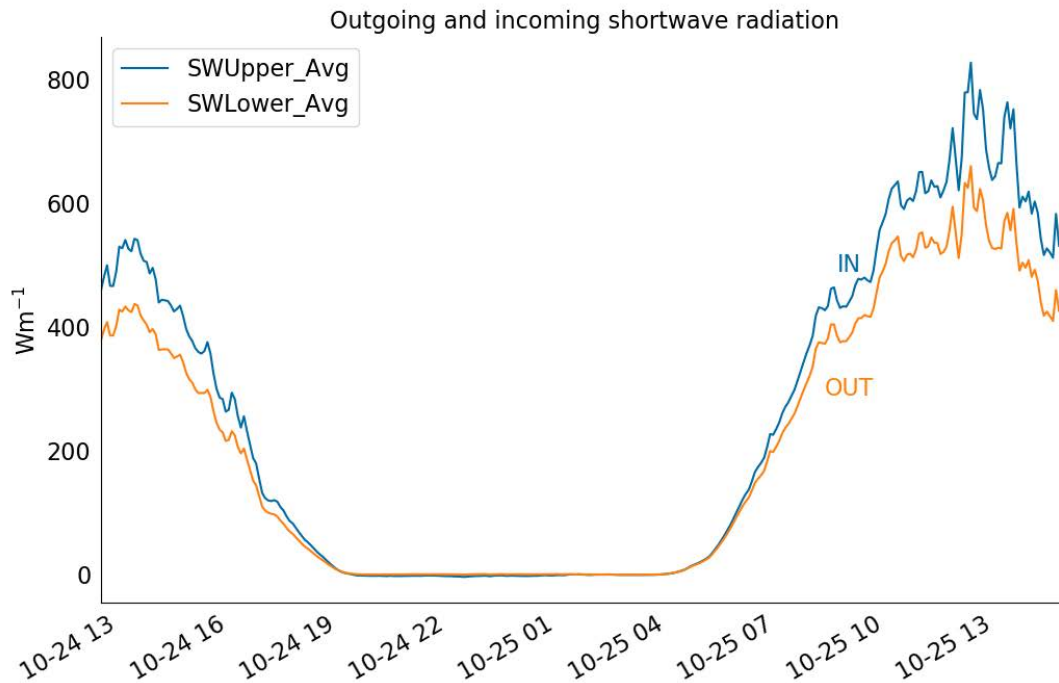


Figure 4.8: Timeseries of incoming and outgoing shortwave radiation.

The surface albedo was calculated as the ratio of the reflected and incoming shortwave radiation. Albedo measurements are not reliable for low radiation flux magnitudes, or under large solar zenith angles ( $> 80^\circ$ ), which for this location and time of year means that albedo is not reliable between 6 pm and 6 am GMT. The mean albedo for the deployment period is 0.83 (Figure 10). The increase in albedo on 25 October may be related to the snowfall overnight (fresh snow was observed during recovery). There was a clear effect of the ship on the albedo – it increased from 0.73 to 0.81 when the ship moved away from the mast location to start CTD operations nearby. We therefore discarded all the data before 12:30 GMT on 24 October to avoid any effects from the ship.

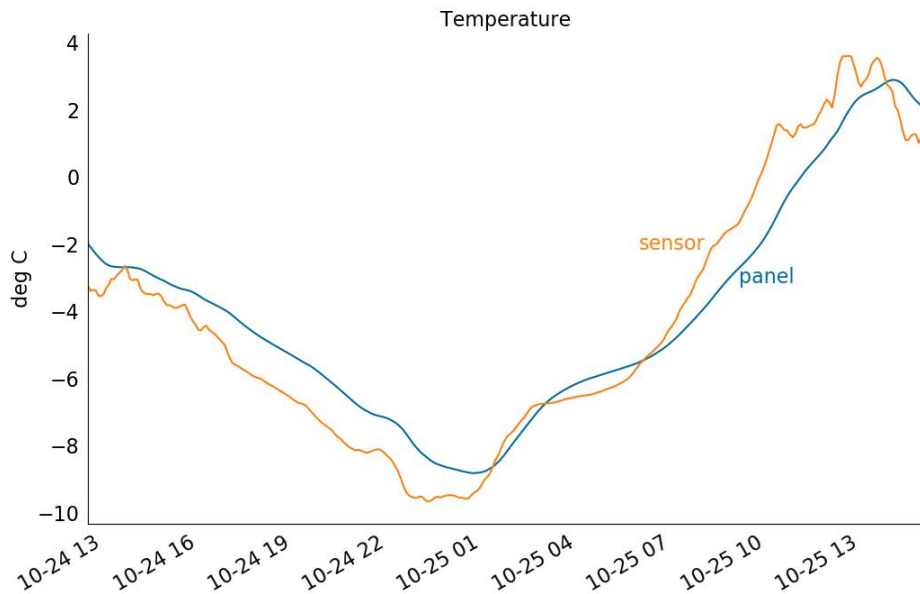


Figure 4.9: Timeseries of temperature measured by the radiometer (sensor, orange) and inside the data logger (panel, blue).

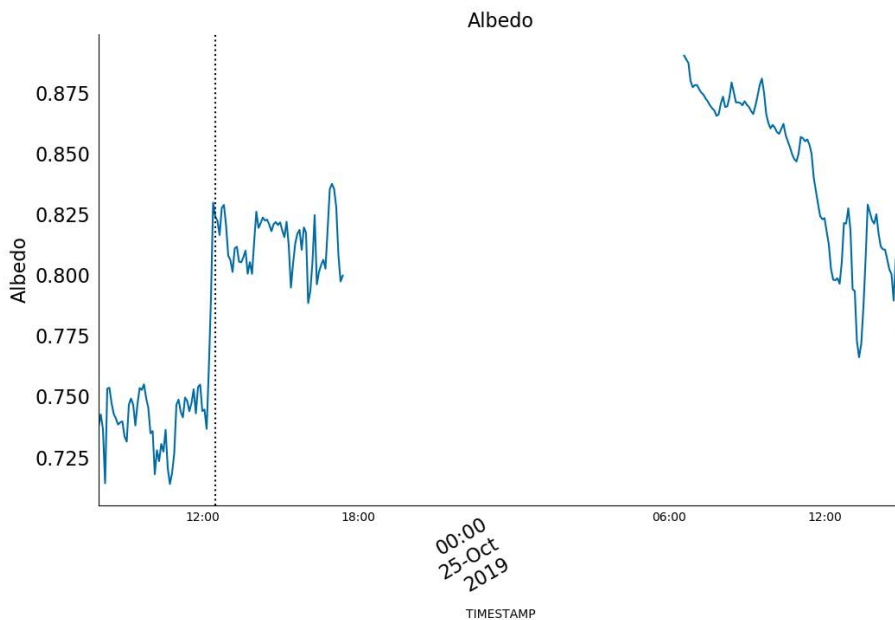


Figure 4.10: Timeseries of albedo for solar zenith angles less than  $80^\circ$ . The vertical dotted line shows the time when the ship moved away from the station.

Longwave radiation was negative throughout the measurement period (Figures 4.11 and 4.13). Variations in the outgoing radiation emitted by the snow surface are determined by

the surface temperature and the emissivity of water. These variations were small (orange line in Figure 4.11, amplitude  $20 \text{ W m}^{-1}$ ) and appeared to be dominated by the diurnal cycle in surface temperature (Figure 12), assuming that the air temperature is a proxy for the surface temperature. The incoming radiation is more variable ( $\sim 60 \text{ W m}^{-1}$ ) – incoming radiation depends on the temperature and emissivity of the overlying water vapour, fog, or cloud layers.

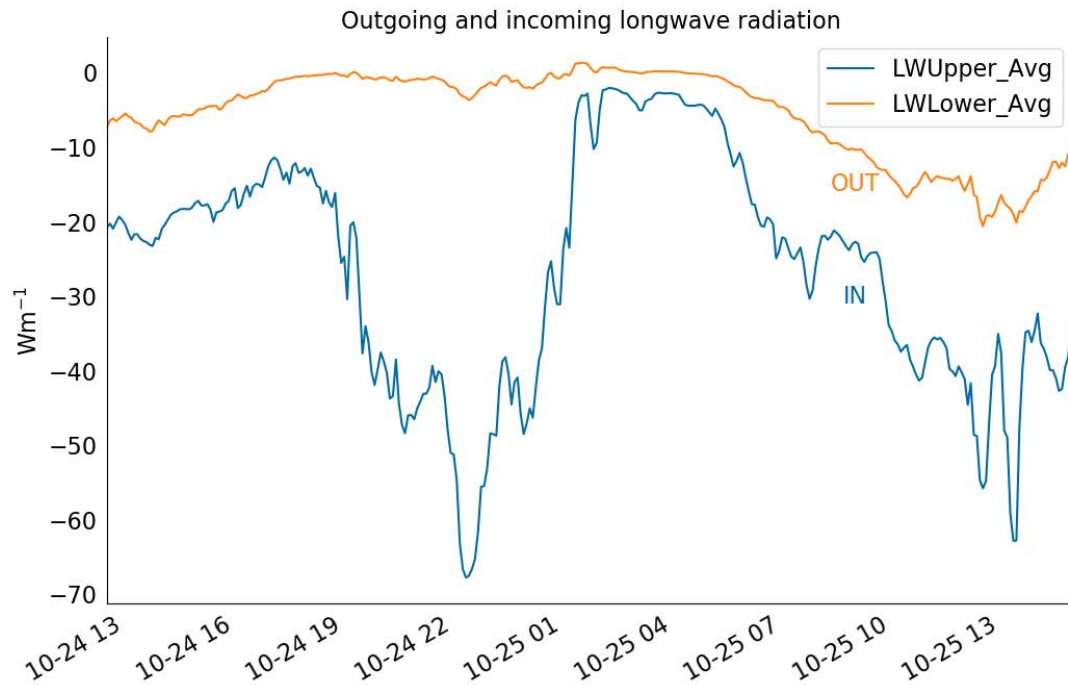


Figure 11: Timeseries of incoming and outgoing longwave radiation.

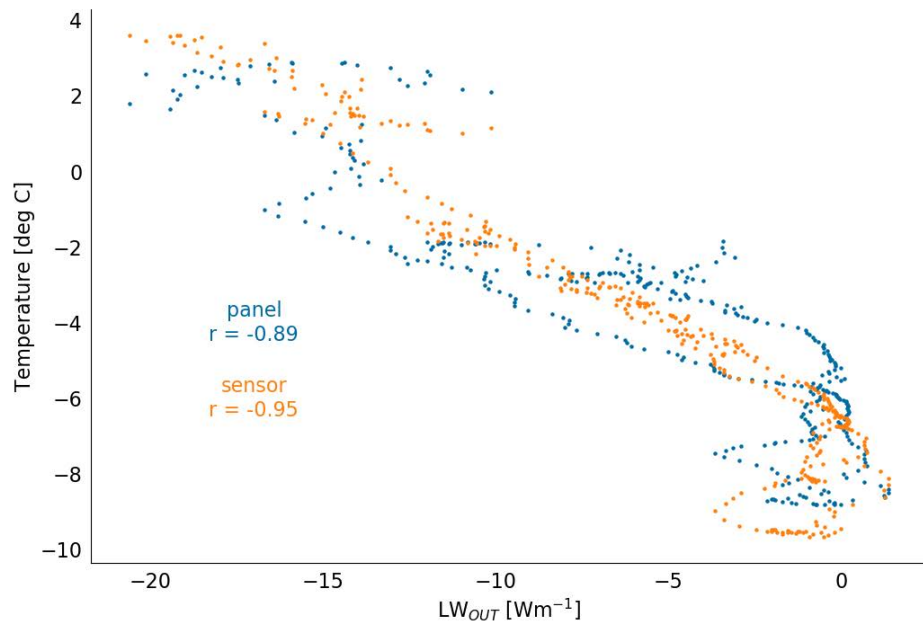


Figure 12: Dependence of the outgoing longwave radiation on air temperature.

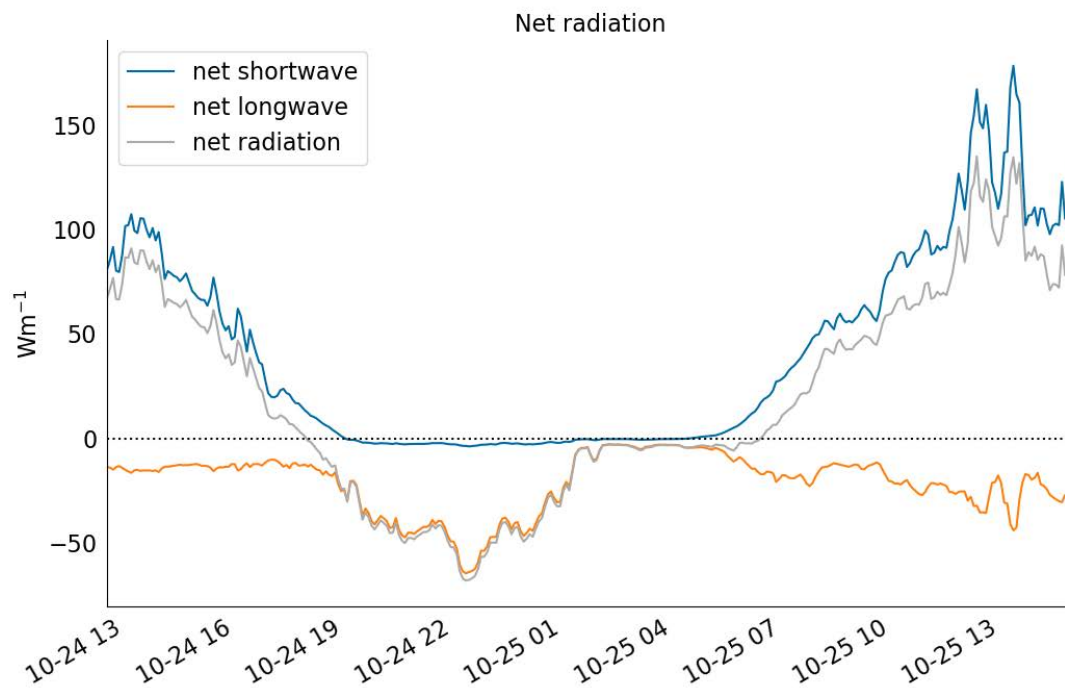


Figure 13: Timeseries of net radiation.

Net radiation was positive (upward) during the day and negative (downward) at night.

#### 4.3.3. Profile Experiments: MIZ5/MIZ7/MIZ8

Our IMU was not working and we were therefore unable to remove the movement of the instruments from the data. It is unlikely that all the instruments remained level during the deployment period due to wind influences and ship motion. The following results are therefore merely illustrative. At MIZ5 the instruments were too close to the gondola (Figure 5). We improved the design by attaching the instruments to the mast rather than to the gondola but then there was an issue with the data logger at MIZ7 and MIZ8 (Figure 6). The data logger only collected the first hour of measurements at MIZ7 (the 2m and 5 m measurement) and the first 40 minutes at MIZ8 (the 2 m measurement). The mean values for each of the 2 m stations are shown in Table 2. We think that the problem with the data logger might be related to the internal battery. We will service the data logger on our return to confirm.

Table 4.2: Average measurements at approximately 2 m at MIZ5, MIZ7, and MIZ8

	MIZ5	MIZ7	MIZ8
Time (GMT)	17:50 – 18:29	12:20 – 12:50	14:16 – 14:46
Incoming shortwave	17.60	281.55	196.57
Outgoing shortwave	15.03	249.86	138.56
Incoming longwave	-24.69	-19.74	-18.95
Outgoing longwave	-2.42	-11.27	-2.84
Net radiation	-19.70	23.23	41.90
Albedo	0.86	0.89	0.70

The ice was much thinner with less snow cover at MIZ8 and that can be seen in the decreased albedo (Table 4.2).

#### 4.3.4. Turbulent fluxes

Our system configuration measures sonic sensible heat flux, momentum flux, temperature, humidity, horizontal wind speed, and wind direction. Wind stress (momentum) and sensible and latent heat fluxes are classified as turbulent fluxes. They depend on nonlinear, covarying terms. Eddy Covariance is a method to measure vertical flux of heat, water or gases. Flux is calculated as a covariance of instantaneous deviations in vertical wind speed and instantaneous deviations in the entity of interest (temperature for the sensible heat and water vapour for the latent heat). The method relies on the prevalence of the turbulent transport, and requires state-of-the-art instruments. Accurate measurement of vertical velocity is critical for covariance estimates of turbulent fluxes. It

uses complex calculations, and utilizes many assumptions. However, it is the most direct approach to measuring fluxes.

Apart from emitted longwave radiation, the sensible and latent heat fluxes are the only means of transporting energy from the surface into the atmosphere. The turbulent heat fluxes are often dismissed as being one to two orders smaller than the radiation fluxes, but they become significant when compared to the net radiation. The rate of heat transfer by turbulent fluxes depends on the roughness of the surface, wind speed, boundary layer stability, and the size of the temperature and water vapour gradients.

15% of the data collected by the anemometer registered as NaNs and these data were very noisy and difficult to despik. We don't provide any preliminary results for the turbulent fluxes as we need to optimize our despiking routines for noisy data. Once despiked, we will apply a double rotation tilt correction method suitable for flat, horizontal, isotropic terrains with extended fetches to rotate the raw  $u$ ,  $v$ ,  $w$  data into a reference frame aligned with the mean streamline so that  $\langle w \rangle = \langle v \rangle = 0$ . We will then remove any linear trends from each averaging period to prevent long-term trends not related to turbulence from turning into artificial flux contributions. The determination of the averaging period represents a trade-off between remaining in a "spectral gap" where the realization averaging time will capture most of the eddy events, but where changes in the mean flow speed and direction will not adversely affect covariance statistics. Details on the treatment of the data will be available with the processed data set at a later stage.

#### **4.3.5. Evaporation (mass) fluxes**

We have no results from the evaporation experiment. The pan was fully iced within a few hours of setting it up. However, even before then there was too much sloshing about in the pan to make decent measurements. Even if we come up with a way to keep the pan flat (i.e. using some sort of stability platform), we would still have to contend with the ship vibrations, which cause ripples on the water surface. We need to develop an alternative method to measure the evaporative fluxes over sea ice.

#### **4.4. References**

Bitz, Cecilia M., and William H. Lipscomb. 1999. "An Energy-Conserving Thermodynamic Model of Sea Ice." *Journal of Geophysical Research* 104 (C7): 15669-- 15677.

Bourassa, Mark A., Sarah T. Gille, Cecilia Bitz, David Carlson, Ivana Cerovecki, Carol Anne Clayson, Meghan F. Cronin, et al. 2013. "High-Latitude Ocean and Sea Ice Surface Fluxes: Challenges for Climate Research." *Bulletin of the American Meteorological Society* 94 (3): 403–23. <https://doi.org/10.1175/BAMS-D-11-00244.1>.

Kennicutt, Mahlon C., David Bromwich, Daniela Liggett, Birgit Njåstad, Lloyd Peck, Stephen R Rintoul, Catherine Ritz, et al. 2019. "Sustained Antarctic Research: A 21st Century Imperative." *One Earth* 1 (1): 95–113. <https://doi.org/10.1016/j.oneear.2019.08.014>.

Parkinson, Claire L. 2019. "A 40-y Record Reveals Gradual Antarctic Sea Ice Increases Followed by Decreases at Rates Far Exceeding the Rates Seen in the Arctic." *Proceedings of the National Academy of Sciences*, July, 201906556. <https://doi.org/10.1073/pnas.1906556116>.

Swart, Sebastiaan, Sarah T. Gille, Bruno Delille, Simon Josey, Matthew Mazloff, Louise Newman, Andrew F. Thompson, et al. 2019. "Constraining Southern Ocean Air-Sea-Ice Fluxes Through Enhanced Observations." *Frontiers in Marine Science* 6 (July): 421. <https://doi.org/10.3389/fmars.2019.00421>.

## 5. TEAM GLIDER

### 5.1. Overview

Team Glider was responsible to deploy instruments for two research interests: (1) in occupying the Sub-Antarctic Zone (SAZ) and Polar Upwelling Zone (PUZ) to study the impact of storms associated with fronts and (2) to manage and extend the ROAM-MIZ (Robotic Observations And Modelling of the Marginal Ice Zone) field campaign which aims to study the activity of submesoscale processes at the boundary between the Marginal Ice Zone and open ocean. Through these combined projects, the following platforms were deployed between the two SCALE cruises:

1. Six buoyancy gliders (Seagliders),
2. Three surface gliders (one Sailbuoy and two Wavegliders),
3. Two SWIFT wave buoys (deployed and recovered on both cruises)
4. Two Seasonal Ice Mass Balance buoys
5. Underway CTD (UCTD)

In addition to the platform deployments, calibration CTDs were taken, which followed the SOCCO procedures for water sampling depths for dissolved oxygen, salinity and chlorophyll. The logging of the pyranometer on the main mast was also regularly checked to ensure data for incoming heat fluxes. A summary of deployment/recovery locations are summarised below in Tables 5.1 and 5.2 and shown in Figures 5.1 and 5.2.

Table 5.1: Platforms deployed during SCALE winter cruise, including sensors, deployment date and location and, where applicable, recovery information

Serial number	Platform type	Installed Sensors	Deployment location	Deployment time	Recovery location	Recovery time
542 (CSIR)	Seaglider (1000 m)	CTD, dissolved oxygen, PAR, EcoPuck	43°00.008' S, 8°29.850' E	21/07/2019 10:15	--	13/12/2019 08:10
574 (CSIR)	Seaglider (1000 m)	CTD, dissolved oxygen, PAR, EcoPuck	53°59.979' S, 0°0.530' E	24/07/2019 08:00	53°59.337' S, 0°01.791' E	24/07/2019 11:06
662 (GU)	Seaglider – Ogive fairing (1000 m)	CTD, dissolved oxygen, PAR, EcoPuck	56°00.079' S, 0°0.095' E	25/07/2019 11:15	--	--
SB1812A (GU)	Sailbuoy	Airmar, CT	56°00.019' S, 0°0.017' E	25/07/2019 11:42	--	2/12/2019
SWIFT20 (1)	SWIFT buoy	Airmar, IMU, GoPro camera	56°00.154' S, 0°0.105' E	25/07/2019 11:57	55°51.767' S, 0°23.846' E	26/07/2019 10:37
SWIFT20 (2)	SWIFT buoy	Airmar, IMU, GoPro Camera	56°59.907' S, 0°0.851' E	26/07/2019 22:58	56°40.488' S, 0°26.322' E	28/07/2019 14:45
SWIFT21	SWIFT buoy	Airmar, IMU, GoPro Camera	57°07.143' S, 0°0.323' W	27/07/2019 01:19	56°48.172' S, 0°17.521' E	28/07/2019 09:27
SIMB1	Seasonal Ice Mass Balance Buoy	Extended thermistor string, acoustic sounders, air temperature	58°05.887' S, 0°02.055' W	27/07/2019 15:01	--	--

		and pressure				
--	--	--------------	--	--	--	--

Table 5.2: Platforms deployed during SCALE spring cruise, including sensors, deployment date and location and, where applicable, recovery information

Serial number	Platform type	Installed Sensors	Deployment location	Deployment time	Recovery location	Recovery time
#027 (CSIR)	Waveglider	CTD, PCO2, Dissolved oxygen, Airmar Weather, Airmar Waterspeed, SeaFET (PH), XEOS Tracker	47°00.051' S, 5°16.430' E	17/10/2019 12:23	--	--
#052 (CSIR)	Waveglider	CTD, PCO2, Dissolved oxygen, Airmar Weather, Airmar Waterspeed, XEOS Tracker	47°00.051' S, 5°16.430' E	17/10/2019 12:23	42°54.655' S, 009°49.224' E	15/11/2019 15:42
574 (CSIR)	Seaglider (1000 m)	CTD, dissolved oxygen, PAR, EcoPuck	54°02.428' S, 0°01.597' E	19/10/2019 13:43	--	19/02/2020 18:45
537 (UEA)	Seaglider (1000 m)	CTD, dissolved oxygen,	55°01.206' S, 0°02.713' E	20/10/2019 08:50	--	18/02/2020

		PAR, EcoPuck				
640 (GU)	Seaglider – Ogive fairing (1000 m)	CTD, dissolved oxygen, PAR, EcoPuck	55°01.206' S, 0°02.713' E	20/10/201 9 08:50	--	18/02/20 20
SWIFT20	SWIFT buoy	Airmar, IMU, GoPro Camera	56°55.380' S, 0°02.766' E	22/10/201 9 23:08	54°36.618' S, 0°04.370'E	7/11/201 9 10:01
SWIFT21	SWIFT buoy	Airmar, IMU, GoPro Camera	57°53.596' S, 0°00.835' E	23/10/201 9 11:55	56°35.622' S, 3°54.126'E	7/11/201 9 21:08
SIMB2	Seasonal Ice Mass Balance Buoy	Temperatur e string, acoustic sounders, air temperature and pressure	59°18.467' S, 0°05.489' E	24/10/201 9 07:43	--	--

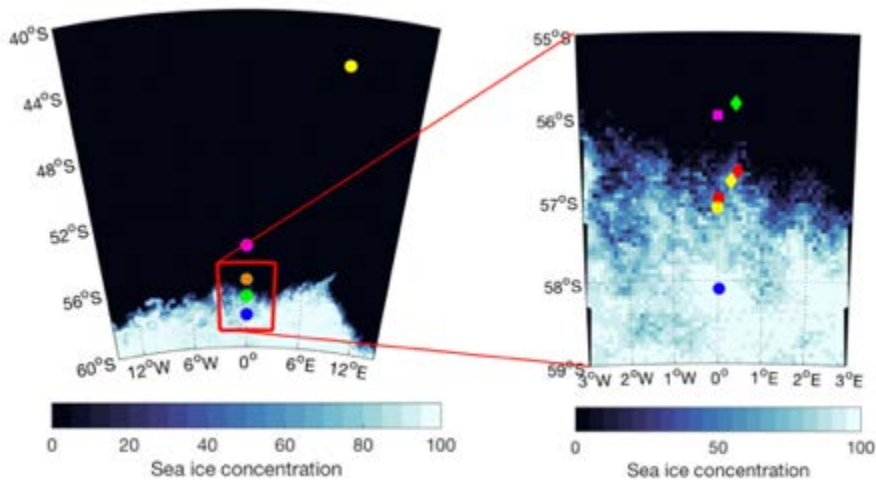


Figure 5.1: Deployment and recovery locations of platforms during SCALE winter cruise 2019, using sea ice concentration from July 27<sup>th</sup> 2019. Left: overview of all deployments, SG542 (yellow), SG574 (pink), SG662, Sailbuoy and SWIFT20 (orange), SWIFT20 and SWIFT21 (green) and the SIMB (blue). (b) Right: zoom of the ROAM-MIZ deployment,:

SG662, Sailbuoy and SWIFT20(1) (purple square), SWIFT20(1) recovery (green diamond), SWIFT20 (red) and SWIFT21 (yellow) deployments (dot) and recoveries (diamond) and SIMB (blue).

## **5.2. Wave Gliders**

### **5.2.1. Introduction**

Wave gliders are autonomous ocean science vehicles that consist of a surface float with an array of solar panels, multiple sensors, batteries and the control unit, as well as an undersea sub-unit that is 8m under the water level which is responsible for the movement and steering of the vehicle. A wave glider is completely propelled by wave/swell energy and the solar panels are only used to power the electrical sensors, control unit and to move the rudder for steering. The science sensors on the wave gliders are a Seabird "Prawler" CTD, Airmar weather station (200WX), Seabird SeaFET PH sensor, Seabird dissolved oxygen and veGAS-pCO<sub>2</sub> (Versatile Glider, Atmospheric and Ship pCO<sub>2</sub> High Precision pCO<sub>2</sub> analyzers) sensor, a CSIR developed pCO<sub>2</sub> system. Two Liquid Robotics SV3 wave gliders were deployed on the SCALE spring cruise, these were SV3\_052 and SV3\_027. These two wavegliders had modified extended hulls and this deployment would be the first long term test of the new extended hulls.

### **5.2.2. Pre-deployment checks**

In order to run through the full set of pre-deployment checks the wave gliders need to be strapped down to the heli-deck (deck 5) whilst in their storage trolley. Then the wave glider can be switched on and a laptop is used to log into the wifi network of the wave glider. Here a full pre-deployment check-list is available and every item must be checked and be in the expected operating ranges. Such as the control of the thruster unit on the sub, the weather station readings, the charging of the batteries via solar panels, all three GPS connections to the iridium satellite network need to be functioning (the airmar mast has a gps antenna as well as the control unit and the PCO<sub>2</sub> system). It is also important to let a pilot back on land send commands to the wave glider and to confirm they are receiving its data. Once this and the whole pre-deployment checklist has been completed then the wave gliders can be switched off and stored inside the heli-hanger again. The pre-deployment should happen the day before the deployment at least.

### **5.2.3. Deployment**

For deployment the wave gliders inside the trolley are switched on and the land pilots must be notified of this, then it is lifted by the starboard/aft crane with two straps and lowered down to deck 3. From here the land pilots will perform some necessary check and once they are happy they must give the go ahead to deploy the wave glider. Then the lifting straps that were used to lift the wave glider with the crane are replaced with rope and attached to a main quick release mechanism that will drop the wave glider into the ocean from the aft A-frame on the ship. Next the supporting ratchet straps keeping the wave glider in the cradle/trolley are removed and a single quick release strap is placed between the wave glider float and sub unit, this is used to separate the float and sub unit

once it is “dropped” into the ocean from the main quick release mechanism. The deck crew will lift the wave glider with the A-frame up and over the aft end of the ship (off the poop-deck) and when they give the command the responsible technician will pull the quick release mechanism. The deployments were on the **17/10/2019** at **12:23**.

It should be noted that the most ideal conditions for deploying a wave glider is as little swell and wind as possible. With swell present the wave glider runs the risk of being damaged upon being released from the A-frame. This happened with the deployment of wave glider SV3\_027 where the quick release mechanism did not function correctly because of the swell and the ropes got tangled in the weather station and ripped it off the float hull.

After the deployment of wave glider a pCO<sub>2</sub> calibration circle from the ship must be performed. The land pilots will gain control and give the glider a fixed heading and relay this information to the ship. The ship will then encircle the wave glider while travelling at a slow speed and always maintaining a 500m distance from the wave glider. This is because the pCO<sub>2</sub> system on the ship will be in equilibrator mode and samples are taken at fixed intervals for the calibration.

#### **5.2.4. Recovery**

After almost a month after the deployment the wave gliders encountered problems where their steering could no longer be controlled and they were then drifting roughly 45km a day with the wind and ocean currents. A recovery was then planned by the ship’s crew and only performed with wave glider SV3\_052 because it was close enough to the return leg of the cruise. The land pilots relayed the gps location of the wave glider frequently and this was relayed to the ships navigational officers in order to track the wave glider. With many spotters on the bridge and on the deck above the wave glider was spotted about 1-2nm from the ship. The recovery was performed by the ship’s crew by using a big net and the starboard/aft crane to scoop the wave glider out of the water. It is important to note that this was possible because it was known that the sub-unit of the wave glider, that is normally 8m underwater and attached to the float with an umbilical cable, was missing. This is what allowed the float part of the wave glider to be scooped up by the net otherwise the umbilical cable would normally get in the way.

The recovery was on the **15/11/2019** at **15:42**.

#### **5.3. Seagliders**

The Seaglider is a buoyancy glider that samples between the surface and 1000 m in a V-shaped profile. It dives or climbs by pumping oil between internal/external bladders to change its buoyancy, accompanied by battery movement that can change the pitch and roll. It is a largely autonomous system, communicating via satellite at the end of each dive to transfer data and pick up commands such as targets to aim for and sampling rates for the science sensors. The data from all three Seagliders deployed during SCALE winter cruise are uploaded to the CSIR or Kongsberg basestations and then shown on the University of Washington IOP server. The two CSIR gliders were equipped with ARGOS

tags, which act as independent locating devices if the Iridium system were to fail. In the SCALE spring cruise, each Seaglider reports to a different basestation: CSIR (SG574), Kongsberg (SG640) and UEA (SG537). Data can be found either on the University of Washington IOP server or ROAM-MIZ website. Both the UEA and CSIR gliders were equipped with ARGOS tags.

Five of the gliders (all except SG537) were equipped with Seabird CT sails, Aanderaa dissolved oxygen optodes (AA4831), PAR sensors and WetLabs triplet ECOpuck (measures responses in 470, 695 and 700 nm wavelengths that correspond to chlorophyll, coloured dissolved organic matter and backscatter). SG537 was equipped with the same sensors, but excluded the PAR sensor. In order to run pre-deployment tests, the gliders must be placed in a position on the heli-deck where they are able to connect to Iridium satellites in the region. We found that the port side of the heli-deck, away from the main structure of the ship, was sufficient for this (Figure 5.3).

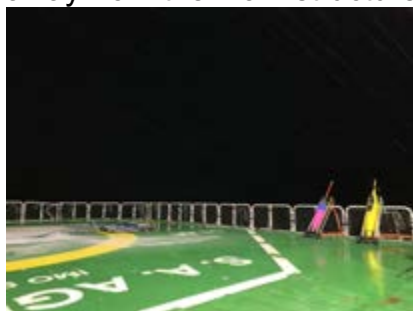


Figure 5.3: SG574 and SG662 on the heli-deck undergoing testing on the winter cruise

Following a completed Sealaunch procedure and after receiving the “OK to launch” from pilots back on land, the serial cable is disconnected from the glider and the glider is carried down the stairs to the poop deck. Here the wings and rudder can be attached and the sensor caps removed. The gliders were lowered using the aft A-frame and were deployed using a quick release that was fastened around the lifting point on the rudder. After deployment the ship moved forwards at 0.5-1 knots whilst the on-board team observed how the glider was sitting in the water and confirmed to pilots on land that the first dive could be initiated. Whilst the ship is still on station and the glider is on its first few dives, a calibration CTD should be taken (ideally within 4 hours of deployment for best practices of chlorophyll a calibrations).

*Typical timings for a deployment:*

T-1 day: Run any remaining hardware self-tests and/or simulation dives. Pilots clean basestation and prepare cmdfiles for the Sealaunch.

T-2 hours: Take Seaglider out onto heli-deck, connect and prepare pilots for Sealaunch

T-1.5 hours: Initiate Sealaunch

*Approx T-1 hour: Receive prompt “Pilots to give OK to launch?”*

T-30 mins: Move Seaglider down to Poop Deck, attach wings and rudder

T-10 mins: Remove sensor caps and attach quick release.

SG542 – SAZ deployment on winter cruise

### *Pre-deployment checks*

Following a successful autonomous self-test, sim dives and sea trials in Cape Town the week before departure, the only pre-deployment check for SG542 was an autonomous self-test. This was performed on the morning of 21/08 and approximately 3 hours before deployment. For this check the glider was strapped to the railing of the stairs on heli-deck at an angle of about 70°. This test was successful other than an issue with the iridium satellite connection, thus the Seaglider was moved further back on the heli-deck and strapped to the side railings for the sea launch process. At this stage the ARGOS tag 'animal tracker' was also put into start mode.



Figure 5.4: Deployment of SG542; photo Emma Bone

### *Deployment*

Once the sea launch process completed and the pilot gave the go-ahead message, we moved the Seaglider to the aft deck to install the rudder and wings, as well as to remove all sensor caps. We then waited for a further confirmation message from the pilot before the actual deployment of the Seaglider. This was done with the Aft A-Frame Crane using a hand-pulled quick release mechanism. The Seaglider was confirmed to be positioned (or 'sitting') correctly in the water and after approximately 10-15 minutes it went under for its first dive.

Due to bad weather conditions with swell heights of 3-4m and a constant wind speed of 35 knots, the decision was made to cancel the CTD calibration cast on deployment day but to attempt it on the return leg of the cruise. The CTD calibration cast was taken on 03/08/2019.

### SG574 – PUZ deployment on winter cruise

#### *Pre-deployment checks*

The same pre-deployment checks as with SG542 were performed with SG574 including those done in Cape Town before departure. However, this time we covered the CT sail with a towel so that it remained dry as the air temperature was well below zero and water could freeze and crack the glass sensor. The Autonomous self-test was conducted the night before (or 12 hours prior to) the actual deployment to save time and to allow for smoother operations at the deployment station. This was performed on 23/08 and allowed us the time to ensure an iridium connection was made during the autonomous self-test.



Figure 5.5: Left: Deployment set up of SG574, Right: A good buoyancy position post deployment

#### *Deployment*

The exact same deployment procedure that was used for SG542 was followed for SG574. The deployment day was 24/08. After the Seaglider was released it also took approximately 10-15 minutes to go under for its first dive of 50m depth. The dive took approximately 40 minutes and encountered a high number of VBD retries so the decision was made by the pilot to recover the Seaglider about 10 minutes after the dive.

The calibration CTD cast was performed with this deployment, however due to the recovery of the Seaglider the Niskin bottles were not fired at the desired depths.

#### *Recovery*

Following the message from the pilot to recover the Seaglider the chief scientist was immediately notified and he then notified the bridge of the situation. The pilot then proceeded to send the current GPS position of the Seaglider every 5-10 minutes, which were used to plot the drift of the Seaglider. It was helpful to notify the Team Leader WhatsApp group of the cruise of the situation so that each team can send as many volunteers as they can around the ships perimeter to help spot the Seaglider on the surface.

Once the Seaglider was spotted, we kept a constant eye on it until the officers could see it as well. During this time the ship's crew prepared a net on the heli-deck for the recovery with the crane as it was not possible to recover the Seaglider with a small boat in the weather conditions.

The net that was used was not ideal for a Seaglider recovery as it was the net normally used for the collection of pancake ice and thus had a hole size that was too large. This meant that the Seaglider slipped through a hole and was only supported by its wings and the CT sail. This caused damage to the temperature probe on the CT sail as it was bent 90° and broke off half of the Seaglider's rudder. Other than the net issue the recovery was very well performed by the ship's crew and navigation officers. After the recovery, the Seaglider and sensors were rinsed off with warm fresh water and stored inside the heli-hanger.



Figure 5.6: SG574 on recovery, with the pancake ice net SG662 – ROAM-MIZ deployment on the winter cruise

#### *Pre-deployment checks*

Following successful self-tests and sim dives before departure from Cape Town, problems were found with the basestation server at Kongsberg. To ensure correct communications we needed to perform multiple sets of sim dives, which took place on 23/07, 24/07 and the morning of deployment on 25/07. These tests also acted to confirm that the new ICE glider software was working correctly, and as the tests were taking place during cold temperatures (air temperature around -10 °C) we covered the CT sail with a towel to try to keep the cell dry and warm.

#### *Deployment*

As with previous deployments, the Seaglider was released from the aft crane using a quick release clip. The glider took approximately 10 minutes to fill with water and to be confirmed to have a good position in the water. Upon confirmation with the piloting team back on land, the glider was placed on her first dive. During this dive, VBD retries were encountered. However, these errors were not repeated on later dives and the decision was made to leave the glider in.

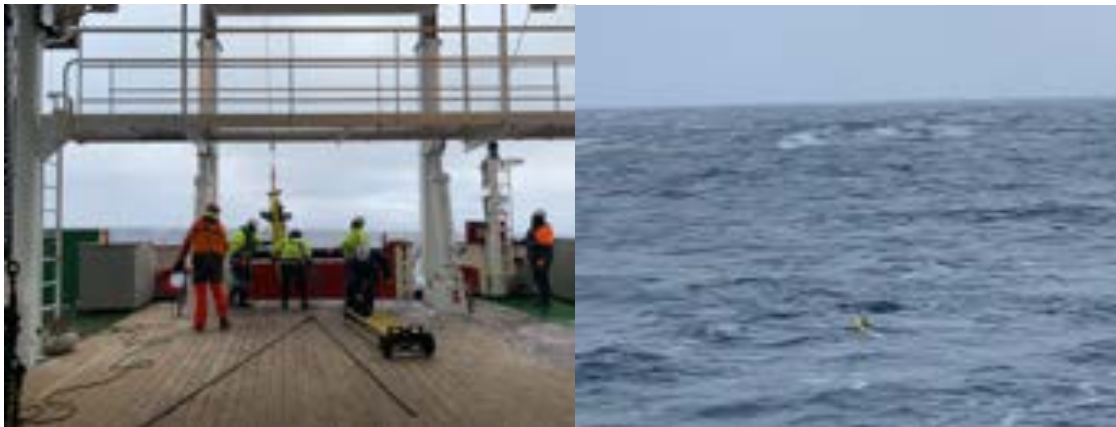


Figure 5.7: Deployment of SG662 (left), and the buoyancy position in the water after 5 minutes (right)

#### SG574 – PUZ deployment on spring cruise

#### *Pre-deployment checks*

A similar pre-deployment check process as performed with SG574 and SG542 on winter cruise were performed with SG574 on the SCALE Spring cruise, including all the tests and seatrials done in Cape Town the week before departure. However, this time it was important to test SG574 more thoroughly because of its issues on winter cruise that caused the glider to be recovered. This was done by performing multiple simulation dives (sim-dives) the day before the deployment as requested by the land pilots, instead of an autonomous self-test. This was done by securing the sea gliders to the railings on the heli-deck outside as done with previous pre-deployment self tests. The glider passed the sim dives as it was functioning normally and the land pilots were satisfied with the results and gave the go ahead to launch the next day.

#### *Deployment*

The exact same deployment procedure that was used for SG574 and SG542 on winter cruise were performed with SG574 on the SCALE Spring cruise. The deployment day was 19/10/2019. After the Seaglider was released it also took approximately 10-15 minutes to go under for its first dive of 50m depth, then performed an 80m and 500m dive. The 500m dive was aborted due to an error in the CMD file of the seaglider but this was not an issue and it was then put into the desired 1000m dives. The calibration CTD cast was performed just before the deployment of the seaglider.

#### SG537 and SG640 – ROAM-MIZ deployment on the spring cruise

#### *Pre-deployment checks*

Following seatrials in Cape Town, self tests and sim dives were only performed on one occasion on Friday 18/10 before deployment on both gliders. All tests were passed by the gliders.

#### *Deployment*

Sea state and weather conditions were excellent - winds less than 10 knots and waves smaller than 0.5 m. As with previous deployments, the Seaglider (initially SG537) was released from the aft crane using a quick release clip. The gliders took approximately 10 minutes to fill with water and to be confirmed to have a good position in the water. Upon confirmation with the piloting team back on land, the glider was placed on her first dive. The ship slowly moved away from SG537 at a speed of 0.5 knots. Following confirmation that the glider had dived, the second glider was deployed (SG640). CTD casts were taken pre-deployment at this station.

### **5.4. Sailbuoy**

The Sailbuoy is a 2m long (60 kg) autonomous surface platform manufactured by Offshore Sensing. It is effectively a small sailing boat, capturing power from the wind to travel forwards. It is equipped with solar panels to charge the two 14V batteries that separately power the autopilot and the datalogger. It carries an Airmar WX-200 Ultrasonic Weather Station, mounted on a mast 0.70 m above MSL. The instrument is designed for moving platforms, with the ability to dynamically correct winds using an internal compass and correct up to a 30° pitch in rough seas. The sensor outputs apparent and true wind

speed, wind gust (maximum wind speed over the 10-minute sampling period) and direction (up to  $40 \text{ m s}^{-1}$ ), barometric pressure, air temperature, and GPS location. Each sensor samples at 1 Hz and is then averaged over 10-min bins before transmitting data back to shore. In the keel bulb there is a Neil Brown Ocean Sensors, Inc. CT cell that measures surface ocean temperature and salinity.

#### *Pre-deployment checks*

The Sailbuoy was placed on the helideck on the morning of 25/07/2019 and both magnetic switches were removed to ensure communications to pilots back on shore were active and working. Confirmation on the ship of rudder movement was also made. When these communications were confirmed, the Sailbuoy was moved downstairs to fix the sail, sheets and a final check of fastenings.

#### *Deployment*

Deployment followed previous procedures used on the SA Agulhas II, where a quick release was attached to the weight bearing eye at the bow of the Sailbuoy, with a secondary rope at the stern. The Sailbuoy was carefully lowered into the ocean whilst the ship was travelling forward at a rate of 2-3 knots in a SW direction. The Sailbuoy was programmed to head straight to the northern end of its line of transect.



Figure 5.8: Deployment of the Sailbuoy using the bow ring (left) and post deployment, sailing away from the ship (right)

### **5.5. SWIFT buoys**

SWIFT buoys were provided by Jim Thomson of the Applied Physics Laboratory at the University of Washington. SWIFT20 and SWIFT21 were both equipped with an Airmar sensor (see description above in Sailbuoy section), wave tracking IMU units, GoPro cameras, Geoforce GPS trackers, Iridium communication antenna and had DC40 hunting dog collars attached as a redundancy tracking measure when the ship is within 8 km of the buoy. The buoys are designed to last for 40-day deployments and ideally, two buoys are deployed in two contrasting wave environments.

#### *Pre-deployment checks*

The SWIFT buoys must be activated and placed in clear-sky view at least 6 hours before planned deployment. Iridium and GPS communications were confirmed by the land team, and the Astro DC40 was tested on the ship.

#### *Winter Deployments*

### SWIFT20 (1)

SWIFT20 was deployed after SG662 and Sailbuoy at 56°S, 0°E using the aft crane. The buoy was lowered into the water with a slip line and tension on the attached float line whilst the ship was moving forwards at 3 knots.

### SWIFT20 (2) and SWIFT21

Due to restrictions placed on the ship due to ice, both of these deployments were done from the side door of the environmental hangar. The second deployment of SWIFT20 occurred at approximately 57°S, 0°E and SWIFT21 was deployed 10 nm further south at 57°07'S, 0°E. The buoys were lowered on a slip line and steadied using the attached float lines. To ensure the safety of the buoys, immediately after release the ship thrust away from the buoy, pushing the buoy into the ice.

### *Recovery*

All recoveries utilised the float line, which was captured using the grappling hook and used to assist in hoisting the buoy on board. Below SWIFT20 (1) and SWIFT20 (2) recoveries are outlined due to slight difficulties encountered. After the buoys were back on deck, they were rinsed thoroughly with freshwater and serial connectors were dried with compressed air. The CF cards were removed in order to download all raw data. They were then left ratcheted upright to fully dry out and the Geoforce tracker was switched off before being replaced in the travel cases.

### SWIFT20 (1)

Due to a loss of communications after SWIFT20 was deployed at the ROAM-MIZ location at 56° S, it became essential to collect the buoy as soon as possible. Using 5 hours of transmitted GPS locations together with a hit with the dog collar from 8 km distance, a bearing and drift speed were estimated for the buoy. Overnight, the SWIFT20 was located using the dog collar and spotted by the strobe light. Due to crew restrictions recovery was not possible at that time, but the new location fix was used to re-locate the SWIFT20 the following morning when recovery was possible. Upon recovery, the cause of the loss of communications was seen to be associated with icing of the communication sensors (see Figure 5.9).



Figure 5.9: SWIFT20 upon recovery from the open ocean deployment. All location devices were covered by ice.

### SWIFT20 (2)

Upon locating SWIFT20 after the second deployment it was evident that it was sandwiched between several pancake ice floes. This complicated recovery as it was difficult to get a line or hook around the buoy but not the ice. The ship used its thrusters to try to move the ice away, however, this ice caught on the keel of the buoy and partially submerged the buoy. Upon recovery, the strobe was no longer functioning and crush damage was evident on the yellow float section.

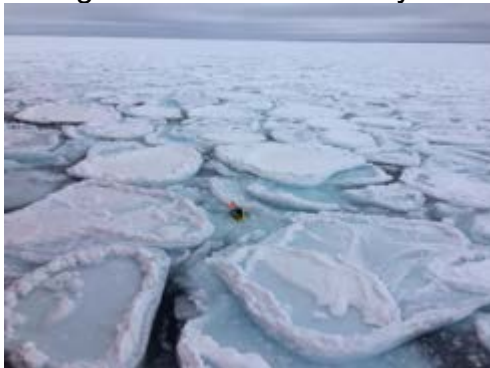
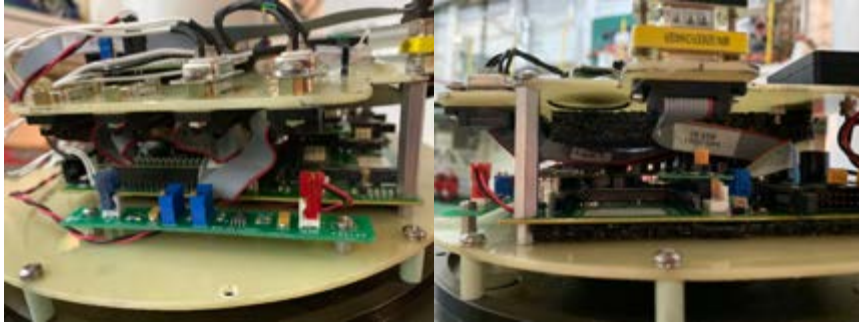


Figure 5.10: SWIFT20 just previous to recovery from the ice mission.

### Complications: SWIFT20

Upon the second deployment of SWIFT20, the DC40 dog collar was not functional, and when the buoy was recovered, the strobe was not flashing and the camera had not taken any images. After the buoy had been fully dried out, these functions were tested again. The strobe light worked immediately, and after an inspection of the circuit board that identified two loose attachments (highlighted below after fixing), the DC40 dog collar also functioned again. The camera capability will be tested back on shore. The loose attachments were likely caused during the initial removal of the CF card to download data, so it is important that in future extra care is taken during this procedure.



CF card holder

Figure 5.11: Highlighting the elements on the SWIFT20 circuit board that can become loose easily.

### *Spring Deployments*

#### SWIFT20

SWIFT20 was deployed upon leaving station on 22/10 at approximately 11pm. It was lowered on a sliprope over the aft A-frame and released on contact with the water as the ship travelled at approximately 0.5 knots.

#### SWIFT21

Unfortunately, during tests on deck, SWIFT21 became dislodged and the Airmar was detached. The Airmar was reattached using epoxy overnight, which resulted in the loss of air temperature and pressure measurements. Wind measurements (speed and direction) were confirmed to still be reliable pre-deployment.



Figure 5.12: The epoxied Airmar on SWIFT21 pre-deployment

SWIFT21 was deployed further into the ice pack, in near consolidated sea ice with minimal wave movement. Upon leaving station, the ship used its thrusters to make a space of open water. SWIFT21 was deployed over the aft A frame with a sliprope and pushed behind the ship.

#### *Recovery*

All recoveries utilised the float line, which was captured using the grappling hook and used to assist in hoisting the buoy on board. After the buoys were back on deck, they were rinsed thoroughly with freshwater and serial connectors were dried with compressed air. The CF cards were removed in order to download all raw data. They were then left ratcheted upright to fully dry out and the Geoforce tracker was switched off before being replaced in the travel cases.



Figure 5.13: The broken Airmar post-recovery on SWIFT20

Both recoveries incurred accidental damage or submersion of instruments. SWIFT20 was located in a region of open water, and, due to 2-3m wave height and rapid surface drift, was swept under the stern hull of the ship. This resulted in a broken Airmar upon recovery. SWIFT21 was located within the marginal ice zone during night operations. Due to the high density of ice floes, the SWIFT buoy was separated from the ship by an ice floe. During recovery, the SWIFT was forced underneath an ice floe, becoming fully submerged. Checks on recovery confirmed no permanent damage.



Figure 5.14: sea ice conditions upon recovery of SWIFT21

### **5.6. Seasonal Ice Mass Balance buoys**

Two Cryosphere Innovations Seasonal Ice Mass Balance (SIMB) buoys were brought to deploy in a region of consolidated ice. These buoys measure 4.8 m in length, approximately 25 cm in diameter and come disassembled into two sections. A thermistor string runs along the outside of the hull, and at the top of the mast is an additional air pressure and temperature sensor. At the top of the mast is an acoustic snow sounder and at the base an acoustic underwater sounder to provide sea ice and snow thickness. One of the buoys (GU#1) was modified to have an extended thermistor string of 10 m in total length, which required attaching to the hull on the ice.

#### *Deployment*

Both SIMBs were activated on the foredeck to confirm Iridium transmissions before they were moved onto the sea ice. The basket hoist was used to transfer scientists and the modified SIMB hull onto the ice, with a second trip to bring the thermistor string to the ice. An area of flat, undeformed ice was selected for the deployment of the SIMB, approximately 2.5 m from a region of sea ice coring undertaken by the sea ice team. The hull was assembled and the two sounders were confirmed to be parallel. As the thermistor string was modified, the power fitting was attached at the head of the mast, and the power cable was attached to the ballast at the base of the hull using clamp bands. The lower half of the thermistor string hung loose.



Figure 5.15: Ice floe that the SIMB was deployed on (in the location of the right-hand group of people)

#### *Winter deployment*

Originally a 25 cm soil auger was brought to core the hole required by the SIMB. However, due to low temperatures the petrol motor used to power the auger did not work, and it was necessary to switch to the smaller 10 cm battery powered ice auger used for the coring. Three cores were originally drilled, with each core hole rapidly freezing over whilst the next holes were being drilled. Upon testing it was found that the three holes were not big enough to fit the SIMB with sounder at the base, and two further holes were drilled. With all 5 scientists assisting with the movement of the SIMB, the buoy was lowered successfully through the ice. However, its final resting position showed a small degree of tilt. This was not measured. Details of floe, sea ice thickness and height of sensors are listed below.

*Floe description:* The ice floe selected was approximately 50 m in diameter and was a consolidation of smaller pancake floes. A pancake of >5 m was used for both the coring operations and SIMB deployment. The closest ridge on the floe was 1.5 m from the SIMB.

*Sea ice thickness:* **0.89 m**

*Snow thickness:* 2 cm

*Height above snow of upper acoustic sounder:* 1.35 m

*Height above ground of top of thermistor string:* 0.92 m



Figure 5.16: Final position of the SIMB, showing a slight tilt. LCB for scale (1.55 m).

### *Spring deployment*

Upon arrival at the drill site, the sea ice team took measurements of snow depth and sea ice thickness. Despite warmer deployment temperatures, the 10cm auger was used to drill the deployment hole during the spring cruise. The drill site was situated furthest away from the ship in order to ensure the least disturbance (approximately 20-30m away). Six core holes were drilled in quick succession, and the SIMB was lowered into the resulting space before it could refreeze. Measurements were made of the height of instruments above the sea ice and snow, with details shown below. There were several other instruments situated at the same location, which are also shown in Figure 17.



Figure 5.17: SIMB post-deployment, LCB for scale.

*Floe description:* The sea ice was well consolidated and the floe used for the SIMB deployment was over 100 m, with no significant ridges visible.

*Sea ice thickness:* **0.455 m**

*Snow thickness:* 11 cm

*Height above snow of upper acoustic sounder:* 1.20 m

*Height above ground of top of thermistor string:* 1.04 m

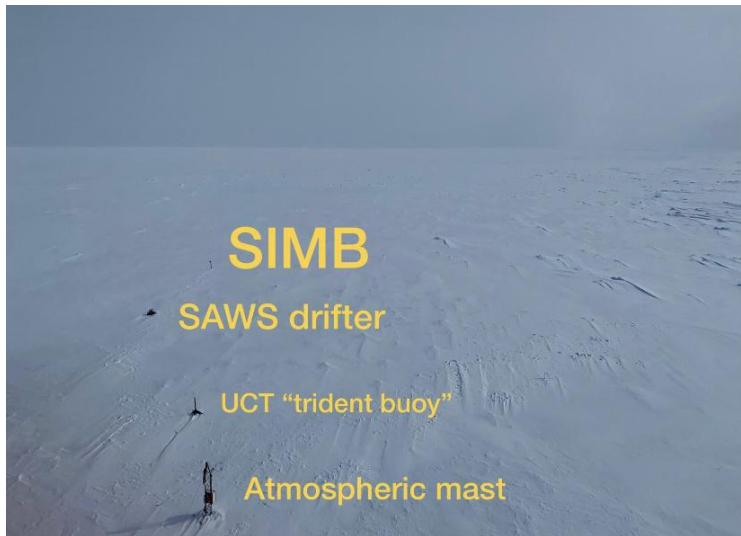


Figure 17: SIMB in location (note large sea ice expanse), together with three other instruments.

## 5.7. High resolution Underway CTD survey at the edge of the Marginal Ice Zone

### 5.7.1. Motivation

Submesoscale flows, energized by fine-scale ( $O(1-10\text{km})$ ) horizontal gradients in density are ubiquitous in the world's oceans. Submesoscale eddies have been modeled and observed at the sea-ice edge in the Arctic ocean. Ongoing observations with Seagliders in the Antarctic Marginal Ice Zone, as part of the ROAM-MIZ project has already started to observe the role that freshwater input from recent sea-ice melt has on setting up horizontal mixed layer density gradients. While Seaglider profiles average a horizontal resolution of  $\sim 3-4\text{km}$ , the internal Rossby radius of deformation at  $55-60\text{ S}$ , is  $< 2\text{km}$ . By deploying the UCTD in a tow-yo method, the horizontal resolution is increased to  $\sim 300\text{m}$ . The aim of the survey is 1) to capture a 3D high-resolution snapshot of the physics of the upper ocean near the Antarctic Marginal Ice Zone and, 2) to augment and compare the data observed by the lower resolution Seaglider profiles collected in the same region.

### 5.7.2. Methods

#### Underway UCTD

A 90560 UCTD (serialnumber: 70200107) was used. The sensors were last calibrated on the 25<sup>th</sup> March 2012 (Temperature, Conductivity) and 21<sup>th</sup> March 2012 (Pressure). Preparations before the deployment followed guidelines from Oceanscience [Oceanscience UCTD Underway Profiling System, User guide and Warranty].

The UCTD was deployed from the port side corner of the lower aft deck of the RV SA Agulhas II to measure temperature and conductivity at a rate of 16Hz using continuous tow-yo casts, with the ship maintaining a speed of 2-3 knots.

For deployment, wire was laid out first, then the probe was carefully lowered to the water surface and the clutch was set to off, so it unspooled. The time was noted when the

downcast began as the probe touched the surface. 150 seconds later the probe reached a depth of about 250m and was slowed down with the break on the winch.

Then the clutch was set to haul in the wire and bring the probe back on surface. When the probe was spotted at the surface and the start of red wire was observed on the winch spool, the winch clutch was switched off again. This was repeated along the whole transect.

At the end of each transect the probe was retrieved by hauling in the wire until it was possible to grab the wire. The probe was then positioned on the side of the vessel and wire was slowly hauled in more until it was possible to grab the probe itself. After the Probe was back on board it was detached from its spooling tail, rinsed with milliQ water, dried, connected for charging and connected to the computer via bluetooth for data transfer.

For data download and to check the battery voltage Sea-Bird Electronics, Inc., 2007 software UCTDTerm 1.1 was used.

## Survey

The UCTD survey was carried out from 11am UTC on the 20th October 2019 to 7pm UTC on the 22<sup>nd</sup> of October 2019, along six transects of 20 km in a box centered between 55S-55.17°S and 0.3°E-0.15°E, with a distance of 3km between transects. The total ship time used for the survey was 26.5 hours. The actual time that the UCTD was sampling was 20 hours, during which an actual distance of 116km was covered horizontally in the water. The final transect was truncated as the winch broke.

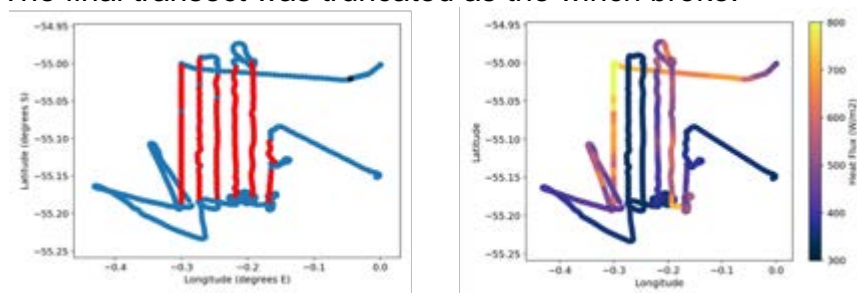


Figure 5.19: a) Survey track (blue dots) completed by RV SA Agulhas with red dots indicating the locations when the UCTD was in the water. b) Heat Flux throughout the survey

## Calibration of salinity sensor

The UCTD conductivity sensor was calibrated with the MIZO CTD station which in turn was calibrated with salinity bottle samples.

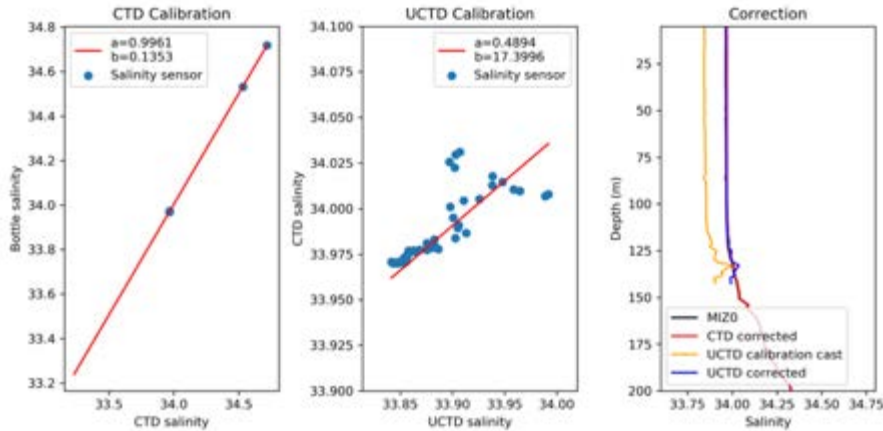


Figure 5.20: Calibration of Conductivity sensor

## Data Processing

The data was initially processed using the SBE Data Processing software, Version 7.19, in which the CTD was aligned with the recommended advance value for the temperature sensor of 0.09, a thermal mass balance correction was also applied using the coefficients  $\alpha=9.5$  and  $\tau$  ( $1/\beta$ ) = 0.12. These values were determined the best after running a sensitivity test on recommended parameters for the UCTD. However, further processing (following Ullman and Hebert, 2013) could improve this correction. Salinity, density and velocity were derived from the raw data and the data was converted to ACSII format.

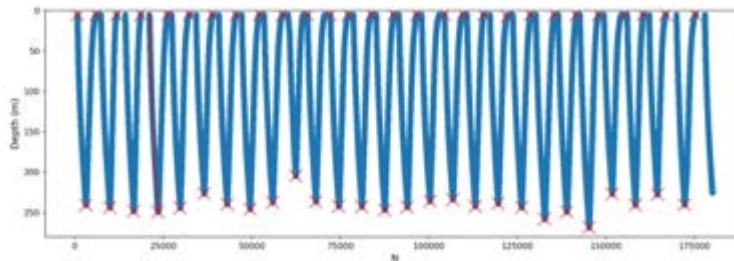


Figure 5.21: Example of tow-yo sampling pattern (Transect 4)

### 5.7.3. Initial results

Five and a half transects were completed consisting of a total of 306 casts, with four full transects (2-5). The diurnal cycle is reflected in temperature, consistent with the ship-board heat flux sensor (Fig 2 ). A fresh water mixed layer eddy is present in all the transects towards the southern end of the survey area. Colder water is also observed to the south and beneath this freshwater eddy (Fig 4,5). On the northern front of the eddy, a warm water tongue is observed extending from below the mixed layer to the surface.

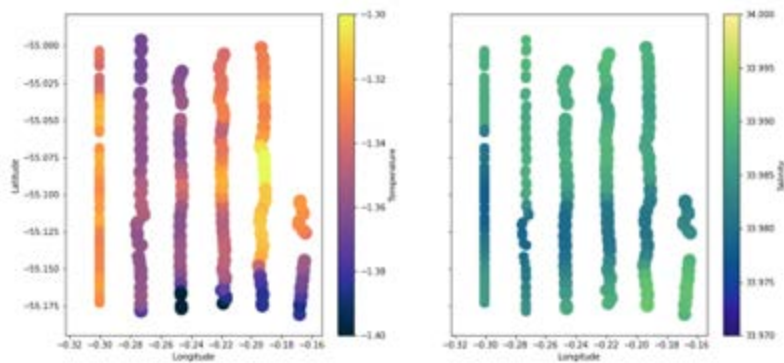


Figure 5.22: 10m temperature and salinity plots along the UCTD transect.

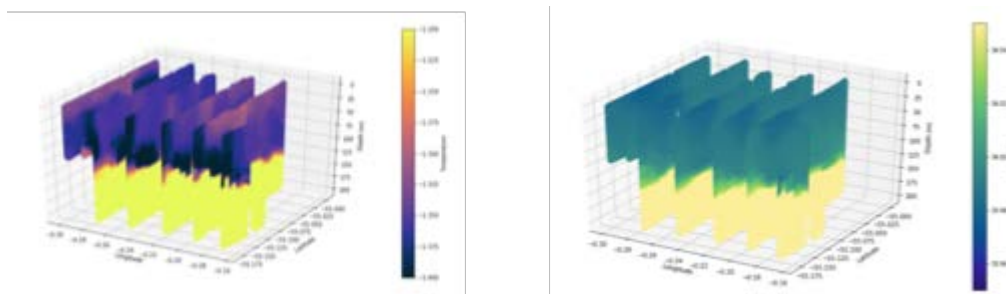


Figure 5.23: 3D plot of temperature and salinity

#### 5.7.4. Challenges and limitations

While the UCTD survey was successful a number of challenges were encountered during deployment as well as in the post-processing phase. During the deployment we were limited by only having one UCTD probe, making it imperative to charge the battery after each transect and therefore decreasing the time available for deployment. Only having one probe also increased the risk of having to cancel the survey if the probe was lost. All the data is stored on the probe and not connected live to the ship so that if the probe is lost so is the data. Applying the level wind and switching the clutch to full when rewinding the probe is also very important as this ensures that the nylon wire does not get entangled, as occurred during one cast after which we had to retrieve the probe to untangle the cord. The winch was both old and the very cold (sub-zero) temperatures caused the winch to be stiff and finally to break during the sixth transect. High winds and large swell which result in increased tension in the wire and winch increasing likelihood of loss of the wire or the winch breaking further limited the survey towards the end where we planned to cut short the survey with an approaching storm.

In post-processing, the inconsistent descent time of the probe in tow-yo mode complicated the thermal-lag correction. The first transect also did not capture the thermocline due to the longer descent time induced by the tow-yo mode as well as the clutch of the winch being stiff, meaning that the clutch had to be off during descent and not on slip as recommended by the guidelines. The lack of a flight model or time stamps during deployment result in inaccurate estimations of distance covered during casts.

Finally, the probe cannot be in contact with ice which limited the proximity to the marginal ice zone that we could survey in.

#### **5.7.5. Conclusions**

The survey was successful producing six transects of which four were full transects of ~20km consisting of 306 up and down casts to an average depth of 250m, with average horizontal resolutions between casts of 380.45m +- 303.37m. Clear horizontal structure in the mixed layer is observed, likely linked with recent ice melt, however this remains to be conclusively determined. It is recommended for future deployments that a spare probe is procured and the winch is either replaced or refurbished.

## 6. TEAM MICROBIOME

**TABLE 6.1. Stations sampled during winter and spring cruises. Stable isotope stations indicated by \*.**

<b>DATE</b>	<b>STATION</b>	<b>SDS</b>	<b>Leg</b>	<b>LATITUDE</b>	<b>LONGITUDE</b>	<b>BOTTOM DEPTH</b>
19 JULY 2019	SOAK	AM01092	S	-35.3841	16.6134	N/A
21 JULY 2019	SAZ	AM01093	S	-43.00057	8.49862	N/A
21-22 JULY 2019	SAZ2	AM01094	S	-45.00095	7.0858	N/A
25 JULY 2019	GT1	AM01097	S	-56.0012	0.00185	1501.1
26 JULY 2019	MIZ1A	AM01100	M	-57.00007	-0.00313	500.7
27 JULY 2019	MIZ2A	AM01104	M	-57.34503	-0.0028	499.9
29 JULY 2019	GT2*	AM01108	N	-54.00088	0.00123	2538.2
31 JULY 2019	GT3	AM01109	N	-51.40167	0.00115	2690.7
1 AUGUST 2019	GT5*	AM01110	N	-46.9999	4.4989	4079.4
2 AUGUST 2019	GT6	AM01110	N	-45.00012	6.59983	4342.7
3 AUGUST 2019	GT7*	AM01111	N	-43.00008	8.50035	3967.5
4 AUGUST 2019	GT9	AM01112	N	-38.59913	11.80077	4667.1
5 AUGUST 2019	GT10	AM01113	N	-36.29938	13.30187	4672.0
13 OCTOBER 2019	SOAK	AM01115	S	-35.76973	14.85912	N/A
16 OCTOBER 2019	SAZ2	AM01116	S	-45.00015	6.60005	4000
19 OCTOBER 2019	PUZ	AM01118	S	-54.0002	0.00078	N/A
24 OCTOBER 2019	MIZ1	AM01123	E	-59.3248	0.06662	500
24 OCTOBER 2019	MIZ2	AM01124	E	-58.98332	0.01188	500
27 OCTOBER 2019	MIZ3	AM01125	E	-59.00072	3.01717	N/A

29 2019	OCTOBER	MIZ5	AM0112 7	E	-59.3645	8.15892	N/A
30 2019	OCTOBER	MIZ6	AM0112 8	E	-59.47255	10.88933	N/A
30 2019	OCTOBER	MIZ7	AM0112 8	E	-59.47255	10.88933	N/A
01 2019	NOVEMBER	MIZ8	AM0112 9	E	-58.5488	17.93818	N/A
08 2019	NOVEMBER	GT1	AM0113 5	N	-55.99467	-0.00682	499.1
09 2019	NOVEMBER	GT2*	AM0113 6	N	-54.00018	-0.00035	2398.7
10 2019	NOVEMBER	GT3	AM0113 8	N	-51.3996	0.00072	2605.6
11 2019	NOVEMBER	GT4	AM0113 9	N	-49.3017	2.30265	3799.7
12 2019	NOVEMBER	GT5	AM0114 0	N	-47.0006	4.49988	3800.3
14 2019	NOVEMBER	GT6	AM0114 2	N	-44.99932	6.60022	4200.3
13 2019	NOVEMBER	GT7*	AM0114 1	N	-43.00007	8.50007	3804.4
16 2019	NOVEMBER	GT8	AM0114 4	N	-40.00048	10.80165	4677.6
17 2019	NOVEMBER	GT9*	AM0114 5	N	-38.6026	11.79955	5000.8
18 2019	NOVEMBER	GT10	AM0114 6	N	-36.29947	13.30282	4800

## 6.1. UNRAVELLING THE ROLE OF IRON ON MICROBIAL COMMUNITIES AND CHEMOAUTOTROPHS FROM THE DEEP SOUTHERN OCEAN

### 6.1.1. Introduction and Rationale

The role and quantitative contribution of chemoautotrophic microbial (picoplanktonic) communities in ocean systems is largely unknown. Previous studies have shown that iron fertilization results in increased productivity of marine phytoplankton. However, little work has been done to elucidate the effect of iron on deep-sea microbes. While the chemical form of iron in high nutrient low chlorophyll (HNLC) regions such as the Southern Ocean remains unknown, it is well established that molecular speciation affects microbial competition for iron uptake. The importance of iron for marine ecosystems and its role in the fixation of CO<sub>2</sub> makes the study of this trace metal of great interest.

### 6.1.2. Aims and Objectives

This experiment aims to assess how trace metals, specifically iron (Fe), influence microbial community composition and functionality using a metagenomic approach combined with a trace metal profile.

### 6.1.3. Research approach and methodology

#### *Winter*

An on-board mesocosm experiment was set up to observe induced changes in iron concentration in two different deep-sea microbial communities. Seawater was collected at two depths (1 200 m and 4 171 m) at the SAZ2 site indicated in Table 1 (AM01094), using Teflon-coated GO-Flo bottles mounted on a trace metal-clean rosette system. 8L samples were incubated in 10 L LDPE carboys for a total duration of 96 hours. Per depth, 5 mesocosms were treated with 0.5 nM FeCl<sub>3</sub>, 5 with 1 nM FeCl<sub>3</sub> with 5 non-iron containing controls for the total experiment. Mesocosms were incubated in the dark at 4°C, with sub-sampling taking place after 1 hour, 36 hours and at the termination point of the experiment. 125 mL of the seawater incubation was collected from each mesocosm in order to measure dissolved iron. Water from each mesocosm was aliquoted for downstream analysis for flow cytometry (preserved in formaldehyde at a final concentration of 2%), single cell genome sequencing (preserved in glycerol-Tris-EDTA buffer) and enzyme activity assays. These samples were stored at -20°C for downstream analysis. Remaining water up to a volume of 3 L was filtered via a dual filtration mechanism and vacuum pump through a 0.22 µm Polyethersulfone (PES) filter and the filters stored at -20°C for microbial community analysis at both the DNA and RNA level.

#### *Spring*

A similar mesocosm incubation was set up to observe changes solely in deep sea microbial community composition induced by the addition of iron. Trace metal free seawater was collected at approximately 4000 m at the November SAZ2 site indicated in Table 6.1 (AM01116), as previously described. 8L samples were again incubated in 10 L LDPE carboys in the dark at 4°C, with sub-sampling taking place after 1 hour, 36 hours and at the termination point of the experiment 96 hours. Two of the mesocosms were terminated at the start of the experiment to function as Baseline samples. Nine mesocosms were inoculated with 0.5 nM FeCl<sub>3</sub>, while 1 nM FeCl<sub>3</sub> was added to another 9 mesocosms. No iron was added to 6 mesocosms, which functioned as a control at each subsampling point.

At each subsampling point water from the mesocosms was aliquoted for dissolved iron measurement, nutrient analysis, flow cytometry and single cell genomics as previously described. To be able to measure microbial iron uptake, 4 × 750 mL water from the control mesocosms was decanted and spiked with either 0.5 nM or 1 nM of the iron isotope <sup>55</sup>FeCl<sub>3</sub>. The remaining water from all incubations (up to a volume of 5 L) was filtered as before for subsequent microbial community analysis at the DNA level.

## 6.2. VIRIO- AND PICO-PLANKTON IN THE SURFACE WATERS OF HYDROTHERMAL VENT SYSTEMS IN THE SOUTHERN OCEAN

### 6.2.1. Introduction and Rationale

Virio- and pico-plankton are very small (<2.0 µm), abundant and diverse life forms in the ocean, that facilitate essential marine biogeochemical cycles. Marine viruses (i.e. virus-like particles; VLPs), are estimated to have a global ocean abundance of  $10^{30}$ , making them the most abundant life form in the ocean. Viral induced lysis via infection, contributes significantly to the cell death of autotrophic and heterotrophic plankton, and results in a process called a “viral shunt”. This ecological event occurs when cellular contents are expelled into the environment, diverting organic material (e.g. carbon, nitrogen and phosphorus) into dissolved pools rather than it being channeled along trophic levels. About 6-26% of the photosynthetically fixed carbon is “shunted” to the dissolved organic matter pool by viral lysis in the pelagic zone. Viruses infect autotrophic picoplankton (Prochlorococcus, Synechococcus and picoeukaryotes), which are the most abundant and ubiquitous primary producers in the epipelagic zone, and they account for >50%, and at times >80%, of the marine primary production. In addition, they infect heterotrophic picoplankton communities which carry out most of the extant ecological processes. Viral dynamics are influenced by environmental and biological factors which modify infectivity, degrade or remove virus particles, adversely affect adsorption to host and proliferation in the host cell, e.g. temperature, UV, nutrients, host physiology. However, the mechanism behind how physico-chemical factors regulate virus dynamics and host–virus interactions is poorly characterised, particularly with regard to seasonality that is likely to influence the microbial ecology.

### **6.2.2. Aims and Objectives**

This study aims to unveil the factors regulating viral dynamics and host-virus interactions of the hydrothermal vent related waters in the SIZ zone near the Antarctic ice margin. To accomplish this, functional metagenomics shall be used to unveil the effect of depth and water masses on virio- and pico-plankton interactions in 2 hydrothermal vent regions. Further, virus precipitation will be performed on the surface water in both hydrothermal sites identified during previous cruises.

### **6.2.3. Research approach and methodology**

During both winter and spring cruises, 20 L of underway water was collected at both GT1 (AM01097, AM01135) and GT2 (AM01108, AM01136) (Table 1, Figure 1), for virus precipitation with Iron (III) Chloride hexahydrate upon return to the University of Pretoria.

### **6.2.4. Progress/preliminary results**

Underway water was filtered via a dual filtration technique using 0.4 µm and 0.2 µm PES filters, and the filters stored at -20°C for downstream DNA extraction as part of a PhD project (see report #6). The remaining water has been stored at 4°C for incubation in Iron (III) Chloride hexahydrate.

## **6.3. DISENTANGLING THE ROLE OF CHEMOLITHOAUTOTROPHS (PICOPLANKTON AND FEMTOPLANKTON) IN THE SEQUESTRATION OF CARBON DIOXIDE**

### 6.3.1. Introduction and Rationale

Marine microbial communities play an underexplored role in the sequestration of atmospheric carbon dioxide. Studies show that there is a discrepancy between biological carbon demand in the deep ocean and the amount of sinking carbon species. Here, we propose that chemolithoautotrophs (microorganisms capable of fixing carbon in the dark by oxidising inorganic compounds) are drivers of carbon sequestration. Our mechanistic understanding of how shifts in microbial communities due to seasonal change affects the rates of carbon fixation and uptake remains ambiguous. Chemolithoautotrophic archaea, bacteria and microbial “dark matter” are involved in rate limiting steps such as iron, sulphur and ammonia oxidation needed to fuel carbon fixation. As a result, their role in global carbon sequestration may be more important than originally assumed. Using classical techniques (isotope incorporation rates) and targeted metagenomics in conjunction with stable isotope probing, we aim to measure the qualitative and quantitative rate of carbon fixation in the Southern Ocean during winter and spring. We hypothesise that changes in seasonal nutrient input and quality does not affect the rate of carbon fixation and uptake, and rather results in the enrichment of specific chemolithoautotrophs.

### 6.3.2. Aims and objectives

The aim of this project is to study the role and contribution of dark carbon fixing microorganisms towards the sequestration of carbon in the Southern Ocean by following the objectives listed below.

- determine the quantitative rates of dark carbon fixation the Southern Ocean zones
- determine the taxonomy and biochemical pathways used for carbon fixation.

### 6.3.3. Research approach and Methodology

Seawater was collected for nutrient and chemistry analysis, flow cytometry and isotope incorporation productivity assays at 12 stations (GT1-10, MIZ1-2) (Table 1, Figure 1). For all stations, seawater was collected from 8 depths which were denoted as surface (5-200m) and deep (500m-deepest depth).

#### ***Stable isotope probing***

Four litres of water was collected via the Niskin CTD at each station (GT2, GT5, GT7 in winter, GT2, GT7, GT9 in spring) at depths of 300 m, 1500 m and the deep zone. Seawater was collected for nutrient and chemistry analysis, flow cytometry and isotope incorporation productivity assays. Thereafter, SIP incubations were prepared by spiking 1L subsamples with 4 mM of C<sup>14</sup>-Sodium Carbonate for 24hrs. The microbial water samples were filtered through membrane filters (0.2 µm) using a dual-filtration system and a vacuum pump. A further 30 L of water was collected from the marine snow catcher during spring cruise at 10m below the mixed layer in the suspended fraction (GT1, GT3, GT10). Here, 10L of water was incubated with 230 µM of C<sup>14</sup>-Sodium Carbonate for 48hrs

and filtered as before. All SIP filters were stored at -80°C. Samples for nutrient analysis were stored at 4°C. Filters for DNA extraction were stored at -20°C.

### ***Bacterial and Archaeal Productivity (at all stations, 8 depths)***

Productivity was determined by incubating samples with Leucine and C<sup>14</sup>-Sodium carbonate to measure heterotrophic and autotrophic productivity respectively. For Leucine, 1.5 mL samples in triplicates (two experiments and one control) were spiked with 5 nM of Leucine with the addition of 80 µl to the killed control. Incubation were performed at ±2°C *in-situ* temperature for 1hrs surface samples and 24hrs for deep samples. The incubations were terminated by the addition of 80 µl TCA. Archaeal productivity was performed by spiking 45 mL samples with 3 µCi of C<sup>14</sup>-Sodium carbonate. 2% formaldehyde was added to the control. Incubations were performed at ±2°C *in-situ* temperature for 48hrs surface samples and 72hrs for deep samples. The experiments were terminated by the addition of 2% formaldehyde and filtered through a 0.22 µm membrane filters.

### ***DNA extraction, sequencing and data analysis***

All downstream analysis will be performed at the University of Pretoria following previous methods.

#### **6.3.4. Progress/preliminary results**

Bacterial heterotrophic production (BHP) during winter was measured using a Tri-Carb T2800 liquid scintillation analyser. The results reveal that BHP was two orders of magnitude lower than measurements from studies conducted at the Pacific and North Atlantic Oceans. We observed a general decrease in BHP from surface to deep samples ranging from 0.2 to 0.001 nmolC<sup>-1</sup>L<sup>-1</sup>d<sup>-1</sup> (dilution factor of leucine = 2, Standard deviation ≤ 30) respectively. The relatively low values of BHP suggest that autotrophic modes of growth are utilised by microorganisms in which inorganic nutrients may be sources of energy rather than organic molecules.

## **6.4. NITRITE OXIDISING BACTERIA IN THE SOUTHERN OCEAN**

### **6.4.1. Introduction and Rationale**

Microorganisms are present in all ecosystems, including the world's oceans. Marine microbial communities play a key role in the oceanic carbon cycle. Phytoplankton and photosynthetic bacteria have been studied widely. However, the involvement of bacteria in carbon cycling in the mesopelagic and bathypelagic zones of the ocean remains to be explored. To perform metabolism, chemoautotrophic prokaryotes use inorganic carbon and energy obtained from the oxidation of inorganic compounds such as sulphur and nitrite, among other compounds. The role of nitrite oxidising bacteria in carbon uptake in the Southern Ocean is partially known and needs to be further investigated.

### 6.4.2. Aims and Objectives

The aim of the study is to investigate the role of nitrite oxidising bacteria in the Southern Ocean during two seasons: Winter and Spring. In order to achieve this the potential taxa and functions of chemolithotrophs linked to carbon assimilation process in the Southern Ocean will be studied. Thereafter, the role of nitrite oxidising bacteria in carbon fixation processes will be examined by the use of single cell genomics. Finally, the contribution of nitrite oxidising bacteria to total inorganic incorporation will be investigated by catalysed reporter deposition – fluorescent in situ hybridisation combined with microautoradiography (MICRO-CARD-FISH).

### 6.4.3. Research approach and methodology

#### *Winter*

Water samples were collected at 8 different depths (5 m, 50 m, 200 m, 500 m, 1 000 m, 1 250 m, 1 500 m, deep) using both Niskin and GO-Flo CTD samplers at stations MIZ1, MIZ2, and all stations from GT1 to GT10 (Table 1, Figure 1). At each depth 9 mL of water was preserved in formaldehyde (final concentration of 2%) bacterial and archaeal cell counting by flow cytometry. An additional 6 mL was aliquoted and fixed with glycerol-Tris-EDTA for fluorescence-activated cell sorting (FACS), followed by single cell sequencing, to study the potential functionality of nitrite oxidising bacteria in the Southern Ocean. Moreover, at stations GT2, GT5 and GT7 50 mL of sample was collected and fixed with formaldehyde to a final concentration of 2%, followed by filtration and freezing at -20°C for micro-CARD-FISH analysis.

#### *Spring*

The winter cruise sampling strategy was replicated during spring, collecting aliquots for flow cytometry, FACS and single cell genomics at the same stations and depths. These were preserved and stored as previously described. Samples for micro-CARD-FISH were collected at six stations (GT1, GT2\*, GT4, GT5, GT7\*, GT9\*). Each station was located in a different Southern Ocean zone and 3 (marked with \*) correlated with stable isotope probe (SIP) metagenomics studies (see report #3) (Table 2).

**Table 6.2. Details of the micro-CARD-FISH sampling depths and stations. Note that at SIP stations (see report #3) samples were collected at 300 m instead of 200 m to coincide with the metagenomic data.**

<b>STATION ID</b>	<b>OCEAN ZONE</b>	<b>DEPTHS SAMPLED</b>
<b>GT1</b>	SIZ	200 m, 500 m, 1500 m, bottom
<b>GT2</b>	PUZ	300 m, 500 m, 1500 m, bottom
<b>GT4</b>	PF	200 m, 500 m, 1500 m, bottom

<b>GT5</b>	PFZ	200 m, 500 m, 1500 m, bottom
<b>GT7</b>	SAZ	300 m, 500 m, 1500 m, bottom
<b>GT9</b>	STZ	300 m, 500 m, 1500 m, bottom

The micro-CARD-FISH sampling and treatment procedure required three 50 mL samples to be collected per depth (two replicates and one killed control). Each was spiked with C<sup>14</sup> (final concentration 100 µCi), incubated for 30 hours, fixed with formaldehyde (final concentration 4%) and filtered through a polycarbonate membrane filter of 0.22 µm pore size. The filters were stored at -20°C to be further analysed by catalysed reporter fluorescence *in situ* hybridisation using specific oligonucleotides for nitrite oxidising bacteria, followed by microautoradiography.

## **6.5. ELUCIDATING MICROBIOMES ASSOCIATED WITH THE DEGRADATION OF MICROPLASTICS IN THE SOUTHERN OCEAN**

### **6.5.1. Introduction and Rationale**

Microplastics pollution in marine environments as an emerging field of research has gained much concern due to ecotoxicological risks posed on the associated biota and ecosystem. With small sizes of less than 5mm, microplastics can easily interfere with the marine food web through ingestion and transfer across trophic levels. More so, they may act as carriers of chemical pollutants or pathogens. Most evaluation of the distribution of microplastics in marine environments have been within the context of the Northern hemisphere. Hence, the status of microplastics pollution in the Southern Ocean remains unclear, especially as it relates to microbial degradation.

### **6.5.2. Aims and Objectives**

The main aim of this project is to elucidate the effects of microplastics on microbial communities and their functions in the Southern Ocean by:

- Assessing the distribution of microplastics in SO
- Identifying taxa linked with biodegradation of microplastics
- Bioprospecting of enzymes involved in microbial degradation

### **6.5.3. Research approach and methodology**

#### ***Winter***

Seawater was collected from a depth of 5m using the Niskin CTD at all stations on the northbound leg from Antarctica to South Africa (Table 1, Figure 1). Water was filtered through 0.45 µm and 0.22 µm pore filters, which were stored at -20°C. Samples for chemistry and nutrient analysis were stored at 4°C.

Aliquots were also collected for single cell genomics (2 mL), flow cytometry (10 mL) and enzyme assays (200 mL).

#### ***Spring***

10 L of water was sampled from the underway inflow system at stations PUZ, GT1 – GT10, as well as from the suspended fraction of marine snow catchers deployed at both 10 and 110m below the mixed layer depth at stations PUZ, MIZ1, MIZ3, MIZ5 and GT1, GT3, GT5, GT7, GT9. Ice cores collected from MIZ3 and MIZ7 and snow collected from MIZ6, MIZ7, 8MIZ were melted at 4°C. For all samples collected, 50 mL of water was stored in falcon tubes at -20°C. All water samples were filtered through Whatman Glass Fiber filters with pore size of 0.5 µm and subsequently through 0.2 µm polycarbonate filter which were then stored at -20°C. Glass fiber filter samples and 50 mL samples collected in falcon tubes were stored at -20°C for identification and polymer characterisation of microplastics using FTIR (Fourier Transform Infra-Red) or Raman Spectroscopy /

Microscopy. The 0.2 µm filter samples will be used for DNA extraction and metagenomics analyses to elucidate the microbiome associated with the degradation of microplastics. At station PUZ, two independent microcosm experiments were initiated for the duration of the cruise. They consisted of 2L of water collected in triplicate from the underway system and marine snow catcher and were incubated at 4°C for 30 days. Test incubations (2 × 2 L) were amended with microplastics (polyethylene and polyethylene terephthalate particles), with glass beads as control (1 × 2 L). Due to filtering time constraints, after termination, the microcosms were transported back to the University of Pretoria for further processing.

#### **6.5.4. Progress/preliminary results**

Samples collected with 0.45 µm filters during the winter cruise expedition have been analysed for polymer detection and characterisation using FTIR spectroscopy at the National Centre for Nano-structured Materials facility in CSIR, Pretoria. Result spectra are still being compared with known libraries.

### **6.6. MOLECULAR CHARACTERIZATION OF KETOSYNTHASE GENES FROM THE SOUTHERN OCEAN**

#### **6.6.1. Introduction and Rationale**

The rising antibiotics resistance has necessitated the quest for the discovery of novel antibacterial compounds (polyketides) that can salvage the problem. Oceans, which cover more than 70% of the earth, are presumed to be a source of microorganisms with the potential to produce these valuable novel products (polyketides and nonribosomal peptides). Therefore, the marine environment is currently being explored and the Southern Ocean is presumed to harbour these compounds because of its unique nature. Polyketide synthase (PKS) and Non ribosomal peptide synthetase are enzymes that mediate the biosynthesis of polyketides with enormous structural complexity and chemical nature by combinatorial use of various domains. Ketosynthase and Adenylation (A) domains are the most phylogenetically conserved domains and can therefore be used to determine their diversity. Hence, characterization of both ketosynthase and adenylation genes in the Southern Ocean waters can reveal compounds of great medicinal importance.

#### **6.6.2. Aims and objectives**

The primary aim of this project is to characterize ketosynthase and adenylation genes in the Southern Ocean (SO). This will be achieved through

- Metagenomic DNA extractions from SO depth profile samples collected from MIZ1, MIZ2, GT1-GT10
- Targeted amplicon sequencing of KS domain and A domain
- Bioinformatic screening for KS and A
- Fosmid library construction of certain zones in SO
- Screening of the fosmid libraries

### **6.6.3. Research approach and methodology**

#### ***Winter***

A total volume of 3 L seawater was collected from depths of 1500 m and 3750 m using the GO-Flo CTD at MIZ1, MIZ2, GT1-GT10 stations (Table 1, Figure 1). An additional 5 L was collected at 5 m, 50 m, 200 m, 500 m, 1 000 m, 1 250 m, 1 500 m using the Niskin CTD. Sample aliquots were retained for enzyme assay measurements, flow cytometry, single cell genomics, and physico-chemistry parameters (DIC, DOC, TIC, TOC). The remaining water was filtered through 0.45 µm and 0.22 µm PES filters which were stored at -20°C for DNA extraction and metagenomic sequencing. Seawater samples for chemistry and nutrient analysis were stored at 4°C. Samples for single cell genomics and enzyme assays were all stored at -20°C. Flow cytometry water was preserved at a final concentration of 2% formaldehyde and stored at -80°C. An additional 20 L of water was collected from the underway at GT1 and GT2 and stored at 4°C for filtering upon return to the University of Pretoria.

#### ***Spring***

Water was collected from the 8 previously specified depths via the Niskin CTD at 12 stations mentioned above (Table 6.1). An additional 20 L of seawater was collected from the mixed layer of the MIZ3 (from the marine snow catcher suspended fraction) and underway at stations PUZ, GT1, GT2 and GT3 for formed library construction, filtered through 0.45 µm and 0.22 µm PES filters which were also stored at -20°C.

### **6.6.4. Progress/preliminary results**

DNA extraction has been performed on all winter cruise DNA filters. Further, winter cruise underway water has been filtered as previously described and the filters stored at -80°C.

### **6.7. Highlights and concerns of the research accomplished during the winter trip**

The Ocean Microbiome team succeeded in obtaining a sufficient number of stations spanning the SAZ, PF, PUZ, PFZ and MIZ zones of the Southern Ocean, successfully sampling the water column at 11/13 previously indicated sampling stations along the latitudinal transect. While 2 stations were skipped (GT4 and GT8) due to inclement weather and poor timing for our return to the SA coastline, we believe the extant samples offers the opportunity to investigate how biogeography and depth impacts the microbial communities and their quantitative and qualitative contributions to microbial processes during the winter. We look forward to characterising these winter communities and spring communities and their abundances in the next SCALE expedition, for a clearer picture on seasonal affectations on the Southern Ocean microbiome.

### **6.8. Highlights and concerns of the research accomplished during the spring trip**

As a result of great weather conditions and some strategic station re-organising, all stations that were important to the team were sampled at.

However, at the SAZ2 station we encountered a miscommunication between CTD operators and scientists that led to incorrect sampling for the mesocosm study. This resulted in experimental re-design and a degree of incomparability to the winter samples and analysis that was not necessary.

Due to station scheduling and fast inter station sailing, very often, members of the team had to go 24-36 hours without sleep, having done repetitive manual labour for 6- 8 hours, which isn't optimal for sample acquisition as technical errors increase with a decrease in cognitive ability. Further, the team has expressed that it felt like excellent, accurate and contamination-free science was less of a priority than rushing to the next station, which should not have been the case given the abundance of extra sailing days.

Nevertheless, the team has already proceeded with land based processing and analysis and look forward to the results of this informing their MSc, PhD and postdoctoral research.

Team Microbiome would like to thank all the organisers, DEFF, SA Agulhas II & crew, and our PI for the amazing opportunity afforded to us via SCALE.

## **7. TEAM NATM & NOCE**

### **7.1. Nitrogen cycling in the Southern Ocean**

#### **7.1.1. Introduction**

A key uncertainty facing our current understanding of the Earth's climate system is the role played by biology in the Southern Ocean. Observations show that nitrate (an essential macro-nutrient to phytoplankton) is never fully consumed in Antarctic surface waters, likely due to a combination of iron and light limitation of phytoplankton (Martin et al. 1991; Sunda and Huntsman 1997), although the role of planktonic community composition remains poorly understood. On an annual basis, phytoplankton growth in the sunlit upper ocean that is fuelled by nitrate supplied from below (i.e., "new production") is balanced by the export of sinking organic matter into the ocean interior (i.e., "export production"; Dugdale and Goering 1967; Eppley and Peterson 1979), thus driving CO<sub>2</sub> sequestration. Phytoplankton growth can also be supported by nitrogen (N) forms such as ammonium and urea that are recycled in surface waters (i.e., "regenerated production"); in net, regenerated production results in no removal of CO<sub>2</sub> to the deep ocean.

The biologically-driven flux of carbon (C) from surface waters (i.e., the ocean's "biological pump") acts to transfer CO<sub>2</sub> to the isolated waters of the deep ocean, lowering the atmospheric concentration of this greenhouse gas. The high nitrate - low chlorophyll state of the present-day Southern Ocean represents a "leak" in the global ocean's biological pump since by consuming nitrate more completely, Antarctic phytoplankton could lower atmospheric CO<sub>2</sub>. Indeed, a more efficient biological pump at high latitudes is a leading hypothesis for the decrease in atmospheric CO<sub>2</sub> that characterized the ice ages (Sigman and Boyle 2000; Sigman et al. 2010). Understanding the controls on biological nitrate utilization in the modern Antarctic Ocean is thus central to our understanding of its outsized role in setting atmospheric CO<sub>2</sub> today and in the past, and in absorbing CO<sub>2</sub> in the future (Sarmiento and Toggweiler 1984).

Because the low latitudes receive nutrients that are subducted into the thermocline in the Southern Ocean, the efficiency of the Southern Ocean's biological pump controls the efficiency of the global ocean's biological pump. In Antarctic waters, biological pump efficiency is set by the point at which phytoplankton switch from assimilating upwelled NO<sub>3</sub><sup>-</sup> to assimilating NH<sub>4</sub><sup>+</sup> recycled in surface waters (i.e., switch from new- to regenerated production). This "switch" defines the moment at which the upper ocean ecosystem stops sequestering atmospheric CO<sub>2</sub>. Previous work conducted in the Antarctic suggests that i) Antarctic phytoplankton do switch from reliance on NO<sub>3</sub><sup>-</sup> to reliance on NH<sub>4</sub><sup>+</sup>; and ii) this switch likely occurs in late summer/early autumn, after the cessation of the spring and early summer period of NO<sub>3</sub><sup>-</sup> drawdown (Smart et al. 2015; Kemeny et al. 2018). However, due to a paucity of seasonal data, our view of the Antarctic N cycle is heavily biased towards the conditions characteristic of early- to mid-summer. A seasonally-resolved dataset is required to verify the occurrence and timing of the hypothesized switch, as well as to understand its implications.

The major goal of the project is to describe and probe the seasonal evolution of the Antarctic Ocean's N cycle in order to better understand the controls on  $\text{NO}_3^-$  drawdown and export production (and thus  $\text{CO}_2$  removal) in this region. The SCALE cruises therefore provided the opportunity to collect data for the winter and spring period, which will be compared to data collected in early and late summer 2018/19.

*Experimental overview:* Primary production is an indicator of the amount of energy available to an ecosystem, which is centrally important to ecological processes and biogeochemical cycling. To assess the wintertime fertility of the Southern Ocean and the relative importance of different phytoplankton groups for driving production, simulated *in situ* experiments ( $^{13}\text{C}$  and  $^{15}\text{N}$  incorporation; Cullen 2001; Dugdale and Goering 1967) were conducted to measure rates of net primary production, and new and regenerated production by both the bulk and size-fractionated phytoplankton community. Rates of nitrification (the regeneration of nitrate from ammonium) and ammonium regeneration were also quantified (Peng et al. 2018; Mduyana et al. *in prep*). The rate data will allow for accurate calculation of the f-ratio (shorthand for “flux ratio”; Eppley and Peterson, 1979), which provides an indication of the strength of the region's biological pump and thus its capacity for biological  $\text{CO}_2$  removal.

In addition to the bulk and size-fractionated community N transformation experiments, a series of  $^{15}\text{N}$  incubations (urea,  $\text{NO}_3^-$  and  $\text{NH}_4^+$  uptake) were undertaken. The resultant particle samples collected at the end of the incubations will be flow cytometrically-sorted and measured for N isotopes. These data will allow for the quantification of taxon-specific rates of urea,  $\text{NO}_3^-$  and  $\text{NH}_4^+$  uptake (e.g., by *Synechococcus*, eukaryotes, diatoms, heterotrophic bacteria). This will enhance our understanding of the role of different phytoplankton groups in driving the biological pump, with implications for future Southern Ocean biogeochemistry given predictions that phytoplankton community composition is likely to change under conditions of global warming.

The natural abundance N isotopic composition ( $\delta^{15}\text{N}$ ) of suspended particles (PN) has been used as a tracer of the dominant N source supporting production (i.e., new vs. regenerated N). For example, the consumption of subsurface nitrate yields high- $\delta^{15}\text{N}$  PN whereas ammonium uptake yields low- $\delta^{15}\text{N}$  PN (Rau et al. 1990; Treibergs et al. 2014). Inferring N source from bulk PN  $\delta^{15}\text{N}$  is problematic, however, because this pool includes heterotrophs and detritus in addition to phytoplankton (Fawcett et al. 2011, 2014). This can be overcome by coupling fluorescence activated cell sorting (FACS) and high sensitivity N isotope analysis (Fawcett et al. 2011; 2014; Treibergs et al. 2014). Using this approach, important biological populations can be isolated from mixed environmental samples and population-specific  $\delta^{15}\text{N}$  can be measured. This yields an integrated (over the organism lifetime) view of the primary N source supporting different phytoplankton groups, revealing their role in new and export production and complementing the rate experiments, which integrate over only a few hours.

## **7.1.2. Methods**

### **7.1.2.1. Field collections**

*Seawater samples:* Seawater samples were collected underway for nutrients and  $\text{NH}_4^+$  and  $\text{NO}_3^-$  isotopes every 2 or 4 hours (Figure 7.1) and from hydrocasts at each CTD station (Figure 7.2). From each cast, water was collected at regular intervals between the surface and bottom and then frozen at  $-20^\circ\text{C}$ . Phosphate ( $\text{PO}_4^{3-}$ ), nitrite ( $\text{NO}_2^-$ ) and  $\text{NH}_4^+$  were measured onboard, while  $\text{NO}_3^-$ , silicate and urea will be measured in the Marine Biogeochemistry Laboratory at UCT (MBL-UCT) by flow injection analysis. The  $\delta^{15}\text{N-NH}_4^+$  and  $\delta^{15}\text{N-NO}_3^-$  will be measured in the MBL-UCT via the method of Zhang et al. (2007) and Sigman et al. (2001), respectively. At selected stations, samples for net community production (NCP) and  $\delta^{15}\text{N-N}_2\text{O}$  were collected (Table 1 and 2). These samples will be analysed using Elementar Americas PrecisION isotope ratio mass spectrometer at the University of South Carolina. During the winter cruise, seawater samples were also collected from all depths at all stations for the later analysis of water isotopes (i.e.,  $\delta^{18}\text{O-H}_2\text{O}$ ). The  $\delta^{18}\text{O-H}_2\text{O}$  will be measured using a Picarro L2140-i isotope and gas concentration analyser at UCT.

*N isotopes of bulk particles and specific phytoplankton taxa:* Water samples for bulk N isotopic analysis of particulate organic nitrogen biomass (PN) were collected every four hours from the underway and from six euphotic zone depths on each hydrocast. At each underway station, three 4 L HDPE bottles were filled with seawater that was then filtered under gentle vacuum through pre-combusted GF/F filters with nominal pore sizes of 0.3  $\mu\text{m}$ , 2.7  $\mu\text{m}$  and 25  $\mu\text{m}$ . At each CTD station, 4 L of seawater was collected and filtered for the  $>25$   $\mu\text{m}$  size-class, and 0.5 mL each for the 0.3-2.7  $\mu\text{m}$  and 2.7-25  $\mu\text{m}$  size-classes. After filtration, the filters were folded in half using ethanol-cleaned forceps and stored in ashed tinfoil envelopes at  $-80^\circ\text{C}$  pending analysis.

Water samples for taxon-specific nitrogen isotopes were collected at the four hourly underway stations and from three euphotic zone depths on various hydrocasts (Table 1). At these stations two 4 L bottles of seawater were taken from each depth of interest. Seawater was filtered through a polycarbonate (PC) membrane filter with a nominal pore size of 0.4  $\mu\text{m}$  under gentle vacuum. After filtration, the PC filters were placed in 4 mL cryovials to which  $\sim 4$  mL of filtered seawater and 100  $\mu\text{L}$  of glutaraldehyde were added in order to resuspend the cells from the filters and preserve them. The cryovials were subsequently stored in the fridge for 1-4 hours and thereafter frozen at  $-80^\circ\text{C}$  pending analysis.

*Incubation experiments:* Tracer incubation experiments were conducted at multiple stations to directly quantify rates of carbon fixation (i.e., primary production), urea,  $\text{NO}_3^-$  and  $\text{NH}_4^+$  uptake (Table 1; “PP”) and  $\text{NH}_4^+$  and  $\text{NO}_2^-$  oxidation (Table 1; “NTR”). Water samples were collected in 1 L PC bottles (uptake) and 250 mL black HDPE bottles (nitrification) from three euphotic zone and three to four sub-euphotic zone depths. Seawater was pre-screened through a 200  $\mu\text{m}$  nylon mesh to remove large grazers. Duplicate 1 L bottles from each euphotic zone depth were amended with  $^{15}\text{NO}_3^-$  or  $^{15}\text{NH}_4^+$  or  $^{15}\text{urea}$  (for N uptake), and duplicate 250 mL bottles from all depths are amended with  $^{15}\text{NH}_4^+ + ^{14}\text{NO}_2^-$  carrier or  $^{15}\text{NO}_2^-$  (for  $\text{NH}_4^+$  and  $\text{NO}_2^-$  oxidation, respectively). The isotope tracers were added at  $\sim 10\%$  of the ambient nutrient concentration. Two of the six

1 L bottles from each depth were also amended with  $^{13}\text{C}$ -bicarbonate in order to quantify net carbon fixation.

Prior to incubation, 40 mL subsamples ( $T_0$ ) were collected from all nitrification bottles and frozen at  $-20^\circ\text{C}$ . All bottles (for uptake and nitrification) were then placed in a custom-built on-deck incubator equipped with neutral density screens to simulate *in situ* light levels and a supply of circulating seawater to maintain a constant temperature. Uptake experiments were incubated for 4-6 hrs and nitrification experiments for 20-30 hrs. A second 40 mL subsample ( $T_f$ ) was collected from each nitrification bottle at the end of the incubation. The N uptake and carbon fixation incubations were terminated by size-fractionated filtration (0.3-2.7  $\mu\text{m}$ , 2.7-25  $\mu\text{m}$ , 25-200  $\mu\text{m}$ ) onto ashed GF/Fs that were then oven dried at  $40^\circ\text{C}$  and pelletized into tin cups for analysis at the Stable Light Isotope Laboratory at UCT.

In addition, a series of  $^{15}\text{N}$  incubations (urea,  $\text{NH}_4^+$  and  $\text{NO}_3^-$  uptake) were terminated via filtration onto PC filters so that the samples can later be sorted using fluorescence activated cell sorting (e.g., for *Synechococcus*, eukaryotes, diatoms, heterotrophic bacteria, etc.). Samples were incubated, filtered, and preserved as described above for *N isotopes of specific phytoplankton taxa*. In the laboratory, these samples will be sorted and measured for  $^{15}\text{N}$  enrichment as outlined below. Samples were also collected for flow cytometric counting of phytoplankton particles, which aid in the quantification of different phytoplankton groups; this information is critical for ground-truthing the FACS data.

*Plankton taxonomy:* At all CTD stations, phytoplankton and zooplankton samples were collected using a drift net and bongo net, respectively. The mesh size of the drift net was 50  $\mu\text{m}$  and the bongo net had two cod ends with mesh sizes of 90  $\mu\text{m}$  and 200  $\mu\text{m}$ . Nets were lowered to 200 m and then immediately raised again. The collected samples were preserved in a mixture of seawater + glutaraldehyde in HDPE bottles until later analysis via light and scanning electron microscopy. Flowcytometry samples were also collected at each underway and CTD stations in order to better characterize the phytoplankton community. These samples were analysed onboard using a custom built flowcytometer (see section 7.2).

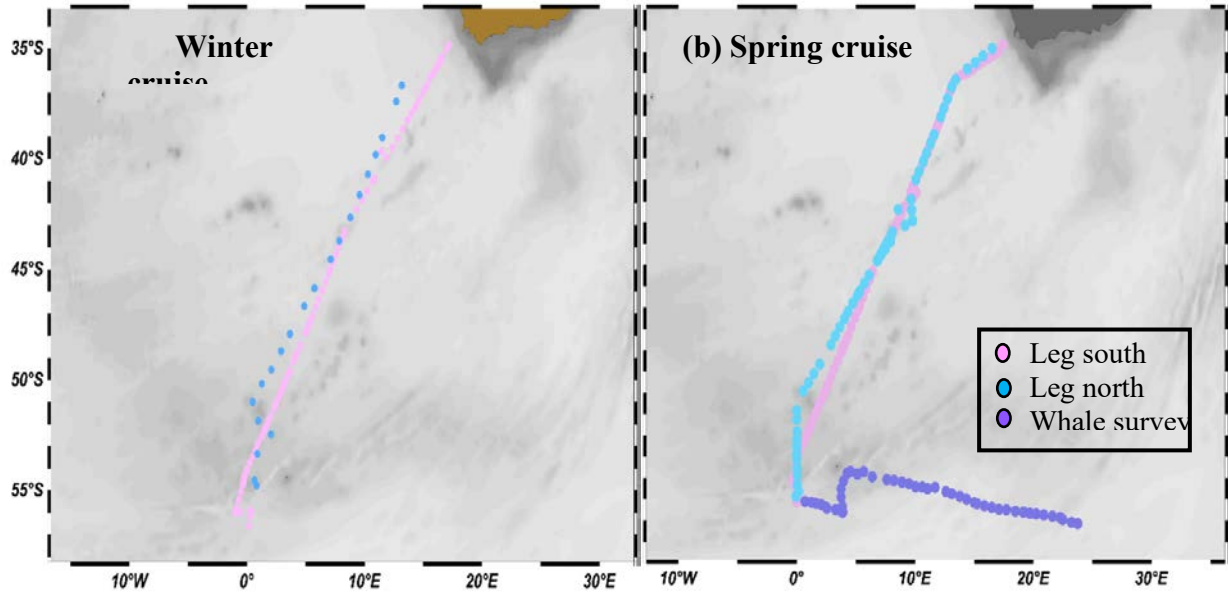


**Figure 7.1.** The position of the underway stations during (a) the winter cruise and (b) the spring cruise. The pink dots represent the underway stations along the southbound legs, the purple dots the stations along the whale survey and the blue dots stations on the northbound legs.

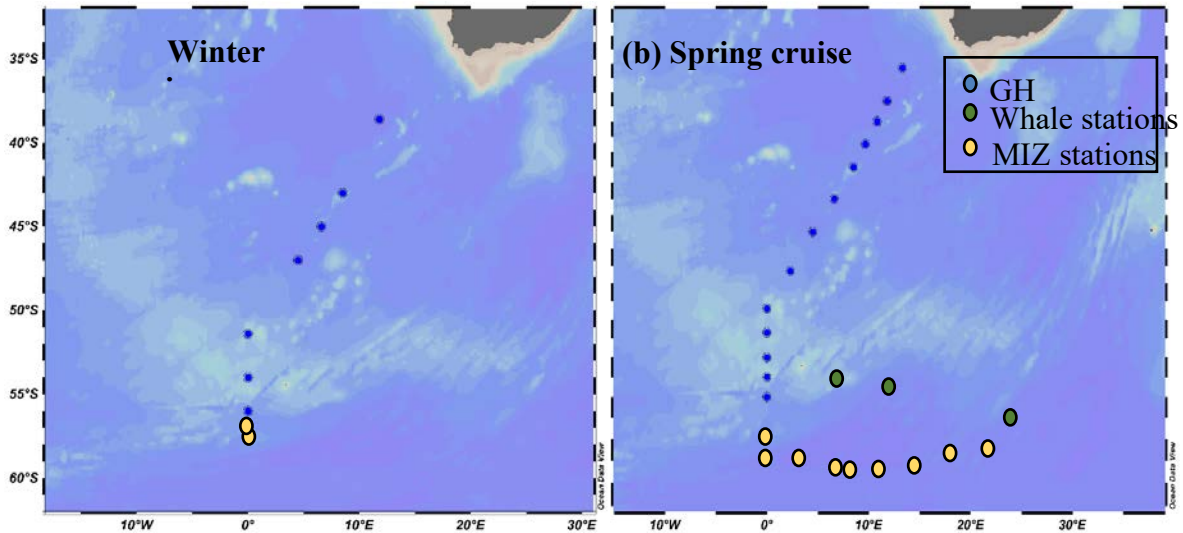


**Figure 7.2.** Position of the CTD stations during (a) the winter cruise and (b) the spring cruise. The blue dots represent the CTD stations along the Good Hope (GH) line, the green dots the stations along the whale survey and the yellow dots the marginal ice zone (MIZ) stations.

**Table 7.1.** List of parameters sampled from each CTD cast during the SCALE winter cruise

Station	Nutrients	NH <sub>4</sub> <sup>+</sup>	NH <sub>4</sub> <sup>+</sup> isotope	NO <sub>3</sub> <sup>-</sup> isotope	Flow cytometry	PON	FACS NA	N <sub>2</sub> O	NCP	δ <sup>18</sup> O seawater	PP	NTR	FACS N uptake	Bongo	Zoo vacuum
SAZ2														x	
MIZ1	x	x	x	x	x	x	x	x		x		x		x	x
MIZ2	x	x	x	x	x	x	x	x		x		x		x	x
GT1	x	x	x	x	x	x	x	x		x		x	x	x	
GT2	x	x	x	x	x	x		x		x	x	x	x	x	
GT3	x	x	x	x	x	x			x	x	x	x	x	x	
GT5	x	x	x	x	x	x			x	x	x	x	x	x	
GT6	x	x	x	x	x	x	x	x		x		x		x	
GT7	x	x	x	x	x	x			x	x	x	x	x	x	
GT9	x	x	x	x	x	x	x	x		x		x	x		
GT10	x	x	x	x		x							x		

**Table 7.2.** List of parameters sampled from each CTD cast during the SCALE spring cruise

Station	Nutrients	NH <sub>4</sub> <sup>+</sup>	NH <sub>4</sub> <sup>+</sup> isotope	NO <sub>3</sub> <sup>-</sup> isotope	Flow cytometry	PON	FACS NA	N <sub>2</sub> O	NCP	PP	NTR	FACS N uptake	Bongo	Zoo incubation	Zoo vacuum
SAZ2	x	x	x	x	x	x	x			x	x	x	x	x	
PUZ	x	x	x	x	x	x	x	x	x	x	x	x	x	x	
MIZ0	x	x	x	x	x	x		x	x	x	x	x	x	x	
MIZ1	x	x	x	x	x	x		x	x	x	x	x	x		
MIZ2	x	x	x	x	x	x	x	x	x		x		x	x	
MIZ3	x	x	x	x	x	x	x	x	x		x		x	x	x
MIZ4	x	x	x	x	x	x		x	x	x	x	x	x	x	
MIZ5	x	x	x	x	x	x	x	x	x		x		x		x
MIZ6	x	x	x	x	x	x	x	x	x		x		x		x
MIZ7	x	x	x	x	x	x		x	x	x	x	x	x		x
MIZ8	x	x	x	x	x	x	x	x	x		x		x		
MIZ9	x	x	x	x	x	x		x	x	x	x	x	x		
WS1	x	x	x	x	x	x	x	x	x		x		x		
WS2	x	x	x	x	x	x		x	x	x	x	x	x	x	
WS3	x	x	x	x	x	x	x	x	x		x		x		
GT1	x	x	x	x	x	x	x	x	x		x		x	x	
GT2	x	x	x	x	x	x	x	x	x	x	x	x	x	x	
GT2b	x	x	x	x	x	x	x			x	x	x			
GT3	x	x	x	x	x	x	x	x	x	x	x	x	x		
GT4	x	x	x	x	x	x	x			x	x	x	x		
GT5	x	x	x	x	x	x	x	x	x		x		x	x	
GT6	x	x	x	x	x	x	x	x	x	x	x	x		x	
GT7	x	x	x	x	x	x	x	x	x	x	x	x	x	x	
GT7b	x	x	x	x	x	x	x			x	x	x	x		
GT8	x	x	x	x	x	x	x				x				
GT9	x	x	x	x	x	x	x	x	x	x	x	x			
GT10	x	x	x	x	x	x	x			x		x			

### 7.1.3. Laboratory methods

*Nitrate and silicate analysis:* Nitrate and silicate concentrations will be measured on a Lachat QuickChem Flow Analysis platform in MBL-UCT following published auto-analysis protocols (Diamond, 1994; Grasshoff, 1976). The configuration typically used gives the Lachat QuickChem Flow Analysis platform a detection limit of 0.1  $\mu\text{M}$ .

*Nitrite analysis:* Nitrite concentrations were determined shipboard using the benchtop colorimetric Greiss reaction (Bendschneider and Robinson, 1952; Parsons et al., 1984). Absorbance was measured using a Thermo Scientific Genesys 30 Visible spectrophotometer at a wavelength of 543 nm. The method has a detection limit of 0.05  $\mu\text{M}$ .

*Phosphate analysis:* Phosphate concentrations were determined shipboard using the Strickland and Parsons colourimetric method (Strickland and Parsons, 1968). Samples and standards were measured using a Thermo Scientific Genesys 30 Visible spectrophotometer at a wavelength of 880 nm. The method has a detection limit of 0.05  $\mu\text{M}$ .

*Ammonium analysis:* Ammonium concentrations were determined using the Holmes fluorometric method (Holmes et al., 1999). Samples and standards were measured using a Turner Designs Trilogy Fluorometer 7500-000 equipped with a UV module. The method has a detection limit of 0.05  $\mu\text{M}$ . Since  $\text{NH}_x$  samples are easy to contaminate, precautions were taken to prevent contamination during sample collection and processing. Following the addition of the orthophthaldialdehyde (OPA) working reagent to frozen samples, a water bath was used to defrost the samples. Once at room temperature, the samples and standards were allowed to react for four hours. The matrix effect, from the comparison of seawater samples and standards made with type-1 ultrapure water, was calculated according to the standard addition method (Saxberg & Kowalski, 1979). Final concentrations were corrected for the matrix effect.

*Nitrate isotope analysis:* The  $\delta^{15}\text{N}$  of  $\text{NO}_3^-$  (and its  $\delta^{18}\text{O}$ , which offers additional constraints on  $\text{NO}_3^-$  cycling) will be measured in the MBL-UCT using the newly-installed “denitrifier-isotope ratio mass spectrometer (IRMS)”. Briefly, denitrifying bacteria lacking a terminal nitrous oxide ( $\text{N}_2\text{O}$ ) reductase quantitatively convert sample  $\text{NO}_3^-$  (and  $\text{NO}_2^-$ ) to  $\text{N}_2\text{O}$  (Sigman et al. 2001; Casciotti et al. 2002) that is then measured using a Thermo Delta V Plus IRMS and purpose-built on-line  $\text{N}_2\text{O}$  extraction and purification system. Precision for  $\delta^{15}\text{N}$  and  $\delta^{18}\text{O}$  is  $\leq 0.1\text{‰}$  and  $\leq 0.3\text{‰}$ , respectively, for  $\text{NO}_3^-$  concentrations  $\geq 0.5 \mu\text{M}$ .  $\text{NO}_2^-$  removal, if necessary, will be undertaken via the method of Granger and Sigman (2009) prior to sample analysis.

*FACS-N isotope analysis:* Central to this project is the coupled flow cytometry-N isotope protocol (Fawcett et al. 2011; 2014; Treibergs et al. 2014). All sorting will take place at the UCT Flow Cytometry Core Facility. Vials are thawed in the dark and gently vortexed to dislodge cells from filters. Re-suspended cells are filtered through a 35  $\mu\text{m}$  mesh; the  $>35 \mu\text{m}$  particles are archived for future analysis. All sorts will be conducted using a BD

FACS Jazz Cell Sorter equipped with a 488 nm blue laser. Samples will be sorted for *Synechococcus* and total eukaryotic phytoplankton according to Fawcett et al. (2011), as well as cryptophytes and heterotrophic bacteria (Marie et al., 2007). We also aim to optimize the flow cytometry protocol for sorting diatoms; we will begin with the approach of McNair et al. (2015) and Hansman and Sessions (2015).

Sorted PN will be converted to  $\text{NO}_3^-$  at MBL-UCT using the persulfate oxidation method of Knapp et al. (2005) as modified by Fawcett et al. (2014). Briefly, sorted particles are filtered onto ashed 0.3  $\mu\text{m}$  GF-75s, then transferred to combusted 4 mL glass Wheaton vials to which 2 mL of persulfate oxidizing reagent (POR) is added. POR is also added to triplicate vials containing a GF-75 blank plus varying amounts of two L-glutamic acid isotope standards, USGS-40 and USGS-41 (Qi et al. 2003); this allows for quantification of the N content and  $\delta^{15}\text{N}$  of the blank. POR is made by dissolving 1-2 g of NaOH and 1-2 g of 4-times recrystallized, methanol-rinsed potassium persulfate in 100 mL of DI water. After POR addition, vials are autoclaved at 121°C for 55 mins on a slow-vent setting. Sample pH is lowered to 5-8 and vials are centrifuged at 3000 rpm for 10 mins to separate residual GF-75 from the liquid sample. The concentration of the resultant  $\text{NO}_3^-$  is measured via chemiluminescent analysis (Garside 1982; Braman and Hendrix 1989) using a NOx analyzer (Teledyne T200) with custom-built front-end at MBL-UCT. The  $\delta^{15}\text{N}$  of the oxidized  $\text{NO}_3^-$  is analysed using the denitrifier method. The precision of the full collection/cytometry/N isotope protocol is  $\sim 0.4\%$  (Fawcett et al. 2011; 2014).

## **7.2. Characterizing the Southern Ocean phytoplankton community**

### **7.2.1. Introduction**

Flow cytometry samples will be used in conjunction with nutrient, physical (using thermosalinograph data), and net primary productivity data to provide us with a high-resolution determination of the surface phytoplankton community structure and group specific contributions to biogeochemical cycling and carbon export across the Atlantic sector of the Southern Ocean. This project will capitalize on a new collaboration between the Department of Oceanography, UCT and the Department of Bioscience, Aarhus University, Denmark. To more accurately, reliably, and rapidly determine phytoplankton community composition across the latitudinal gradients of the Southern Ocean, we will make use of a CytoSense pulse-shape recording flow cytometer (PFCM) supplied by our collaborators at Aarhus University. Access to this sophisticated instrument and our collaborators' phyecological expertise will allow us to process a large number of samples in a feasible time-frame. The PFCM has been demonstrated to provide count results comparable to that of traditional microscopy, while only requiring roughly 10 ml and about 30 minutes, per sample, to run (Haraguchi et al., 2017). Additionally, the PFCM provides us with a method of determining phytoplankton community composition that is more powerful in comparison to traditional flow cytometry; with the ability to look at the fluorescent and scatter profiles of every individual particle measured (Figure 3).

### **7.2.2. Methods**

Samples were collected at 2-hour intervals from the ship's underway system and at 7 depths within the mixed layer from each Niskin cast. In winter, 25 ml of these samples

were fixed with Gluteraldehyde to a final concentration of 0.1% (v/v) (Marie et al., 2005; Vaultot et al., 1989) and stored at 4°C in the dark to slow the rate of pigment degradation brought on by the fixation. The fixed samples will be used to ground-truth a fixation method for use with the PFCM. The PFCM is equipped with red (FL Red; emission: 650–700 nm), orange (FL Orange; emission: 600–650 nm), and yellow (FL Yellow; emission: 550 nm) fluorescence sensors. In addition, the instrument is equipped with sideward (SWS) and forward scatter (FWS) sensors that record light scattered orthogonally and parallel to the incident laser beam, respectively. The large size range among phytoplankton cells (0.5 to >1000 µm) produces signal intensities varying over several orders of magnitude. Therefore, the instrument is equipped with duplicate pairs of all sensors (except for the FWS): a standard (for large cells) and a high-sensitivity (for smaller nano- and pico-sized cells) sensor, allowing the instrument to cover the full size-range of phytoplankton cells. As an example, the red fluorescence sensor is configured in two versions, namely FL Red (normal sensitivity) and FL Red HS (high sensitivity). In addition, this PFCM is equipped with a camera that was set up to take photos of a random subset of the analysed particles (a limit of 300 pictures per sample was set in this study), which were used to support further identification. Samples were run according to Haraguchi et al. (2017) with one run of 0.5 ml (25 mV FLR-hs trigger) to determine the total community structure and absolute counts (Figure 7.3) and a second run of 10 ml (225 mV FLR-hs trigger) targeted at having an adequate representation of larger cells to aid in identification.

### **7.2.3. Preliminary results**

The equipment is sensitive enough to separate some of the recorded taxa into different physiological states (i.e. dividing and/or dying cells) and assigning them as separate clusters (Takabayashi 2006, McFarland et al. 2015). Furthermore, based on default algorithms, this PFCM technique allows particle length to be easily determined for all cells exceeding the width of the laser sheet (5 µm). However, it is important to highlight that cells <5 µm are recorded by the optical sensors (as represented in Figure 7.4) and that their integrated signal amplitude will be proportional to their volume. This allows distinction of smaller cells, provided that the cell produces a signal exceeding the pre-set trigger level. However, their precise length determination requires the use of other algorithms (McFarland et al. 2015) or calibration beads (Thyssen et al. 2008). Preliminary data are shown in Figures below. The absolute particle concentrations are immediately determined from sample runs (Figure 7.3A) and each sample run is represented by thousands of particle profiles (e.g. Figure 7.4) which are plotted in cytogram space using a wide selection of optical sensor parameters (e.g. Figure 7.3B).

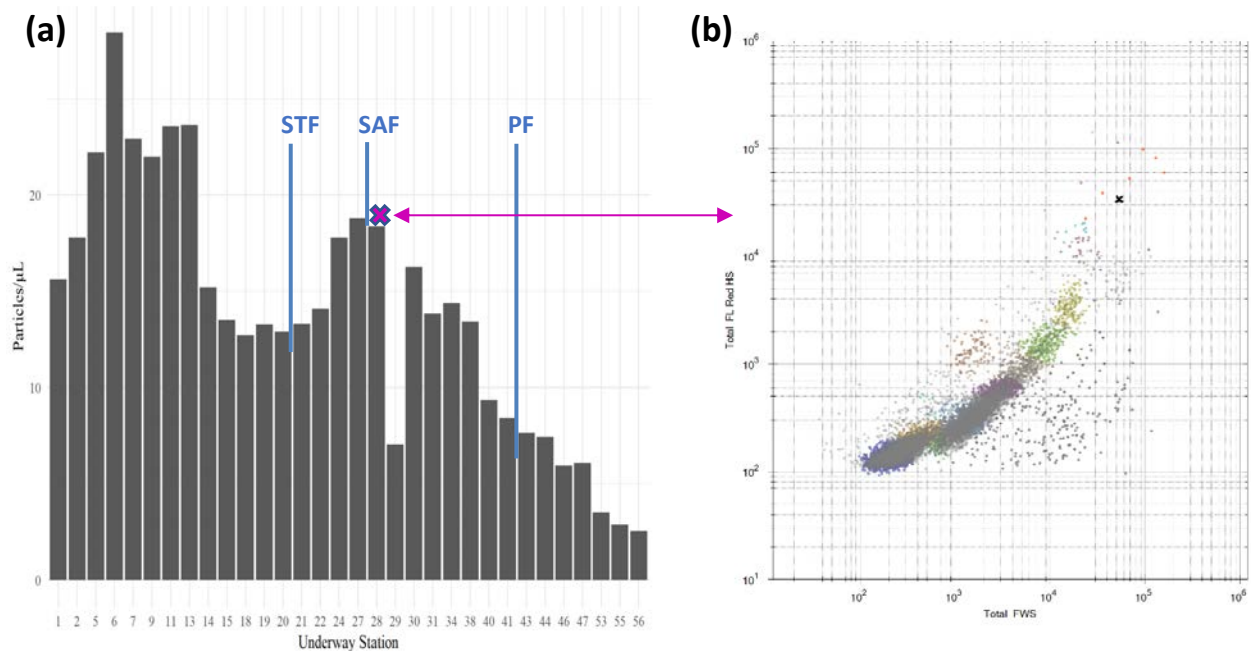


**Figure 7.3. a)** Particle concentrations (per  $\mu\text{L}$ ) for selected underway stations taken between Cape Town and MIZ1. The position of the Sub-Tropical Front (STF), Subantarctic Front (SAF), and Polar Front (PF) are indicated by the blue lines. **b)** Cytogram of underway station 28 (indicated) in total fluorescence, for the FL Red HS sensor, vs. total forward scatter space. Colours indicate differing plankton groupings (defined by using multiple cytograms in conjunction with this one). Larger phytoplankton tend toward the top right of the graph and large detritus towards the bottom right.

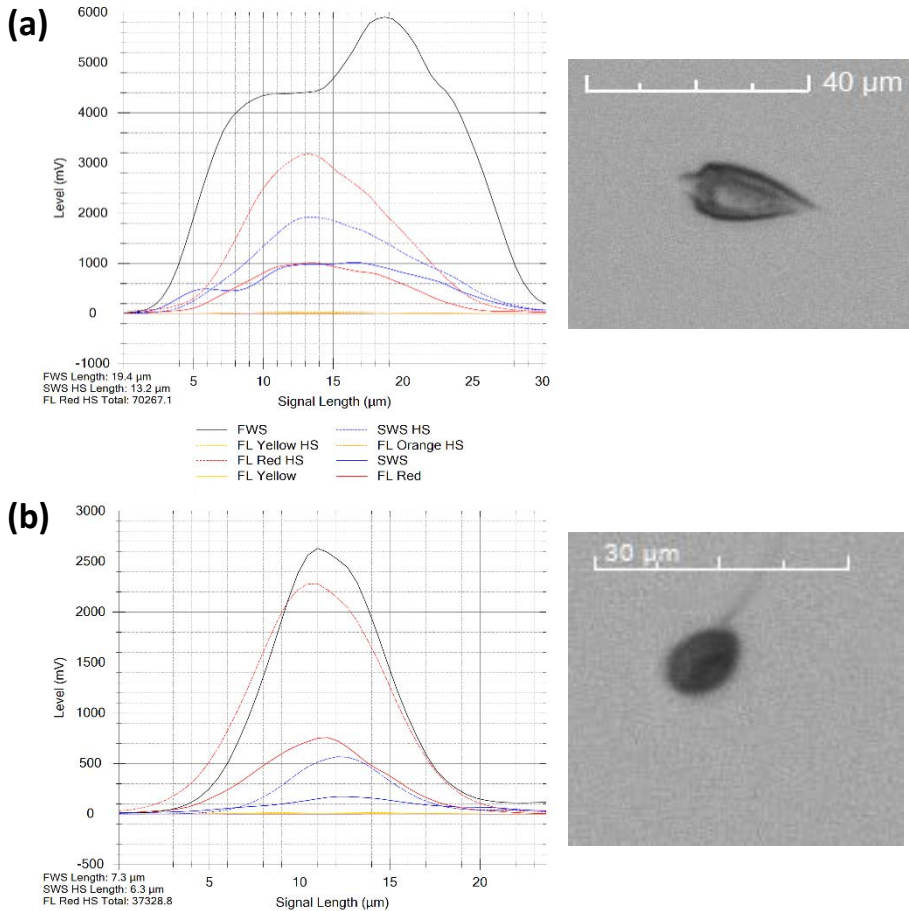


**Figure 7.4.** Two optical profiles of phytoplankton present at underway station 28 are shown here: **a)** A dinoflagellate of the *Oxytoxum* genus (Guiry & Guiry, 2019),  $\sim 19.4 \mu\text{m}$  in length. **b)** A nanoflagellate of  $\sim 7.3 \mu\text{m}$  in length. The various fluorescence's shown are: forward Scatter (FWS; black solid line), high-sensitivity Sideward Scatter (SWS HS; blue dashed line), high-sensitivity Yellow fluorescence (FL Yellow HS; yellow dashed line), high-sensitivity Orange fluorescence (FL Orange HS; orange dashed line), high-sensitivity Red fluorescence (FL Red HS; red dashed line), Sideward Scatter (SWS; blue solid line), Yellow fluorescence (FL Yellow; yellow solid line), and Red fluorescence (FL Red; red solid line).

### 7.3. Secondary production and plankton activity during the winter season in the Southern Ocean

#### 7.3.1. Introduction

Marine phytoplankton represent a crucial link in the Earth's climate system as they convert atmospheric  $\text{CO}_2$  dissolved in surface waters into organic carbon (C) through photosynthesis (primary production). In the Southern Ocean (SO), while this important activity is higher in spring and summer, when light irradiance and light-time are at maximum, during winter phytoplankton productivity is limited also by the little amount of available amount of light, suggesting the establishment of an unproductive marine

system. However, during the previous winter-cruise to the Antarctic Marginal Ice Zone (MIZ) in 2017, a surprisingly higher abundance of sea-algae within consolidated ice and fragmented ice (“pan-cakes”) was determined, though their role in marine ecosystem and their role in carbon-regulation during winter are still unclear and perhaps underestimated. Furthermore, there is no quantitative information on relationship and carbon-export from sea-algae to zooplankton organisms during the winter season in the MIZ.

During the SCALE 2019 cruises to the MIZ, we investigated winter and spring productivity and activity of mesozooplankton in response to possible interactions with high concentration of sea-algae in the sea ice. We aimed to investigate the changes in the zooplankton community between the open ocean and the MIZ by (1) quantifying abundance and biomass of zooplankton, (2) evaluating the amount of eggs spawned as a proxy for secondary production, and (3) evaluating the trophic role of the plankton organisms and the transfer of biomass and energy by using stable isotopes analysis.

In MIZ and along the Good Hope Line transect, various stations were investigated (Tables 1 and 2) towing vertically a drift-net with 50  $\mu\text{m}$  mesh for phytoplankton collection, and a Bongo set with two mesh sizes: 200  $\mu\text{m}$ , for taxonomy identification analysis; and 90  $\mu\text{m}$ , for isotope analysis and incubation of female copepods. In the MIZ, additional zooplankton samplings were conducted using a zooplankton pump. These samples were conducted within the sea ice-water interface in an attempt to collect the zooplankton below the pancakes.

### **7.3.2. Objectives**

The importance of the winter and spring season in the driving  $\text{CO}_2$  drawdown in the Southern Ocean still remains to be quantified. Using measurements of nutrients, stable isotopes of carbon and nitrogen and biological (phytoplankton, sea-ice algae, zooplankton) diversity, combined with a numerical model, we aim to develop an integrated view of the SO productivity during winter, with implications for MIZ nutrient cycling, ecosystem function, and  $\text{CO}_2$  removal.

### **7.3.3. Mesozooplankton distribution and biomass**

At all CTD stations, phytoplankton and zooplankton samples were collected using a drift net and bongo net, respectively. The mesh size of the drift net was 50  $\mu\text{m}$  and the bongo net had two cod ends with mesh sizes of 90  $\mu\text{m}$  and 200  $\mu\text{m}$ . Nets were lowered to 200 m and then immediately raised again. Samples collected using 200  $\mu\text{m}$  net were stored in plastic bottles and preserved with buffered formalin 10% (final concentration 2%) for taxonomy identification and measurement of body biomass will be conducted at UCT. Samples collected using the 90  $\mu\text{m}$  were size-fractionated and filtered down onto GF/F. These samples will undergo massspectrometry for isotopic analysis back at UCT.

### **7.3.4. Preliminary results**

Mesozooplankton distribution changed along the Good Hope Line towards the MIZ, showing biological characterization of the different water masses within the MIZ and between the several fronts: Subantarctic Polar Front (APF) and Antarctic Front (AF). Within the Cape Line transect, biodiversity of mesozooplankton was dominated by small copepods: mostly *O. similis* and Clausocalanidea species. Here, bigger copepods species and Euphausiid were almost absent, however, fish larvae were relatively abundant. No key copepods species were found (e.g. *C. propinquus*). In the MIZ, although smaller copepods dominated in numbers, biodiversity was higher compared to the transect. The number of bigger copepods (e.g. *Calanus propinquus*, Figure 5), amphipods, Euphausiids and Chaetognaths was also high. These results might denote the establishment of two different marine ecosystems in the two systems: in MIZ, a more productive and richer system than the one in the open ocean.



**Figure 7.5.** Female of *C. propinquus* from MIZ2 winter cruise incubated for egg spawning.

### **7.3.5. Egg spawning and secondary productivity**

As much as 60-80% of the zooplankton biomass in the SO food web is composed of calanoid copepods, tiny crustaceans of roughly 1 to 10 mm body length. Because of their sheer abundance and rather complicated life-history features, copepods are very suitable for studying lifecycle traits as well as for estimating secondary production.

Studies on life-cycle strategies of dominant copepod species have been carried out in the SO (notably the Weddell Sea) since the 1980s. One of the most interesting aspects is the adaptation of herbivorous species to the distinct seasonality in light, ice cover and primary production, i.e. they have to cope with prolonged periods of food shortage during the long and dark winter season, when phytoplankton growth is significantly reduced. Therefore, different species have adopted often substantially different life-cycle strategies to survive in these unfavourable winter conditions. They have developed specific adaptations to utilize short-term food pulses and endure long periods of food scarcity in the water column. During spring and early summer, they ascend from the depths where they overwinter in a so-called diapause state to the surface layers where they actively feed on phytoplankton and reproduce. These ontogenetic and seasonal vertical migrations associated with diapause (overwintering) are known adaptations for copepods to escape temporarily from unfavourable conditions and food scarcity during the unproductive winter season. Diapausing species migrate mainly as pre-adults to greater depths, often in

excess of 1000 m, where they reside for several months in an inactive state of overwintering. Diapause is characterized by reduced swimming activity, arrested development, cessation of feeding, and reduced metabolic rates. Pre-adult stages accumulate large amounts of food reserves as depot lipids during spring and summer, which are almost exclusively composed of wax esters, in order to fuel diapause in autumn/winter as well as – to some extent – reproduction in the following spring. In contrast to the Arctic Ocean, only one calanoid copepod, *Calanoides acutus*, which is a dominant species in the SO copepod community, is known to have adopted this particular overwintering strategy. Whether *Rhincalanus gigas*, another dominant species, is also an ontogenetic migrant, still remains uncertain. Wintertime observations in 2012 during the SA *Agulhas II* Shakedown cruise, however, showed that this species exclusively occurred in deep waters (>400 m), possibly providing evidence of such an overwintering strategy. Most of the other Antarctic copepods, including *Calanus propinquus* and *C. simillimus*, do not appear to have a resting stage in their life cycle and remain active during winter adjusting their feeding behaviour, e.g. by switching from a phytoplankton-based summer diet to a wider food spectrum in winter. These species also accumulate fat reserves, albeit of a different chemical make-up.

Daily egg production rates (EPRs) were measured using a simple technique, called the 'bottle incubation method'. Typically, single specimens of adult female copepods were carefully placed into 1-L glass incubation bottles. These were filled with ambient sea surface water that contains natural phytoplankton assemblages, but this water was filtered through a 50- $\mu\text{m}$  mesh to avoid possible contamination with eggs that might already be present in the water. All bottles were maintained in an incubator in the walking fridge at a constant temperature of 4° C. After 48 hours, the incubations were terminated, the condition of females in the bottles was assessed and the eggs that were spawned during the incubation period were counted under a microscope onboard. The number of eggs produced per female during a 48-hr period is a measure of fecundity or daily EPR. Experiments where females were found dead or moribund were not considered for inclusion in the dataset. Specimens of females and eggs were collected for further analysis of stable isotopes, and ammonium concentration and  $\delta^{15}\text{N}$  of ammonium will be also measured for each bottle to evaluate the zooplankton contribution to nitrogen cycling.

### 7.3.6. Preliminary results

4 incubation experiments were conducted during the winter cruise, while 12 incubation experiments were conducted during the spring cruise. Due to the different community compositions found it was not possible to incubate the same species for all experiments. In fact, in any experiment, only 6 females of the most representative species of the communities were incubated: two species of Clausocalanidea and *Paraeuchaeta* sp. in the Subantarctic Ocean and *C. propinquus* in the MIZ. It is noteworthy that juveniles, especially late-copepodite stage C5 pre-adults, as well as adult males were observed in fairly high abundances at most of the stations, suggesting that active reproduction (mating and copulation) was imminent once the pre-adults had moulted to adult females. During the winter cruise, of the 24 females incubated individually, 6 had spawned between 0.5 and 1.5 eggs day<sup>-1</sup>, while the remaining 18 produced no eggs, denoting a

low productivity of these organisms. Differences of EPRs between regions are still under analysis.

### **7.3.7. Trophic web analysis using stable isotopes**

Stable isotopes of  $\delta^{15}\text{N}$  and  $\delta^{13}\text{C}$  are commonly used in ecology to determine respectively the trophic position and the food source of any organisms analysed. Isotopic composition of a consumer is the weighted mix of isotopic compositions of its food sources plus a trophic fractionation factor. Determining the trophic structure of the marine ecosystems, such as the plankton system, helps solving complex interactions between organisms and to quantify energy and material flux-transport and the relative exports between each food web level.

In this expedition, we wanted to quantify the structure of mesozooplankton system in the MIZ and its role in the carbon and nitrogen export during winter, comparing it to the open ocean system.

At each station, mesozooplankton were size class fractionated into 7 classes (90-150, 150-250, 250-500, 500-1000, 1000-2000, 2000-5000, >5000  $\mu\text{m}$ ) for bulk analysis and sorted under microscope into different Taxa for species-specific analysis. A minimum of 5 Taxa were collected: Copepods, Chaetognath, Euphausiids, Cladocera and Amphipods but, in most of the stations, copepods were sorted into Genera or species level for a better representation of the food web. Samples will be analysed on land.

## **7.4. Nitrogen cycling in the atmosphere**

### **7.4.1. Motivation**

The emissions of anthropogenic nitrogen (N) to the atmosphere, and its subsequent deposition, have increased greatly since preindustrial times causing substantial impacts on the global N cycle (Galloway et al., 2004). The impacts of this increased anthropogenic N deposition are well documented and have led to a series of consequences for atmospheric chemistry, ecosystems, and human health, referred to as the 'nitrogen cascade' (Erisman et al., 2013; Fowler et al., 2013; Galloway et al., 2003; Vitousek et al., 1997; Elser et al., 2009; Howarth et al., 2000; Peierls and Paerl, 1997). However, the implications of atmospheric deposition of anthropogenic N to the open ocean and the amount of N released to the marine atmosphere from the ocean through natural processes, such as surface ocean photochemistry and biological activity, are still uncertain (Duce et al., 2008). The Southern Ocean is the most remote marine region, which allows for the study of marine emissions without the interference from anthropogenic signals. The results obtained from Southern Ocean studies may also be used to create a proxy for the preindustrial scenario, where, in the case of ammonia gas (the precursor to particulate ammonium), will also give information about the largest preindustrial ammonia source, the surface ocean. The research aims to investigate the surface ocean and lower atmosphere N cycle in the most remote marine region of the global ocean to test the hypothesis that the surface ocean can be a significant source of N to the marine atmosphere, using nitrogen isotopes as a tracer of the marine source in addition to inorganic nitrogen concentrations and NOAA HYSPLIT model (NOAA Hybrid Single-Particle Lagrangian Integrated Trajectory Model) airmass back trajectories.

## 7.4.2. Methods

*High Volume Air Sampler (HV-AS)*: Pre-combusted glass fibre filters (GF/Fs) were used to collect atmospheric samples using a Tisch Environmental high-volume air sampler (HV-AS) fitted with a five-stage cascade impactor, including a sixth filter which acted as a backup sample. The HV-AS was functional during the entire duration of the expedition. A Campbell Scientific Africa sector collector was used to restrict the periods when the HV-AS was active, such that the HV-AS would only switch on if the wind direction was  $<75^\circ$  and  $>140^\circ$  from the bow of the ship for at least ten minutes, such as to avoid contamination from the ship's fume stack. Samples were left until the HV-AS had been switched on for 24 hours. GFF's were mounted and removed from the cascade impactor in an Air Science laminar flow cabinet and the cascade impactor was cleaned with 99.9% reagent-grade ethanol after filters were removed. Samples were placed in individual zip-sealed plastic bags and stored at  $-20^\circ\text{C}$  pending analysis at the Marine Biogeochemistry Lab at the University of Cape Town for inorganic and organic nitrogen concentrations, and ammonium and nitrate nitrogen isotopic compositions ( $\delta^{15}\text{N}$ ).

## 7.5. Quantifying the effects of variable light and iron on the nitrate assimilation isotope effect of phytoplankton

### 7.5.1. Introduction and rationale

A robust characterization of the biological pump requires knowledge of the sources, cycling, and sinks of N and Fe, and how these potentially limiting nutrients interact to modify the biological pump. Increasingly, the N isotopic composition ( $\delta^{15}\text{N}$ ) of nitrate ( $\text{NO}_3^-$ ) is being used to constrain marine N cycling. The US-NSF-funded GEOTRACES program includes measurement of the  $\delta^{15}\text{N}$  of  $\text{NO}_3^-$  as a "key" Trace Element and Isotopic (TEI) analysis. As TEI data from the GEOTRACES sections and other cruises accumulate, the goals of GEOTRACES have shifted to synthesizing the results from the cruises as well as "focusing on the themes of boundary fluxes, internal cycling, and TEIs used as proxies in paleoceanography". One key variable that interpretation of both modern water column  $\text{NO}_3^-$   $\delta^{15}\text{N}$  measurements as well as metrics of paleo-nutrient utilization depend upon, however, is the degree to which  $\text{NO}_3^-$  assimilation by phytoplankton discriminates against the heavier isotope ( $^{15}\text{N}$ ). Here we work towards a deeper understanding of phytoplankton physiological factors driving this correlation.

### 7.5.2. Aims and objective

The overarching hypothesis of the proposed work is that the energy budget of the phytoplankton affects the rate for  $\text{NO}_3^-$  assimilation, with light and Fe stress being primary contributors to physiological energy constraint in Southern Ocean phytoplankton. The SCALE cruise allowed us to evaluate how Fe and light stress in field-based manipulative mesocosms, and in natural Southern Ocean phytoplankton populations affect the rate for  $\text{NO}_3^-$  assimilation, and thus water column  $\text{NO}_3^-$   $\delta^{15}\text{N}$ .

### 7.5.3. Sampling

- Underway nitrate ( $\text{NO}_3^-$ ) samples to measure the isotopic composition of the  $\text{NO}_3^-$
- Underway photophysiology of the phytoplankton community composition to measure photophysiological parameters
- Depth profiles using CTD casts for  $\text{NO}_3^-$  to measure the isotopic composition of the  $\text{NO}_3^-$
- Samples for phytoplankton metagenomics and targeted genomic analysis for Fe stress in phytoplankton.
- Trace metal clean phytoplankton microcosms in custom made incubators to measure the response of the phytoplankton community to iron deplete and replete conditions under different light conditions.

Underway analysis: Samples of phytoplankton variable fluorescence combined with the  $\text{NO}_3^-$   $\text{d}^{15}\text{N}$  and data from other groups on phytoplankton composition and water chemistry will allow us to identify if the residual nitrate isotopic composition is affected by the physiological state of the phytoplankton community, the community composition and or other biological or environmental parameters. Samples and data are currently being processed.

Mesocosm experiment: Two full mesocosms experiments were conducted. Trace metal clean water from the trace metal clean Go-Flo bottles were incubated in 4L polycarbonate bottles. Those incubations ran for approximately 10 -13 days each during which the communities from two different locations (SAZ2 and MIZ) were incubated under in a matrix approach with 2 different light conditions (low light -LL; high light (HL) and two different iron (Fe) conditions (limiting Fe (DFB), replete Fe (Fe). A control with no addition of Fe or Fe-chelating agent was run in addition. Light intensity for the control was set to mimic 15m light intensity as measured during the time of sampling.

### 7.5.4. Experimental setup:

Mesocosm incubations:



Fig. 7.6: Experimental setup for the Mesocosm experiments. Light intensity and temperature were monitored in each incubator (cooler) using HOBO data-loggers. Light was supplied by a custom made LED array which was controlled by Arduino microcontrollers.

Light conditions in acclimations:

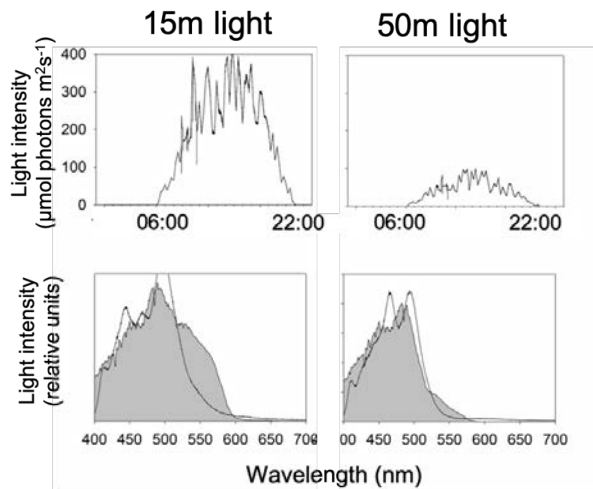


Fig. 7.7: Light intensity and spectrum for the two experimental conditions.

**7.5.5. Preliminary data**

Growth rate response

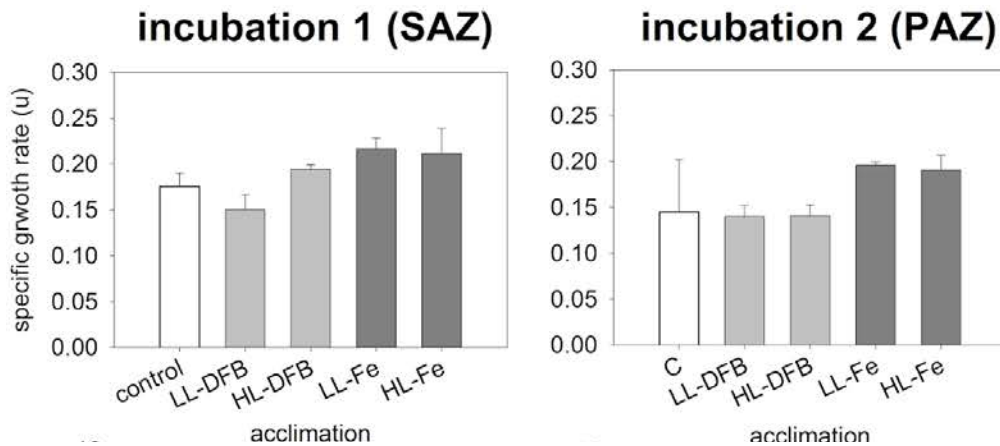


Fig 7.8: Specific growth rates of the two incubations (A) SAZ2 (B) MIZ.

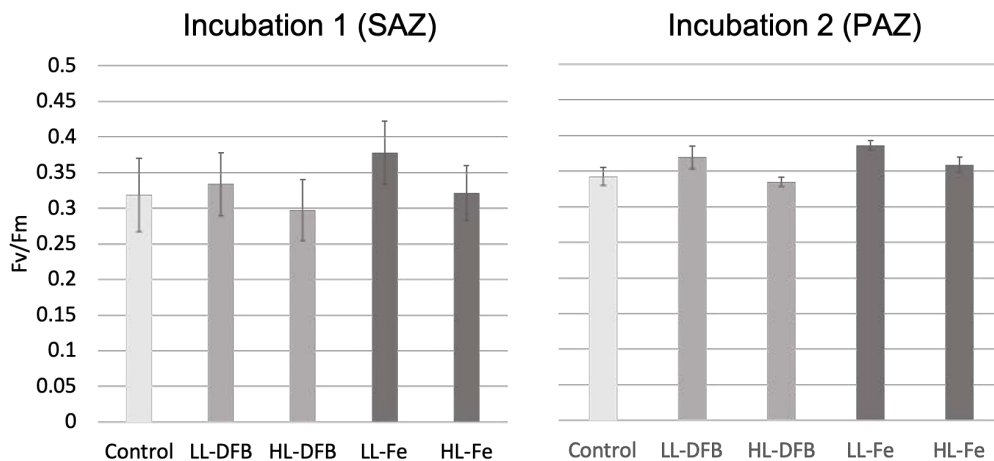


Fig. 7.9: Quantum yield analysis of the two acclimations taken during the mid-exponential growth phase.

Brief preliminary data summary:

Phytoplankton communities treated with Fe addition grew faster compared to the control, in both the SAZ and PAZ samples, indicating that the natural communities were Fe limited. Communities with the added chelating agent DFB showed reduced growth compared to the control. Based on quantum yield measurements (performed in the first 3 hours of the light phase) Fe limitation is expressed within the same light environment resulting in reduced the photophysiological efficiency. These data indicate that Fe limitation induced stress. This was also visible in other photophysiological parameters. Analyses of quantum yield performed throughout a 24h period also indicated that high light acclimated cells were more stressed during the mid-day period compared to low light acclimated cells. Based on our hypothesis on  $\text{NO}_3^-$  uptake and reduction, we would expect a change in cellular  $\text{NO}_3^-$  isotope fractionation. Data on  $\text{d}^{15}\text{N}$  genetics analysis of Fe stress factors and proteomic samples and are still being analyzed.

## 7.6. References

- Bendschneider K and Robinson RJ. 1952. A new spectrophotometric method for the determination of nitrite in sea water. Technical Report No. 8. University of Washington.
- Casciotti KL, Sigman DM, Hastings MG, Böhlke JK, and Hilkert A. 2002. Measurement of the oxygen isotopic composition of nitrate in seawater and freshwater using the denitrifier method, *Anal. Chem.* 74: 4905–4912. doi:10.1021/ac020113
- Cullen, J.J. (2001) Plankton: Primary Production Methods. In: Steele J, Thorpe S, Turekian K (eds) *Encyclopedia of Ocean Sciences*. Academic Press, San Diego, pp 2277–2284.
- Diamond D. 1994. QuikChem Method 10-114-21-1-B: Silicate by flow injection analysis. Lachat Instruments.

Duce, R. A., LaRoche, J., Altieri, K. E., Arrigo, K. R., Baker, A. R., Capone, D. G., Cornell, S., Dentener, F. et al. (2008). Impacts of Atmospheric Anthropogenic Nitrogen on the Open Ocean. *Science*. 320(5878):893-897.

Dugdale RC, Goering JJ. 1967. Uptake of new and regenerated forms of nitrogen in primary productivity. *Limnology and Oceanography*, 12: 196–206.

Elser, J.J., Andersen, T., Baron, J.S., Bergström, A.K., Jansson, M., Kyle, M., Nydick, K.R., Steger, L. and Hessen, D.O., 2009. Shifts in lake N: P stoichiometry and nutrient limitation driven by atmospheric nitrogen deposition. *science*, 326(5954), pp.835-837.

Eppley RW and Peterson BJ. 1979. Particulate organic matter flux and planktonic new production in the deep ocean. *Nature*, 282: 677-680.

Erisman, J., Galloway, J., Seitzinger, S., Bleeker, A., Dise, N., Petrescu, A., Leach, A., and de Vries, W. (2013). Consequences of human modification of the global nitrogen cycle. *Philosophical Transactions of the Royal Society B: Biological Sciences*, 368(1621).

Fawcett, S. E., Lomas, M.W., Ward, B.B., Sigman, D.M. (2014) The counterintuitive effect of summer-to-fall mixed layer deepening on eukaryotic new production in the Sargasso Sea. *Global Biogeochemical Cycles* 28, 86-102.

Fawcett, S. E., Lomas, M.W., Casey, J.R., Ward, B.B., Sigman, D.M. (2011) Assimilation of upwelled nitrate by small eukaryotes in the Sargasso Sea. *Nature Geoscience* 4, 717-722.

Fowler, D., Coyle, M., Skiba, U., Sutton, M.A., Cape, J.N., Reis, S., Sheppard, L.J., Jenkins, A., Grizzetti, B., Galloway, J.N. and Vitousek, P., 2013. The global nitrogen cycle in the twenty first century. *Philosophical Transactions of the Royal Society B: Biological Sciences*, 368(1621), p.20130164.

Galloway, J. N., Aber, J. D., Erisman, J. W., Seitzinger, S. P., Howarth, R. W., Cowling, E. B., and Cosby, B. J. (2003). The Nitrogen Cascade. *BioScience*, 53(4):341–356.

Galloway, J.N., Dentener, F.J., Capone, D.G. et al. *Biogeochemistry* (2004) 70: 153.

Granger J and Sigman DM. 2009. Removal of nitrite with sulfamic acid for nitrate N and O isotope analysis with the denitrifier method. *Rapid communication in mass spectrometry*. 23: 3753-3762

Grasshoff K. 1976. *Methods of seawater analysis*. Verlag Chemie, Weinheim and New York.

Guiry, M.D. & Guiry, G.M. (2019). *AlgaeBase*. World-wide electronic publication, National University of Ireland, Galway (taxonomic information republished from *AlgaeBase* with permission of M.D. Guiry). *Oxytoxum Stein*, 1883. Accessed through: World Register of

Marine Species at: <http://www.marinespecies.org/aphia.php?p=taxdetails&id=109528>  
on 2019-08-10

Haraguchi, L., Jakobsen, H.H., Lundholm, N. and Carstensen, J., 2017. Monitoring natural phytoplankton communities: a comparison between traditional methods and pulse-shape recording flow cytometry. *Aquatic Microbial Ecology*, 80(1), pp.77-92.

Holmes R, Aminot I, K erouel R, Hooker B and Peterson B. 1999. A simple and precise method for measuring ammonium in marine and freshwater ecosystems. *Canadian Journal of Fisheries and Aquatic Sciences*, 56(10): 1801-1808

Howarth, R. (2000). *Nutrient pollution of coastal rivers, bays, and seas*. Washington, DC: Ecological Society of America.

Marie, D., Simon, N., Vaulot, D., 2005. Phytoplankton Cell Counting by Flow Cytometry, in: *Algal Culturing Techniques*. <https://doi.org/10.1016/B978-012088426-1/50018-4>

Martin, J.H., Gordon, R.M., Fitzwater, S.E. (1991) The case for iron. *Limnology and Oceanography* 36, 1793-1802.

McFarland MN, Rines J, Sullivan J, Donaghay P (2015) Impact of phytoplankton size and physiology on particulate optical properties determined with scanning flow cytometry. *Mar Ecol Prog Ser* 531: 43–61

Parsons TR, Maita Y and Lalli CM. 1984. *A Manual of Chemical and Biological Methods for Seawater Analysis*.

Peng X, Fawcett SE, van Oostende N, Wolf MJ, Marconi D, Sigman DM and Ward BB. 2018. Nitrogen uptake and nitrification in the subarctic North Atlantic Ocean. *Limnology and Oceanography*.

Peierls, B. L. and Pearl, H. W.: 1997, 'Bioavailability of atmospheric organic nitrogen deposition to coastal phytoplankton', *Limnol. Oceanogr.* 42, 1819–1823.

Sarmiento, J. L., Toggweiler, J.R. (1984) A new model for the role of the oceans in determining atmospheric pCO<sub>2</sub>. *Nature* 308, 621-624.

Saxberg B and Kowalski W. 1979. Generalised standard edition method. *Analytical Chemistry*, 51(7): 1031-1038.

Sigman, D.M., Boyle, E.A. (2000) Glacial/interglacial variations in atmospheric carbon dioxide. *Nature* 407, 859-869.

Sigman D, Casciotti KL, Andreani M, Barford C, Galanter M and B ohlke JK. 2001. A Bacterial Method for the Nitrogen Isotopic Analysis of Nitrate in Seawater and Freshwater. *Analytical Chemistry*, 73: 4145–4153.

Sigman, D.M., Hain, M.P., Haug, G.H. (2010) The polar ocean and glacial cycles in atmospheric CO<sub>2</sub> concentration. *Nature* 466, 47-55.

Parsons TR, Maita Y and Lalli CM. 1984. A Manual of Chemical and Biological Methods for Seawater Analysis.

Sunda, W.G., Huntsman, S.A. (1997) Interrelated influence of iron, light and cell size on marine phytoplankton growth. *Nature* 390, 389-392.

Takabayashi M (2006) The effect of nutrient availability and temperature on chain length of the diatom, *Skeletonema costatum*. *J Plankton Res* 28: 831–840

Thyssen M, Mathieu D, Garcia N, Denis M (2008) Shortterm variation of phytoplankton assemblages in Mediterranean coastal waters recorded with an automated submerged flow cytometer. *J Plankton Res* 30: 1027–1040

Treibergs LA, and Granger J. (201). Enzyme level N and O isotope effects of assimilatory and dissimilatory nitrate reduction. *Limnology and Oceanography*, 62(1): 272-288.

Vaulot, D., Courties, C., Partensky, F., 1989. A simple method to preserve oceanic phytoplankton for flow cytometric analyses. *Cytometry*.  
<https://doi.org/10.1002/cyto.990100519>

Vitousek, P., Aber, J., Howarth, R., Likens, G., Matson, P., Schindler, D., Schlesinger, W., and Tilman, D. (1997). Human Alteration of the Global Nitrogen Cycle: Sources and Consequences. *Ecological Applications*, 7(3), pp.737-750.



## **8. TEAM OCE**

### **8.1. Winter Cruise**

Listed operations:

- Conductivity, Temperature and Depth (CTD) operations and maintenance of instrument on board.
- Salinity validation samples for CTD sensors – (Salinometer)
- Winch operations (Bongo nets, CTD, Mini Geotrace CTD, McClane Pumps and Marine Snow Catcher)
- CTD Data processing
- Thermosalinograph (TSG) operation and maintenance
- Acoustic Doppler Current Profiler (ADCP)
- Scientific Data System (SDS)

#### **8.1.1. Technical report on Instrumentation**

CTD

Geotrace CTD underwater unit and rosette frame was provided by Sea Technology Services (STS) and Niskin bottles (from CSIR “Miss Daisy” CTD) used for Niskin CTD casts. The GoFlo bottles used for the Geotrace CTD casts were interchanged with the Niskin bottles therefore using a single underwater unit for all CTD operations and all operated off the Kevlar cable on board the SA Agulhas II.

A number of initial problems were encountered with the CTD unit prior to the first deployment and listed below:

- Missing nuts and bolts from the centre frame supporting the bottle firing carousel (entire unit was loose)
- Missing bolts from the altimeter bracket
- Support frame of the underwater unit was loose, did need tightening but was not missing any nuts or washers.
- Niskin bottles from “Miss Daisy” CSIR CTD was not serviced prior to the cruise. 17 spigots and o-rings were replaced, all the firing nylon leads were too short to reach the carousel therefore all 24 leads and crimps for each bottle were changed.

Unfortunately, inadequate number of spares and supplies were sent with the STS interns, however we managed to find bits and pieces of Niskin spares in the scientific store on board the vessel and used to repair the CTD. Please note that any spares used to repair the CTD that did not come from the spare’s boxes supplied by STS will be removed post cruise.

The underwater unit for both the mini Geotrace CTD (Stellies) and “Upright” Geotrace CTD were corrected configured prior to the voyage and deck tested on board prior to any CTD casts. No electronic issues encountered with the sensors. However, in between CTD casts the O2 sensor and pump were flushed with distilled water as standard protocol but encountered freezing of the water in the system which resulted in the pump not switching during a deployment. The CTD was recovered when this issue first arose, and we implemented a “warming of sensors” protocol and “ice check”

of all sensors prior to deployment. This was only required for all MIZ stations beyond the ice edge. The altimeter was bench tested prior to the voyage and deck tested on board and indicated that it was in working condition, but it did not work for majority of the CTD casts. However, it sprung to life on cast 012, but note that nothing was changed to the instrument or config file.

#### Kevlar cable

The Kevlar cable was used for all CTD operations, the cable and compensator were operated according to the standard ship protocols and ensured that all operations were safe for both personnel and equipment. Important to note that CTD operating times are subject to change due to environmental constraints (No CTD operations beyond 30 knt winds with the combination of 4 m-5 m swell) and limitations of the Kevlar cable. The cable is considerably lighter (18kg/km in seawater) than the conventional steel cable and the Geotrace CTD frame is fairly light and weighs very little in water. The average speed for the CTD casts were 0.3m/s – 0.4m/s on the downcast in rough weather and 0.5m/s – 0.6m/s in calmer seas (in ice). The upcast speed ranged between 0.5m/s – 0.8m/s dependent on weather conditions influencing the overall tonnage on the cable. The Kevlar cable performed according to its manufacturing specifications and sustained no damage for the duration of this cruise. During every operation the cable was carefully watched by the cruise to ensure that no “pinching” of the cable between the block and clamp occurred. During the voyage the Bosun and I would “walk” the cable post operations and check for any kinks, nicks or cuts to the outer sheath.

Note: Kevlar cable was load tested on board to 500kg and stretched to 1ton for 15 min increments.

#### Processing of CTD data

All CTD data was processed using SBE Data processing software following the standard filters which were edited to fit the specifications of the two configuration files supplied for the GeoTrace CTD and the Mini CTD.

#### Salinity validation

Salinity samples were taken on every Niskin CTD cast in order to validate the salinity sensor on the CTD – results below:

#### Naming convention for CTD files:

Station	ID	SDS ID	Station	GRID ID	CTD FILE NAME
SOAK	SWIN01	AM01092		VOY-038-SOAK	stn00_GeoSoak
SAZ	SWIN02	AM01093		VOY-038-SAZ	GT01_SAZ
SAZ2	SWIN03	AM01094		VOY-038-SAZ2	GT02_SAZ2

PUZ	SWIN04	AM01095	VOY-038- PUZ	NK03_PUZ
GT1W	SWIN05	AM01096	VOY-038- GT1W	GT04_GT1W
GT1	SWIN06	AM01097	VOY-038- GT1E	GT05_GT1
GT1E	SWIN07	AM01098	VOY-038- GT1E	GT07_GT1E
MIZ1A (MIZ1s)	SWIN08	AM01099	VOY-038- MIZ1	GT08_MIZ1 & NK09_MIZ1
MIZ2A	SWIN10	AM01100	VOY-038- MIZ2	GT010_MIZ2 & NK011_MIZ2
MIZ1E	extra	AM01105	VOY-038- MIZ1	GT012_MIZ1
GT2	SWIN12	AM01107	VOY-038- GT2	GT013_GT2 & NK014_GT2
GT3	SWIN13	AM01108	VOY-038- GT3	GT015_GT3 & NK016_GT3
GT5	SWIN14	AM01109	VOY-038- GT5	GT017_GT5 & NK018_GT3
GT6	SWIN15	AM01110	VOY-038- GT6	GT019_GT6 & NK020_GT6
GT7	SWIN16	AM01111	VOY-038- GT7	NK021_GT7 & GT022_GT7
GT9	SWIN17	AM01112	VOY-038- GT9	NK023_GT9 & GT024_GT9
GT10	SWIN18	AM01113	VOY-038- GT10	GT025_GT010

#### TSG

The TSG unit was flushed with triton-X prior to the pumps being switched on at the start of the voyage. The data collection was broken into "legs" and outlined below:

Leg	File name	Date/Time started (UTC)	Location
Cape Town to Ice Edge	AGU038a	Jul 18 2019 / 21:36:12	34° 11.050 S / 017° 59.743 E
54° S to Ice Edge	AGU038b	Jul 24 2019 / 20:45:33	55° 36.394 S / 000° 48.155 W
Ice edge - MIZ1 into the pancake ice	AGU038c	Jul 26 2019 / 17:24:17	56° 59.991 S / 000° 00.252 E
Ice edge to GoodHope line (North bound leg)	AGU038d	Jul 28 2019 / 19:55:45	56° 21.548 S / 000° 39.233 E
GoodHope line	AGU038e	Aug 03 2019 / 11:34:41	43° 00.005 S / 008° 30.020 E
East London to Cape Town	AGU038f	Aug 10 2019 / 09:20:29	33° 26.433 S / 027° 28.054 E

For the duration of the voyage there were no instrument glitches or sensor failures to report for the TSG system. The TSG was shut down temporarily during the voyage for a mandatory cleaning when the pumps were switched off in ice. A final flush of the system was conducted before leaving East London en route to Cape Town on the return journey.

Note: Suggested replacement of the pipe on the outflow point on the TSG unit.

#### ADCP

ADCP was not operational for the duration of this voyage due to a mechanical fault with the transducer and cable connection during the previous SEAmester cruise.

#### SDS system (AGU038 switched on 20:40 – 18<sup>th</sup> July 2019)

No issues to report regarding the SDS system, all data was successfully logged to the server and downloaded post cruise, the data was sent to STS, East Pier office in order to QC the data.

## **9. TEAM PLANKTON**

### **9.1. Winter Cruise**

#### **9.1.1. Introduction**

As part of the effort to understand the dynamics of food webs and carbon transport within the Southern Ocean and marginal ice zone, phytoplankton type and abundance are two of the most critical parameters that require monitoring. A number of surveys of Southern Ocean phytoplankton have been carried out during the austral summer. However, very little information is available on phytoplankton communities in the austral winter in the Southern Ocean generally and the marginal ice zone specifically. The opportunity provided by this winter cruise, including ice sampling, is unique in investigating phytoplankton communities during sea-ice formation as opposed to those during sea-ice break up during summer. This project has three main aims:

- 1.** To characterize the phytoplankton community composition and biomass across the marginal ice zone. This included sampling of the water column as well as within the ice itself. Investigations of these biological communities are strengthened by the association with the concurrent studies of the physical properties of ice structure by UCT Engineering team led by Dr Keith McKutchon.
- 2.** To characterize the phytoplankton community composition and biomass along the Good Hope line. This work has complemented the proposed research plan by the University of Stellenbosch team of Dr Suzanne Fietz and Prof. Alekendra Roychoudhury. In addition to the routine nutrient measurements, they will be analysing metal concentrations such as iron, and using HPLC to determine phytoplankton pigment characteristics. The envisaged phytoplankton community studies proposed here will greatly enhance our interpretation of the Stellenbosch University team's data. In addition, the data produced on the phytoplankton community composition will also complement the work done by the CSIR (Dr Tommy Ryan-Keogh and team), and Drs Sarah Fawcett and Katy Altieri of the University of Cape Town (Oceanography Department). Their examination of aerosols, carbon exchange and nitrogen fixation will be aided by the insight we provide on the types of phytoplankton communities present.
- 3.** To train and develop capacity in Southern Ocean oceanographic and Antarctic sciences, with particular emphasis on technological capacity. This is identified as a priority within the Marine and Antarctic Research strategy. Cape Peninsula University of Technology is the only UoT to offer a programme in Marine Sciences which advances technical capacity specifically. The annual summer SANAE cruise is not ideal for this purpose due to its length, timing and space limitations. CPUT participated in the July 2016 sea-ice research cruise, and, under Prof. Marcello Vichi, a similar, extended programme was implemented on the 2017 cruise. This cruise built on the experience gained in previous research voyages.

#### **9.1.2. Activity report**

Sampling took place in 3 phases during the cruise.

1. Underway surface samples. These samples for phytoplankton analyses (microscopic and flow cytometry) as well as for total chlorophyll a were taken every 4 hours from leaving Cape Town until the MIZ using the onboard flow-through system. Chlorophyll a samples were processed on board while phytoplankton microscope and flow cytometry samples were taken back to Cape Town for analysis. Phytoplankton samples have been retained at CPUT for further analysis. In addition, the CPUT Plankton team assisted with sampling and sample processing eg filtering of a number of different samples for the CSIR team. This included chlorophyll absorbance, HPLC samples and samples for biogenic silica.

2. Samples as above were taken from ice cores from pancake ice as well as frazil ice retrieved from the MIZ.

3. Samples as above were taken from CTD stations along the Good Hope line. In addition, the CPUT Plankton team also took routine samples from each CTD for oxygen sensor calibration.

### **9.1.3. Chlorophyll-a Results**

#### **9.1.3.1. Underway samples**

Total Chlorophyll a data will be provided as part of the CSIR cruise report. All samples (both underway and CTD were also size fractionated at pore sizes 20, 2.7 and 0.3  $\mu\text{m}$ . This data will form part of ongoing student projects.

#### **9.1.3.2. Marginal Ice Zone chlorophyll a samples**

Samples were taken from top, middle and bottom of ice cores provided by UCT Engineering. These were analysed for chlorophyll a and samples taken for later microscopic phytoplankton analysis. This data will form part of an MTech in Oceanography by Ms Simone Louw.

#### **9.1.3.3. Oxygen data**

At all CTD stations, samples were taken by the CPUT Plankton team and immediately fixed for Winkler titration oxygen analysis. Thanks to Dr Warren Joubert for his assistance with training students to carry out these analyses. The data was collated by Ms Sonya de Waardt and analysed in a report for submission as part of her Work Integrated Learning modules (see below).

### **9.1.4. Dissolved Oxygen**

#### **9.1.4.1. Introduction**

Dissolved oxygen is one of the most important gases to measure in the ocean, if there is not enough dissolved oxygen in the ocean it can lead to mortalities of living organisms because it can lead to hypoxic conditions (Helm et al, 2019). According to Helm et al (2012) dissolved oxygen concentration has been decreasing in the ocean, making it vital to monitor it. The Southern Ocean Seasonal Experiment (SCALE) is “an interdisciplinary experiment that spans seasonal to decadal time scales in the south east Atlantic sector of the Southern Ocean” (SCALE,2018). Jacobs (2006) stated that the Southern Ocean was observed to be in a disequilibrium in the last few decades.

He also mentioned that global warming could be contributing to the change in physical properties in the Southern Ocean such as salinity, temperature and dissolved oxygen. It has been suggested that global warming has contributed to climate change and that climate change might lead to an increase in anoxic conditions in the ocean (Bopp et al., 2002; Matear et al., 2000; Plattner et al., 2001; Sarmiento et al., 1998). Furuya et al (1995) noted that knowing the concentration of dissolved oxygen can also assist in studies on biological productivity in the Southern Ocean.

Instrumentation plays an important role in collecting data on dissolved oxygen. There are various methods that have been developed over the years to measure dissolved oxygen in seawater. The Winkler Titration Method is one of the most well-known and is seen as the only true primary method for determining dissolved oxygen in seawater (Helm et al., 2009). Limitations to this method is that it is very time consuming, provides limited data and requires training. Due to these limitations new instruments were developed to get large quantities of data and that is a lot less time consuming, these instruments include

Amperimetric Sensors and Optical Sensors which get attached to CTDs (Conductivity-Temperature-Depth Instrument), where the SB 43 Oxygen Sensor is an amperimetric sensor which uses a membrane to determine dissolved oxygen. Although using these sensors to determine dissolved oxygen is a much simpler and quicker method compared to using the Winkler Titration Method, it also comes with its own limitations (Helm et al, 2009). They noted that these instruments need continuous calibration to get accurate readings, therefore making the Winkler Titration method necessary to get the precise measurements required for determining dissolved oxygen.

#### **9.1.4.2. Aim**

The aim of the project is to describe how the SBE 43 Dissolved Oxygen Sensor can be calibrated using the Winkler Titration method from data collected during the Southern Ocean Seasonal Experiment 2019.

#### **9.1.4.3. Objectives**

- To determine the dissolved oxygen concentration of water samples collected on SCALE 2019 using the Winkler titration method
- To compare results calculated using the Winkler Titration Method with data collected from SBE 43 Dissolved Oxygen Sensor on the Sea-bird CTD during SCALE 2019.
- To determine if the oxygen sensor readings drifted in the duration of the cruise
- To determine the calibration factor to correct the oxygen data.

#### **9.1.4.4. Methods**

##### **Study Area**

The study area for the project took place onboard the SA Agulhas 2 during the Southern Ocean Seasonal Experiment 2019. Samples and Oxygen readings were collected along the Good Hope Line as seen in Figure 1. Ten stations were selected to conduct the study, locations and dates of collection can be seen in Table 1.

Station	Date	Latitude (°S)	Longitude(°E)
PUZ	24/7/2019	-54,00017	0,01123
GT1	25/7/2019	-56,0012	0,00185
MIZ 1	27/7/2019	-57,00007	-0,00313
MIZ 2	28/7/2019	-57,34503	-0,0028
GT 2	30/7/2019	-54,00088	0,00123
GT3	31/7/2019	-51,40167	0,00115
GT5	2/8/2019	-46,9999	4,4989
GT6	3/8/2019	-45,00012	6,59983
GT7	3/8/2019	-43,00008	8,50035
GT9	5/8/2019	-38,59913	11,80077

Table 9.1: Sampling stations with coordinates and dates of sampling events

### **Background and History of the Winkler Titration Method**

The measurement of dissolved oxygen in seawater was originally determined by the chemical method that was proposed by Winkler in 1888 (Hansen,1999). Other methods were developed as modifications of the original method such as Scholander et al in 1995 and Weiss and Craig in 1973. These modifications were mainly to improve the technical details of the procedure (Hansen, 1999). Hansen (1999) stated that the Winkler Titration method is a form of an iodometric titration. He explained the method to be a multistep oxidation that needs to be performed using manganese in order to allow dissolved oxygen in seawater to directly oxidize the iodide ion to iodine. The method was modernized through the development of instruments that improved the accuracy of the titration results by using a computer-controlled titration procedure which automatically detects the endpoint (Hansen, 1999). One of these instruments is the Metrohm 848 Titrono Plus which is an ideal instrument to ensure that the results of the titration method are accurate. This instrument is compact and ideal to use when performing dissolved oxygen titrations on board a vessel.

#### **9.1.4.5. Sampling Procedure**

During the cruise niskin bottles along with the Sea-bird CTD were deployed at 10 different stations as seen in Figure 2. Seawater samples were collected from depths ranging from approximately 5 meters to 1500 meters. Dissolved oxygen samples were collected in glass flasks with glass stoppers. The flask volumes ranged between 114 mL and 119 mL; this was taken into account in the final formulas to determine the dissolved oxygen content of the sample. The flask was filled and allowed to overflow for the amount of time it took to fill the bottle e.g. if it took 10s to fill the flask, the flask must be allowed to overflow for 10s. This prevented any air bubbles from external sources to be in the sample. Once the sample was collected, 1 mL of Manganese chloride and 1 mL of Alkaline iodide was added to the sample using a syringe pipette. After adding the reagents, the flask was shaken vigorously until the sample turned an

orange colour. The sample was then stored in a dark cupboard for 6-8 hours to allow the precipitate to settle.



Figure 9.2 The Deployment of the CTD with Niskin bottles.

### **Application of the Metrohm 848 Titrino Plus**

The Metrohm 848 Titrino Plus was used to perform the Winkler Titration method for the determination of dissolved oxygen in seawater. The components of the instrument can be seen in Figure 3. The instrument was filled with a known concentration of sodium thiosulphate. The instrument was equipped with a measuring beaker containing a stirring magnet, an electrode and a bottle containing the prepared thiosulphate solution. The instrument had a display screen which showed the endpoint, volume of thiosulphate and pH of the sample.

### **Preparation of the Sodium Thiosulphate Solution**

The sodium thiosulphate was prepared by filling the measuring cylinder with 50 mL of sodium thiosulphate and 500 mL deionized water. The solution was placed in a bottle that is part of the instrument. The solution was dispensed into a beaker to ensure that there are no air bubbles in the dispenser. Once the instrument was set up, the instrument needed to be standardized in order to get the known concentration of the thiosulphate. The standardization was performed every 24 hours, the standardization values had to have a standard deviation of 0.05 before using it to process the samples collected from the niskin bottles. The procedure to standardize the solution consisted of adding reagents to the beaker that was filled with 50 mL of deionized water. The reagents that were added was 1 mL of sulphuric acid, 1 mL of alkaline iodide, 1 mL of manganese chloride and 10 mL of the standard. The beaker containing the solution was swirled before adding each of the reagents. After completing the standardization, the values of the volume of sodium thiosulphate and pH was logged for data processing.

#### **9.1.4.6. Sample Processing**

The samples were processed by adding sulphuric acid with a syringe pipette to the glass flask containing the settled sample, the flask was vigorously shaken to allow the sulphuric acid to mix with the sample. The beaker containing the stirring magnet was filled with the sample and placed on the instrument. The electrode with the dispenser was placed inside the beaker to begin the titration. Once everything was set up the

instrument started the titration method by dispensing the thiosulphate into the sample. The instrument continued filling the beaker until the sample went from orange to transparent. Once the titration reached the endpoint it displayed the results of the volume of the sodium thiosulphate and the pH.

#### 9.1.4.7. Data Processing

##### Winkler Titration

The data was entered into a Microsoft Excel spreadsheet for calculation of the dissolved oxygen in each of the samples. The results of the dissolved oxygen readings are listed in Table 9.2.

The factor that was used in the calculation of the dissolved oxygen was calculated using the data acquired from the standardization. The values of the volume of sodium thiosulphate that had a standard deviation of less than 0.05 were averaged. The final formula of determining the factor is as follows where represents the average volume of thiosulphate.

$$\text{Factor} = \frac{5}{V_{\text{thio}}}$$

The following formula was used to calculate the dissolved oxygen readings from the data acquired from the instrument:

$$\text{Dissolved Oxygen} = \frac{V_{\text{thio}} \times \text{Factor} \times 112}{V_{\text{sample}} - 2}$$

represents the volume of sodium thiosulphate acquired from the instrument, 112 is a constant and represents the volume of the sample collected minus the volume of the reagents added.

#### 9.1.4.8. Calibration of Oxygen Data

The dissolved oxygen values obtained from the Winkler Titration method was used to determine if there was a drift in the oxygen sensor values. This was done by using a scatterplot indicating linear regression in Microsoft Excel 365. The program generated an equation which was used to correct values obtained from the oxygen sensor.

##### Data Presentation

The final results of determining the calibration formula and the regression coefficient which indicated the drift of the sensor is shown in Table 9.2. This was achieved by plotting the data from the Winkler Titrations against the data from the oxygen sensor and using the trendline to get the formulas and regression coefficient as seen in Figure 9.3. The drift of the oxygen sensor at each of the stations is illustrated in Figure 9.4. After determining the calibration formulas for each of the stations, it was used to calibrate the data retrieved from the dissolved oxygen sensor to get the profile of the oxygen with depth as seen in Figure 9.5.

Station	Formula	Regression Coefficient
Entire Cruise	$y = 0,6283x + 1,4427$	$R^2 = 0,2907$
PUZ	$y = 1,0859x - 0,0915$	$R^2 = 0,9864$
GT1	$y = -0,2425x + 6,1436$	$R^2 = 0,0142$
GT2	$y = 0,7712x - 0,2975$	$R^2 = 0,9238$
MIZ1	$y = 0,8287x + 1,0823$	$R^2 = 0,8599$
MIZ2	$y = 1,356x - 2,5801$	$R^2 = 0,4722$
GT3	$y = 0,7813x - 0,1627$	$R^2 = 0,9963$
GT5	$y = 0,5811x + 1,0423$	$R^2 = 0,9175$
GT6	$y = 0,7487x + 0,4378$	$R^2 = 0,6277$
GT7	$y = 0,7977x - 0,1526$	$R^2 = 0,9982$
GT9	$y = 0,5977x + 0,6663$	$R^2 = 0,6272$

Table 9.2: Calibration Formula and Regression Coefficient for Each of the Stations as well as for the entire cruise

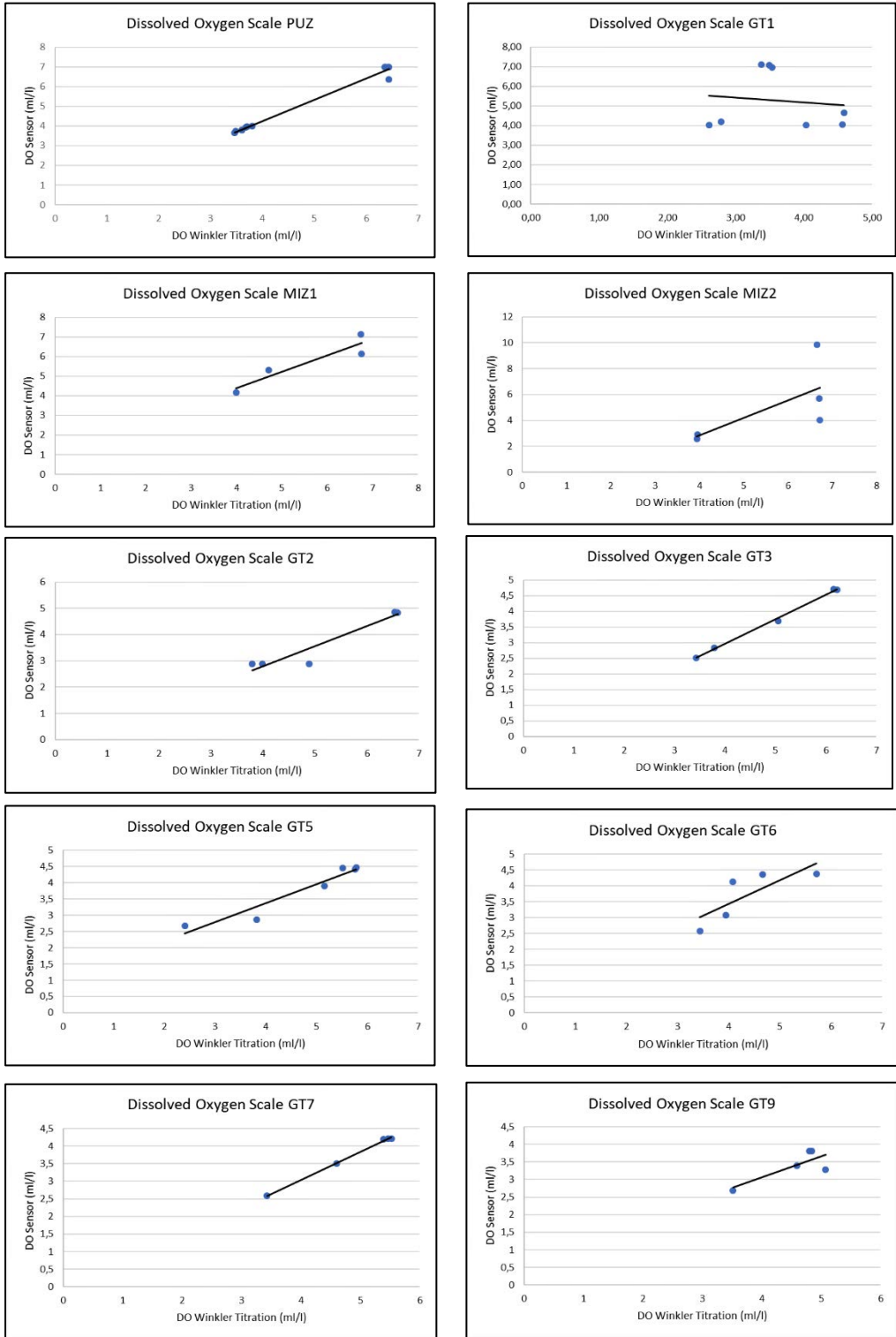


Figure 9.3: Graphical Representation of the comparison between data received from the Oxygen Sensor and the Winkler Titration.

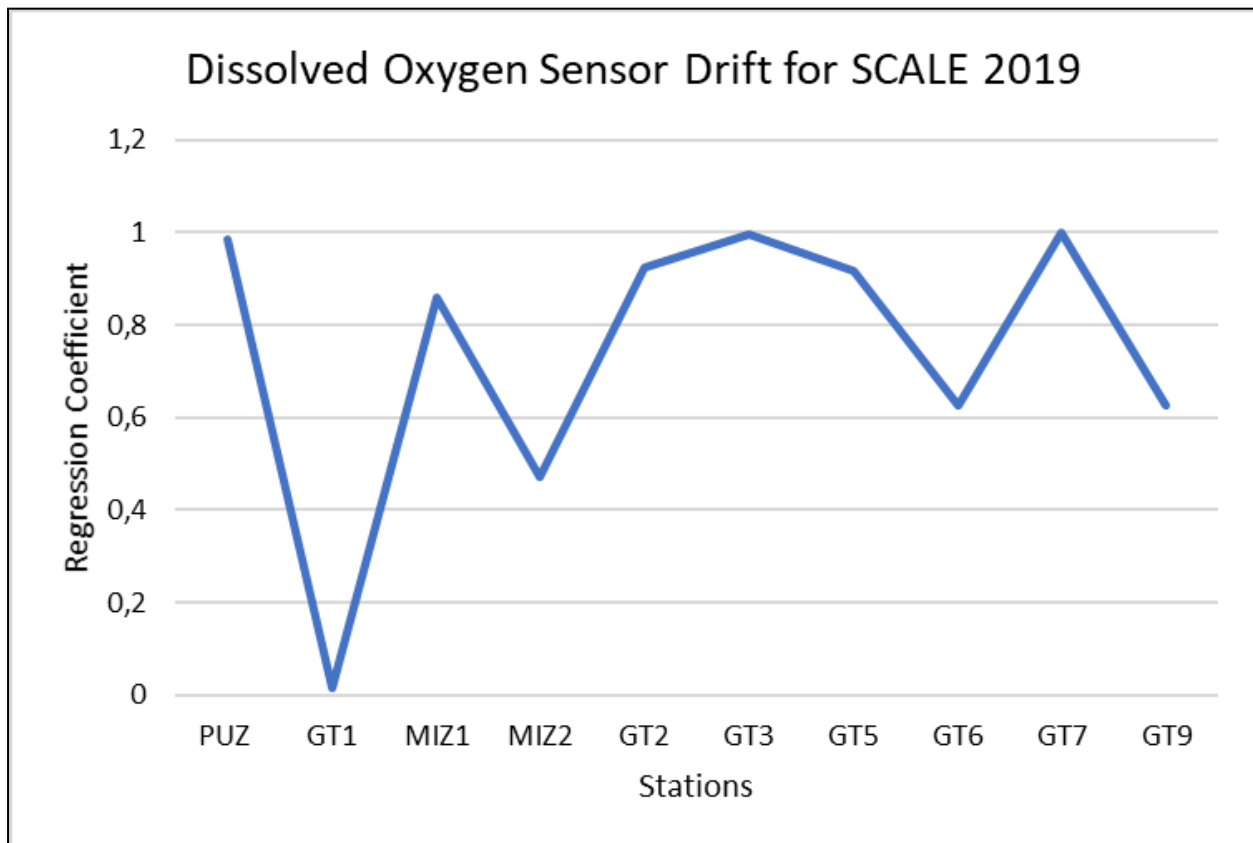


Figure 9.4: The drift in the oxygen data for the entire cruise

#### 9.1.4.9. Data Interpretation

It was clear that there was somewhat of a drift in oxygen data between the stations throughout the cruise when looking at Figure 9.3 and 9.4. Although there was a drift, it was observed that the drift did not occur over time but was instead station specific. At Station PUZ the sensor data had high accuracy readings which differed from station GT1 where it decreased rapidly, this occurred again between station MIZ 1 and MIZ 2 where MIZ 1 had high accuracy readings and decreased rapidly at MIZ 2. After exiting the marginal ice zone (MIZ), the oxygen sensor readings became much more accurate indicating that the drift might be due to environmental reasons. According to the manual published by Sea-Bird Electronics (2011) for the SBE 43 Dissolved Oxygen Sensor, there needs to be a constant flow of water pumping through the membrane to get accurate results. During the sampling of the water at MIZ 2 it was observed that the sensors on the CTD as well as the water in the niskin bottles froze and could have contributed to the restriction of water being pumped through the membrane. As seen in Figure 5, oxygen data from MIZ 2 does not show realistic profiles of oxygen with depth. The error could have come from both the Winkler Titrations and the dissolved oxygen sensor. The Winkler Titration error could have possibly come from the water being frozen in the niskin bottle, this led to a delay in time before collecting the samples. The water sample probably got contaminated from the ambient air whilst waiting for the water to defrost. The dissolved oxygen sensor error could have resulted from it being frozen, restricting flow of water through the membrane as stated earlier. The oxygen with depth profiles shown in Figure 5 indicated a high variation in dissolved oxygen levels at the surface. This could have been caused by the sensor being extremely sensitive to sudden changes in environment from the atmosphere to

the seawater, needing time to adjust to the new environment before lowering it further down through the water column. Another environmental factor to consider when looking at the drift in sensor data is temperature. Temperature impacts the diffusion rate of the dissolved oxygen through the sensor's membrane and as temperature decreases the measured dissolved oxygen readings also decreases (Edaphic Scientific, 2019). This might be one of the reasons why there were inaccurate readings in the Marginal Ice Zone.

#### **9.1.4.10. Conclusion**

It can be concluded that there is a definite need to use the Winkler Titration Method to determine oxygen as well as the need in using an oxygen sensor. The oxygen sensor allows for high volumes of data to profile dissolved oxygen with depth. Although the sensor is convenient, it does drift due to environmental conditions that impact the constant flow of water being pumped across the membrane. It is unclear if the sensor is vulnerable to drift caused by fouling of the membrane over time throughout the cruise, but it is clear that the drift is station specific and dependent on local environmental conditions.

#### **9.1.4.11. Recommendations**

- It is advised to collect more duplicate samples from certain depth to get a more information on where in the water column the drift might have occurred.
- It is recommended to profile temperature with depth to confirm if it had an impact on the sensor readings.
- Collect samples from niskin bottles as soon as it is retrieved.

#### **9.1.5. References**

Bopp, L., C.; Le Que´re´, M.; Heimann, A. C.; Manning, & P. Monfray. 2002. Climate-induced oceanic oxygen fluxes: Implications for the contemporary carbon budget. *Global Biogeochem. Cycles*, 16(2), 1022, doi:10.1029/2001GB001445.

Edaphic Scientific. 2019. Dissolved Oxygen Probes, Sensors & Meters Australia. <https://www.edaphic.com.au/oxygen/dissolved-oxygen-sensors-and-meters/> [14/10/2019].

Furuya, K. & Harada, K. 1995. An Automated Precise Winkler Titration for Determining Dissolved Oxygen on Board Ship. *Journal of Oceanography*, 51:375-383.

Hansen, H.P. (1999). 'Determination of oxygen', in Grasshoff, K.; Kremling, K. & Ehrhardt, M. (ed). *Methods of Seawater Analysis*. New York: Wiley-VCH, pp 75-89. 1999.

Helm, I.; Jalukse, L.; Vilbaste, M. & Leito, I. 2009. Micro-Winkler titration method for dissolved oxygen concentration measurement. *Analytica Chimica Acta*, 648:167-173.

Helm, I.; Jalukse, L. & Leito, I. 2012. A highly accurate method for determination of dissolved oxygen: Gravimetric Winkler method. *Analytica Chimica Acta*, 741: 21-31.

Jacobs, S. 2006. Observations of change in the Southern Ocean. *Philosophical Transactions of the Royal Society*, 364: 1657-1681.

Matear, R. J. (2000) Climate change impacts on marine systems, *Aust. Microbiol.*, 21(2), 17– 20.

Plattner, G. K.; Joos, F.; Stocker, T.F.&. Marchal, O. 2001. Feedback mechanisms and sensitivities of ocean carbon uptake under global warming. *Tellus Ser. B*, 53(5), 564– 592.

Sarmiento, J. L., T. M. C. Hughes, R. J. Stouffer, and S. Manabe, Simulated response of the ocean carbon cycle to anthropogenic climate warming, *Nature*. 393, 245–249, 1998.

Sea-Bird Electronics, Inc. 2011. SBE 43 Dissolved Oxygen Sensor: Background Information, Deployment Recommendations, and Cleaning and Storage. Bellevue, USA: Sea-Bird Electronics.

## **9.2. Spring Cruise**

### **9.2.1. Introduction**

As part of the effort to understand the dynamics of food webs and carbon transport within the Southern Ocean and marginal ice zone, phytoplankton type and abundance are two of the most critical parameters that require monitoring. A number of surveys of Southern Ocean phytoplankton have been carried out during the austral summer. However, very little information is available on phytoplankton communities in the austral spring in the Southern Ocean generally and the marginal ice zone specifically. The opportunity provided by this Spring cruise including ice sampling, is unique in investigating phytoplankton communities during the sea-ice break up during spring. This project has three main aims:

- To characterize the phytoplankton community composition and biomass across the marginal ice zone. This included sampling of the water column as well as within the ice itself. Investigations of these biological communities are strengthened by the association with the concurrent studies of the physical properties of ice structure by UCT Engineering team.
- To characterize the phytoplankton community composition and biomass along the Good Hope line and sea ice. This work has complemented the proposed research plan by the University of Stellenbosch team of Dr Suzanne Fietz and Prof. Alekendra Roychoudhury. In addition to the routine nutrient measurements, they will be analysing metal concentrations such as iron, and using HPLC to determine phytoplankton pigment characteristics. The envisaged phytoplankton community studies proposed here will greatly enhance our interpretation of the Stellenbosch University team's data. In addition, the data produced on the phytoplankton community composition will also complement the work done by the CSIR (Dr Tommy Ryan-Keogh and team), and Drs Sarah Fawcett and Katye Altieri of the University of Cape Town (Oceanography Department). Their examination of aerosols, carbon exchange and nitrogen fixation will be aided by the insight we provide on the types of phytoplankton communities present.

- To train and develop capacity in Southern Ocean oceanographic and Antarctic sciences, with particular emphasis on technological capacity. This is identified as a priority within the Marine and Antarctic Research strategy. Cape Peninsula University of Technology is the only UoT to offer a programme in Marine Sciences which advances technical capacity specifically. The annual summer SANAE cruise is not ideal for this purpose due to its length, timing and space limitations. CPUT participated in the July 2016 sea-ice research cruise, and, under Prof. Marcello Vichi, a similar, extended programme was implemented on the 2017 cruise. This cruise built on the experience gained in previous research voyages.

### **9.2.2. Activity report**

Sampling took place in 3 phases during the cruise.

- Underway surface samples. These samples for phytoplankton analyses (microscopic and flow cytometry) as well as for total chlorophyll a were taken every 8 and 4 hours, respectively from leaving Cape Town until the MIZ using the onboard flow-through system. Chlorophyll a samples were processed on board while phytoplankton microscope and flow cytometry samples were taken back to Cape Town for analysis. Phytoplankton samples have been retained at CPUT for further analysis. In addition, the CPUT Plankton team assisted with sampling and sample processing eg filtering of a number of different samples for the CSIR team. This included chlorophyll absorbance, HPLC samples and samples for biogenic silica.
- Samples as above were taken from ice cores from pancake ice as well as frazil ice retrieved from the MIZ.
- Samples as above were taken from CTD stations along the Good Hope line. In addition, the CPUT Plankton team also took routine samples from CTD stations for oxygen sensor calibration.

### **9.2.3. Chlorophyll-a Results**

Underway samples

Total Chlorophyll a data will be provided as part of the CSIR cruise report. All samples (both underway and CTD were also size fractionated at pore sizes 20, 2.7 and 0.3  $\mu\text{m}$ . This data will form part of ongoing student projects.

Marginal Ice Zone chlorophyll a samples

Samples were taken from top, middle and bottom of ice cores provided by UCT Engineering. These were analysed for chlorophyll a and samples taken for later microscopic phytoplankton analysis. This data will form part for prospective MTech Oceanography students.

### **9.2.4. Oxygen data**

At CTD stations, samples were taken by the CPUT Plankton team and immediately fixed for Winkler titration oxygen analysis.

## **10. TEAM PLASTICS**

### **10.1. Key objectives**

To investigate heterogeneity in the density, distribution and characteristics of micro-, meso- and macroplastics at sea along a latitudinal gradient.

### **10.2. Data collection: Open water sampling**

#### *Mesoplastics sampling: Neuston net*

We sampled for mesoplastics using a 200  $\mu\text{m}$  neuston net which we deployed from the starboard side of the foredeck. The front crane was used to gently lower the net into the water and tow it for 15 minutes at 2 knots. Upon retrieval, the net was hosed down from the outside to ensure that any material caught on the sides of the net was rinsed into the cod end. We conducted four neuston net tows during the SCALE Winter Cruise 2019 and 17 during the SCALE Spring Cruise 2019 (please see Table 11.1 for details).

The samples were processed in the underway lab and preserved in ethanol for future analyses. Once analysed by our team, the biological material will be given to Luca Stirnmann (NOCE team) to analyse for zooplankton.

#### *Microplastics sampling: Surface water grabs*

We collected replicate surface water samples (40 L) during each neuston net tow by lowering a stainless-steel bucket from the port side of the bow. Samples were filtered in the underway lab on 25  $\mu\text{m}$  (30 L) and 0.7  $\mu\text{m}$  (10 L) filters. Filters were stored in foil packets and frozen for future analyses at the University of Cape Town. Please see Table 1 for details.

#### *Macroplastics sampling: Distance sampling*

We conducted 54 hours of observations during the SCALE Winter Cruise and 71 hours during the SCALE Spring Cruise. We conducted observations either from the observation deck or from the bridge wing and recorded all floating anthropogenic and natural macrodebris items seen in 10-minute transect intervals. For each item seen, the observer recorded the type of material, its colour, approximate size, buoyancy and distance from the ship's track. We only conducted observations during daylight hours while the ship was steaming and when weather conditions permitted. The data will be processed at the University of Cape Town.

**Table 10.1.** Summary of open water samples collected and processed (excluding macro-debris transects) by the Plastics team during the SCALE Winter and Spring cruises 2019

<b>Date</b>	<b>Station</b>	<b>Neuston net tows</b>	<b>Surface water (litres)</b>
<b>Winter</b>			
27/07/2019	MIZ3	0	40
28/07/2019	MIZ1	0	40
31/07/2019	GT3	1	40
01/08/2019	GT5	1	40
02/08/2019	GT6	1	40
03/08/2019	GT7	0	40
06/08/2019	GT-EL	1	40
<b>Spring</b>			
13/10/2019	SOAK	1	40
17/10/2019	ST1	1	40
19/10/2019	PUZ	1	40
20/10/2019	MIZ1a	1	40
11/11/2019	GT4	2	40
12/11/2019	GT5	2	40
14/11/2019	GT7	2	40
15/11/2019	GT6	2	40
15/11/2019	GT7b	2	40
17/11/2019	GT9	1	40
18/11/2019	GT10	2	40
<b>Total</b>		<b>21</b>	<b>720</b>

### **10.3. Data collection: Marginal Ice Zone (MIZ) sampling**

#### *10.3.1. Pancake ice*

We sampled sections of pancake ice during the SCALE Winter Cruise by cutting out rectangular blocks (~10 x 30 cm) with a saw which we melted in a stainless-steel bucket. Care was taken to control for environmental contamination by scraping the sides of the ice blocks with a stainless-steel blade and rinsing each piece with filtered water prior to melting. All equipment was either glass or metal, was triple rinsed before use and was covered with aluminium foil to prevent aerial contamination. We sampled two pancakes from which we filtered 56 L of ice on 25 µm and 38 L on 0.7 µm. We also melted and filtered cores collected from a third pancake by the Sea Ice team (mean volume filtered =  $1.14 \pm 0.10$  L). The samples will be analysed at the University of Cape Town. Please see Table 10.2 for details.

#### *10.3.2. Ice cores*

We collected ice cores during the SCALE Spring Cruise to test for microplastic pollution. At MIZ 2 the Sea Ice Team collected five cores for us. However, upon reflection it was decided that the best way to reduce the chance of aerial contamination from clothing would be if Michael Danial and Eleanor Weideman accompanied the Sea Ice Team onto the ice and collected the safety cores. At MIZ 3, 4, 6 and 7 Riesna Adhu (Sea Ice team) therefore drilled five safety cores at each station using either a plastic

or carbon fibre coring barrel and placed these upwind to reduce the chance of aerial contamination. Our team then placed the cores into pre-rinsed plastic bags.

In the lab, we melted the cores in a pre-rinsed stainless-steel bucket and then filtered the water through 0.7 µm filters (mean volume filtered = 1.97 ± 1.02 L). The filters were stored in clean metal foil and will be analysed at the University of Cape Town (please see Table 10.2 for details).

### 10.3.3. Snow and surface water samples

In addition to ice cores, we also collected replicate snow and surface water samples at each MIZ station. We collected snow samples by scraping snow into pre-rinsed glass jars using a clean metal garden shovel. The snow was then melted and filtered through 0.7 µm filters which were stored in clean metal foil and will be analysed at the University of Cape Town. To reduce the chance of aerial contamination, the snow samples were collected 1 – 2 m upwind of where the last safety core was drilled.

To compare microplastic pollution in ice, snow and surface water, we also collected 40L of surface water by lowering a stainless-steel bucket from the aft deck. This water was also filtered through 0.7 µm filters. Please see Table 10.2 for details.

**Table 10.2.** Summary of samples collected in the Marginal Ice Zone (MIZ) by the Plastics team during the SCALE Winter and Spring cruises 2019

Date	Station	Pancake ice (litres)	Ice cores	Snow	Surface water
<b>Winter</b>					
28/07/2019	MIZ1	99	0	0	40
<b>Spring</b>					
24/10/2019	MIZ2	0	3	6	40
25/10/2019	MIZ3	0	5	5	40
27/10/2019	MIZ4	0	3	0	40
28/10/2019	MIZ5	0	0	5	40
19/10/2019	MIZ6	0	5	5	40
30/10/2019	MIZ7	0	5	5	40
Total		99	21	26	
280					

## 10.4. Results

Results are not available yet as samples will be analysed at the University of Cape Town.

## 10.5. Acknowledgements

We thank chief scientists Thomas Ryan-Keogh (CSIR), Marcello Vichi (UCT) and Sandy Thomalla (CSIR) for the opportunity to participate in the SCALE Cruises and for all their coordination and logistical support. Thank you to the ice team for their support at the MIZ stations and thank you to Captain Knowledge Bengu and the crew of the S.A. Agulhas II for their hospitality and assistance with the scientific work.



## **11. TEAM PRODUCTION**

### **11.1. Bio-optics – Ocean colour**

#### **11.1.1. Motivation & Background**

The Southern Ocean is a well-established carbon dioxide sink and plays an essential role in the global carbon cycle. The in-situ examination of the influence of seasonal cycles and physical drivers on biological production is often spatially and temporally limited. Remote sensing has allowed for regional characterisation by providing routine, synoptic and cost-effective observations at a high frequency and over decadal time scales. Most often remotely sensed data are the only systematic observations available for chronically under-sampled marine environments (e.g. the polar oceans), and there is thus a need to maximise the value of these observations by developing ecosystem-appropriate, well-characterised products.

The CSIR bio-optics suite employed for SCALE includes instruments to measure bulk inherent optical properties (IOPs- scattering, attenuation and absorption), as well as multi-excitation fluorometry used to determine the fluorescence quantum yield of the phytoplankton community. A complementary suite of biogeochemical measurements (as detailed in the Production section) provides the foundation for understanding phytoplankton community composition, on top of which the optical data can be laid, allowing interpretation of all these data towards some understanding of the relationships at play. These systems are complex and a large suite of bio-optical and biogeochemical measurements, over a wide variety of oceanic conditions, is required to achieve this. SCALE's cross section of seasonal conditions provides a valuable opportunity to acquire the requisite data. Together, the bio-optical, biogeochemical and photo-physiological data can be used to parameterise the particle field (the most notable component of which is the phytoplankton community) under a range of different seasonal and biophysical conditions through the quantification of empirical relationships between IOPs and size, pigment and carbon content.

Building on this understanding of observations, empirical relationships can be used in combination with modelled data to form a comprehensive picture of bio-optical drivers and their capacity for inducing optical variability, which can further inform on inherent limitations in the use of bio-optics in phytoplankton community determination, in terms of both ambiguity and signal sensitivity.

This can be taken further with the coupling of IOP models to radiative transfer solutions, allowing sensitivity experiments in both forward and inverse directions, the latter having direct bearing on capability in assessing the utility and contributing to the improvement of existing reflectance inversion algorithms for the retrieval of biogeochemical parameters from spaceborne radiometry.

A particular application of the data collected on the SCALE voyages is towards an assessment of the limits of satellite-based oceanography in terms of phytoplankton identification and quantification via the use of Phytoplankton Functional Types (PFTs): identifying dominant phytoplankton groups in terms of their biogeochemical roles in primary production, nutrient recycling and carbon transport/fixing. As the CSIR/UCT Equivalent Algal Populations (EAP) model of phytoplankton optics matures from

limited application in South African shelf waters towards application in the Southern Ocean, its capability and utility in deriving this information from satellite radiometry is of increasing interest to the global scientific community. There are, however, inherent limitations to the utility of satellite observations due to causal ambiguity in the source of in-water optical signals – and this is the specific area of interest being addressed.

An important aspect of EAP model development is towards a quantification of the role played by organic carbon in the optical identification of PFTs. This is a novel extension to the existing optical model and will inform an improved understanding and assessment of the role of different phytoplankton types in the carbon cycle. The capacity of the Southern Ocean to act as a long term carbon dioxide sink will only be revealed upon a better understanding of the impacts of various forcing mechanisms on phytoplankton physiology and community structure – and the biogeochemical measurements made in the Southern Ocean feed directly into our understanding of these relationships and our ability to model them in pursuit of understanding not only current dynamics, but also those of a future ocean.

It is also through the characterization of these relationships that we are able to exploit optimally the optical data gathered by the gliders in the SOCCO glider project. Each glider has a BB3 measuring particulate backscatter on a continuous basis. From this measurement and together with the coincident fluorometry sensor data, it is in theory possible to isolate the backscatter due to the phytoplankton particulate component and therefore the dominant cell size and concentration of phytoplankton assemblages. These relationships are complex and unique in the Southern Ocean, and these measurements all contribute to the development of appropriate regional algorithms for extracting this information from the sensors we have available.

#### Objectives

The objectives of the SCALE Bio-Optics data collection effort are:

- Continuation of the inter-annual SOCCO dataset of biogeochemical parameters in the Southern Ocean. This addresses the objective of achieving improved understanding of phytoplankton response to event, seasonal and inter-annual variability in ecosystem physical drivers. While the focus has historically been on bloom initiation and onset in winter/spring, the higher productivity of the summer months also provides valuable insight into seasonal dynamics.
- Determine regionally specific relationships between oceanic optical properties and biogeochemistry in the Southern Ocean. A good understanding of regional optical properties, their variability and their relationship with fundamental measurable variables, such as Chl a concentration, is the foundation of any programme which aims to investigate phytoplankton community structure from the measurement of essential variables, as well as any optical remote sensing programme. Empirical observations can be used in the simplest sense to facilitate continuous improvements in regional algorithms for the retrieval of biogeochemical parameters, but the ultimate objective is towards a causal understanding of these relationships. A causal understanding of these highly interconnected and complex relationships will ultimately reveal the inherent biophysical limitations of the use of remotely sensed ocean colour data.
- Causal understanding of bio-optical relationships in phytoplankton communities. A causal understanding of the optical drivers of ocean environments allows for the quantification of the associated variability and

ambiguity inherent in optical observations. This is best achieved by the systematic examination of the respective effects of all optical components, which is achievable only via modelling.

- The unique seasonal characteristics of winter (low biomass), spring (bloom initiation) and summer (higher biomass) all yield excellent opportunities for different aspects of model development, all feeding into a much improved capability to model the varying optical contributions of oceanic in-water constituents: phytoplankton communities (whose assemblage characteristics are generally the primary quantities of interest in optical oceanography) - but also the optical characteristics of non-algal constituents: detrital or waste products (often covarying with phytoplankton), “background” optical contributions from bubbles or viruses, or those of non-algal particles potentially attendant to phytoplankton like bacteria. These constituents are understood to be found in varying proportions at different points in the seasonal cycle, and by examining the dataset as a whole, their respective impacts on the optical environment can be better quantified – resulting in improved modelling capability.
- Extension of the Equivalent Algal Populations (EAP) model of phytoplankton optics into the Southern Ocean. To meet the requirements for investigating the biogeochemical parameters of interest in Southern Ocean research, this extension involves the development of a carbon-driven optical component for incorporation into the model, which currently prioritizes particle size distribution and intracellular pigment density as the optical determinants. Given the widespread distribution of anomalously-scattering coccolithophorid species in the Southern Ocean, this is another aspect of model development required to address the unique biogeochemistry of this region.

### **11.1.2. SCALE Bio-Optical Measurement Suite**

The SCALE Bio-Optics data collection effort comprises three components:

- 1) Continuous measurements performed by the Under Way IOP system. Instruments on the IOP flow-through system include a BB3 (optical scattering at 3 wavelengths), AC-s (absorption and attenuation meter) and MFL (continuous fluorescence).
- 2) Additional optical measurements performed at stations e.g. BB9, acidified BB3 measurements.
- 3) Complementary biogeochemical measurements performed at stations: Coulter Counter (particle size distribution), Fast Repetition Rate Fluorometry, Particulate Absorbance (PAB), High Performance Liquid Chromatography (HPLC) etc.

Underway sampling comprised continuous sampling on the IOP (Inherent Optical Properties) board, and the additional measurements performed at 4 hourly stations were filtrations, size distribution and fluorescence measurements.

Continuous particulate backscatter (BB3) measurements were performed at 3 wavelengths, with the attendant calibration and cleaning procedures. Whereas the lack of certain instruments (detailed in each cruise’s section on data collection) disappointingly prohibited the comprehensive collection of co-incident measurements as intended, their absence did provide time pay detailed attention to the BB3 and run experiments testing sensitivity to flow rates, internal pressure and bubbles. The BB3,

when run in under way mode, is sensitive to small changes in the way in which it is fed sample water – a great challenge in Southern Ocean conditions where the under-way water intake is frequently subjected to pressure variations by active pitching and rolling of the ship. The time for additional experiments investigating this sensitivity has provided valuable data with which to contextualize, post-process and properly interpret measurements across all voyages.



Fig. 11.1 The IOP system

Also, on the BB3 (black box bottom left in Fig. 11.1); a series of filtration experiments were performed to assist in the characterisation of the small particle (detrital) contribution to backscatter. These particles are too small to be quantified by the Coulter Counter but have a significant impact on the particulate backscatter – which must be corrected for in the processing as the intention is to isolate the phytoplankton backscatter from the bulk signal which includes scatter by salt crystals, bubbles, viruses, bacteria and any other non –algal in water constituents. Our current protocols (based on international standards and norms) address backscatter by particles less than 0.1 micron by filtration, but there is still a “missing” size range between 0.1 and 2 micron which we cannot account for in a closure exercise. We performed a series of experiments with the filters available to us to close this gap as far as possible. This is one example of the enormous insight gained from performing the measurements oneself rather than simply processing and interpreting the data – and indicates a significant improvement to our processing methodologies and our ability to better characterize the scattering by these very small particles.

In addition to the need to parameterize non-algal scattering contributions, there is also a need to characterize anomalous phytoplankton scatter – that of coccolithophores, known to be widely distributed in the Southern Ocean. Coccolithophores (*Emiliana* spp.) are armoured with calcium carbonate liths or shell-like structures on their exterior, and these scatter light much more effectively than other phytoplankton. In bloom they are easily identifiable by this unique scattering signal, but in mixed assemblages their elevated scatter contributes to signal ambiguity when determining PFTs based on particle size. We employed an acidification process using Glacial Acetic Acid to dissolve the liths and allow a backscatter measurement without them –

the difference between the bulk and the acidified backscatter can then be attributed to the coccolithophore contribution.

#### Data Collection:

Winter: 18 July – 12 August 2019

Due to a last-minute shipping mishap, the AC-s instrument did not arrive back in Cape Town in time for the cruise, after calibration in the United States. An OSCAR instrument was investigated on-board as an alternative but without the required planning proved complex to operate and prone to leaks.

The BB3 was run continuously, and the BB9 was used on stations to provide co-incident backscatter data. Number of days/stations achieved?

The MFL ran continuously without incident.

Spring: 12 October – 18 November 2019

The MFL ran continuously without incident.

A software control problem with the AC-s prevented measurements on the southbound journey. This was resolved for the return journey, but two LEDs then blew  $\frac{3}{4}$  of the way northwards. A diode on the BB9 blew after 8 days of sampling on the southward journey. It was irreparable by ship technicians.

This meant that the desired dataset of coincident BB3, BB9 and AC-s measurements was not achieved. Co-incident BB3 and AC-s data were recorded between 4 and 13 November, and this period represents the most important bio-optical data collection for this cruise. The 8 days of coincident BB3 and BB9 measurements (14, 15, 17-19 October) are also valuable, particularly in conjunction with the ancillary PAB, Coulter and HPLC data collected.

It is worth noting that continuous BB3 measurements in combination with Chl a on stations, are useful in themselves for regional/zonal studies, despite not being critical to model development.

### 11.1.3. Brief Description of Measurement Protocols

#### Absorbance

##### WETLabs AC-S

The WETLabs AC-S is a hyperspectral instrument measuring attenuation and absorbance in the visible wavelength spectrum at a resolution of 4 nm. It is used in continuous mode on the underway IOP system alongside the BB3 scattering meter. Remembering that  $c = a+b$ , i.e. attenuation is the sum of absorbance plus scattering, when used together, the data from these instruments describes the full set of bulk in-water IOPs in a continuous manner. This is a powerful combination allowing not only the comprehensive characterization of S. Ocean IOPs but also providing much needed data for model development and validation.

The operation of this instrument and processing/interpretation of the data has proved challenging. After suspecting calibration had drifted in early 2019, the instrument was sent to the US and did not arrive back in time for the winter cruise due to a shipping error. It was deployed on the spring cruise but software issues were experienced. On rectifying these, the instrument then worked for about 10 days before blowing two

bulbs simultaneously with no obvious cause. The difficulties with this instrument represent a significant blow to the overall aims of the IOP system.

#### Underway sampling

The AC-S was set up in a flow-through chamber, receiving seawater from the scientific underway ship's supply. The AC-S was run in a continuous underway mode.

#### Cleaning, Calibration and Biofouling

Clean and dirty milliQ runs were each performed twice a day for the purposes of a biofouling correction of the underway data. Once a week, an air calibration was performed on the dry instrument. This provides an indication of instrument drift (a clean and dry instrument should record values very close to zero).

#### Backscattering

##### WetLabs BB9

The WETLabs Scattering Meter (ECO BB9) contains three BB3 instruments, each providing a backscatter measurement for 3 different wavelengths (collectively 412nm, 440nm, 488nm, 510nm, 532nm, 595nm, 650nm, 676nm and 715nm), as well as one data multiplexer, which functions to power the BB3 instruments, to start each data sample, to read all data and to re-format and output the data from all BB3s in a synchronized manner. Scattering and back-scattering are very useful IOPs in terms of describing particle size and composition in ocean environments.

#### Underway sampling

The BB9 was sampled every 4 hours (12, 4, 8 ship time) and / or to coincide with Niskin CTD stations. For a given sample, the chamber is filled from the underway supply, and data are logged for 10 minutes. When the instrument is started, data are checked visually using ECOView123 software, however the data are saved through the python file 'bb9'.

#### Cleaning, Calibration and Biofouling

After data are logged for 10 minutes on the BB9, the detectors on the sensor face are covered with dark electrical tape, the BB9 is then submerged again, and data were logged for approximately 6 minutes (wet dark run). Thereafter, the chamber was drained, and all the chamber walls were cleaned with ethanol. A dry dark (taped) run was conducted (data logged for 6 minutes with the tape still on the detectors, but not submerged in any water). Finally, the tape was removed from the detectors, the optical windows were cleaned and data were logged for approximately 6 minutes (dry empty, cleaned chamber run).

##### WetLabs BB3

The WETLabs Scattering Meter (ECO BB3) provides a backscatter measurement for 3 different wavelengths (470nm, 532nm and 700nm).

#### Underway sampling

The BB3 was set up in a flow-through chamber, receiving seawater from the scientific underway ship's supply. The BB3 was run in a continuous underway mode. Counts

for the wavelengths were continuously checked visually using ECOView123 software, however the data were saved through the python file 'bb3'. BB3 backscattering data were logged continuously but stopped once the ship was stationary. When the Niskin CTD went in the water, data for the bb3 were logged.

#### Cleaning, Calibration and Biofouling

After each BB3 station run was conducted, a filtered sea water was run through the chamber and data were logged for approximately 10 minutes

Every 12 hours, a BB3 chamber was drained and then filled with MilliQ (MQ) and files logged for 6 minutes (dirty MQ run). The BB3 coffin was then drained and cleaned with ethanol, plus the optical windows were cleaned. A dry empty run of the chamber was conducted, and data logged for 6 minutes. The BB3 detectors were then taped, and the data was logged for 6 minutes (dry dark run). The BB3 instrument was then put into a beaker of UW seawater (with the tape still on the detectors) to log data for 6 minutes (wet dark run). After the tape had been removed, the sensor face was cleaned with ethanol, the instrument was put back in place in the coffin, it was filled with MilliQ to conduct a clean MilliQ run, and data were logged for 6 minutes.

#### Fluorescence – MFL

Phytoplankton populations are easily identified by their signature accessory pigments. Chlorophyll is the primary light harvesting pigment, however additional accessory pigments serve to capture light at wavelengths that chlorophyll may not be able to effectively absorb. This umbrella effect is designed to optimise the light capturing potential of phytoplankton. These secondary pigments influence the excitation spectrum of phytoplankton in a species-specific manner, a property that has been exploited by the JFE Advantech Multi Excitation fluorometer (MFL), which serves to discriminate between phytoplankton species based on their accessory pigment composition. It is equipped with a high sensitivity chlorophyll fluorescence detector and 9 excitation LEDs (375nm, 395nm, 420nm, 435nm, 470nm, 490nm, 535nm, 570nm and 590nm), measuring phytoplankton biomass and estimating species composition.

The MFL was run in continuous mode, sampling seawater from the ship's scientific underway supply, by having it pumped under positive pressure to fill the MFL sampling chamber. The software was then initiated to record several minutes of data for each sample. Once a day, the optical window of the MFL was cleaned.

## **11.2. Marine Snow Catcher – Carbon Export**

### **11.2.1. Rationale and Motivation**

The main factors that control material transfer efficiency both on global and regional scales remain unclear. Particle export efficiency is linked with primary production (PP), throughout the water column and a decrease in particle export efficiency was observed at different depths. Positive correlation was observed between the export efficiency and PP by combining export efficiency model estimates of ocean temperature and photosynthetic rates (Laws et al., 2000). While, Maiti et al. (2013) challenged this hypothesis by showing a negative correlation with less sensitivity towards temperature in the SO (Maiti et al., 2013). Carbon export is affected by numerous processes such as remineralization, zooplankton grazing and large export of DOC below the mixed layer depth. The transport of organic material from the euphotic zone to the twilight

zone and to the ocean interior form part of the vertical flux (Pace et al., 1987; Yamanaka & Tajika, 1996). Thus, the vertical flux is determined by the rate of degradation, composition and sinking velocity of the aggregates. The net transfer of carbon from the euphotic zone to the twilight zone is mainly due to the effect of biological carbon pump (BCP) and microbial loop (ML) (Basu & Mackey, 2018). Therefore, increased PP represents an effective BCP, which in turn results in increased carbon export efficiency, where only a small portion of the exported material is removed on a century time scales (Moutin & Raimbault, 2002).

In addition to the ML, a process that enhance carbon export both in the euphotic and twilight zone is referred to as microbial carbon pump (MCP). Which is a conceptual framework for understanding the key role of microbial processes in DOC remineralisation and the production of recalcitrant DOC (RDOC) (Bauer et al., 1992). RDOC produced by microbial remineralisation is resistant to rapid microbial degradation and thus sinks to the ocean interior contributing to carbon export (Hansell et al., 2012). About 91% of the RDOC in the ocean originates from bacterial activity with 1% of labile DOC and 4% semi-labile DOC (Hansell et al., 2009; Hansell, 2013). The labile and semi-labile DOC are further degraded by microorganisms and re-enter the food web, ultimately resulting in RDOC. In addition to POM formed by sinking phytoplankton, aggregates and faecal pellet, there is some POM that contributes to DOC coming from bacterial lysis (Jiao & Zheng, 2011), the leakage or exudation of fixed carbon from phytoplankton (Berman & Wynne, 2005; Moutin & Raimbault, 2002), sudden cell senescence (Agustí et al., 1998), feeding by zooplankton (Buesseler & Boyd, 2009) and the excretion of waste products by zooplankton (faecal pellets) (Cavan et al., 2017; Jiao & Zheng, 2011) which contributes towards the production of labile DOC (Clifford et al., 2017; Lampitt et al., 1990). Thus, bacteria utilize this energy-rich POM for growth (Baltar et al., 2009) and only a small amount of dissolved organic matter (DOM) is utilized by most marine organisms at higher trophic levels. Bacteria introduce this DOM into the food web, additionally contributing to the carbon export to the ocean interior (Francois et al., 2002; Hansell et al., 2012).

This research aims to address the primary key processes that affects the carbon flux. Including some questions regarding the MCP by combining findings about the influence of the PP, particle export efficiency, settling rates, particle composition and bacterial activity as the key concept for carbon flux. Thus, incorporating metagenomics (Sequence-Based Analysis or Random sequencing) and metatranscriptomics to understand microbial communities and function below MLD. Sequence-based analysis involves a complete sequencing of the library to indicate the taxonomic group containing phylogenetic anchors (Handelsman, 2004). Alternatively, random sequencing will be applicable to our research questions, to identify the gene of interest by providing a link of phylogeny with the functional genes. Sequence-based analysis will be supported by the metatranscriptomics analysis that is more into the active genes for carbon metabolism. These processes will be used to connect both carbon fluxes with microbial activity below the MLD to understand the carbon flux and settling rates of each station.

This data will be collected using the Marine Snow Catcher (MSC) which is a large water column or niskin about 100 litres (Baker et al., 2017; Riley et al., 2012). Containing separable top and bottom sections for collection and characterising suspended and sinking particles in the water column. It's used to understand export

processes of the oceanic organic carbon cycle. Also, it can be used to predict how these processes may change in the future. Deployment details are shown in Table 11.1, the depth was determined after the deployment of the deep cast GoFlo.

Table 11.1. Winter MSC deployment details

Grid	Station Name	Latitude	Longitude	Depth MLD + 10m	Deployment Date Time
VOY-38-GT1E	GT1	56° 00.157' S	00° 00.115' W	110m	25-July-2019 20:09
VOY-38-MIZ1	MIZ1s	56° 59.986' S	00° 00.474' E	150m	26-July-2019 20:02
VOY-38-MIZ2	MIZ2	57° 18.045' S	00° 00.975' E	140m	27-July-2019 01:57
VOY-38-GT2B	GT2	54° 00.048' S	00° 00.075' E	160m	30-July-2019 02:48
VOY-38-GT5	GT5	46° 59.994' S	04° 29.963' E	150m	01-August-2019 18:07
VOY-38-GT7	GT7	43° 00.006' S	08° 30.021' E	210m	03-August-2019 12:52

Table 11.2. Spring MSC deployment details

Grid	Station Name	Latitude	Longitude	Depth 1 MLD + 10m	Depth 2	Deployment Date Time
------	--------------	----------	-----------	-------------------	---------	----------------------

VOY-40-PUZ	PUZ	54° 00.406' S	00° 00.586' W	110m	210m	19-October-2019 09:20
VOY-40-MIZ1	MIZ1	57° 57.672' S	00° 00.584' E	85m	110m	23-October-2019 09:30
VOY-40-MIZ3	MIZ3	58° 58.349' S	00° 01.564' E	110m	120m	24-October-2019 23:14
VOY-40-MIZ5	MIZ5	59° 18.701' S	06° 37.101' E	95m	110m	28-October-2019 15:40
VOY-40-GT1	GT1	56° 00.016' S	00° 01.890' E	80m	110m	08-November-2019 19:18
VOY-40-GT3	GT3	51° 23.981' S	00° 00.032' E	80m	110m	11-November-2019 03:35
VOY-40-GT5	GT5	47° 00.015' S	00° 30.000' E	50m	110m	12-November-2019 14:21
VOY-40-GT7	GT7	42° 59.999' S	08° 30.337' E	110m	150m	13-November-2019 19:28
VOY-40-GT9	GT9	38° 36.157' S	11° 47.970' E	50m	110m	17-November-2019

## 11.2.2. Methodology

### 11.2.2.1. Snow Catcher Deployment Protocol

1. To set snow catcher mechanism in open position push the central pole (D) upwards until the two pin holes are aligned, and the pin can be located to hold it in place (E)– done lying down on deck

2. Take the pole and plunger (B) from the base and locate into the pole running through the length of the snow catcher (C). The poles should be secured together with a pin thus must be aligned correctly – vertically held by crane
3. Gently lower into base locating the bottom of the pole into the hole in the clear Perspex base (J).
4. Clip shut (K) the base and top of snow catcher and cable tie the clips for extra security. It will only locate in one orientation indicated by the notched part in the base and metal frame. Use ratchet straps to secure
5. Lift over side of deck and hold vertically to allow for steps 6-8
6. Attach the release mechanism (F) to the rope/wire:
  - Slot rope into groove (G) in release mechanism.
  - Tighten slightly to prevent it falling out using small spanner (H)
  - Adjust position of the release mechanism so the release rope attached to the snow catcher is taught (I) when the pole inside is pushed into the open position.
  - Once in place tighten release completely. However, do not over tighten as the threading is brass and it may be damaged.
7. Remove the pin (E) from the top of the snow catcher holding the mechanism open (this should be only one when snow catcher is upright. The central pole with closing valves should only move very slightly when the pin is removed.
8. Ensure the two taps are closed so it doesn't leak (L).
9. Deploy and stand by for 10 minutes, then fire by sending messenger down on the rope – ensure messenger is secured on properly so is not lost.
10. Bring back on deck and stand upright for 2-3 hours.
11. Open the top tap (L) all the way to air in. Slowly open the bottom tap and allow top 95 L of water to drain out slowly. This is to ensure that not too much turbulence is created, and particles are re-suspended.
12. Gently lift the top of the snow catcher away from the base.
13. Put lid on tray and take away for analysis.

N.B. Don't put end of snow catcher which locates into the base directly on the ground as it may be damaged and affect the seal.

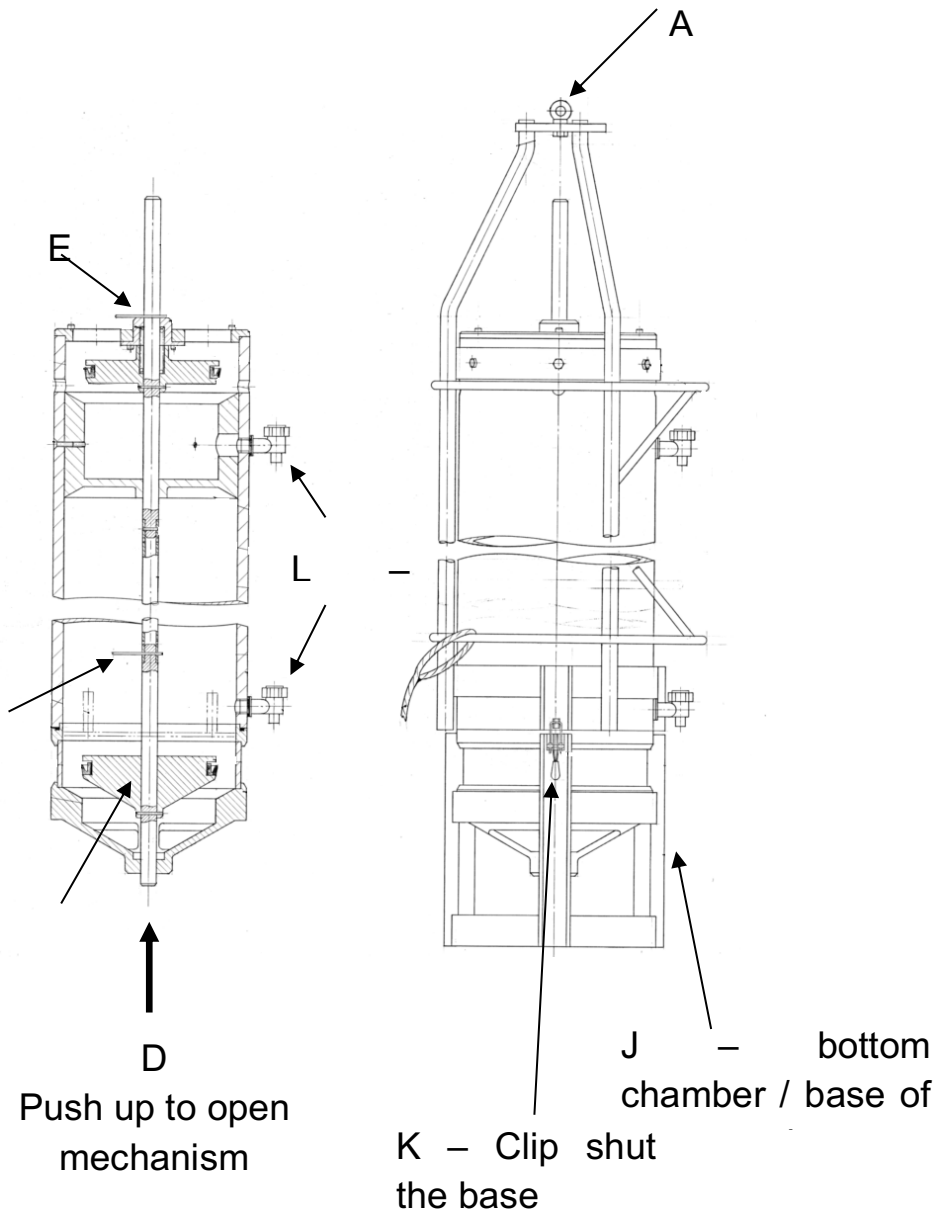


Figure 11.2: Internal and External Schematics of Snow Catcher.

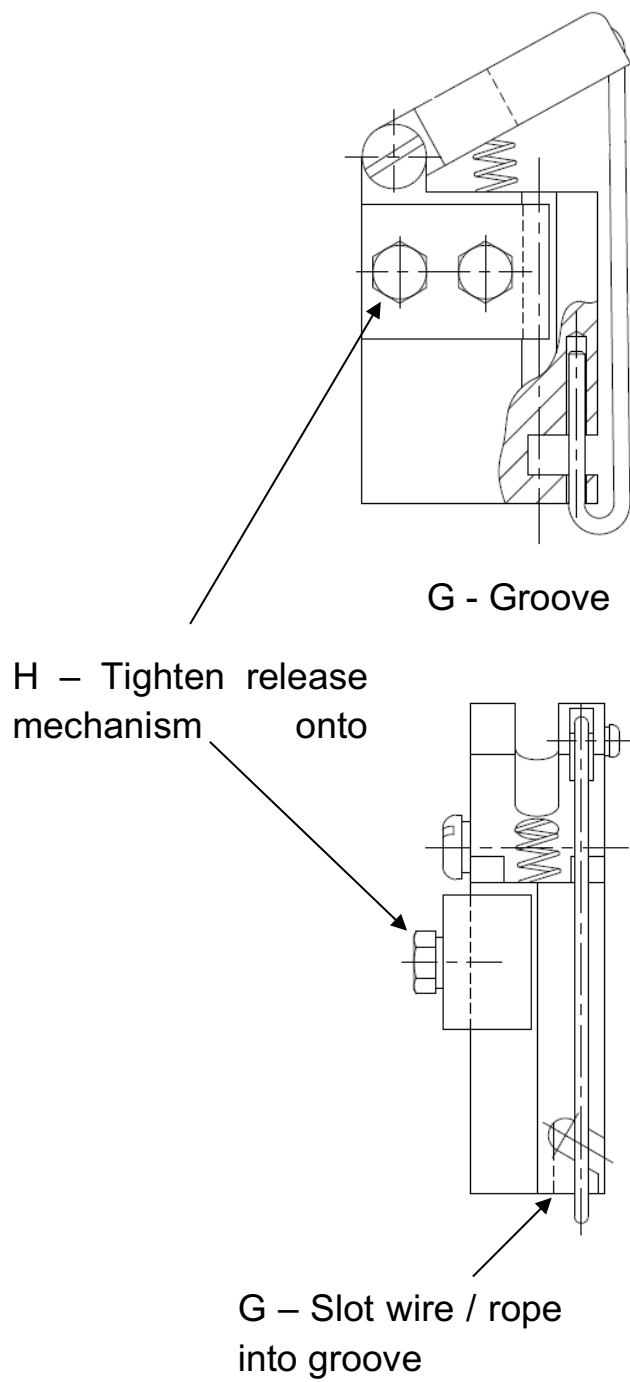


Figure 11.3: Release Mechanism (F).

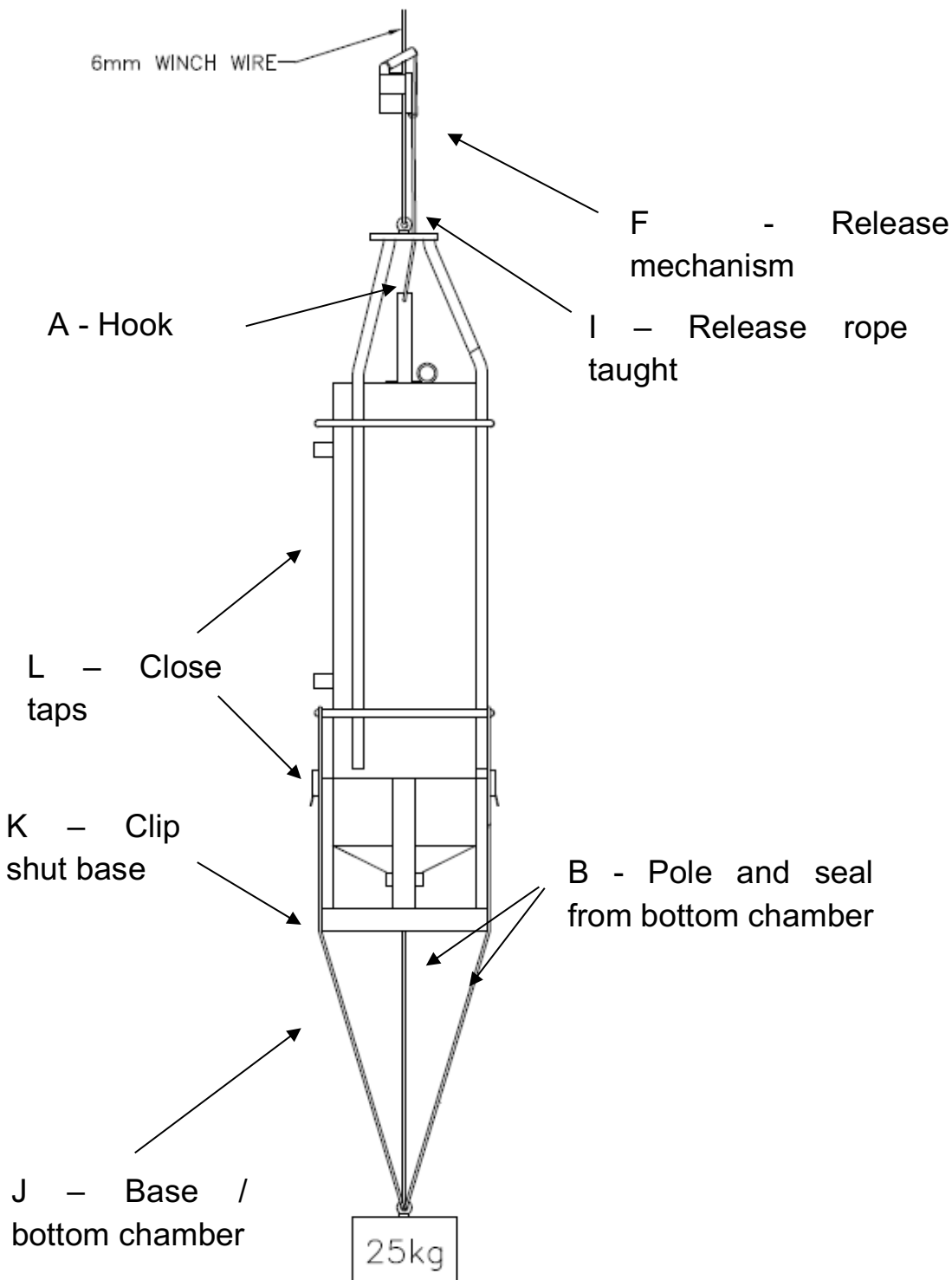


Figure 11.4: General diagram of MSC.

### 11.2.3. Sampling the MSC

The top suspended fraction (8 litres) is collected into a 25 litres bottle and discard the remaining water till the bottom 8 to 12 litres. The bottom slow sinking fraction (~8 litres) is collected into a 10 litres bottle. Whist, the fast sinking fraction (~3.5 litres) is collected using a bucked by open the bottom chamber (J) of the MSC.

The collected water samples are then split into four parts using Folsom splitter for POC, total carbon, Biogenic Silica (BSi) and metagenomics. The Glass Fibre Filters (GFF) were combusted overnight (5 pm – 8 am) in a muffle furnace at 400 °C prior to the cruise. The 25 mm GFF pre-combusted filters were used for POC and total carbon filtration followed by HCl acid fume overnight in for the POC samples, thereafter, oven dried overnight. The filters were stored in a small petri dish after filtering sample for POC, total carbon and BSi to avoid contamination. While, for total carbon the filters were oven dried immediately after filtration. BSi sample fractions were filtered onto 0.8 µm Poly carbonate filters then oven dried overnight. While, for metagenomics analysis 0.2 µm PC filters are used and stored in -80°C freezer.

After 24 hours, the POC and total carbon oven dried GFF filters were prepared for analysis using 12 mm Punch. Then folded into foil cups in a labelled 96-well plate for POC and total carbon analysis.

#### **11.2.4. General comments and Suggestions**

The MSC deployed and standing for 10 minutes can be increased to 30 or 45 minutes for collection of more particles. Additionally, two MSCs can be deployed at the same depth and allow to settle for 2 hrs and 4 hours to investigate the settling time. As suspended fraction might contain some of the slow sinking particles that takes time to equilibrate to its density position or sink. Therefore, it would be an interesting comparison to evaluate settling time as an important factor contributing to carbon export.

The trigger mechanism is too sensitive, it needs to be improved because small waves can trigger the mechanism and close the MSC.

### **11.3. Short-term (24-hour) Nutrient addition Incubation Experiments**

#### **11.3.1. Rationale**

The Southern Ocean is known to be a High-Nutrient, Low-Chlorophyll (HNLC) region, limited particularly during peak phytoplankton primary productivity (bloom season) by iron. Iron is an essential micronutrient in the electron transport chain for photosynthesis. Following a seasonal progression study from Austral Autumn, during SCALEI (Winter: July – August 2019), and SCALEII (Spring: October – November 2019), a total of 30 short-term (24-hour) incubation experiments were completed across the SCALE cruises along the Good Hope Line, on-board the SA Agulhas II, in the Atlantic sector of the Southern Ocean. Experimental locations ranged between the Marginal Ice Zone (MIZ), along the ice edge, the Polar Frontal Zone (PFZ), through to the Sub-Antarctic Zone (SAZ) and the Sub-Tropical Zone (STZ). The experiments investigated the phytoplankton photophysiology, chlorophyll-a growth and macronutrient nutrient drawdown, as well as the photochemical efficiency over different timescales. One additional experiment was terminated after 66-hours for comparison purposes during Spring, and one experiment during Winter was subsampled after 72hrs, following termination and subsampling again after 96hrs. Seawater was sampled into 1L polycarbonate bottles using Trace Metal Clean (TMC) sampling techniques, and were inoculated with 2.0 nM of the Micronutrient iron (Fe) and allowed to incubate under natural light and in situ temperature conditions over 24-hours, with experiments setup either in a fridge or deck incubator, followed by termination (subsampling) under clean conditions. Five supplementary treatments to

Fe-addition were carried out as experiments SC\_01, SC\_02, SC\_15, and SC\_19 in Spring as shown in Table 2 below. These experiments included addition of Al, FeAl, FeCo, FeMn, and FeAlCoMn.

All experimental treatments were conducted in triplicates, with initial sample analysis measured as above. Five experiments, corresponding to sampling locations of the Winter cruise, were repeated in Spring, complementing the seasonal study after approximately 3 months. Two experiments: SC\_15 and SC\_19 were sampled twice – on the downward leg and return leg of the Spring cruise.

### **11.3.2. Aims and Objectives**

A seasonal study from Winter to Spring in the Atlantic sector of the Southern Ocean, along the Good Hope Line gives us an overview of the seasonal progression of the phytoplankton. The incubations run for 24-hours (short-term bioassays) aimed to analyse the rapid changes in (photo-)physiology and photochemical efficiency upon Fe addition. Short-term incubations avoid changes in the biomass and community structure of the samples. Hence, the immediate response could be detected through photophysiological fluorescence measurements and chlorophyll pigment concentrations.

### **11.3.3. Methods**

Incubations of the collected trace metal clean seawater were performed in 1L polycarbonate bottles. All bottles used for the incubations were passed through a rigorous cleaning process involving a Decon wash and a soak in 50% HCl for 1 week, followed by rinsing then storage with acidified Milli-Q prior to sailing.

Trace metal clean seawater for the incubations were collected using two methods: 1) a trace metal clean torpedo FISH towed alongside the ship, submerged at approximately 2 – 5 m depth and 2) GoFlo bottles from a GEOTRACES CTD rosette equipped with clean 24 x 12L GoFlo bottles, deployed on a conducting Kevlar cable (General Oceanics, USA) with TMC seawater collected at ~25 m depth. Each of the polycarbonate bottles used for the incubations were rinsed three times and filled to the 1L mark with TMC seawater for triplicate control and triplicate Fe-spiked samples (to a concentration of 2.0 nM). Each bottle top was sealed with Parafilm, and the bottles were enclosed into double zip lock bags, and randomly placed inside a fridge incubator set to the average Photosynthetically Active Radiation (PAR) at each latitude of the collected water, and at in situ seawater temperature for the duration of the sunrise and sunset at the given location. The deck incubations followed the same procedures highlighted above, with the exception that they were placed in a square Perspex box which was a water bath of flowing seawater, under natural light conditions and seawater temperature. All incubations were terminated and subsamples after approximately 24 hours.

Prior to the commencement of each incubation, 1L of the sample was retained for initial comparison and information of the sampling set (TZero). After each 24-hour experiment was terminated and the incubation bottles removed from the incubator, they were subsampled inside a trace metal clean environment. The initial bottle, as well as the each of the controls and Fe-spiked bottles were sampled for 50 mL nutrients (analysis onland), 500 ml chlorophyll filtrations each onto 25mm Whatman

(Glass Fibre Filter) GF/F filter (nominal pore size 0.7  $\mu\text{m}$ ), and Fast Repetition Rate fluorometry (FRRf) run on a FastOcean FRRf, Chelsea Scientific Instruments Fastracka™ Mk II FastOcean FRRf incorporating a FastAct™ laboratory system for each sample, along with a blank correction (filtrate after syringe filtering the sample through a 0.2  $\mu\text{m}$  filter) for determining the photochemical efficiency ( $F_v/F_m$ ) of the biomass. A Fluorescent Light Curve (FLC) was run for TZero, the control sample with the smallest  $F_v/F_m$  value, and an FLC for the Fe-spiked sample with the highest  $F_v/F_m$  value. Each experiment was linked to a GoFlo and CTD incubation station for the trace metal concentrations and other biogeochemical parameters, respectively. In the case of the torpedo FISH, the experiment was linked to an underway station.

Bottle filling and all manipulation steps including spiking and sub-sampling were performed within the dedicated Class-100 filtered air and under clean laminar flow, inside a trace metal clean certified container. A complete list of sampling locations and relevant information is provided in Table 11.3 and Table 11.4 below, corresponding to the Winter and Spring cruises respectively. The FRRf data was analysed with the “Phytoplankton Photophysiology Utilities” package in Python.

Table 11.3: Experiment number, sampling positions, and linked station for the short-term micronutrient iron addition incubation experiments during Winter 2019.

Exp	Link	Latitude	Longitude	Sampling method	Start date	Termination date
WC19_01	23/07/19 10h00 UTC (UW 46)	-50.817	2.650	Fe fish	23/07/19	24/07/19
WC19_02	GT 01	-56.003	-0.002	GoFlo	25/07/19	26/07/19
WC19_03	GT 02	-54.001	0.013	GoFlo	30/07/19	31/07/19
WC19_04	GT 03	-54.402	0.011	GoFlo	31/07/19	01/08/19
WC19_05	GT 05	-46.999	4.499	GoFlo	01/08/19	02/08/19
WC19_06	GT 07	-43.000	8.503	GoFlo	03/08/19	04/08/19
WC19_07	GT 09	-38.599	11.801	GoFlo	04/08/19	05/08/19

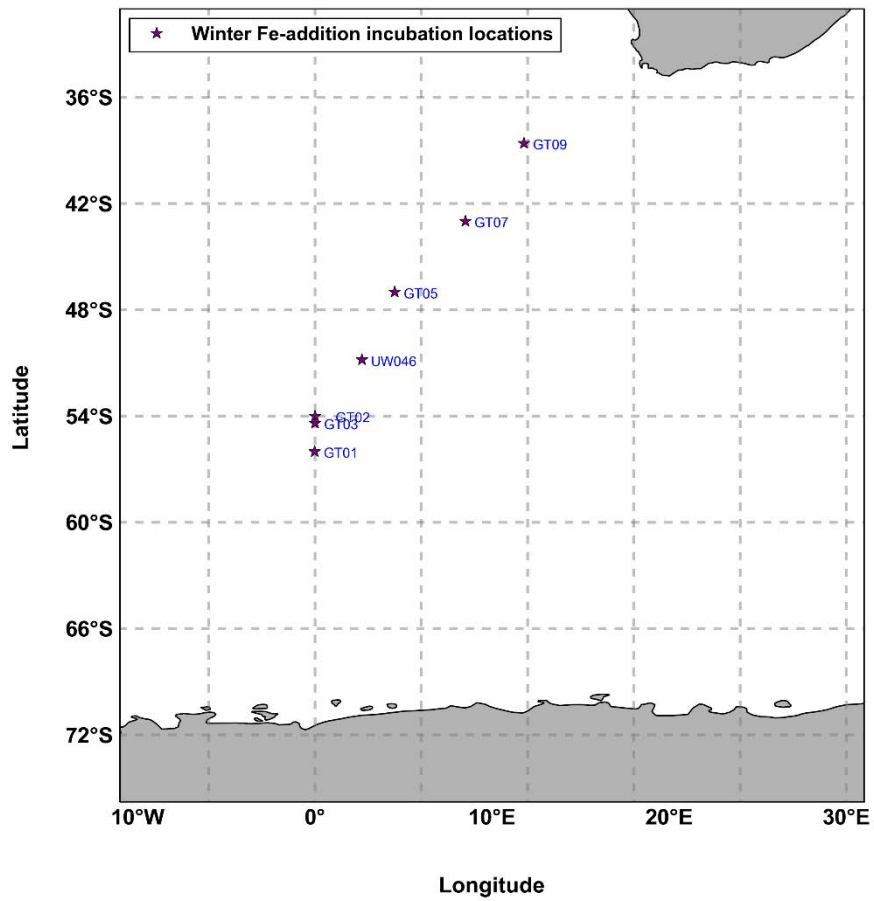


Figure 11.5: Sampling locations of SCALE Winter incubation experiments.

Table 11.4: Experiment number, sampling positions, and linked station for the short-term micronutrient iron, and other trace metal addition incubation experiments during Spring 2019.

Exp	Link	Latitude	Longitude	Metal addition	Start date	Termination date
SC19_01	GT01 SAZ2 *(in PFZ)	-45.000	6.600	Fe, Al, FeAl, FeMn, FeCo, FeAlMnCo	16/10/19	17/10/19
SC19_02	PUZ GT 05	-54.007	-0.011	Fe, Al, FeAl, FeMn, FeCo, FeAlMnCo	19/10/19	20/10/19
	(WC: GT 02)					
SC19_03	MIZ0A GT 06	-55.001	0.000	Fe only	20/10/19	21/10/19
SC19_04	MIZ1b GT 08	-57.964	0.010	Fe only	23/10/19	24/10/19
SC19_05	MIZ2 GT 10	-59.320	0.072	Fe only	24/10/19	25/10/19
SC19_06	MIZ4 GT 14	-59.000	3.018	Fe only	27/10/19	28/10/19
SC19_07	MIZ5 GT 16	-59.339	6.616	Fe only	29/10/19	30/10/19
SC19_08	MIZ6 GT 18	-59.364	8.160	Fe only	29/10/19	30/10/19
SC19_09	MIZ7 GT 21	-59.469	10.918	Fe only	30/10/19	31/10/19
SC19_10	MIZ8 GT 23	-58.541	17.969	Fe only	01/11/19	02/11/19

SC19_11	WS01 GT 26	-57.152	23.995	Fe only	04/11/19	05/11/19
SC19_12	WS02 GT 29	-55.378	11.965	Fe only	06/11/19	07/11/19
SC19_13	WS03 GT 31	-55.001	6.997	Fe only	07/11/19	08/11/19
SC19_14	GT1 GT 33	-55.996	0.004	Fe only	08/11/19	09/11/19
	(WC: GT 01)					
SC19_15	GT2 GT 36	-54.000	0.000	Fe, Al, FeAl, FeMn, FeCo, FeAlMnCo	09/11/19	10/11/19
	(WC: GT 02)					
SC19_16	GT3 G 41	-51.400	0.001	Fe only	10/11/19	11/11/19
SC19_17 Deck	GT4 GT 44	-51.400	2.303	Fe only	11/11/19	12/11/19
SC19_17	GT4 GT 44	-51.400	2.303	Fe only	11/11/19	13/11/19
SC19_18 Deck	GT7 GT 50	-43.000	8.500	Fe only	13/11/19	14/11/19
	(WC: GT 07)					
SC19_18	GT7 GT 50	-43.000	8.500	Fe only	13/11/19	14/11/19
	(WC: GT 07)					

SC19_19	GT6 GT 53	-44.999	6.600	Fe, Co, Fe, FeMn, FeCo, FeMnCo	14/11/19	17/11/19
SC19_20	GT8 GT 57	-40.001	10.802	Fe only	16/11/19	17/11/19
SC19_21	GT9 GT 63	-38.603	11.800	Fe only	17/11/19	18/11/19
	(WC: GT 09)					

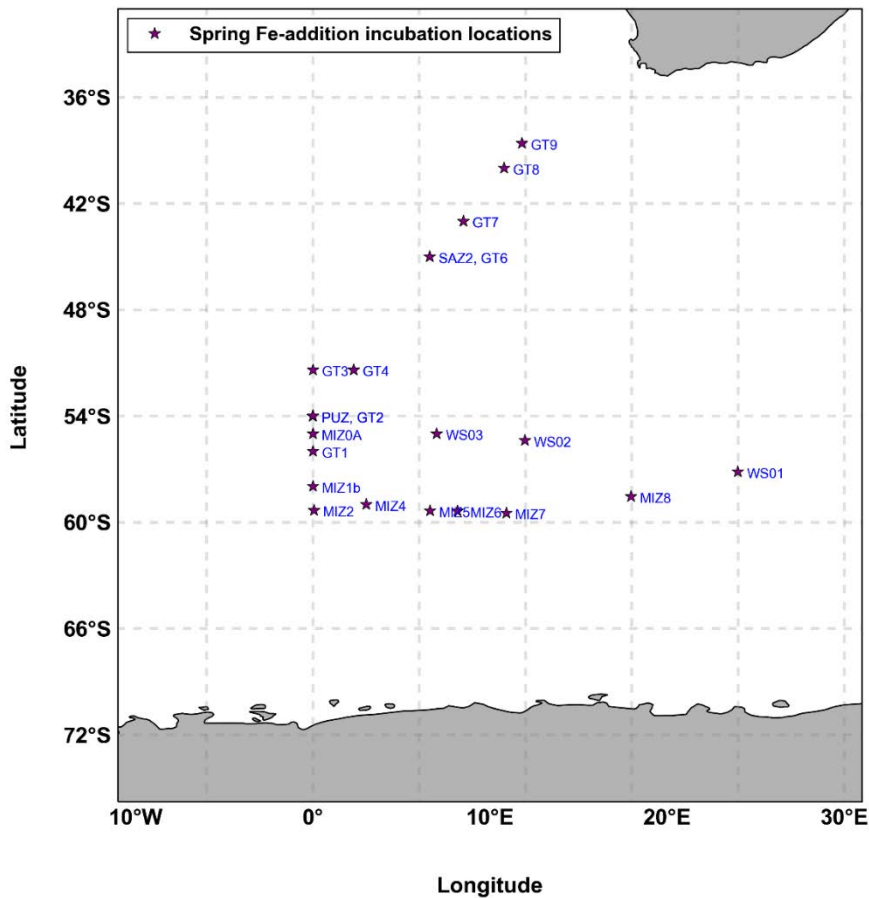


Figure 11.6: Sampling locations of SCALE Spring incubation experiments.

### 11.3.4. Conclusion

Initial photophysiological results show a minimal iron limitation in the South Atlantic region of the Good Hope Line from similar photochemical efficiencies ( $F_v/F_m$ ) between

the control and iron-spiked samples. Further rigorous analysis of the photophysiology coupled with the biogeochemical parameters will give additional information on the iron limitation across the seasons, and to establish the physiological adaptation of phytoplankton to low levels of trace element iron for primary production. Furthermore, the chlorophyll-a concentrations were all within the same standard deviation for each treatment and experiment, with most experiments having chlorophyll-a concentrations less than  $1 \mu\text{g}\cdot\text{L}^{-1}$ . Any minor discrepancies in the photochemical efficiency and chlorophyll-a concentration between the initial and control samples could be linked to phytoplankton being constrained to a closed system.

### **11.3.5. Challenges**

Some of the challenges experienced during both cruises included instrument usage (FRRf and chlorophyll-a filtration system) between stations (Trace Clean (GoFLo), CTD, and Underway), as well as use of the Trace metal clean containers for other projects, which prevented immediate subsampling of the incubations, and sometimes resulted in waiting times of a few hours. The deck incubations were not successful, as the deck heating was turned on sometimes during the 24hr incubation period, and the water pressure was too low to supply adequate flowing seawater through the square box incubator, with additional overcast days. The torpedo FISH had a number of challenges with regards to its deployment, with most being on the account of weather, rough seas, and ice, preventing water collection at the required time. The Fe-spike of  $\text{FeCl}_3$  was not delivered in time for sailing, so elemental Fe was prepared in a diluted acid for the 2.0 nM concentration.

## **11.4. Productivity vs Irradiance Experiments**

### **11.4.1. Methods**

#### **11.4.1.1. PE Experiment**

A total of 11 experiments were carried out on the winter cruise and 18 experiments on the spring cruise. 8 x 2000 mL water samples and 3 x 800 mL water samples (obtained from ice core samples) were collected in covered polycarbonate bottles. From the 2000 mL and 800 mL respectively, 60 mL of water was decanted into 12 vials. Each vial was inoculated with  $40 \mu\text{L C}^{14}$  (5ml  $\text{NaC}^{14}\text{CO}_3$  in 5 ml seawater) spikes and this represented a  $20 \mu\text{Ci}$  activity spike. From 3 random vials (of the 12 vials),  $100 \mu\text{L}$  was transferred into 6 ml Scintillation vials with  $200 \mu\text{l}$   $\beta$ -phenylethylamine and 5 ml of UltimaGold scintillation cocktail was added to each vial and the vials were stored for further analysis. The photosynthetron was placed inside an incubator fridge which was used to control the temperature. The 12 vials were incubated in the Photosynthetron with artificial light source to mimic water-column light attenuation for 2 hours. LED lights were used as a light source with differing light intensities with the third slot blacked out. After 2 hours of incubation, the samples were filtered onto  $0.2 \mu\text{m}$  ash filter papers and placed into Scintillation vials. The samples were further acidified with 0.5 ml of 0.5 M HCl for 24 hours, and after 24 hours 5 ml UltimaGold scintillation cocktail was added to the samples and stored for further analysis.

#### **11.4.1.2. NPP and Calcification Experiments**

Seawater (2000 ml) from three different depths were collected from the Niskin CTD. Five hundred millilitres of seawater was decanted into nine 500 ml Schott bottles respectively and these were inoculated with 30  $\mu\text{l}$   $\text{C}^{14}$  spike. From the Schott bottles, 100  $\mu\text{l}$  was transferred into 6 ml Scintillation vials with 200  $\mu\text{l}$   $\beta$ -phenylethylamine and 5 ml of UltimaGold scintillation cocktail was added to each vial and the vials were stored for further analysis. The nine 500 ml Schott bottles were incubated outside for 24 hours in incubators with different light levels to mimic the different depths the water was collected from. After 24 hours of incubation, the samples were filtered in the dark onto 0.2  $\mu\text{m}$  ash filter papers and rinsed extensively with 0.2  $\mu\text{m}$  filtered seawater. The filter papers were placed in glass vials with gas-tight septum and a bucket containing ash filter paper soaked in  $\beta$ -phenylethylamine attached to the lid. Zero point five millilitres of 0.5 M HCl was injected through the septum into the bottom of the vial and left for 24 hours. After 24 hours, the filter papers were placed in separate scintillation vials and 5 ml UltimaGold scintillation cocktail was added to the samples and stored for further analysis.

#### **11.4.2. Problems encountered**

1. The first two experiments, the filtration rig gave problems and hence could not filter. In some of the experiments during filtration, some of the samples leaked.
2. Only 11 experiments were carried out since the  $\text{C}^{14}$  spike ran out during the Winter Cruise.
3. The second batch of spike during the Spring Cruise was never delivered.

#### **11.5. CTD and UW Sampling**

##### **11.5.1. Chlorophyll-a**

Seawater was collected from 6 different depths; 500 mL of seawater was filtered through 0.3  $\mu\text{m}$  and 2.7  $\mu\text{m}$  filters, and 1 L was filtered through a 20  $\mu\text{m}$  filter. All filters were placed in glass vials containing 90% acetone and stored at  $-20^{\circ}\text{C}$  for  $\sim 24$  h. Samples were allowed to acclimate to room temperature before the raw chl-a fluorescence was measured using a Turner Trilogy Benchtop Fluorometer (non-acidification module). Seawater was also collected from the ship's underway scientific seawater supply every 1, 2 or 4 hours at various stages of the cruise. Samples were processed as above.

Known Issues:

1. Fluorometer requires a calibration which will be performed post cruise
2. The following samples have issues and should be treated with caution or excluded from further analysis:
  - a.

##### **11.5.2. Total particulate absorbance (PAB)**

Seawater was collected from 3 different depths or from the ship's scientific seawater supply every 4 hours (4, 8, 12 ships time). Approximately 2 L seawater was filtered through 25 mm GF/Fs (0.7  $\mu\text{m}$  nominal pore size). Filters were placed in petri-dishes,

flash frozen in liquid nitrogen, wrapped in tin foil and stored at  $-80^{\circ}\text{C}$  for analysis on land.

### **11.5.3. Particulate organic carbon (POC)**

Seawater was collected from 6 different depths or from the ship's scientific seawater supply every 4 hours (4, 8, 12 ships time). Approximately 2 L seawater was filtered through 25 mm ashed (pre-combusted) GF/Fs ( $0.7\ \mu\text{m}$  nominal pore size). The ashed filters were combusted in a muffle furnace at  $400^{\circ}\text{C}$  overnight, prior to the cruise. Following filtration, filters were placed into petri-dishes and incubated at  $50^{\circ}\text{C}$  for 24 h. Filters were then placed in a fume hood, in a desiccation chamber that contained a beaker of concentrated HCl, at room temperature for 24 h. Filters were then punched using a size 13 punch, folded into tin cups, and placed into a labelled 96-well plate, for analysis on land. As a control, a blank ashed filter was punched, folded into a tin cup, and placed in the 96-well plate during each round of punching. The filtrate was also filtered onto pre-combusted GF/Fs and followed the same treatment to give an approximation of the dissolved inorganic carbon (DOC) that is adsorbed onto the filter during the filtration process.

### **11.5.4. BSi**

Seawater was collected from 3 different depths or from the ship's scientific seawater supply every 4 hours (4, 8, 12 ships time). Approximately 1 L seawater was filtered through  $0.2\ \mu\text{m}$  isopore polycarbonate filters. Filters were placed in petri-dishes and incubated at  $50^{\circ}\text{C}$  for 24 h. The petri-dishes were then sealed with parafilm and stored at room temperature, for analysis on land.

### **11.5.5. Particle-size analysis (Coulter counter)**

Seawater was collected from 3 different depths or from the ship's scientific seawater supply every 4 hours (4, 8, 12 ships time). Particle-size analysis was performed using a Beckman Coulter-Multisizer, as per the manufacturer's instructions. The  $140\ \mu\text{m}$  aperture tube was used for all CTD measurements, using the SCALE SOP, which sampled 20 runs of 2 mL seawater per run. Corresponding blank measurements were performed using  $0.2\ \mu\text{m}$  isopore polycarbonate filtered-seawater sampled from the same depths as the particle measurements.

### **11.5.6. Active chlorophyll fluorescence**

Measurements of the photochemical efficiency ( $F_v/F_m$ ), the effect absorption cross-section of PSII ( $\sigma_{\text{PSII}}$ ) and electron transport rates were performed with a Chelsea Scientific Instruments FastOcean™ integrated with a FastAct™ laboratory system. Seawater was collected from 6 different depths. Measurements were made in triplicate, and corresponding blanks ( $0.2\ \mu\text{m}$  filtered seawater) were recorded. Size fractionated FRRf measurements were recorded for surface water (either from the surface Niskins or the underway supply every 4 hours); approximately 2 L seawater was filtered through a 47 mm isopore polycarbonate filter ( $5.0\ \mu\text{m}$  nominal pore size). The filtrate constituted the  $<5.0\ \mu\text{m}$  component. The filter was placed in a 50 mL Falcon tube, which was filled with  $0.2\ \mu\text{m}$  filtered seawater, where following gentle mixing the

cells were resuspended, and constituted the >5.0 µm sample. Measurements of both size fractions were made in triplicate, and corresponding blanks were recorded.

Fluorescence light curves were performed every 4 hours (4, 8, 12 ships time) using water from the ship's scientific seawater supply and were also performed from the shallowest niskin at all CTD stations.

During the south bound leg on the winter cruise and spring cruise quenching tests were performed by placing an underway sample of seawater into the cuvette chamber, turning on the FastAct light to 10 µE m<sup>-2</sup> s<sup>-1</sup> and measuring every minute for 30 minutes. All other samples were low light acclimated prior to measurement by either being placed in a LEE filter screened box or in the FastAct chamber at 10 µE m<sup>-2</sup> s<sup>-1</sup> for 30 minutes.

#### **11.5.7. Proteins**

Two litres of surface seawater (either from the surface Niskins or the underway supply) was filtered through 25 mm GF/Fs (0.7 µm nominal pore size), in triplicate. Filters were placed in cryo-vials, before being flash frozen in liquid nitrogen and stored at -80°C, for analysis on land.

#### **11.5.8. HPLC**

Approximately 2 L of seawater from the ship's scientific seawater supply were collected every 4 hours (4, 8, 12 ships time) and filtered through 25 mm GF/Fs GF/Fs (0.7 µm nominal pore size). Filters were placed in cryo-vials, before being flash frozen in liquid nitrogen and stored at -80°C, for analysis on land.

#### **11.5.9. Low-temperature (77K) excitation spectra**

Approximately 2 L of seawater from the ship's scientific seawater supply were collected every 4 hours (4, 8, 12 ships time) and filtered through 25 mm GF/Fs GF/Fs (0.7 µm nominal pore size). Filters were placed in petri dishes, before being flash frozen in liquid nitrogen, wrapped in tin foil and stored at -80°C for analysis on land.

### **11.6. References**

Agustí, S., Satta, M. P., Mura, M. P., & Benavent, E. (1998). Dissolved esterase activity as tracer of phytoplankton lysis rates in the NW Mediterranean. *Limnology and Oceanography*, 43(8), 1836–1849.

Baker, C. A., Henson, S. A., Cavan, E. L., Giering, S. L. C., Yool, A., Gehlen, M., Belcher, A., Riley, J. S., Smith, H. E. K., & Sanders, R. (2017). Slow-sinking particulate organic carbon in the Atlantic Ocean: Magnitude, flux, and potential controls. *Global Biogeochemical Cycles*, 31(7), 1051–1065. <https://doi.org/10.1002/2017GB005638>

Baltar, F., Aristegui, J., Gasol, J. M., Sintes, E., & Herndl, G. J. (2009). Evidence of prokaryotic metabolism on suspended particulate organic matter in the dark waters of the subtropical North Atlantic. *Limnology and Oceanography*, 54(1), 182–193. <https://doi.org/10.4319/lo.2009.54.1.0182>

Basu, S., & Mackey, K. R. M. (2018). Phytoplankton as key mediators of the biological carbon pump: Their responses to a changing climate. *Sustainability (Switzerland)*, 10(3). <https://doi.org/10.3390/su10030869>

Bauer, J. E., Williams, P. M., & Druffel, E. R. M. (1992). <sup>14</sup>C activity of dissolved organic carbon fractions in the north-central Pacific and Sargasso Sea. *Nature*, 357(6380), 667–670. <https://doi.org/10.1038/357667a0>

Berman, T., & Wynne, D. (2005). Assessing phytoplankton lysis in Lake Kinneret. *Limnology and Oceanography*, 50(2), 526–537. <https://doi.org/10.4319/lo.2005.50.2.0526>

Buesseler, K. O., & Boyd, P. W. (2009). Shedding light on processes that control particle export and flux attenuation in the twilight zone of the open ocean. *Limnology and Oceanography*, 54(4), 1210–1232. <https://doi.org/10.4319/lo.2009.54.4.1210>

Cavan, E. L., Henson, S. A., Belcher, A., & Sanders, R. (2017). Role of zooplankton in determining the efficiency of the biological carbon pump. *Biogeosciences*, 14(1), 177–186. <https://doi.org/10.5194/bg-14-177-2017>

Clifford, E. L., Hansell, D. A., Varela, M. M., Nieto-Cid, M., Herndl, G. J., & Sintes, E. (2017). Crustacean zooplankton release copious amounts of dissolved organic matter as taurine in the ocean. *Limnology and Oceanography*, 62(6), 2745–2758. <https://doi.org/10.1002/lno.10603>

Francois, R., Honjo, S., Krishfield, R., & Manganini, S. (2002). Factors controlling the flux of organic carbon to the bathypelagic zone of the ocean. *Global Biogeochemical Cycles*, 16(4), 34-1-34–20. <https://doi.org/10.1029/2001GB001722>

Handelsman, J. (2004). Metagenomics: Application of Genomics to Uncultured Microorganisms. *Microbiology and Molecular Biology Reviews*, 68(4), 669–685. <https://doi.org/10.1128/MMBR.68.4.669-685.2004>

Hansell, D., Carlson, C., Repeta, D., & Schlitzer, R. (2009). Dissolved Organic Matter in the Ocean: A Controversy Stimulates New Insights. *Oceanography*, 22(4), 202–211. <https://doi.org/10.5670/oceanog.2009.109>

Hansell, D. A. (2013). Recalcitrant Dissolved Organic Carbon Fractions. *Annual Review of Marine Science*, 5(1), 421–445. <https://doi.org/10.1146/annurev-marine-120710-100757>

Hansell, D. A., Carlson, C. A., & Schlitzer, R. (2012). Net removal of major marine dissolved organic carbon fractions in the subsurface ocean. *Global Biogeochemical Cycles*, 26(1), 1–9. <https://doi.org/10.1029/2011GB004069>

Jiao, N., & Zheng, Q. (2011). The microbial carbon pump: From genes to ecosystems. *Applied and Environmental Microbiology*, 77(21), 7439–7444. <https://doi.org/10.1128/AEM.05640-11>

Lampitt, R. S., Noji, T., & von Bodungen, B. (1990). What happens to zooplankton faecal pellets? Implications for material flux. *Marine Biology*, 104(1), 15–23. <https://doi.org/10.1007/BF01313152>

Laws, E., Falkowski, P., & Smith, W. (2000). Temperature effects on export production in the open ocean. *Global*, 14(4), 1231–1246. Retrieved from <http://onlinelibrary.wiley.com/doi/10.1029/1999GB001229/full>

Maiti, K., Charette, M. A., Buesseler, K. O., & Kahru, M. (2013). An inverse relationship between production and export efficiency in the Southern Ocean. *Geophysical Research Letters*, 40(8), 1557–1561. <https://doi.org/10.1002/grl.50219>

Moutin, T., & Raimbault, P. (2002). Primary production, carbon export and nutrients availability in western and eastern Mediterranean Sea in early summer 1996 (MINOS cruise). *Journal of Marine Systems*, 33–34, 273–288. [https://doi.org/10.1016/S0924-7963\(02\)00062-3](https://doi.org/10.1016/S0924-7963(02)00062-3)

Pace, M. L., Knauer, G. A., Karl, D. M., & Martin, J. H. (1987). Primary production, new production and vertical flux in the eastern Pacific Ocean. *Nature*, 325(6107), 803–804. <https://doi.org/10.1038/325803a0>

Riley, J. S., Sanders, R., Marsay, C., Le Moigne, F. A. C., Achterberg, E. P., & Poulton, A. J. (2012). The relative contribution of fast and slow sinking particles to ocean carbon export. *Global Biogeochemical Cycles*, 26(1), 1–10. <https://doi.org/10.1029/2011GB004085>

Yamanaka, Y., & Tajika, E. (1996). The role of the vertical fluxes of particulate organic matter and calcite in the oceanic carbon cycle: Studies using an ocean biogeochemical general circulation model. *Global Biogeochemical Cycles*, 10(2), 361–382. <https://doi.org/10.1029/96GB00634>

## **12. TEAM SAWS**

### **12.1. Winter Cruise**

#### **12.1.1. Scope**

This section shall describe the activities of SAWS personnel during the 2019 Southern Ocean SeAonal Experiment (SCALE) Winter Cruise. A broad overview of the different work packages is presented, along with a high level summary of major activities along cruise legs. It is not exhaustive and data and/or analysis should be requested separately.

#### **12.1.2. Work Packages and Pre-departure Prep**

Broadly, SAWS activities onboard can be categorised as follows:

*Work Package 1:* Three-hourly surface synoptic weather observations & daily upper air soundings

*Work Package 2:* Ozone soundings

*Work Package 3:* Sea ice charting pilot project

*Work Package 4:* Decision support for science and navigation

#### **Work Package 1: Three-hourly Surface Synoptic Weather Observations & Upper Air Soundings**

Three-hourly surface synoptic observations (SYNOPS) are coded weather messages which are compiled and transmitted from the vessel to the local SAWS office. There, they are quality controlled and transmitted to the World Meteorological Organisation's (WMO) Global Telecommunication System (GTS). Thereafter, they are made available as part of an open source marine safety information system and accessed in the interest of navigational safety. The messages contain a coded combination of data measured by instrumentation onboard the ship (e.g. temperature, pressure, humidity, wind direction, wind speed) as well as a vast array of visual observations conducted by meteorological personnel (e.g. cloud cover, type and bases, wave conditions, precipitation, visibility etc.). The data they contain are also assimilated into global numerical weather prediction models. This process assists greatly in constraining errors in weather forecasts, and the impact is especially important in otherwise-data sparse regions (such as the one traversed during this cruise). This work also forms part of the VOS programme.

Upper air soundings are measurements of the atmospheric profile in the vicinity of the vessel. They are conducted by means of helium-filled weather balloons carrying radiosonde measuring temperature, pressure, humidity and position. The system ascends through the atmosphere to altitudes of around 22, 000 m, giving a clear picture of the entire tropospheric profile (and extending into the lower stratosphere). This work also forms part of the ASAP programme.

Preparation for this work package involved ensuring that the SAWS instruments onboard the vessel were calibrated and verified according to WMO protocols, in order to ensure accuracy throughout the duration of the cruise. This was completed on the 11<sup>th</sup> July 2019 by the Port Meteorological Officer (PMO). The upper-air system was also checked, and the required helium gas quantity and supplies of radiosondes and latex balloons acquired.

#### **Work Package 2: Ozone Soundings**

Ozone soundings are a relatively new addition to the SAWS workflow onboard the SAAll, with the first soundings having been performed on the 2018-19 SANAE takeover voyage some seven months prior. The ozone sonde calibration equipment was installed onboard the SAAll in preparation for that cruise. The only additional physical preparation required was thus the loading of the required balloons, helium gas and sufficient chemicals for the chemical cell.

Preparation prior to the cruise included conducting training sessions at both the Cape Town Weather Office (CTWO), as well as onboard. Initial training sessions at the CTWO were held during June 2019.

### Work Package 3: Sea Ice Charting Pilot Project

This work package is related to the interest SAWS has in providing routine sea ice charting services, in order to satisfy service provision recommendations of the WMO for NMSs with METAREA responsibilities. This cruise was seen as an opportunity to run an initial pilot project. The aim of the pilot project would be to:

- 1) Develop a basic workflow for ice edge detection (edge detection being the first step towards charting and satisfying GMDSS MSI requirements). This would include identifying suitable data sources and software to be used.

- 2) Assess the suitability of the 15 % concentration convention (a northern hemisphere-centric) for the definition of the ice edge from a maritime safety point of view.

- 3) Gather data which can be used to “ground-truth” satellite data and derived products, as well as for use in training material to future forecasters who might become responsible for constructing ice charts.

In order for this to be achieved, several tasks were conducted prior to departure. The first was the identification of suitable data sources to be used by the scientists piloting the process. In this regard, 7 standard sources were selected. Routine protocols were set up in the CTWO Marine Unit to pull these data operationally and process them. Processing protocols were built to allow easy downloading via the severely-limited bandwidth available on the ship.

Next, a low-bandwidth webpage was built to host the various resources which had been assembled to support the pilot project. This webpage would allow the researchers to pull the daily sea-ice concentration maps and KML files of the same data which were being generated in the CTWO Marine Unit, to the ship. Sea-ice edge detection and charting could then be conducted onboard.

Next, the data service interface which SAWS procured along with the sea ice buoys purchased from MetOcean was configured and tested to ensure it was set up correctly. This was linked to the webpage to allow access by researchers onboard to the data being transmitted by the sea ice buoys. The buoys themselves were then float tested (to ensure they float upright, with the antenna straight up to facilitate proper data transmission), and then loaded on the ship.

Having developed a bespoke SAWS Sea Ice Charting Tool, the Marine Unit installed the tool on the vessel’s weather office computers for use in the pilot project during the cruise. This constitutes a large body of work, which has merit in and of itself, far beyond the scope of this cruise report.

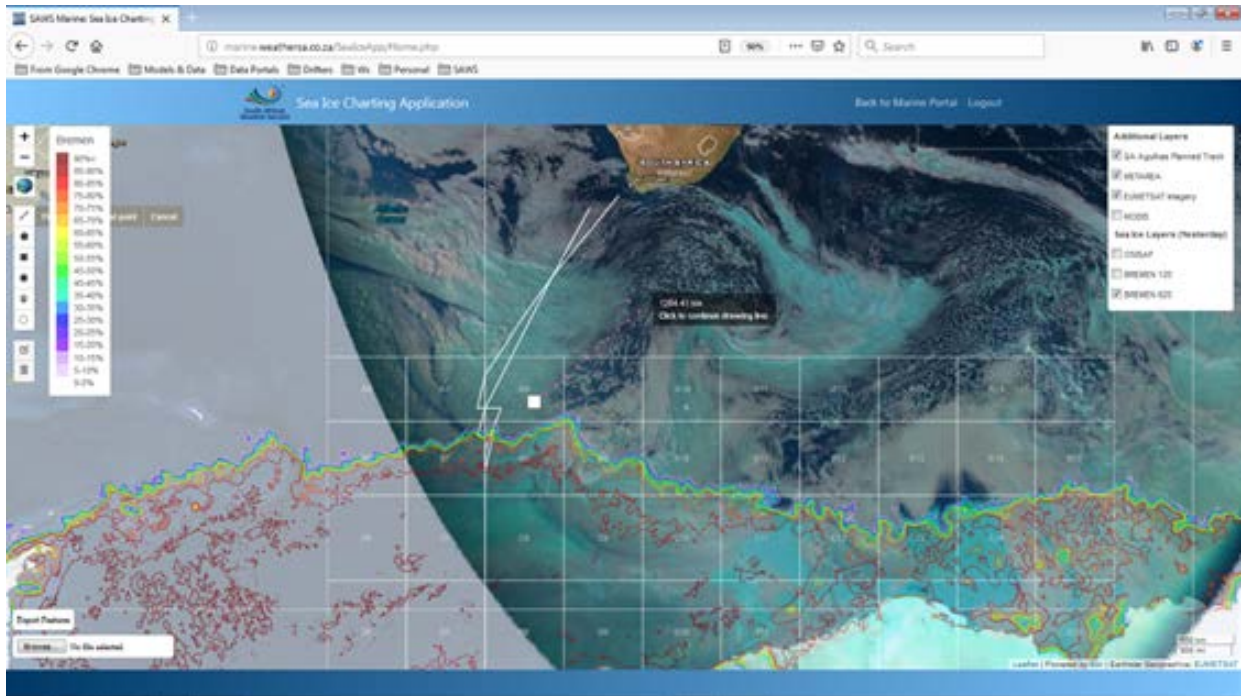


Figure 12.1. The SAWS Marine Sea Ice Charting Tool, developed in-house.

#### Work Package 4: Decision Support for Science and Navigation

The winter cruise is usually a series of significant scientific and navigational challenges. Timeframes are tight and consequences, both financial and other (such as equipment damage) potentially severe. As such, the SAWS Marine Unit undertook to provide a comprehensive decision support package to the vessel crew and science teams. This package goes well beyond the normal service extended to the SAAI. It included new, customized data feeds and visualisations, daily (and as often as required) consultation with the vessel Master, Chief Scientist and team leaders and posting of comprehensive printed material in key areas of the ship. In order to facilitate this, protocols and programmes were written to acquire, and process various open-source weather forecast data operationally. The outputs from these programmes were hosted on the cruise support webpage.



Figure 12.2. The dedicated research cruise decision support webpage which was set up for the SCALE project. This resource was used to access data for use in the sea ice charting pilot project, as well as all information which was supplied to the crew and science teams. Information and data were tailored to this cruise plan, and the site was set for use with low-bandwidth connections. All information was also made available via direct links, for occasions where connectivity was particularly poor.

### 12.1.3. Southbound Leg to MIZ

#### Surface Synoptic Observations

SYNOPS began from 06h00Z on the morning of the 19<sup>th</sup> July, with the whole team shadowing the PMO for the first shift. Thereafter, shifts ran as per normal until 21h00Z on the 7<sup>th</sup> August. Vessel SYNOP systems performed as expected.

#### Upper Air Soundings

The first upper air sounding was conducted at approximately 23h45Z on the 19<sup>th</sup> August. This sounding was conducted by the PMO, with the rest of the team shadowing for additional training. The timing of the balloon release was designed to coincide with the 00h00Z global NWP runs such that the data would be available for assimilation. Preparation began at 23h00Z each day, with the actual release normally around 23h45Z.

All upper air systems functioned normally. Except for one release during particularly heavy wind conditions, all releases were successful, with radiosondes reaching altitudes of around 21,000 m.

During the unsuccessful release, the balloon was released on the 7<sup>th</sup> deck outside the balloon hangar, along the centre longitudinal line of the ship. It would appear that the airflow along this centre line adheres to the general plan of the ship, meaning that there is a downdraft which the balloon encountered. It was unable to overcome this

downdraft and was pushed into the ocean. This effect is exacerbated (and only really a problem) in wind speeds of 40 kt, from what personnel were able to observe. In such cases, it may be helpful to release the balloon from the port corner of the deck outside the balloon hangar, where the airflow may be slightly less uniform, allowing the balloon a chance to climb.

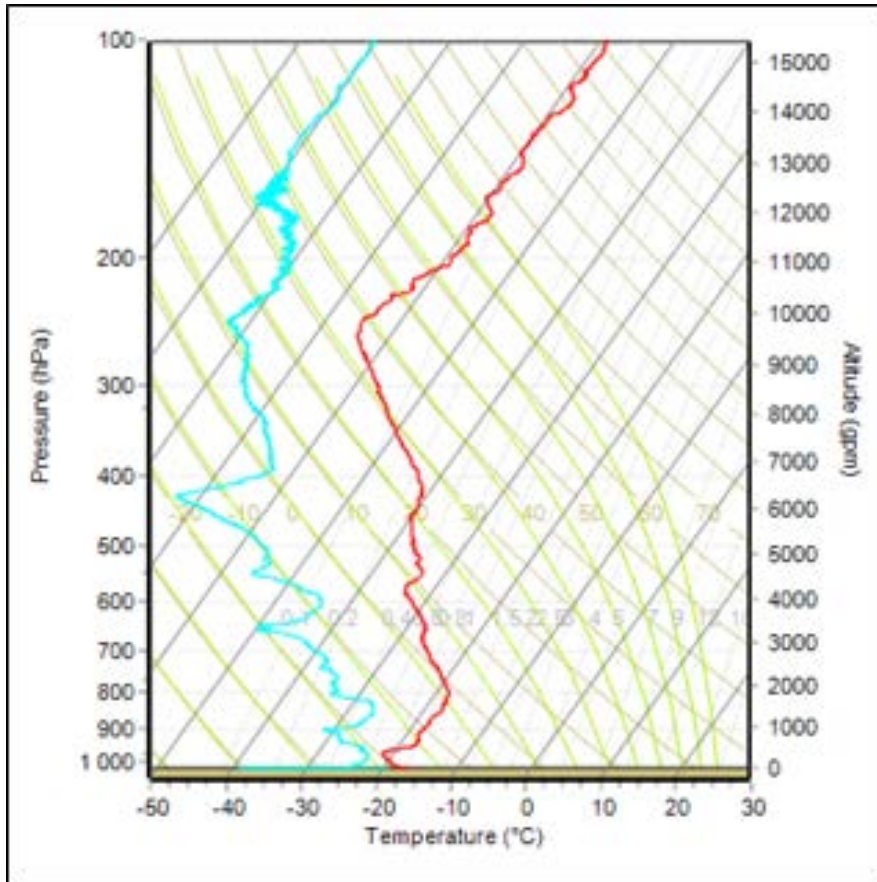


Figure 12.3. A skew-T plot generated from an upper-air atmospheric sounding at around XYZ. Where the dew point temperature (blue) and temperature (red) curves near each other, the relative humidity increases, indicating the likely presence of clouds.

#### Met-ocean Decision Support

Speaking to *Winter Cruise, Work Package 4*, SAWS provided daily met-ocean products including maps of wind speed and direction with isobars, significant wave height and mean direction, sea ice classification, sea ice concentration, sea-surface temperature, air temperature, precipitation and composite maps of sea level pressure, swell height and direction and sea ice concentration. Selected time steps for these fields as well as the shipping chart were printed and assembled into a daily weather information pack which was posted on noticeboards in the 6<sup>th</sup> and 7<sup>th</sup> deck lounges, outside the dining hall and in the environmental hangar where most of the science work was conducted.

In addition to this, Meteorological Trainer (Marine) Christina Liesker provided expert interpretation of the model forecasts each day during a daily briefing between her, the Chief Scientist and the Captain and Chief Mate. Over the course of the cruise, numerous requests for specific information or insight were received.

#### Ozone Sounding

In total, 3 ozone soundings were conducted. These operations require significant training (prior to cruise departure), as well as considerable preparation immediately prior to each sounding. The PMO was responsible for ozone soundings on this cruise, and began preparation for soundings approximately 7 days ahead of the planned release time. Broadly speaking, preparation involves 3 stages. These are conducted approximately 7 days, 3 days and 24 hours before launch. Preparations include the introduction of cathodic and anodic chemicals to the cell, the calibration of the cells by introducing ozone to the sonde and the checking of the sonde's reaction time with and without ozone.

For the first ozone sounding conducted on the southbound leg, a regular 600 g balloon was used. This is the standard recommended balloon type for ozone soundings. Due to the standard helium nozzle (used for standard meteorological radiosonde releases) being too small, resulting in a loose fit of the balloon, the first balloon worked itself off the nozzle and was lost. A second balloon had to be used and held manually to ensure it did not come free from the nozzle (it could also be secured with a length of string or similar). For subsequent releases, 2x 350 g balloons were used in each case as no further 600 g balloons were available. This technique appears to have been successful.



Figure 12.4. Preparation and deployment of an ozone sonde.

<b>Date</b>	2019-07-24	2019-07-27	2019-07-29
<b>Time</b>	08:53Z	12:07Z	16:41Z
<b>Latitude (° N)</b>	-53.999778	-58.127472	-54.001028
<b>Longitude (° E)</b>	0.011083	-0.011139	0.001611
<b>Sounding #</b>	UA_932817600	UA_933076800	UA_933249600
<b>Max Altitude (m)</b>	15, 547	20, 279	19, 625

Table 12.1. Ozone sounding deployment details.

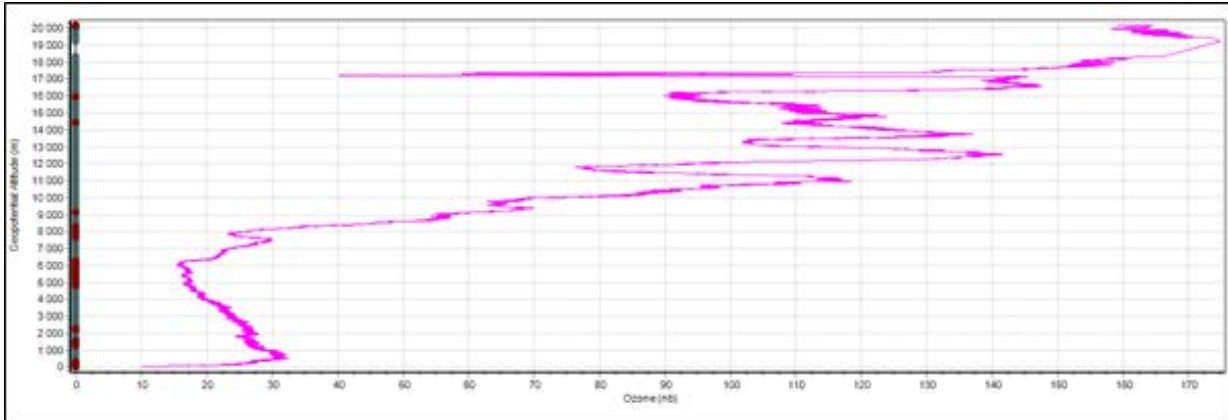


Figure 12.5. An example of the data collected by the ozone sonde. Ozone partial pressure (nano bar; nb) in the atmosphere over 58.127 °S

### iSVP Buoy Deployment

Two standard iSVPs were deployed prior to arrival at the MIZ. This was aimed at obtaining some idea of confirmed open water in relation to the MIZ (where polar iSVPs would be deployed). Further, the drifters would become part of the Global Drifter Program (GDP) of the Data Buoy Cooperation Panel (DBCP) and thus contribute data for assimilation into NWP.

Deployments were uneventful, and success was confirmed by colleagues from the CTWO Marine Unit who were able to detect the buoys from the GTS.

Deployment details are as follows:

<b>Date</b>	24 July 2019	24 July 2019
<b>Time (UTC)</b>	10h24	17h30
<b>Position (° N/E)</b>	-54.000, 0.000	-54.99385, 0.49075
<b>Ship Speed (kt)</b>	0	10.97
<b>Height above MSL (m)</b>	2	2
<b>Deployment position</b>	Stern	Stern
<b>Buoy Serial Number</b>	300234066434240	300234066432480
<b>WMO Number</b>	1701559	1701559

Table 12.2. Deployment details for two standard iSVP buoys slightly north of the MIZ.



Figure 12.6. Deployment of a standard iSVP buoy from the stern.

### Sea Ice Edge Detection

Each day, the range of satellite and model derived sea ice products was downloaded from the cruise webpage during the 06, 09 and 12Z shifts (as each became available from the CTWO Marine Unit).

These were archived into the correct directories on the AWS computer, so as to facilitate the charting exercise.

Starting on the 19<sup>th</sup> July, a SAWS personnel meeting was held each day to discuss the ice conditions and changes thereof as determined from the various sea ice data products being used.

The work flows prepared prior to departure were used to construct ice edges, and these were archived for analysis later on. Notes were also made of common challenges and patterns which were noticed (in respect of how the ice evolves from day to day).

In addition to this, various data products were received via the weather office email address onboard from Mr. Neal Young in Australia. Neal is a sea ice expert, having worked with sea ice data analysis and remote sensing in the Southern Ocean for many years. He has provided valuable guidance to the SAWS Marine Unit, since connecting with them via the International Ice Charting Working Group (IIWCG) meeting in 2018. This proved particularly helpful when synthetic aperture radar (SAR) images became available for the area of interest, as Neal's imagery was georeferenced, compared to derived products and annotated for use in planning MIZ work.

#### **12.1.4. Transit Through MIZ**

Upon first noticing (any) sea ice, SAWS personnel were tasked to take regular photographs, as well as join the team observing sea ice from UCT on the bridge, to learn from and support their operations. The aim of this exercise was to assemble a large photographic dataset, which could be time/location referenced, such that the in-situ ice distribution could be compared to the space/time corresponding sea ice data products. It was envisaged that this would allow something to be said about the accuracy of the products, as well as for lessons to be learnt regarding care in their use. Further, the photographic dataset would form the backbone of a training resource with which to explain changes within the MIZ to prospective SAWS ice charters (forecasters).

In addition to sea ice observations, routine SYNOPs continued as normal.

The deployment of the 3 polar iSVP buoys was also conducted in the MIZ. One of these buoys was deployed into water, with drifting sea ice around it, and the other two were deployed directly onto large pancake sea ice floes. This activity forms a critical

component of the ice charting pilot project, whereby an objective handle on the movement of known sea ice can be obtained. Further, the sea-level pressure (SLP) data collected by the ice buoys will allow an assessment of model accuracy to be made, where numerical model weather data (e.g. reanalysis) are used in correlating sea ice evolution with meteorological forcing.

Finally, an ozone sounding was conducted at the southern-most station of MIZ 3. Details can be found in Table 12.1.



Figure 12.7. SAWS scientists deploying a polar iSVP buoy on an ice floe.

<b>Date</b>	2019-07-27	2019-07-27	2019-07-28
<b>Time (UTC)</b>	00:01	17:09	05:07
<b>Position (° N/E)</b>	-57.058667, 0.106917	-57.9174, -0.0176	-57.1658, -0.0044
<b>Ship Speed (kt)</b>	0	0	0
<b>Height above MSL (m)</b>	2	0	0
<b>Deployment position</b>	Starboard quarter	Starboard side via crane	Starboard side via crane
<b>Buoy Number</b>	<b>IMEI</b> 300234067003010	300234066992870	300234067002060

Table 3. Deployment details for the 3 Metocean polar iSVP buoys

### 12.1.5. Northbound Leg from MIZ

After reaching 57.91 °S, the vessel turned around and began heading slowly northwards. Strictly speaking, the final ice buoy deployment occurred during this leg, but for ease of reading it is detailed in the previous section. All activities associated with the various work packages continued during this leg, as described in detail in Section 5. An ozone sounding was conducted at 54.001028° S, as detailed in Table 1.

On the north bound leg to East London, upper air soundings were terminated after the ascent on the 5th August (given proximity to the coast < 150 nm), and SYNOPSIS after the 21h00Z observation for the 6<sup>th</sup> August.

During this leg, preparations were made to showcase the work which SAWS had undertaken during the cruise for the purpose of the SAAll open day being held in the Port of East London.

## **12.2. Spring Cruise**

### **12.2.1. Scope**

This report shall describe the activities of SAWS personnel during the 2019 **S**outhern **O**cean **S**easonal **E**xperiment (SCALE) Spring Cruise. To this end, it shall provide selected figures and tables representative of the data collected and analysed during the cruise, for the various different work packages. Data and the analyses should be requested separately. Broadly speaking, the report focuses on four main work packages which formed part of the SAWS activities onboard:

*Work Package 1:* Three-hourly surface synoptic weather observations & upper air soundings

*Work Package 2:* Automated sea ice observations

*Work Package 3:* Sea ice charting pilot project

*Work Package 4:* Decision support for science and navigation

### **12.2.2. Work Packages and Pre-departure Prep**

Significant preparation related to the various work packages was conducted prior to departure.

*Work Package 1: Three-hourly Surface Synoptic Weather Observations & Upper Air Soundings*

Preparation for this work package involved ensuring that the SAWS instruments onboard the vessel were calibrated and verified according to WMO protocols, in order to ensure accuracy throughout the duration of the cruise. This was completed on the 11<sup>th</sup> October 2019 by the Port Meteorological Officer (PMO) and Chief Technologist. The upper-air system was also checked, and the required helium gas quantity and supplies of radiosondes and latex balloons acquired.

Next, training was provided by the PMO to all personnel who would be conducting surface synoptic observations and upper air soundings during the cruise. This was conducted over 2 sessions.

*Work Package 2: Automated Sea Ice Observations*

Weather-proof action cameras were purchased to begin building a photograph database of sea ice conditions during the MIZ legs. The Marine Unit prepared the action camera positioning and mounting prior to departure to ensure a known

geometry for later processing. Calibration was also performed to allow for size information to be extracted from photographs.

#### Work Package 3: Sea Ice Charting Pilot Project

This work package is related to the interest SAWS has in providing routine sea ice charting services, in order to satisfy service provision recommendations of the WMO for NMSs with METAREA responsibilities. Whilst an edge detection pilot project was run on the Winter cruise, during Spring, the focus was on the deployment of instrumentation and creation of the photo dataset.

#### Work Package 4: Decision Support for Science and Navigation

The same decision support package as was made available during the winter cruise (see Winter Cruise, Work Package 4) was made available during the spring cruise. This included the same range of bespoke data products, webpages and consultation with forecasters and researchers from SAWS.

### **12.2.3. Southbound Leg to MIZ**

#### Surface Synoptic Observations

SYNOPS began from 06h00Z on the morning of the 13<sup>th</sup> October, with the whole team shadowing the PMO for the first shift. Thereafter, shifts ran as per normal until 21h00Z on the 19<sup>th</sup> November. Vessel SYNOP systems performed as expected, except for some instances when spurious humidity values were obtained from the temp/humidity sensor. These would ultimately be removed during the post-cruise quality control processing.

#### Upper Air Sounding

The first upper air sounding was conducted on the 14<sup>th</sup> October 2019 and followed an every-other-day routine. This sounding was conducted by the PMO, with the rest of the team shadowing for additional training. The timing of the balloon release was designed to ensure that the completion of the ascent coincided with the 12h00Z global NWP runs such that the data would be available for assimilation. Preparation began at 11h15Z, with the actual release normally around 11h45Z.

All upper air systems functioned normally with no problems encountered. Except for two releases during particularly heavy wind conditions, all releases were successful, with radiosondes reaching altitudes of around 21, 000 m.

#### Met-ocean Decision Support

Routine and on-demand met-ocean support was provided throughout the cruise in the same format as was done during the Winter Cruise (see Winter Cruise, Met-ocean Decision Support). For the spring cruise, this included deliberations from the Marine Unit personnel based in the CTWO regarding the sea ice edge and conditions.

### **12.2.4. Transit Through MIZ and Eastwards track**

The sea ice cameras were programmed to take photos every minute whilst the SA Agulhas II was in the ice. Sea ice thickness was also observed every 2 hours for the duration of the eastwards. In addition to sea ice observations, routine SYNOPS and upper air ascents continued as normal.



Figure 12.8. A photo from the mounted action camera showing sea ice conditions and the buoy used to measure sea ice thickness.

### iSVP Buoy Deployment

Specially-designed frames were built around three standard iSVP buoys to allow them to be deployed on sea ice floes in the MIZ. The frames ensured that they would operate as ice trackers and barometers on the ice, and function as normal Global Drifter Program (GDP) drifters after the melting of the floes. This would enable them to continue to collect data for assimilation into NWP.

Deployments were uneventful, and success was confirmed by colleagues from the CTWO Marine Unit who were able to detect the buoys from the GTS.

Deployment details are as follows:

Date	24/10/2019	28/10/2019	29/10/2019
Time (UTC)	11:30Z	n/a	11:30Z
Position (° N/E)	-55.33, 0.06	-59. 36, 6.57	-59.38, 8.15
IMEI Number	30023406643305 0	300234066434000	300234066434250

Table 12.4. Deployment details for three standard iSVP buoys on purpose-built ice frames in the MIZ.



*Figure 12.9. Deployment of a standard iSVP buoy on specially-designed cradle, on a floe in the MIZ.*

This activity feeds into the sea ice charting project in the same way as the polar iSVP buoys deployed during the winter cruise.

#### **12.2.5. Northbound Leg from MIZ**

After reaching 56.0 °S, the vessel turned north-east and began heading slowly for Cape Town with 12 CTD stations. The SAWS team continued with normal routine SYNOPS and upper air ascents.

#### **12.3. Acknowledgements**

As with most scientific expeditions, the work conducted by the cruise team was enabled and supported by -various people behind the scenes. The SAWS cruise teams would like to thanks those who ensured the smooth running of operational feeds from the CTWO, as well as Mr. Neal Young for his insight and guidance.



### 13. TEAM SEAICE

Sea ice research during the SCALE cruises was a joint effort between several teams. It was led by the UCT Polar Team, which comprised the Department of Oceanography, Civil Engineering, Chemical Engineering, Electrical Engineering and international collaborators from the University of Duisburg-Essen. The team also supported the tasks undertaken on ice or involving collected ice samples by teams WAVE, FLUX, TRACEX, NOCE, PLASTICS and SAWS that are described in their respective chapters.

The aim of the SEAICE team was to obtain a quantitative characterization of the Marginal Ice Zone features (MIZ) during the advancing phase of sea ice in winter and during the retreat in spring.

The team commissioned a specialized mobile polar laboratory (Figure 13.1) that was loaded on the ship for both cruises. The refrigerated container, so-called reefer, is equipped with stainless steel benches and a specialized bandsaw, which allowed the scientists to carry out the processing of specimens at  $-10^{\circ}\text{C}$ . The reefer was located on the port side of Level 3 deck, closer to the entrance, due to the need to minimize vibrations and risks when cutting the samples with the bandsaw.



Figure 13.1 The UCT mobile polar laboratory loaded on the SA Agulhas II

The sections below illustrate the activities that assisted sea-ice navigation, observations and the collection of sea ice and snow samples. Details are also provided on the measurements of physical and mechanical properties of sea ice, from collected pancake or brash ice and from the field cores.

Ice navigation and planning was assisted this year by two new products: 1) a dedicated tool developed by SAWS, which is described in Chap. 12, and 2) a preliminary remote

sensing product describing sea ice type concentrations developed by Dr Melshaimer from the University of Bremen. This product distinguishes the different ice types (young ice, first year ice and multi-year ice) based on the combination of passive microwave and scatterometer data using an algorithm developed by Environment Canada (ECICE) and adapted to Antarctic sea ice by Bremen Institute of Environmental Physics. Figure 13.2 shows that the winter station MIZ3 was expected to be in FYI conditions, which was confirmed on site as detailed below in the fieldwork section. The MIZ extent with unconsolidated ice conditions, composed of pancake ice of about 1 to 5 m diameter extended for about 200 km southward as indicated by the YI map features.

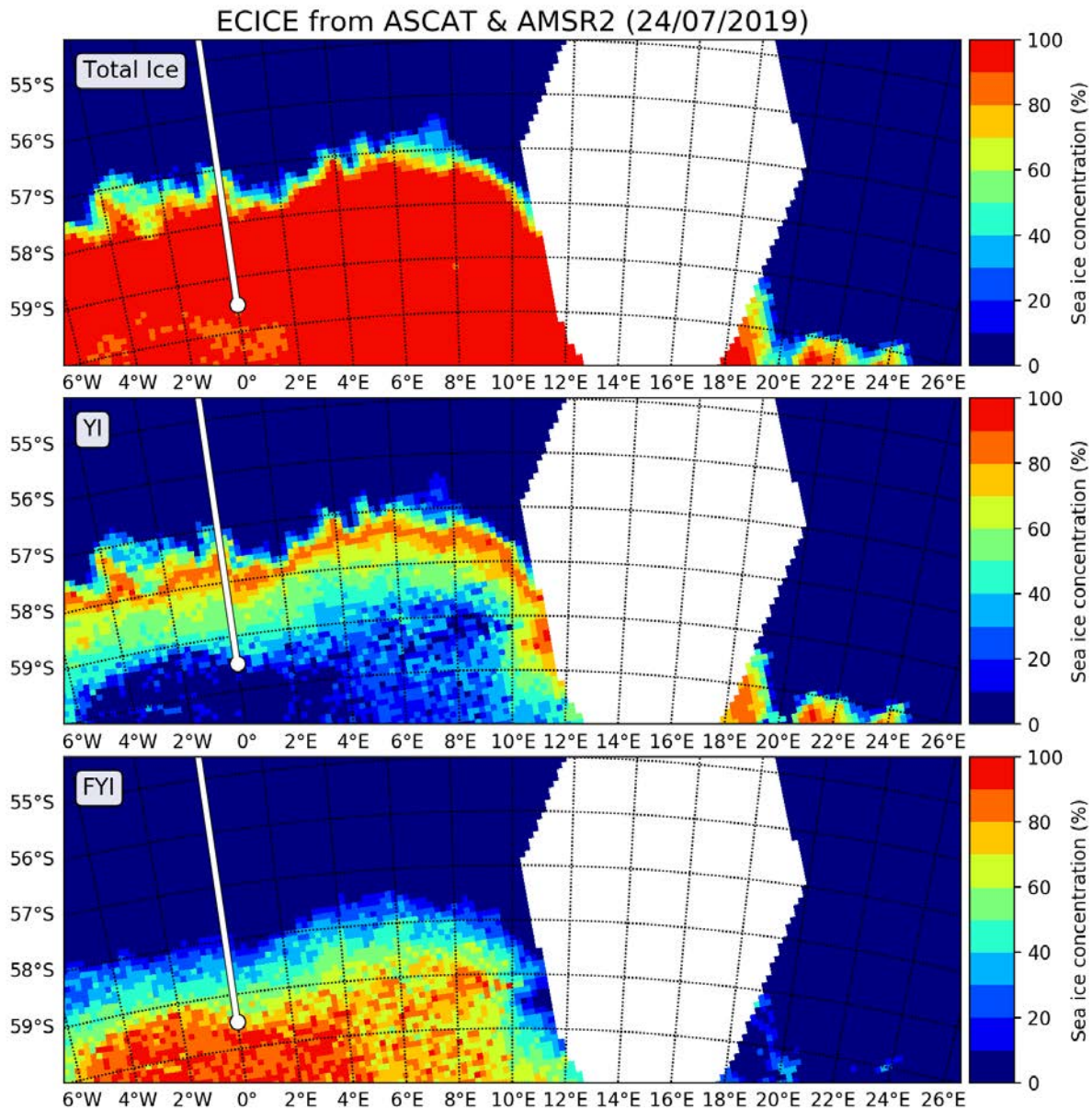


Figure 13.2 Sea ice type concentration from the IUP product developed by the University of Bremen. Daily concentration of total ice, young ice (YI) and first-year ice (FYI) on the 24<sup>th</sup> July prior to the ship entering the MIZ. The cruise plan and the southernmost station are also shown. The large region of missing data is due to an issue with the sensor.

The conditions during the spring cruise were characterized by rather similar sea ice features along the Good Hope line (Figure 13.3). The sea ice edge at this longitude extended northward about 150 km since the winter cruise. The major difference was observed in the eastern sector, where the sea ice advanced northward and reached about the same latitude as in winter. According to the satellite images, sea ice along the Good Hope line was already in the retreat phase since mid-October, as shown by the timeseries at 56S (Figure 13.4).

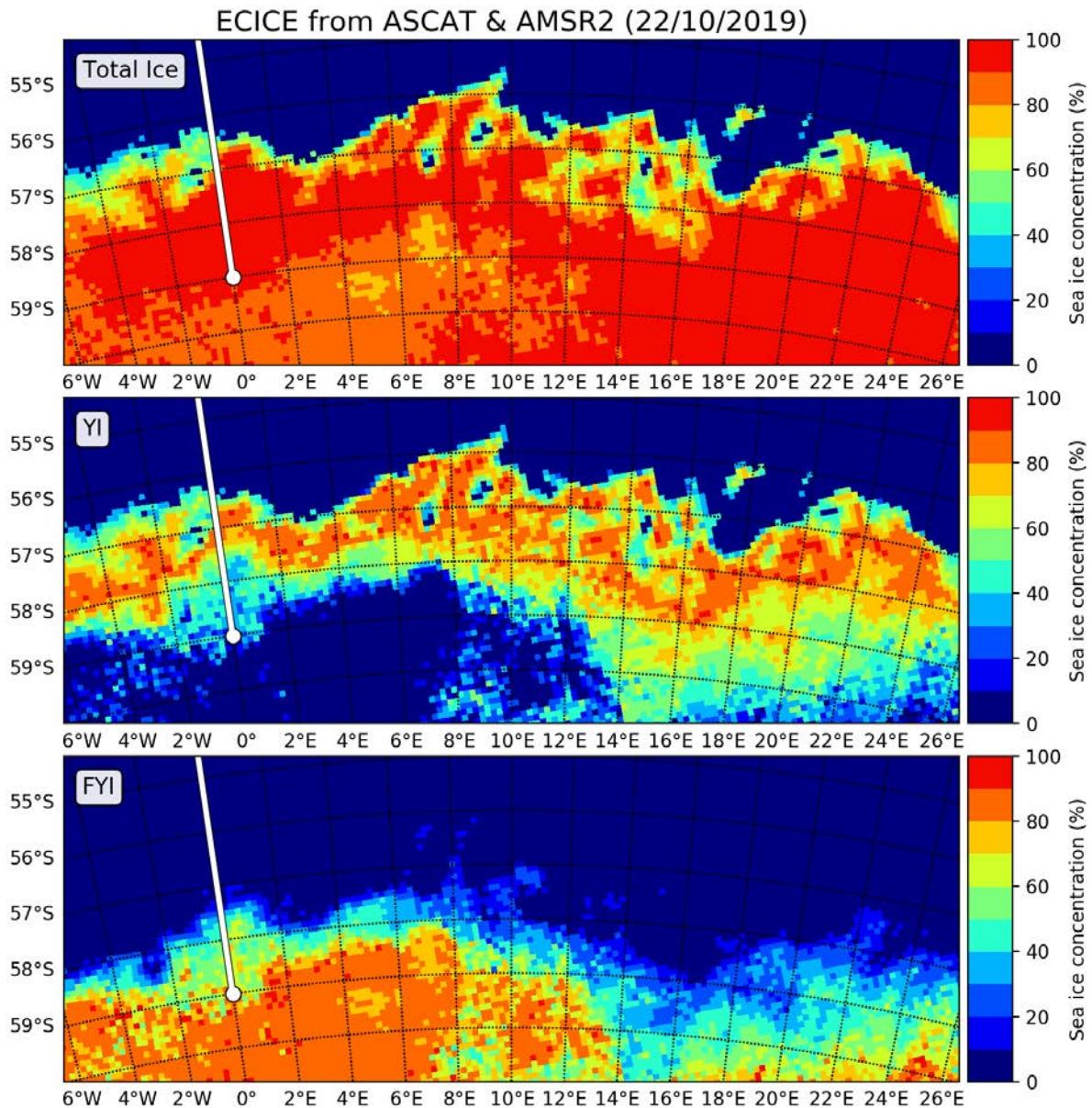


Figure 13.3 As in the previous figure but for the spring cruise, before entering the ice on 22<sup>nd</sup> October.

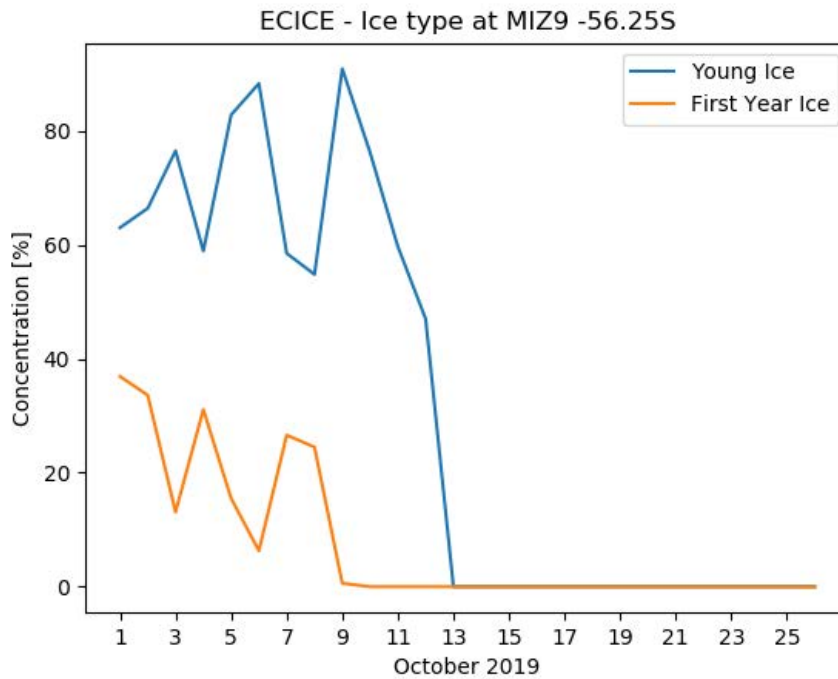


Figure 13.4 Time series of ice type concentration at the planned station MIZ9 at -56.25 degrees (this station was moved further South because sea ice retreated quicker than expected from climatological data).

During the **winter cruise** the ship entered the ice on the 26<sup>th</sup> July at 13:00 and exited on the 28<sup>th</sup> July at 20:30. Figure 13.5 shows an overview of the stations according to the naming convention used in Table 1 in the report introduction. The station plan was designed to resolve the gradient of sea ice features from the open ocean into more consolidated sea ice conditions. Due to contingency and time optimization, the sequence of stations did not follow the original design. The naming convention was extended to preserve the original geographic distribution of MIZ1 being at the edge with the open ocean, MIZ2 at intermediate conditions and MIZ3 in pack ice. Stations are therefore turned into clusters, where the different activities as indicated in Table 1 took place.

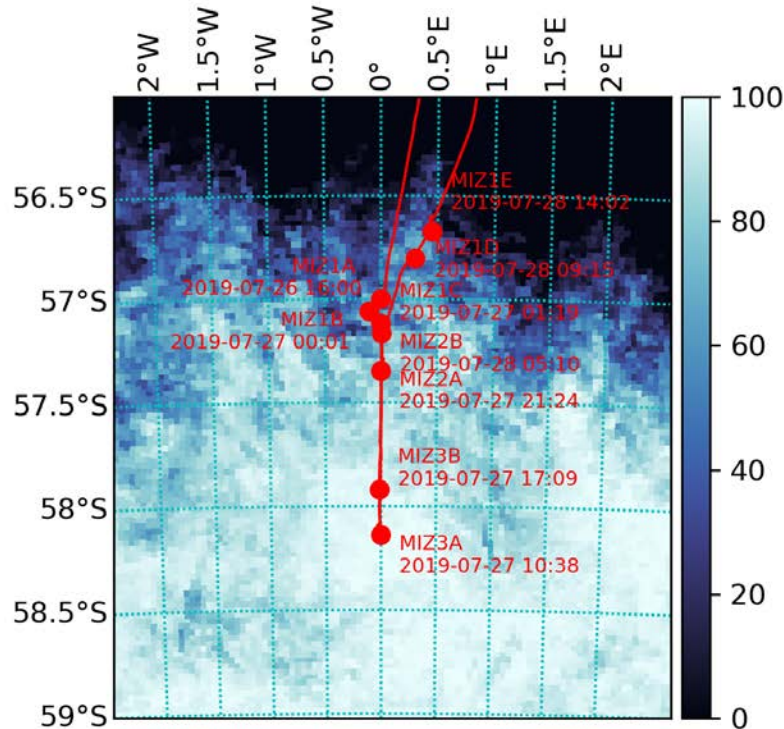


Figure 13.5 Map of the winter MIZ stations with date and time of the starting of operations. The ship entered from the westernmost course and exited from the easternmost course. Sea ice concentration is from the University of Hamburg ASI-AMSR2 processing for the 26<sup>th</sup> July 2019

The longer **spring cruise** repeated the winter MIZ3 station and allowed for a zonal transect to obtain sea ice conditions across the longitudes (Figure 13.6). The spring MIZ3 was moved about 80 km to the South with respect to the winter location. The ship encountered a large variability in the sea ice features that did not match the required safety conditions for field operations.

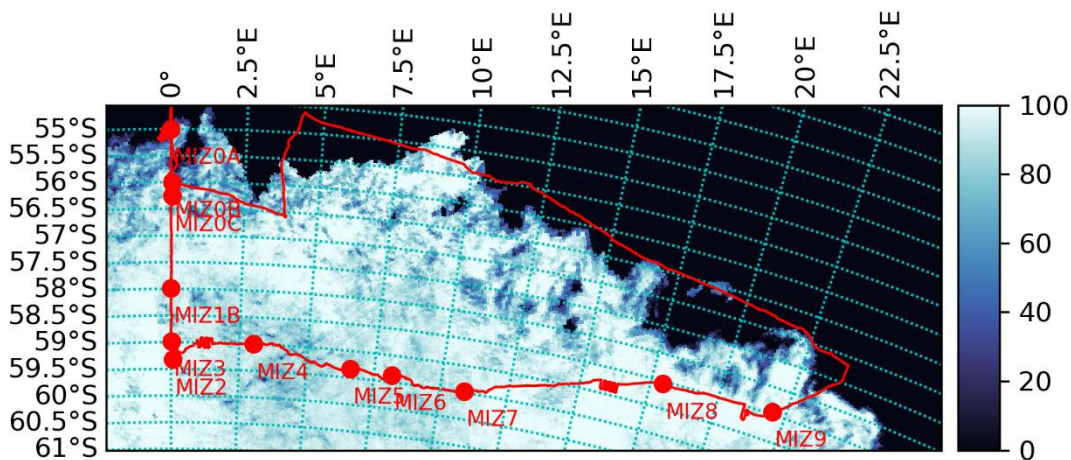


Figure 13.6 Map of the spring cruise MIZ stations (they will be indicated as SMIZx in the text). Sea ice concentration is from the 28<sup>th</sup> October 2019.

The table below illustrates the activities that were undertaken during the cruises.

<b>Activity</b>	<b>Winter</b>	<b>Spring</b>
Sea ice observations	Yes	Yes
Ice coring + under ice sampling	Yes	Yes
Floe lifting	Yes (pancake)	Yes (brash)
Ice-tethered buoy deployments	Yes	Yes
Frazil ice sampling and testing	Yes	No
Compression tests	Yes	Yes
Ultrasound tests	Yes	No (on land)
Thermal conductivity	Yes	No
Crystallography and cross-polarization	Yes	No (on land)
Permeability	No	Yes

### 13.1. Sea Ice Observations

*PI: Marcello Vichi*

*Winter cruise members: (on the ship) Ehlke de Jong (leader), Armand van Zuydam, Nicole Taylor, Martinique, Jesslyn Bossau, Tor Magnus Aarskog; (on land) Wayne de Jager, Sejal Pramlall*

*Spring cruise members: Martinique Engelbrecht (leader), Jesslyn Bossau, Kelsey Kaplan, Wayne de Jager, Sejal Pramlall, Andrei Sandru (on land) Ehlke de Jong, Marcello Vichi*

This activity started a couple of months before the voyages with the analysis of sea ice evolution using satellite remote sensing. The AMSR2 sensor data processed by the University of Hamburg and the University of Bremen in Germany are used because they allow higher resolution down to 3.125 km. The preliminary ECICE data illustrated in the introduction were a valid help during the cruise, especially to inform the navigation during the longitudinal transect in spring.

Observations on the ship were done jointly with team VIBRATION. In order to combine the different requirements, a complete set of sea ice observations was done every 10 minutes from the bridge. Observations are collected according to the Antarctic Sea Ice Processes and Climate (ASPeCt) protocol – the international standard of observing Antarctic sea ice. Ice is classified according to primary, secondary and tertiary types, for which the estimated concentrations, floe sizes and features are given separately with specific codes (Figure 13.7). The higher frequency observations were eventually combined into the hourly frequency required by ASPeCt. The abridged versions of the forms submitted to the Australian data centre at the University of Tasmania are provided at the end of this section.

ICE TYPE (ty)	FLOE SIZE (f)	TOPOGRAPHY (t)	SNOW TYPE (s)
10 Frazil 11 Shuga 12 Grease  20 Nilas 30 Pancakes 40 Young grey ice, 0.1-0.15 m 50 Young grey-white ice, 0.15-0.3 m 60 First year, 0.3-0.7 m 70 First year, 0.7-1.2 m 80 First year, >1.2 m 85 Multiyear floes 90 Brash 95 Fast ice	100 Pancakes 200 New sheet ice 300 Brash/broken ice 400 Cake ice, <20 m 500 Small floes, 20-100 m 600 Medium floes, 100-500 m 700 Large floes, 500-2000 m 800 Vast floes, >2000 m	100 Level ice 200 Rafted pancakes 300 Cemented pancakes 400 Finger rafting 5xy New, unconsolidated ridges (no snow) 6xy New ridges filled with snow or a snow cover 7xy Consolidated ridges (no weathering) 8xy Older, weathered ridges  x values: 0 0-10% areal coverage 1 10-20% 2 20-30% 3 30-40% 4 40-50% 5 50-60% 6 60-70% 7 70-80% 8 80-90% 9 90-100%  y values: 1 0.5 m av. sail height 2 1.0 m 3 1.5 m 4 2.0 m 5 3.0 m 6 4.0 m 7 5.0 m	0 No snow observation 1 No snow, no ice or brash 2 Cold new snow, <1 day old 3 Cold old snow 4 Cold wind-packed snow 5 New melting snow (wet new snow) 6 Old melting snow 7 Glaze 8 Melt slush 9 Melt puddles 10 Saturated snow (waves) 11 Sastrugi

ICE CONcn (c)
to be expressed in tenths

SEA ICE (z) AND SNOW THICKNESS (sz)
to be expressed in centimetres

OPEN WATER
0 No openings 1 Small cracks 2 Very narrow breaks, <50m 3 Narrow breaks, 50-200 m 4 Wide breaks, 200-500 m 5 Very wide breaks, >500 m 6 Lead/coastal lead 7 Polynya/coastal polynya 8 Water broken only by small scattered floes 9 Open sea

Figure 13.7 ASPeCt codes for reporting ice features

### **Winter cruise**

Observations started when entering the ice (26.07.2019 at 13h00 pm) and ended when exiting the ice (28.07.2019 at 20h30). The designated observation sites are the Bridge and Monkey Island for camera recordings. The camera recordings consisted of an automated system jointly operated by team SEAICE and team WAVE, which is described in Chapter 17, and a backup system comprising a laptop for recording sea ice observations and two TomTom Bandit cameras for recording the sea ice environment. Operations in the Bridge were quiet and calm, thanks to the collaboration with the ship Officers' crew. Monkey Island was exceptionally windy (with wind speeds of up to 40 knots) and cold (wind chills of up to -50°C). Besides the team leader, this observation team experienced the ice environment for the first time during winter 2019 cruise. Therefore, lack of experience resulted in subjective biases. However, they were well-trained and keen to learn which resulted in them doing relatively well. To gain insight into predicting the sea ice edge, the team worked closely with the South African Weather Service (SAWS). This was a success and through more expeditions together we can gain the experience and understanding of forecasting the ice edge.

Sea ice observations have been taking place aboard the S.A. Agulhas II since winter 2016. This winter 2019 Antarctic expedition was the sixth where ASPeCt observations were conducted. Much has been improved since the first ASPeCt observations in 2016. Momentarily, there is not very much to improve apart from increasing the skills and expertise of the sea ice observers.

### **Spring cruise**

Brash ice was first observed at 8:40 on the 22<sup>nd</sup> October at a latitude of 55° 48'. The last floe was observed at 16:20 on the 8<sup>th</sup> November. Six ice observers, who learned standard Antarctic Sea ice Processes and Climate (ASPeCt) protocols as well as sea ice observation methodologies, operated on the bridge when conducting ice

observations. The ASPeCt protocol and definitions were used when sea ice data was collected. These characteristics and definitions included:

- Total concentration: the fraction of the ocean covered by any type of sea ice, estimated to the nearest 10%;
- Categories and concentrations: the dominant ice types present in the pack were divided into primary (most dominant), secondary (second-most dominant), and tertiary (third most dominant);
- Ice type;
- Ice thickness;
- Cloud cover;
- Visibility;
- Weather;
- Air and sea surface temperature.

ASPeCt sea ice observations took place in conjunction with the Stellenbosch sea-ice team. Therefore, in addition to the above-mentioned observations, ramming and vibrations were recorded. Observations were recorded once per minute and began and ended the moment the ship entered and exited the sea ice region. TomTom Bandit cameras were used to continuously record the sea ice state as in the previous cruises. For safety, when going outside to change the cameras, the sea ice observer harnessed themselves to the ship. If the wind was greater than 35 knots or if it was too dark, the observer did not go outside to change the cameras.

Changes to be made for future expeditions:

The team worked well together. However, since they were inexperienced with sea ice observations, their recordings were not on par with ASPeCt standards. More experienced ice observers will be needed for future expeditions. To limit subjective bias, the number of ice observers needs to be as low as possible. However, conducting observations every minute for Stellenbosch requirements proved to be challenging with 6 observers. There should, therefore, be two additional observers. Since more experienced observers are needed and the number of observers should be increased, a new strategy for ice observations needs to be considered for future expeditions.



Figure 13.8 Coring field at the winter MIZ3 station showing the cemented pancakes with sizes varying between 3 and 15 m

### **13.2. Ice coring and fieldwork**

*PI: Marcello Vichi, Sebastian Skatulla, Tokoloho Rampai, Keith MacHutchon*  
*Winter cruise members: Emmanuel Omatuku Ngongo (team leader, University of Cape Town - UCT). Coring team (Riesna Audh (UCT), Benjamin Hall (UCT) and Emmanuel Omatuku Ngongo (UCT)); Logging and Transfer team (Andrea Cook (UCT), Rutger Marquart (UCT), Ashleigh Womack (UCT), Jean Looek (Stellenbosch University – SU), SU students from the Trace Metal and Vibration groups, and Cape Peninsula University of Technology (CPUT) students from the Phytoplankton group.)*  
*Spring cruise members: Justin Pead and Riesna Audh (team leaders), Rutger Marquart, Felix Paul, Siobhan Johnson, Mark Hambrock, Kelsey Kaplan, Boitumelo Matlakala, Tshepang Khoboko, Hasham Taujoo, Sejal Pramlall, Wayne de Jager, Jonathan Rogerson*

#### **Winter cruise**

Fieldwork operation during the winter cruise took place at station MIZ3 on 27 July 2019 between 10h00-16h00 (UTC). The coring operation and temperature measurement of cores took place overboard on a piece of consolidated pancake ice located off the starboard bow. The operation occurred in daylight in extreme conditions. The temperature was  $-17^{\circ}\text{C}$  and the wind speed 20 m/s, according to the onboard equipment of the South African Weather Services. During operation, the ship shielded the activity area from the wind to protect the coring team from the wind chill.

Various equipment was used in this activity. The ship forward crane, gondola platform and personnel cradle were used for the transportation of the coring team and equipment between the foredeck and consolidated pancake ice. A corer, temperature

probe, and other related equipment were used to collect ice cores and snow cover, and to measure temperature and snow cover.

A total of 26 cores were collected and distributed as follow: 5 (TraceEx - SU), 2 (Isotope - UCT), 3 (Overboard temperature, biomatter and nutrients, salinity – UCT), 2 (Phytoplankton group – CPUT), 1 (Biomatter culturing – UCT), 2 (CT scanning – UCT), 2 (Cross-polarization – UCT), 3 (Onboard ultrasound – UCT), 3 (Onboard thermal conductivity, indentation and uni-axial compression – University of Duisburg-Essen), 3 (Honours projects – UCT). Temperature was measured on 3 cores immediately after coring. For this purpose, the cores were placed on a plastic holder made of half a gutter pipe with marking for drill points 5 cm apart from each other. The temperature probe was put into pre-drilled holes, and temperature readings were recorded. The snow cover was measured using a ruler.

After sea ice core collection at MIZ3, a 3D printed Niskin bottle was deployed through two core cavities to retrieve samples of the water at the ice-ocean interface. The niskin 3d deployment yielded two water samples of approximately 700 ml each. These samples were processed for biogeochemical properties (nutrients, flow cytometry, chlorophyll-a concentration, n-isotopes) and salinity. The same tests were run on the frazil ice samples and the sea ice cores that were collected at both MIZ3 and MIZ1.

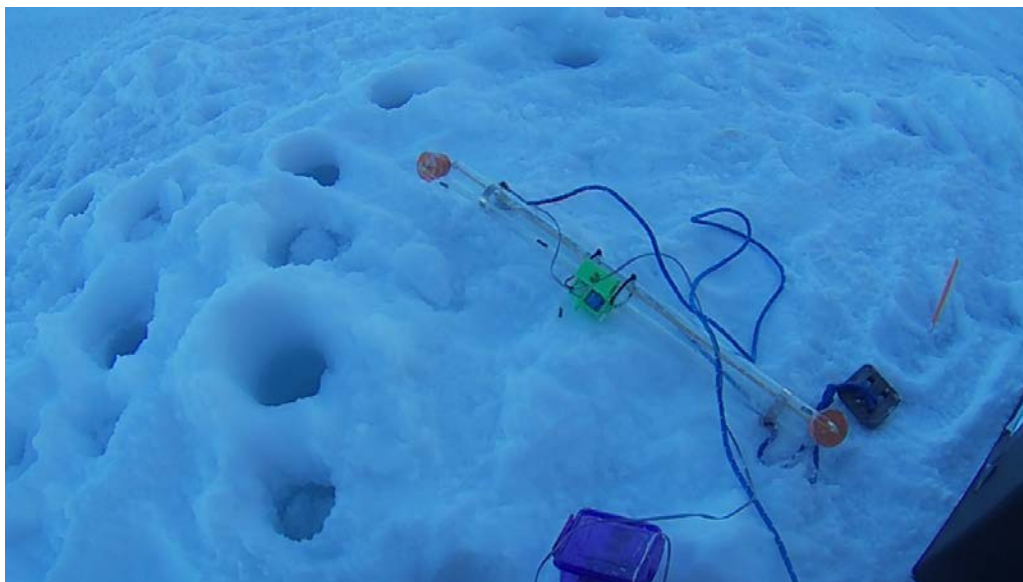


Figure 13.9 Image of the Niskin 3d in the field during station MIZ 3

Snow samples from the sea ice floe at MIZ3 and from the pancake ice collected at MIZ1n were collected using a plastic spade and stored in clean, labeled ziploc bags. The samples were allowed to melt at 5 deg C.

Sub-sampling of the sea ice and snow samples were conducted in the Wet Geology Laboratory aboard the SA Agulhas II. Sub-sampling included allowing the samples to melt in a fridge at 5 degC. Once melted, the volume of the samples was measured using a graduated beaker. The measured samples were transferred from individually marked containers used during initial sampling into amber bottles for salinity testing, 50 ml nutrient tubes and HDPE bottles for biogeochemical testing using methods described in the biogeochemistry section of this report. A total of 15 sea ice cores, 29 frazil ice and water samples, 2 sea water samples and 6 snow samples were prepared for further testing. At the time of writing, nutrient data are not available as biogeochemical analysis will be conducted at the Department of Oceanography's Biogeochemistry Laboratory at UCT.

### *Issues encountered*

#### 1. Overboard coring of consolidated pancake ice

The research objectives of the overboard coring of consolidated pancake ice were met. The results from this fieldwork are extremely important as they will lead to a better understanding of pancake ice. This activity has also helped build experience within the Sea Ice team on in-situ coring of sea ice. However, one of the coring team members was a victim of frostbite due to the wetting of gloves during ice coring and their removal for other operations that required more precise handling of instruments. Frostbites present unusual symptoms for African participants who have rarely experienced extreme cold conditions for prolonged periods. To prevent cold injuries in future expeditions, the following recommendations have been implemented for the spring cruise:

- Rotation of coring teams/members with a maximum coring shift of 2 hrs.
- Implementation of a buddy-check system so that participants do not work with wet gloves and/or are replaced if needed.
- Training on cold-injury prior to expeditions: This will include education of participants about signs and symptoms of cold-related injuries and illnesses, rewarming techniques, first-aid treatment, appropriate clothing, and eating and drinking.
- Schedule of coring activities during the warmest hours of the day, with activity areas shielded from wind to reduce wind chill.
- Further investment in cold gear and heat sources: This will include the use of waterproof gloves or adequate substitutions and the use of heat sources, e.g. mitten gloves.
- Participants to wear eye protection (e.g. skiing goggles) when exposed to blowing snow and ice crystals.



Figure 13.10 Coring operations at spring SMIZ2 (top) and SMIZ5 (bottom). SMIZ5 was abandoned due to unsafe texture of the ice matrix after the exploratory cores.

### ***Spring cruise***

This second cruise allowed for improvement on the issues encountered during the first cruise, especially in terms of safety. Most operations were conducted on consolidated floes. Stations were along the predefined track from the cruise plan, while the specific ice fields for overboard coring were chosen according to ice type (consolidated floes), topography (minimal ridging, cracks, flooding), ice thickness (in excess of 45 cm).

For the duration of each station, the ice team had one member on deck overwatching ice activities, conducting regular check-ins with the teams on ice via hand signals and one team leader on deck to liaise with deck crew and assist with personnel changes. Up to 4 different fully-equipped shifts were organized before each station, with rotation

every two hours. Ice team leader was present on deck until the station closed as done in the winter cruise. Equipment was prepared in advance and the shifts were exposed to cold conditions right before going on ice; at the end of each shift the equipment was stored in the forward hold by other members of the team and cores taken to respective freezers and labs for processing.

*SMIZ2 24/10/2019 12:35:*

Assessment team out first, floe deemed suitable and safe for activities. TracEx, Plastics teams brought on ice to begin core collection. Shift 2 on ice for handover with shift 1, joined by TracEx snow collection. Gondola off ice with shift 1 cores, shift 1 off ice via personnel carrier. Shift 3 on ice for handover, Shift 2 off ice, TracEx team still on ice for snow collection. Only 3 shifts needed to fulfil core requirements as teams worked faster than expected.

*SMIZ3 24/10/2019 19:45:*

Assessment team out first, floe deemed safe and suitable for activities. SIMB and MAST teams brought onto ice for respective deployments. Once SIMB and MAST were deployed and calibrated, teams were taken off the ice and core collection procedures began. First was TracEx cores, which were collected by the sea ice assessment team and assisted by a TracEx team member. Second sea ice team shift brought onto ice for handover and to begin second batch collection, gondola brought on board with shift 1 cores and equipment from the completed deployments. Shift 3 completes a handover with shift 2 at the end of shift 1. Same procedure followed with gondola, shift changes. Shift 5 personnel included the SAWS buoy deployment team. Final shift on standby, but not used.

*SMIZ4 27/10/2019 03:04:*

This station was deemed suitable but later abandoned. Assessment team out on ice, before completing safety assessment, TracEx and Plastics teams were put onto ice. Assessment team found that the station location was unsafe when a core of less than 30 cm length with a slush texture was extracted. All personnel on ice were immediately taken off ice and the station was abandoned. Team leads, chief scientist and deck crew were all in agreement for station abandonment.

*SMIZ5 28/10/2019 11:32:*

This was another problematic station. Assessment team went on ice but the cores collected were questionable. The team was brought back on deck with collected core for consultations. Ship moved forward to a new location and a new assessment team comprising experienced team members were put on ice for the floe assessment, to enable immediate feedback and decision making (Figure 13.10). Floe was deemed unsuitable for activity due to core structure and flooding under the snow layer. Station abandoned after consultation between the team leaders, bridge, deck crew and chief scientist. Ice field was not suitable for miles ahead of the vessel.

*SMIZ6 29/10/2019 12:31:*

Assessment team on ice, floe deemed suitable for activities. TracEx, Plastics teams on ice to begin collection. Shifts cut to one hour long by order of the Captain due to weather. This complicated the core collection as teams had to be shuffled and experienced ice team members (part of the assessment team) were brought off the ice too soon for exceeding one-hour time limit. Shift changes and equipment

exchanges identical to the previous stations. New team on ice in shift 3 for ZooVac operation. All cores collected and teams returned to ship.

SMIZ7 30/10/2019 11:26:

Ice type: unconsolidated floes – melting stage (late season)

Stations were within predefined coordinates from the cruise plan, while ice fields for floe lifting were chosen according to ice type, size and ship manoeuvrability during floe lifting. The assessment team on ice deemed the floe suitable for activities. Core collection completed in three shifts, with a SAWS buoy deployment, TracEx snow collection and ZooVac collection.

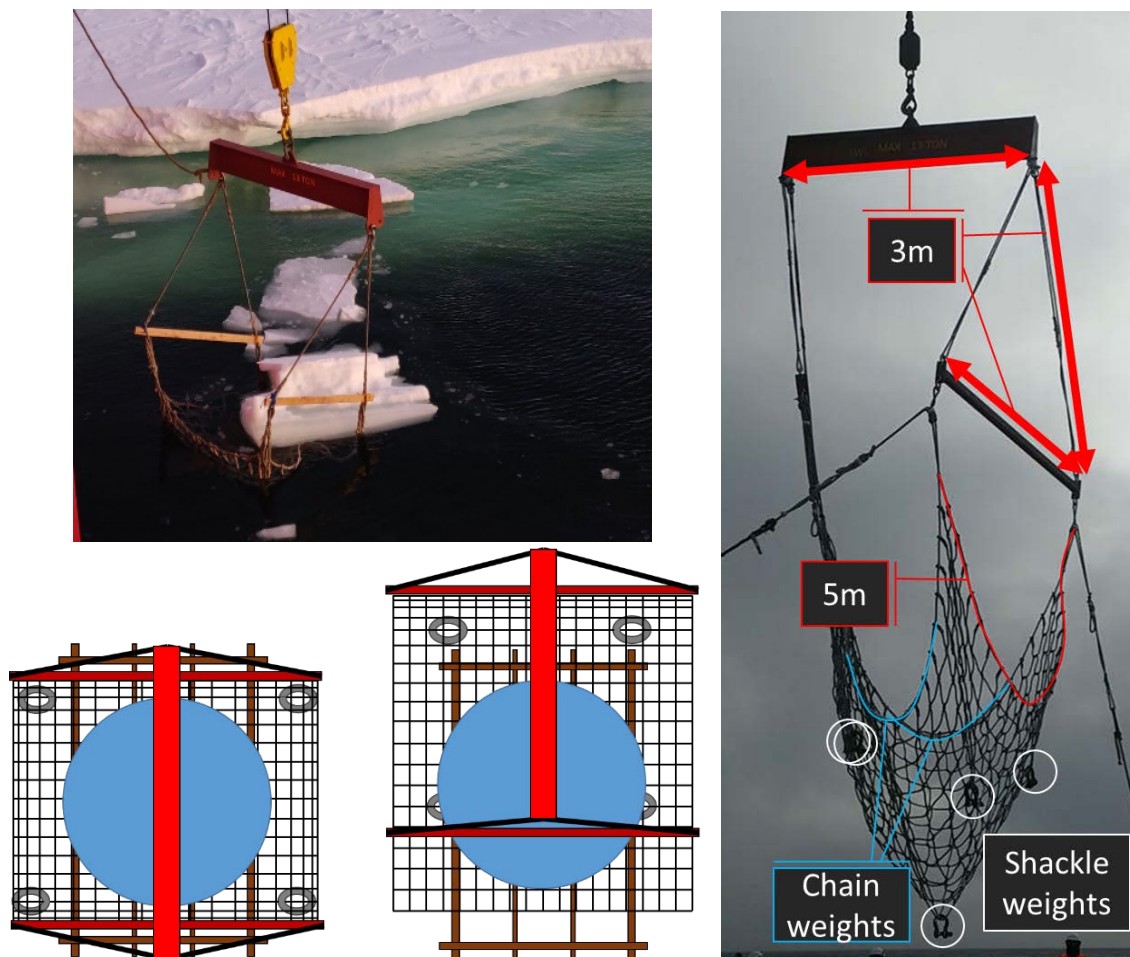


Figure 13.11 a) [top left] Ice collection from summer cruise 2018-19 b) [bottom left] Heli-deck pancake placement c) Contraption dimensions

### 13.3. Floe lifting

PI: Sebastian Skatulla, Tokoloho Rampai, Keith MacHutchon

Winter cruise members: Benjamin Hall and Mark Hambrock (team leaders), same members as in Sec. 13.2

Spring cruise members: Justin Pead and Mark Hambrock (team leaders), Rutger Marquart, Felix Paul, Siobhan Johnson, Riesna Audh, Kelsey Kaplan, Boitumelo

*Matlakala, Tshepang Khoboko, Hasham Taujoo, Sejal Pramlall, Wayne de Jager, Jonathan Rogerson*

The scientific aim of this activity was to define the features of pancakes and other kinds of individual floes at different stages of development, fully characterizing their physical, chemical and biological features. The main challenge is the preservation of the liquid-ice mixture and reduction of the gravity drainage of brine. For the SCALE cruises, it was decided to prioritize efficiency and the diversity of samples, acknowledging that drainage is inevitable.

### ***Winter cruise***

This activity was carried out at station MIZ1 North: [56,802 - 56,803] °S | [0.030 - 0,303] °E on 28/07/2019 between 10:45 – 16:00

Pancakes were fished from the ocean using the Helideck crane and pancake catching contraption, and subsequently placed onto wooden beam grids on the Helideck. Calm ocean and wind conditions allowed for quick selection and isolation of pancakes, resulting in processing becoming the bottleneck to the overall procedure.

Following the ice retrieval operations of the summer of 2018 (see Figure 13.11a) a similar approach with altered dimensions and improved catching capabilities was envisioned for retrieval of pancakes which are too small to safely support in-situ coring. An image with dimensions of the contraption is shown in Figure 13.11c. The contraption consists of a net, attached to two steel spreader-beams at the corners which, in turn, are attached to a large steel I-beam.

The net has square sides of 5-meter length is weighted with five shackles near the centre of the net: four of the shackles are attached at the corners of the 3-meter centre square of the net and the remaining shackle at the centre. Weight shackles are indicated in Figure 1b in grey and Figure 1c with white circles. The 3-meter centre square was chosen in order to ensure that the additional weight does not cause additional contraction of the net but lies directly below the support beams. The two steel spreader-beams and I-beam have lengths of 3 meters respectively, with the spreader-corner-to-beam distance being 3 meters, forming an equilateral triangle.

The contraption is designed to be able to dynamically support a 3-ton floe. Assuming pancakes to have the density of water and a half-ellipsoid shape (e.g. pancake in Figure 13.12), the largest pancakes that can safely be lifted with the contraption are those with a diameter of 3 meters and a height of 0.6 meters.



Figure 13.12 a) [left] Pancake catching 2019 b) [right] Manoeuvre to remove pancake B from net

Four pancakes were collected and placed onto individual grids through the procedures indicated above. Two rafted pancakes were also lifted; however, they were deemed unusable due to the high likelihood of fracture upon contact with the grid and the subsequent removal procedure from the net. Pancake D shattered into six large pieces during removal from the net (see Figure 13.14). Details on the different pancake dimensions and duration of the operations are given below

Pancake		A	B	C	D
Lifting duration (minutes)		2	2	1	4
Temperature core processing durations (minutes)	1	3	7	27	19
	2	23	22	40	41
	3	28	28	48	46
Total coring duration (minutes)		95	193	202	161
Dimensions (meters)	Height	0.40	0.37	0.45	0.37
	Length	2.42	2.49	2.42	2.95
	Width	1.83	2.33	1.83	2.51

This table shows that the time needed to extract cores, relative to the short catching and lifting time, unfortunately resulted in prolonged drainage and potential contamination-exposure of the pancakes on deck. For future operations, it is recommended that new pancakes are only brought on deck once a prior pancake has been fully cored.



Figure 13.13 On board pancake coring during the winter cruise

All collected pancakes had rafted edges, snow-layers and did not have visible biologically active layer. Each pancake was measured for its dimensions. The depth and a sample of the snow-layer were taken before each pancake was manoeuvred out of the net. Cores were taken from the pancakes (as shown in Figure 3 and Figure 6) and distributed to the respective research groups as detailed in Table 2 to Table 5. Due to time constraints only one cluster was extracted from each pancake, with pancake C and D being the only pancakes from which trace metal cores were extracted. The cluster layout is shown in Figure 4.

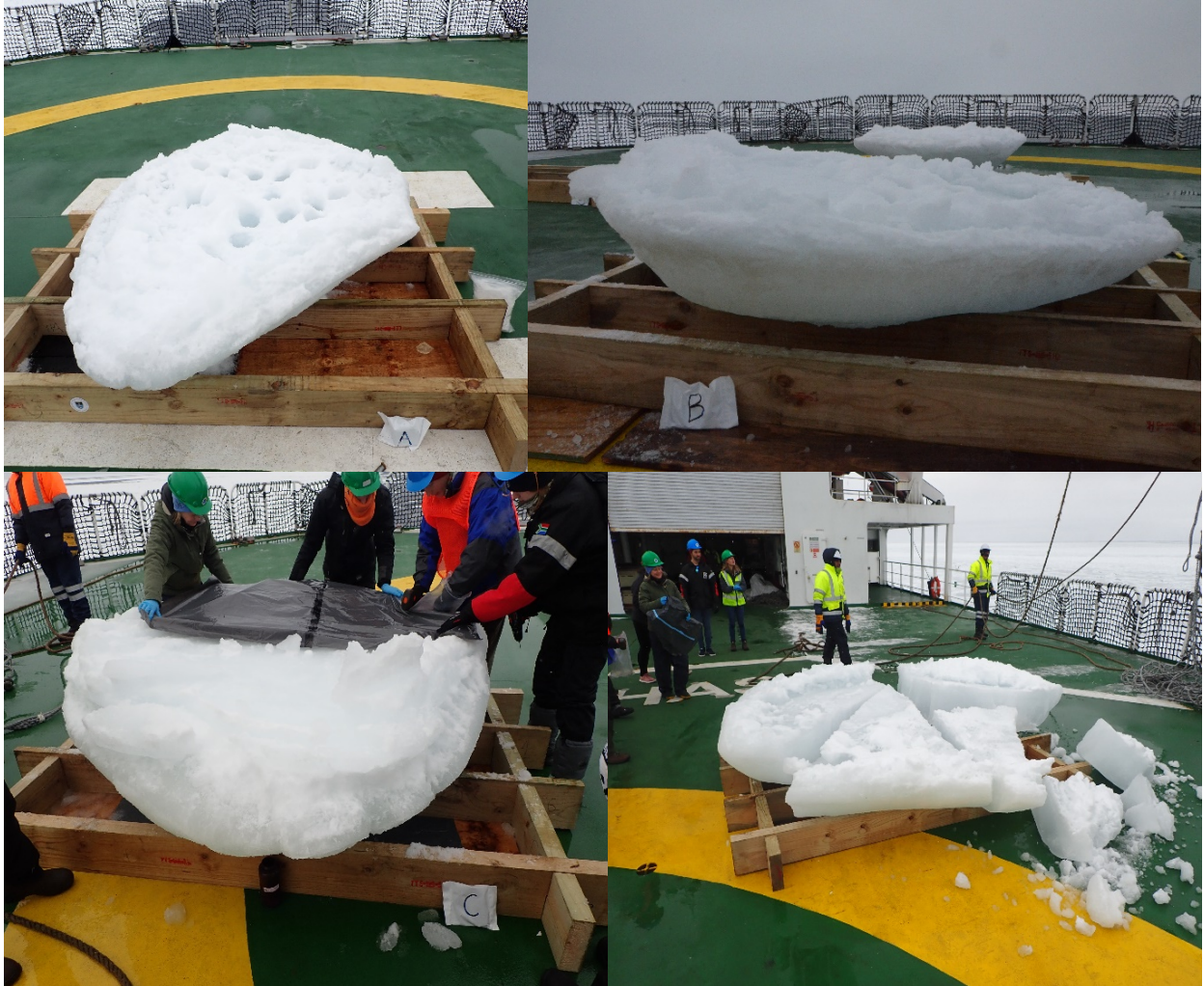


Figure 13.14 a) Pancake A after the coring operation [top left]; b) Pancake B [top right]; c) Pancake C being sampled for trace metals [bottom left] d) Pancake D shattered after the removal of the net [bottom right] The wooden beam structure that prevent the contamination of the samples is visible under the floes.

First and foremost, it must be stated that the performance of the crew during the fishing procedure was exceptional, reducing the time of draining during lifting to as low as a single minute. The unfortunate event of the shattering of pancake D shows that the pancake catching contraption requires improvement to allow for easier removal in order to prevent unwanted shattering in the future.

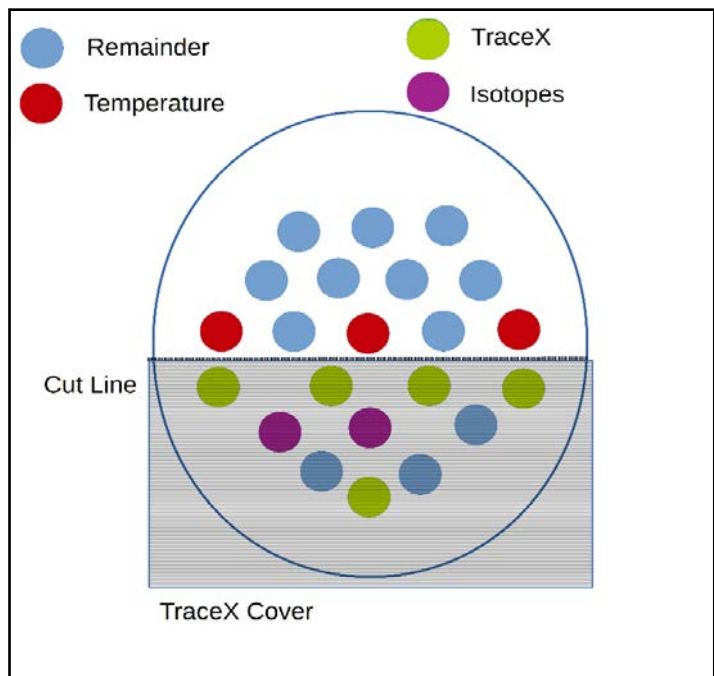


Figure 13.15 Ideal single cluster coring layout

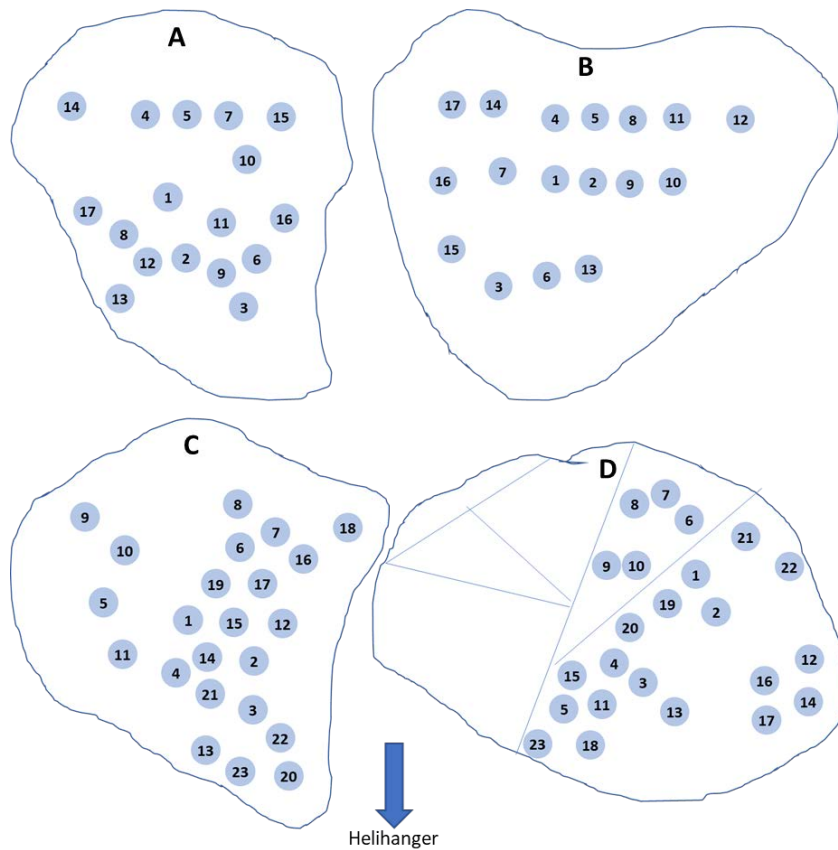


Figure 13.16 Pancake core number layout

Table PA Pancake A coring information

<b>CORE ID</b>	<b>CORE TYPE</b>	<b>CORE NAME</b>	<b>TEAM</b>	<b>DATE CORED</b>	<b>TIME CORED</b>
1	Physical	M01-PHY-01-A	UCT PERG	19/07/28	10:50
2	Isotope	M01-BGC-01-A	UCT PERG	19/07/28	11:05
3	Physical	M01-PHY-02-A	UCT PERG	19/07/28	11:10
4	Isotope	M01-BGC-02-A	UCT PERG	19/07/28	11:12
5	Physical	M01-PHY-03-A	UCT PERG	19/07/28	11:15
6	CPUT	M01-CPUT-01-A	CPUT	19/07/28	11:30
7	CPUT	M01-CPUT-02-A	CPUT	19/07/28	11:32
8	CT	M01-CT-01-A	UCT PERG	19/07/28	11:50
9	CT	M01-CT-02-A	UCT PERG	19/07/28	11:52
10	CP	M01-CP-01-A	UCT PERG	19/07/28	12:01
11	CP	M01-CP-02-A	UCT PERG	19/07/28	12:05
12	US	M01-US-01-A	UCT PERG	19/07/28	12:06
13	US	M01-US-02-A	UCT PERG	19/07/28	12:11
14	US	M01-US-03-A	UCT PERG	19/07/28	12:13
15	DE	M01-DE-01-A	DE	19/07/28	12:18
16	DE	M01-DE-02-A	DE	19/07/28	12:19
17	DE	M01-DE-03-A	DE	19/07/28	12:22

Table PB Pancake B coring information

<b>CORE ID</b>	<b>CORE TYPE</b>	<b>CORE NAME</b>	<b>TEAM</b>	<b>DATE CORED</b>	<b>TIME CORED</b>
1	Physical	M01-PHY-01-B	UCT PERG	19/07/28	11:05
2	Isotope	M01-BGC-01-B	UCT PERG	19/07/28	11:18
3	Physical	M01-PHY-02-B	UCT PERG	19/07/28	11:20
4	Isotope	M01-BGC-02-B	UCT PERG	19/07/28	11:24
5	Physical	M01-PHY-03-B	UCT PERG	19/07/28	11:26
6	CPUT	M01-CPUT-01-B	CPUT	19/07/28	11:35
7	CPUT	M01-CPUT-02-B	CPUT	19/07/28	11:40
8	CT	M01-CT-01-B	UCT PERG	19/07/28	11:57
9	CT	M01-CT-02-B	UCT PERG	19/07/28	11:59
10	CP	M01-CP-01-B	UCT PERG	19/07/28	12:35
11	CP	M01-CP-02-B	UCT PERG	19/07/28	12:47
12	US	M01-US-01-B	UCT PERG	19/07/28	12:50
13	US	M01-US-02-B	UCT PERG	19/07/28	12:52
14	US	M01-US-03-B	UCT PERG	19/07/28	01:38
15	DE	M01-DE-01-B	DE	19/07/28	02:06
16	DE	M01-DE-02-B	DE	19/07/28	02:09
17	DE	M01-DE-03-B	DE	19/07/28	02:11

Table PC Pancake C coring information

<b>CORE ID</b>	<b>CORE TYPE</b>	<b>CORE NAME</b>	<b>TEAM</b>	<b>DATE CORED</b>	<b>TIME CORED</b>
1	Physical	M01-PHY-01-C	UCT PERG	19/07/28	01:05
2	Isotope	M01-BGC-01-C	UCT PERG	19/07/28	01:06
3	Physical	M01-PHY-02-C	UCT PERG	19/07/28	01:18
4	Isotope	M01-BGC-02-C	UCT PERG	19/07/28	01:22
5	Physical	M01-PHY-03-C	UCT PERG	19/07/28	01:26
6	TraceX	M01-TM-01-C	TraceX	19/07/28	01:47
7	TraceX	M01-TM-02-C	TraceX	19/07/28	01:53
8	TraceX	M01-TM-03-C	TraceX	19/07/28	01:56
9	TraceX	M01-TM-04-C	TraceX	19/07/28	02:14
10	TraceX	M01-TM-05-C	TraceX	19/07/28	02:18
11	CP	M01-CP-01-C	UCT PERG	19/07/28	02:23
12	CPUT	M01-CPUT-01-C	CPUT	19/07/28	03:40
13	CPUT	M01-CPUT-02-C	CPUT	19/07/28	03:42
14	CT	M01-CT-02-C	UCT PERG	19/07/28	03:44
15	CT	M01-CT-01-C	UCT PERG	19/07/28	03:45
16	CP	M01-CP-02-C	UCT PERG	19/07/28	03:47
17	US	M01-US-01-C	UCT PERG	19/07/28	03:50
18	US	M01-US-02-C	UCT PERG	19/07/28	03:51
19	US	M01-US-03-C	UCT PERG	19/07/28	03:53
20	DE	M01-DE-01-C	DE	19/07/28	03:57
21	DE	M01-DE-02-C	DE	19/07/28	03:58
22	DE	M01-DE-03-C	DE	19/07/28	04:00

Table PD Pancake D coring information

<b>CORE ID</b>	<b>CORE TYPE</b>	<b>CORE NAME</b>	<b>TEAM</b>	<b>DATE CORED</b>	<b>TIME CORED</b>
1	Physical	M01-PHY-01-D	UCT PERG	19/07/28	01:13
2	Isotope	M01-BGC-01-D	UCT PERG	19/07/28	01:16
3	Isotope	M01-BGC-02-D	UCT PERG	19/07/28	01:30
4	Physical	M01-PHY-02-D	UCT PERG	19/07/28	01:35
5	Physical	M01-PHY-03-D	UCT PERG	19/07/28	01:40
6	TraceX	M01-TM-01-D	TraceX	19/07/28	02:34
7	TraceX	M01-TM-02-D	TraceX	19/07/28	02:36
8	TraceX	M01-TM-03-D	TraceX	19/07/28	02:39
9	TraceX	M01-TM-04-D	TraceX	19/07/28	02:42
10	TraceX	M01-TM-05-D	TraceX	19/07/28	02:44
11	CPUT	M01-CPUT-01-D	CPUT	19/07/28	02:52

12	CPUT	M01-CPUT-02-D	CPUT	19/07/28	02:55
13	CT	M01-CT-01-D	UCT PERG	19/07/28	02:59
14	CT	M01-CT-02-D	UCT PERG	19/07/28	03:02
15	US	M01-US-01-D	UCT PERG	19/07/28	03:07
16	US	M01-US-02-D	UCT PERG	19/07/28	03:11
17	US	M01-US-03-D	UCT PERG	19/07/28	03:14
18	CP	M01-CP-01-D	UCT PERG	19/07/28	03:19
19	CP	M01-CP-02-D	UCT PERG	19/07/28	03:20
20	DE	M01-DE-01-D	DE	19/07/28	03:22
21	DE	M01-DE-02-D	DE	19/07/28	03:26
22	DE	M01-DE-03-D	DE	19/07/28	03:30
23	CPUT	M01-CPUT-03-D	CPUT	19/07/28	03:35

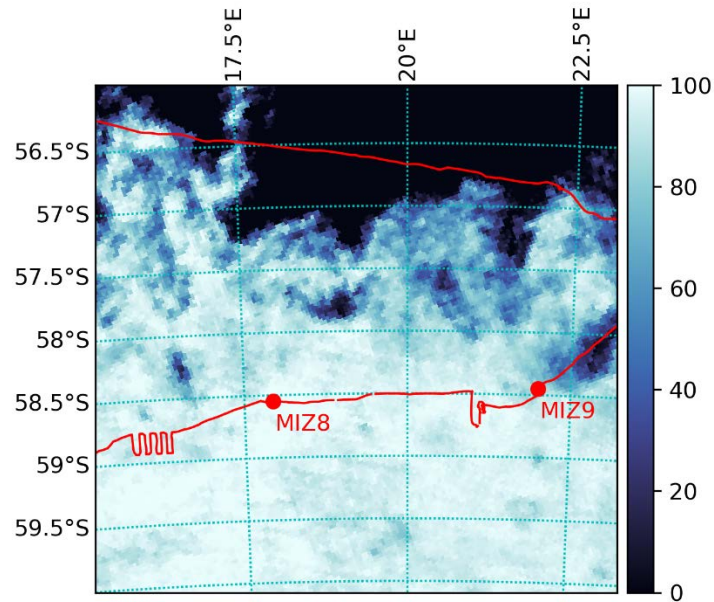


Figure 13.17 Top: AMSR2 sea ice concentration from 1<sup>st</sup> November 2019 (date of SMIZ8). Bottom: sea ice conditions at MIZ8 during the floe lifting operations

## ***Spring cruise***

Spring station SMIZ1 was planned to be a floe lifting station. Due to the open draft conditions, the sea state was rough and did not allow for any sample collection. After a few attempts, the station was abandoned. Lifting operations were done at Stations SMIZ8 and SMIZ9, with conditions as shown in Figure 13.17.

All equipment was set up before station opening. One ice team lead on bridge, one on deck. Ice field was selected from the bridge, individual floes were selected from deck with consultation with the bridge.

The typical sequence was as following. Once each floe is selected, it is brought on deck via net attached to the helideck aft crane. Once on deck, floe is removed from net and coring begins. Cores are subsequently taken to polar lab or freezers. A new floe is brought on deck after temperature cores are extracted from current floe. Once coring operations are concluded the station is closed, the deck is cleared of equipment, and floes are strapped to the deck. Floes are removed once they have melted and are easily moved from beams. At the completion of the lifting stations the beams were removed from deck and stored in helihangar.

Two floes were collected at SMIZ8 and 1 floe at SMIZ 9. Their features indicated the melting conditions, with presence of discoloration just below the freeboard as shown in Figure 13.18. The features, dimensions and collected cores are listed in Figure 13.19.



Figure 13.18 Floe B collected at SMIZ8

Date	01/11/2019	Pancake Dimensions							
		Snow Depth	10 cm	Length	2,4 m	Height	45 cm	Width	
<b>Core ID</b>	<b>Core Name</b>	<b>Pancake Sketch</b>							
1	DE-03A								
2	PHY-01A								
3	PHY-02A								
4	US-25A								
5	US-26A								
6	MRI-09A								
7	US-27A								
8	CT-17A								
9	CT-18A								
10	CP-09A								
11	DE-02A								
12	DE-01A								
13	PER-01A								
14	DMS-01								
15	PER-02A								

Date	01/11/2019	Pancake Dimensions									
		Snow Depth	10,6 cm	Length	2,22 m	Width	170 cm	Port Height	81 cm	Staboard Height	73 cm
<b>Core ID</b>	<b>Core Name</b>	<b>Pancake Sketch</b>									
1	PHY-01B										
2	INC-01B										
3	NTS-01B										
4	NTS-02B										
5	PHY-02B										
6	NTS-03B										
7	BGC-50A										
8	MRI-10D										
9	PHY-03B										
10	BGC-49A										
11	RUAN-01B										
12	RUAN-02B										
13	CPUT-01B										
14	CPUT-02B										
Riesna Box	7D										

Date	03/11/2019	Pancake Dimensions									
		Snow Depth	5,5 cm	Length	3,9 m	Width	2,7 m	Port Height	50 cm	Staboard Height	50 cm
<b>Core ID</b>	<b>Core Name</b>	<b>Pancake Sketch</b>									
1	PHY-01A										
2	DE-01A										
3	NTS-01A										
4	PHY-02A										
5	DE-02A										
6	DE-03A										
7	PHY-02A										
8	NTS-02A										
9	INC-01A										
10	CMP-28A										
11	CMP-29A										
12	CMP-30A										
13	MRI-01A										
14	CT-01A										
15	CT-02A										
16	CP-01A										
17	CMP-01A										
18	CMP-02A										
19	DMS-02A										
20	PER-02A										
21	PER-01A										
22	BGC-59A										
23	BGC-57A										
24	DMS-01A										

Figure 13.19 Features and cores extracted from floes A, B (SMIZ8 01/11) and C (SMIZ9, 03/11)

### 13.4. Ice-tethered buoys

*PI: A/Prof Amit Mishra, A/Prof Marcello Vichi*

*Winter cruise members: Robyn Verrinder (leader), Jaimie Jacobson, Ehlke de Jong*

*Spring cruise members: Justin Pead (leader), Kelsey Kaplan*

This task is a collaboration between a few national and international projects to develop a series of low-cost autonomous devices for measuring sea ice properties in the MIZ. The ice-tethered buoys are designed to be expendable and easily manufactured in South Africa, which poses major challenges in terms of the reliability of some components. The project code name is Southern Hemisphere Antarctic Research Collaborative (SHARC).

#### **Winter cruise**

Six SHARC buoys and tripods were produced by the Department of Electrical Engineering and Department of Oceanography, UCT for potential deployment during the 2019 SCALE Winter Cruise at three stations in the marginal ice zone (MIZ1, MIZ2 and MIZ3). However, during onboard testing the buoy's boost converter, used in the power supply circuit, was found to have stability problems and it was then decided only to deploy two buoys in the Marginal Ice Zone. One buoy at MIZ1S (2019-WC-SB01) and the other at MIZ2N (2019-WCSB02) using alternative power supply methods (off-the-self rechargeable Li-ion battery pack with 5 V, 2 A output (2019-WC-SB01) and direct connection from the output of the 3.6 V Lithium Thionyl Chloride battery pack (2019-WC-SB02)). An additional buoy (2019-WC-SB03) was configured using the same settings as 2019-WC-SB02 and deployed onboard the SA Agulhas II's helideck for continuous testing for the duration of the voyage from MIZ1N to East London.

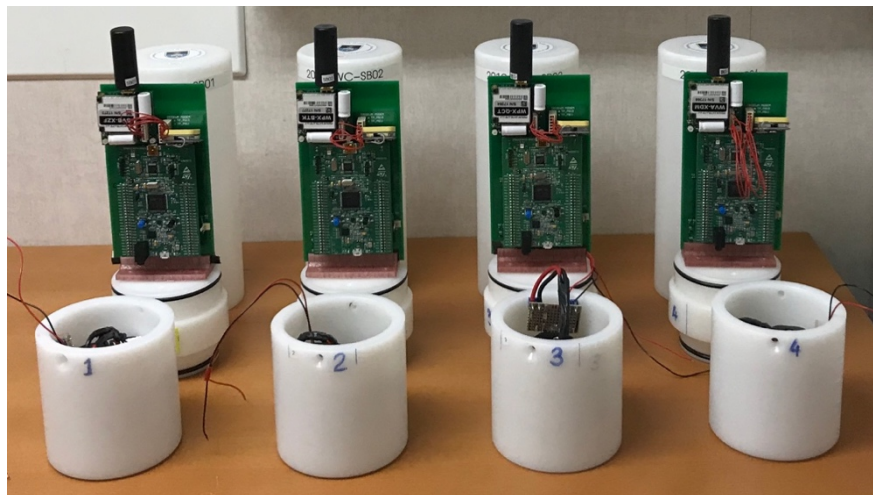


Figure 13.20 Four SHARC buoys showing the internal electronics and external enclosure

Before deployment each SHARC buoy was configured and tested on board the ship in the Electronics Laboratory to ensure correct operation. This included configuring the uBlox NEO 7M GPS sensor in uCentre v1.6 (uBlox) with the following configuration settings:

- Communication: UART; 115200 baud; 8-bit; 1 stop bit; no parity; LSB first
- Message: NMEA message type; GLL (coordinates); GSA (diagnostics); ZDA (time and date)
- Model configuration: Dynamic model (sea); 2D fixed mode; minimum of three satellites maximum of six.

The Iridium modem was tested (UART; 19200 baud; 8-bit; 1 stop; no parity; LSB first). The Buoy firmware was reloaded onto the device and the batteries and power supply were then connected to the buoy. Buoys were configured to record GPS data every 30 minutes and transmit data via the Iridium Modem link after four successive GPS readings (every two hours). LEDs onboard the buoy were used to visually check that each subsystem was working as expected. Once it was established that the buoy's electronics were working correctly, they were securely fastened in the buoy enclosure and each enclosure was mounted and fastened to the cradle in the tripod ready for deployment.

Three team members were used to deploy the buoys on suitably sized ice pancakes from the crane operated personnel basket. Buoy tripods were placed on the personnel basket on deck (Figure 2b) and the basket was then lowered from the side of the ship. Suitable ice pancakes were visually identified by team members on the basket and had to be large enough (> 2 m diameter) enough to support the buoy tripod. Once a suitable pancake had been identified, the buoy and tripod were manually deployed from the crane operated basket and positioned in the centre of the selected ice pancake. The tripod was attached to the ice via four pins. The GPS position, environmental and ship conditions were recorded from the ships bridge at the time of deployment.

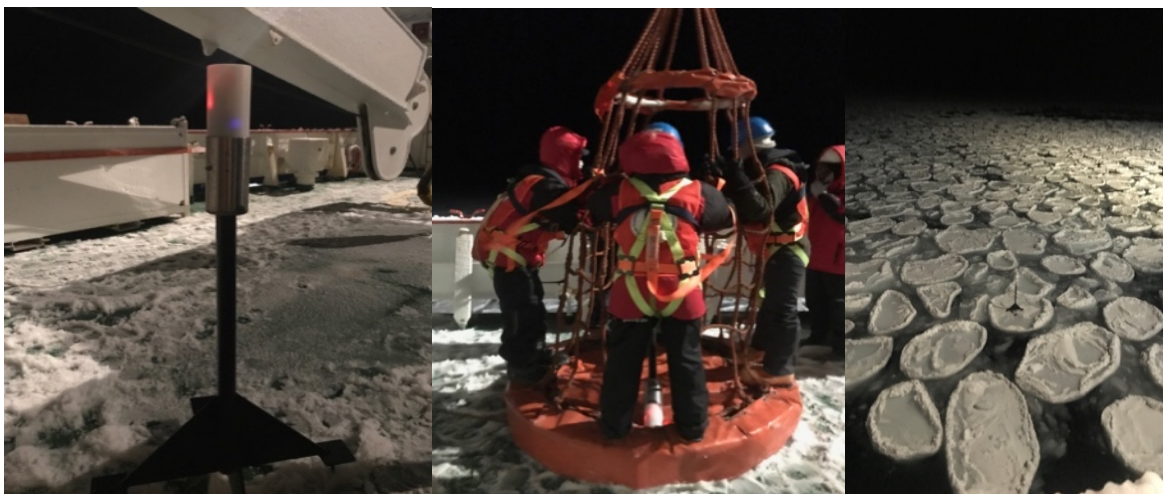


Figure 13.21 Left: SHARC buoy SB01 in the enclosure and tripod ready for deployment. Centre: SHARC buoy and team on personnel basket for deployment at station MIZ1A. Right: SB01 after deployment on a pancake ice floe.

Buoy 2019-WC-SB01 was deployed at MIZ1A. After tethering, it transmitted one message via the Iridium satellite network before communication with the buoy was lost. A second attempt was done at MIZ2A. Buoy 2019-WC-SB02 did not communicate with the Iridium satellite network once it was deployed. It is believed that the buoy may

have been damaged during deployment and stopped working. Deployments were suspended to save the components and improve the design.

### **Spring Cruise**

The buoys were re-assembled for the cruise, but the short period between the two legs did not allow to finalize the operations. A few components needed to be completed while on board, and this generated an issue with the proper establishment of the GPS links. A series of other issues affected the power system. Despite all efforts of the land team members Verrinder and Jacobson who prepared various firmware versions, the system was not sufficiently reliable to be deployed. SHARC buoys were thus not utilized during the spring cruise. To complement the other buoys deployed by SAWS and the Gothenburg University, we deployed one Trident tracker that was successfully used in the 2017 cruise.

### **13.5. Frazil ice**

*PI: Sebastian Skatulla, Jörg Schröder, Doru Lupascu*

*Winter cruise members: Felix Paul (team leader), Mark Hambrock, Tommy Mielke, Carina Nisters, Jörg Schröder*

This was the first time that frazil ice viscosity was measured in situ. Other in situ activities focus more on the thermodynamic properties of frazil ice by means of an instrument called frazilometer, but the mechanical properties of the frazil ice are largely unknown. This work was a joint activity with the University of Duisburg-Essen.

The Frazil sampler (Figure 13.22) is an ad-hoc instrument designed and manufactured by the German team. It is lowered from the A-frame using the smaller plankton net winch. By means of a system of pulley it closes the bottom and captures the upper portion of the water containing the floating frazil ice. The system demonstrated acceptable perturbation to the sample.

All operations took place in the environmental hangar, and frazil sampling was always the first activity at the station. Water was very calm during all stations. The ship propeller was switched off before arriving at the station and the keel was left to glide over ice for a while until complete stop. This manoeuvre minimized the impact to the interstitial ice. A gap between pancake ice floes was then identified and the A-frame was directed on top of the gap to allow for a vertical entry.

The following instruments were used:

1. Frazil sampler
2. Thermometer
3. Ruler
4. Rheometer
5. Sheet
6. Scale
7. Different boxes to measure the volumes

We mainly tested the viscosity of frazil ice in the top layer. Further we took the temperature, salinity and weight of frazil ice and water. The physical and mechanical property were tested with different devices. The viscosity was measured with a rheometer (eBTV Rheometer, Figure 13.23) inside the frazil sampler. The temperature was tested with the GMH 3750 and GTF 401. The weight of the frazil ice was measured by releasing the ice into the filtering sheet and hanging it from the scale.



Figure 13.22 Example of operations with the frazil sampler

Samples were collected at the following stations:

- Session/Station: MIZ1s: 26.07.2019 17:23:00 to 18:16:00
  - 3 samples of frazil ice were taken out of the water
  - 2 measurements were made per sample, except for the last sample
  - Dimensions and weights can be seen on the excel file
- Session/Station-name: MIZ2: 27.07.2019 21:35:00 to 22:33:00
  - 6 samples of frazil ice were taken out of the water
  - 2 measurements were made per sample
  - Dimensions and weights can be seen on the excel file
- Session/Station-name: MIZ1n: 28.07.2019 15:01:00 to 15:30:00
  - 3 samples of frazil ice were taken out of the water
  - 2 measurements were made per sample
  - Dimensions and weights can be seen on the excel file

The operation with the team went well. The ship crew was very helpful. For the next time the sheet to drain the water must be prepared against freezing. Instead of the sheet a sieve could also be used.

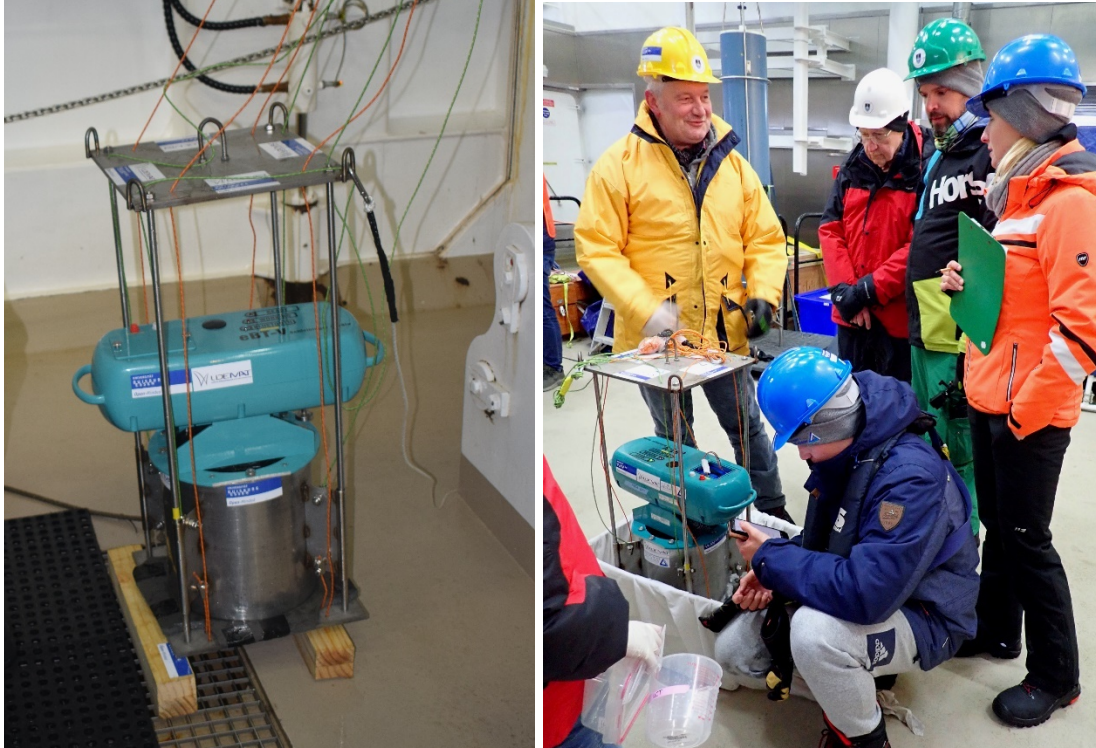


Figure 13.23 The rheometer inserted into the frazil sampler and during the operation with the filtering sheet.

### 13.6. Compression test

*PI: Sebastian Skatulla, Jörg Schröder*

*Winter cruise members: Tommy Mielke (team leader), Felix Paul, Jörg Schröder*

*Spring cruise members: Felix Paul*

Cores were brought to the polar laboratory for the compression test. The length of the cores were measured with a tape measure and photos were taken. It was decided and noted how to cut the cores into samples. Most of the samples were cut into 3-4 samples. The bandsaw operator and an assistant cut the samples in 13.5 cm long pieces. Length of the samples was checked with the folding ruler. Samples were placed in the uniaxial GCTS Compression Test (Figure 13.24). A stopwatch was used to apply the force uniformly. The device was connected to a smartphone which showed the results from the compression test (Figure 13.25). All samples were photographed after the test.



Figure 13.24 The sample in the GCTS machine and after the test completion

The table below summarizes the processed samples

<p>Session/Station: MIZ3</p> <ul style="list-style-type: none"> <li>▪ 3 cores per cluster/pancake</li> <li>▪ Core numbers: M03-DE-01-A; M03-DE-02-A; M03-DE-03-A</li> <li>▪ 8 specimens tested</li> <li>▪ Specimen numbers: M03-DE-01-A-C; M03-DE-01-A-D; M03-DE-01-A-G; M03-DE-01-A-H M03-DE-02-A-E; M03-DE-03-A-C; M03-DE-03-A-H; M03-DE-03-A-I</li> <li>▪ Dimensions of specimen: d: 90 mm ; h: 133-135 mm</li> </ul>	<p>Session/Station: MIZ1n</p> <ul style="list-style-type: none"> <li>▪ 3 cores per pancake (12 cores)</li> <li>▪ Core numbers: M01-DE-01-A; M01-DE-02-A; M01-DE-03-A M01-DE-01-B; M01-DE-02-B; M01-DE-03-B M01-DE-01-C; M01-DE-02-C; M01-DE-03-C M01-DE-01-D; M01-DE-02-D; M01-DE-03-D</li> <li>▪ 19 specimens tested</li> <li>▪ Specimen numbers: M01-DE-01-A-C; M01-DE-02-A-C; M01-DE-03-A-C; M01-DE-01-B-C M01-DE-01-B-D; M01-DE-02-B-A; M01-DE-02-B-B; M01-DE-03-B-A M01-DE-03-B-B; M01-DE-01-C-C; M01-DE-01-C-D; M01-DE-02-C-A M01-DE-02-C-B; M01-DE-03-C-A; M01-DE-03-C-B; M01-DE-01-D-A M01-DE-01-D-B; M01-DE-02-D-A; M01-DE-03-D-A</li> <li>▪ Dimensions of specimen: d: 90 mm ; h: 133-135 mm</li> </ul>
--	---

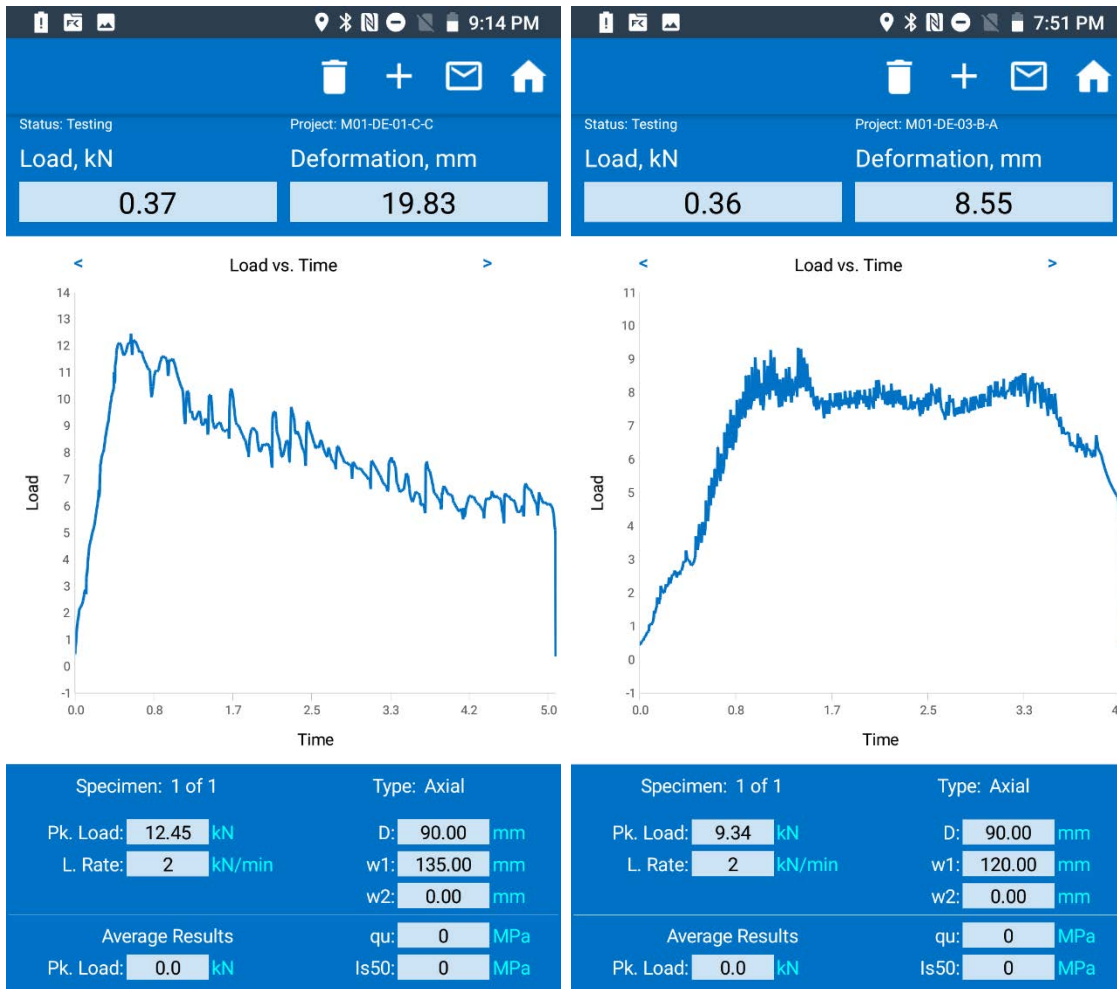


Figure 13.25 Example of compression test results for two different cores from MIZ1. The second sample shows a much smaller deformation indicating larger compaction

### Spring cruise

The methodology was identical to the winter cruise. The higher number of stations and the lower number of people processing the samples put a considerable strain on the testing operations.

The table below reports all the collected samples.

<p>Session/Station SMIZ0:</p> <ol style="list-style-type: none"> <li>Number of cores: 1 core from lifted floe (test).</li> <li>Number of samples tested: 3 samples tested.</li> <li>Core/frazil sample description (dimension, condition): Length: 51 cm</li> <li>Core/frazil specimens (number, type): MIZ0-DE-TE51</li> </ol>	<p>Session/Station-name: SMIZ2</p> <ol style="list-style-type: none"> <li>Number of cores: 3 cores from consolidated ice.</li> <li>Number of samples tested: 9 samples tested.</li> <li>Core/frazil sample description (dimension, condition): Length: 52 cm Length: 56 cm Length: 53 cm</li> </ol>
---	---

	4. Core/frazil specimens (number, type): SMIZ2-DE-07, SMIZ2-DE-08, SMIZ2-DE-09
<p>Session/Station SMIZ3:</p> <p>1. Number of cores: 3 cores from consolidated ice.</p> <p>2. Number of samples tested: 13 samples tested.</p> <p>3. Core/frazil sample description (dimension, condition): Length: 60 cm Length: 78 cm Length: 81 cm</p> <p>4. Core/frazil specimens (number, type): SMIZ3-DE-01, SMIZ3-DE-02, SMIZ3-DE-03</p>	<p>Session/Station SMIZ4.1:</p> <p>1. Number of cores: 2 cores from consolidated ice.</p> <p>2. Number of samples tested: 7 samples tested.</p> <p>3. Core/frazil sample description (dimension, condition): Length: 60 cm Length: 86 cm</p> <p>4. Core/frazil specimens (number, type): SMIZ4.1-DE-security, SMIZ4.1-DE-01</p>
<p>Session/Station SMIZ4.2:</p> <p>1. Number of cores: 2. 4 cores from consolidated ice.</p> <p>3. Number of samples tested: 12 samples tested.</p> <p>4. Core/frazil sample description (dimension, condition): Length: 58 cm Length: 61 cm Length: 60 cm Length: 58 cm</p> <p>5. Core/frazil specimens (number, type): SMIZ4.2-DE-00 SMIZ4.2-DE-01 SMIZ4.2-DE-02 SMIZ4.2-DE-03</p>	<p>Session/Station SMIZ7:</p> <p>1. Number of cores: 3 cores from consolidated ice.</p> <p>2. Number of samples tested: 10 samples tested.</p> <p>3. Core/frazil sample description (dimension, condition): Length: 70 cm Length: 65 cm Length: 75 cm</p> <p>4. Core/frazil specimens (number, type): SMIZ7-DE-01 SMIZ7-DE-02 SMIZ7-DE-03</p>
<p>Session/Station SMIZ8:</p> <p>1. Number of cores: 5 pancake cores.</p> <p>2. Number of samples tested: 12 samples tested.</p> <p>3. Core/frazil sample description (dimension, condition): Length: 45 cm Length: 46 cm Length: 47 cm Length: 84 cm Length: 80 cm</p> <p>4. Core/frazil specimens (number, type): MIZ8-DE-01A, MIZ8-DE-02A, MIZ8-DE-03A, MIZ8-DE-01B, MIZ8-DE-02B</p>	<p>Session/Station SMIZ9:</p> <p>1. Number of cores: 3 pancake cores.</p> <p>2. Number of samples tested: 6 samples tested.</p> <p>3. Core/frazil sample description (dimension, condition): Length: 63 cm Length: 53 cm Length: 59 cm</p> <p>4. Core/frazil specimens (number, type): MIZ9-DE-01A, MIZ9-DE-02A, MIZ9-DE-03A</p>

### 13.7. Ultrasound test

*PI: Sebastian Skatulla, Keith MacHutchon*

*Winter cruise members: Rutger Marquart, Siobhan Johnson, Andrea Cook and Keith MacHutchon*

Non-destructive measurement of the elastic modulus of transverse isotropic ice was carried out using ultrasound techniques. Ultrasound measurements were conducted using a Proceq Ultrasound Testing Unit, which employs S and P waves to find the different elastic modulus of the sample in longitudinal and transverse direction. For this the samples needed to be cut such that it had two flat parallel faces in longitudinal and transverse direction, respectively. Sample preparation and testing was conducted at  $-10^{\circ}\text{C}$  in the mobile polar laboratory. The start of the test was initiated on the device interface and the resulting waves appeared on-screen. The resulting image was saved, and the test stopped. Each of the test results were downloaded later to find the P and S waves and their respective velocities. Using the installed Proceq software, the P and S wave arrival time and velocities were found by selecting the point at which these waves are first detected. The corresponding time and velocity of each wave was then subsequently used to calculate the transverse isotropic elastic moduli and shear moduli. Once a sample has been tested, it was cut into three equal sections and each section was tested again in the same way to obtain an indication of the longitudinal variability.

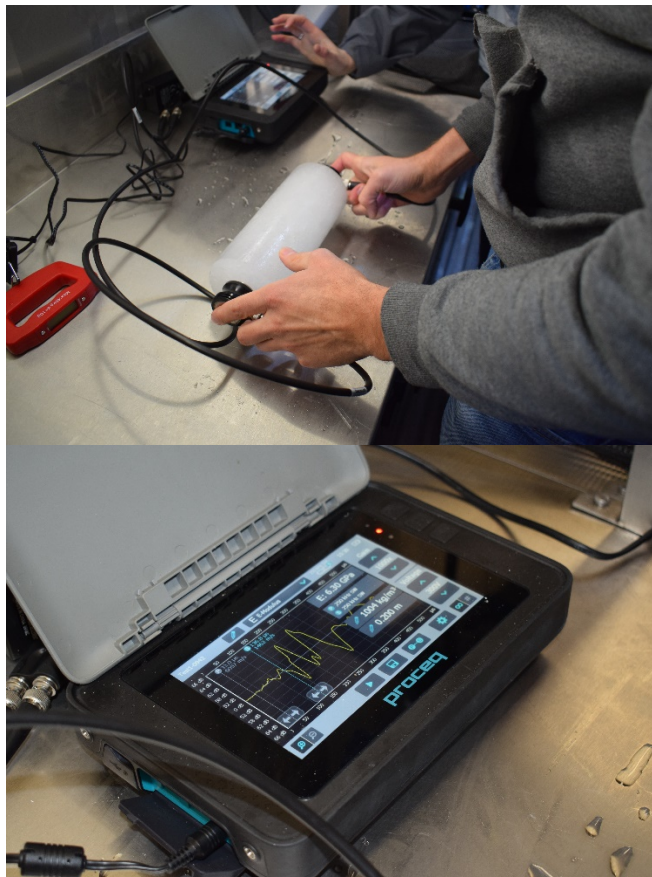


Figure 13.26 The sample is cut to size and then tested with ultrasound to measure the elasticity

The following aspects should be considered in the future:

- Cores broke during coring, and so planned segment sizes had to be adapted.
- Motion of the ship in MIZ1 timeslot 2 made weight measurements difficult. This affects the density calculation of the core. A better scale is required.
- Processing of the cores could not be done immediately due to processing the physical cores first.
- We have been able to process all necessary cores within 24 hours.
- The use of the band saw resulted in flat surface cuts in minimal time.
- All obtained results are relative values, no absolute values.
- We should additionally test the ice samples with a specialized shear-wave transducer, as the used combined transducer made is sometimes difficult to identify the start of the S-wave.

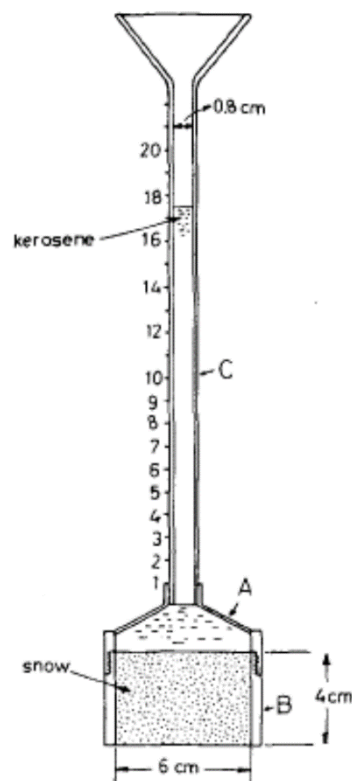


Figure 13.27 Schematic of the Falling Head Permeability Test [Kuroiwa 1967] and the permeability testing prototype used on the ship.

### 13.8. Permeability

PI: Sebastian Skatulla

Spring cruise members: Rutger Marquart, Hasham Taujoo

As part of a BSc Honours project, a sea ice permeability testing prototype was designed and subsequently used in form of a feasibility study during the cruise. The design was based on the so-called “Falling Head Permeability test” as shown in Figure

13.1 which makes use of the continuity equation equating the volume of the falling liquid head to that entering the specimen. Since the experiment will be performed on ice specimens, water cannot be used as the measuring fluid as it will either freeze or melt the sample. A suitable fluid is kerosene which has a freezing point of  $-40^{\circ}\text{C}$  and its kinematic viscosity is similar to that of brine for the range of temperature in which the experiment is meant to take place. Furthermore, brine and salts are insoluble in kerosene so that it could be reused for subsequent testing.

The equipment (Figure 13.27) consists of an 8 mm ID Perspex pipe, 110 mm to 50 mm PVC pipe reducer, adaptor from the Perspex pipe to the 50 mm end of the reducer, custom silicon sleeve, band saw, kerosene, retort stand with clamps, stopwatch, marker, bucket, 2x funnels. The ice core was cut in several samples along the length of the core, with following dimensions: 4.5 mm x 4.5 mm x 5.5 mm and placed in the silicon sleeve as depicted in Figure 13.28. The following experiment is performed on Deck 3, because kerosene is too hazardous to be used inside the Mobile Polar Lab.

This operation is done on Deck 3. Each sample is placed in the silicon sleeve. The sleeve is placed in the apparatus, which is subsequently filled with kerosene. The head is measured once the stopwatch is started and after 120 s both the height of the kerosene in the pipe at the start and end of the experiment is logged.

Ambient temperature was approximately  $-7.2^{\circ}$ ,  $-3.1^{\circ}$  and  $-5.3^{\circ}$  on the 24th, 25th and 26th, respectively, while doing the experiment. The ship was slowly moving in the ice, no waves and therefore no rigid body motions of the ship.

Albeit, successful permeability measurements were taken, the following issues were noticed:

- In contrast to consolidated ice, pancake ice has a very high permeability so that the methodology had to be changed from fixed time to fixed height.
- It was not clear how much air voids in the ice specimen influenced the measured permeability, as it allows for free flow of the fluid for the length of the void.
- The sample slipped out of the silicon sleeve and had to be additionally fixed with a nylon cord.
- The cold temperature made the silicon sleeve brittle so that mounting of the ice continuously damaged the sleeve over time until it would not properly seal anymore.
- The outside experiment made controlled temperature conditions impossible.

### References

Kuroiwa, D. 1967. Liquid Permeability of Snow. Hokkaido University

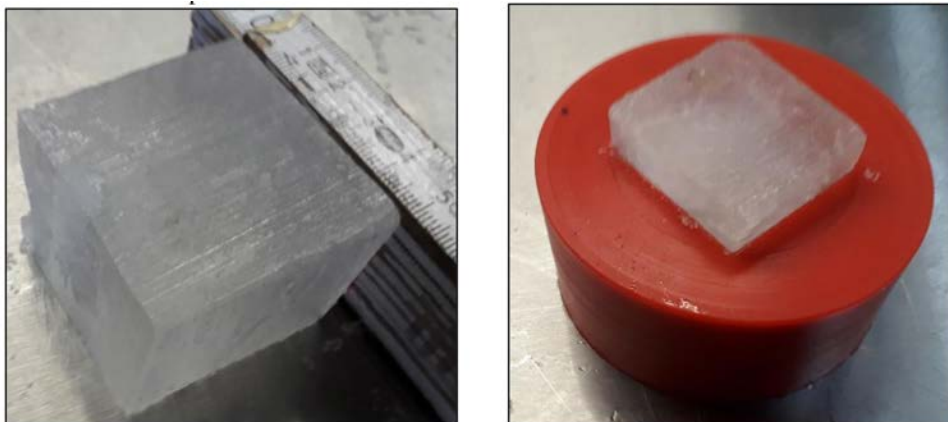


Figure 13.28 Processed ice sample after cutting operations and sample in silicon sleeve

### 13.9. Crystallography

*PI: Keith MacHutchon, Tokoloho Rampai*

*Winter cruise members: Siobhan Johnson, Carina Nisters*

This task is meant to measure the crystal structure and ice morphology by means of cross-polarization techniques. It was conducted on samples of frazil ice and ice cores. At station MIZ1 the frazil was collected by means of the purposely designed frazil sampler, developed by the University of Duisberg-Essen in Germany. The sample was immediately taken into the Mobile Polar Laboratory (MPL) where it was thinly spread onto a glass slide at -10 deg. C and imaged between two sheets of polarised paper. The frazil slide was then stored in the laboratory in a specimen slide rack, for later ongoing analysis. Images of the crystal morphology are shown below in Figure 13.29

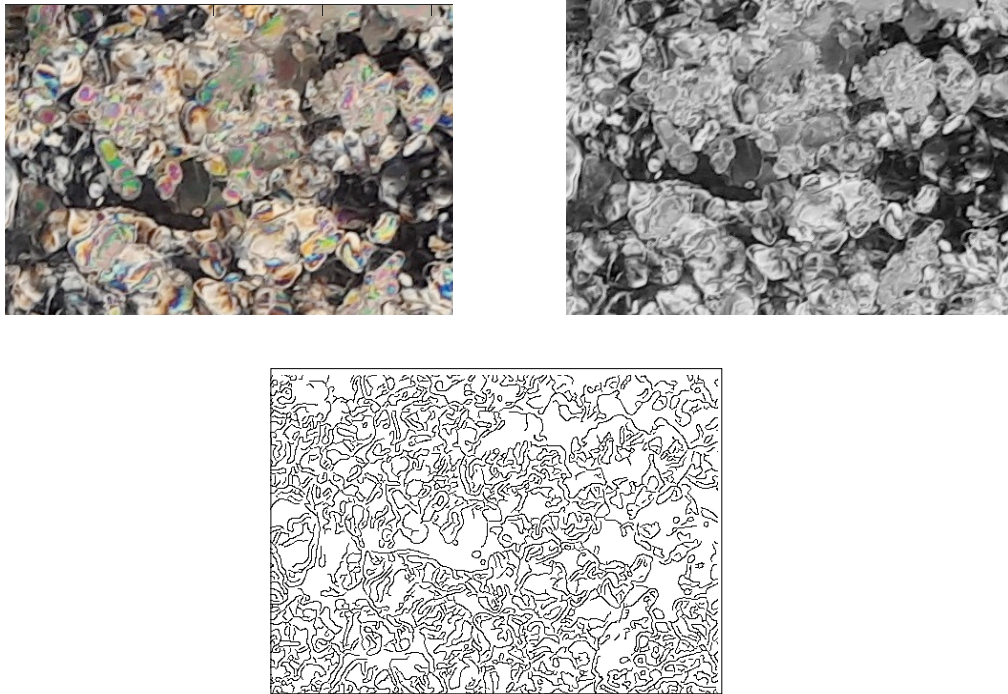


Figure 13.29 Colour image of typical frazil crystals (top left), grayscale image (top right), outlines of frazil crystal edges (bottom)

The frazil that was collected at MIZ 2 was imaged, analysed and stored for later ongoing analysis as described above. A colour image of the frazil crystals has been shown together with a black and white image and crystal edge images in Figure 13.30.

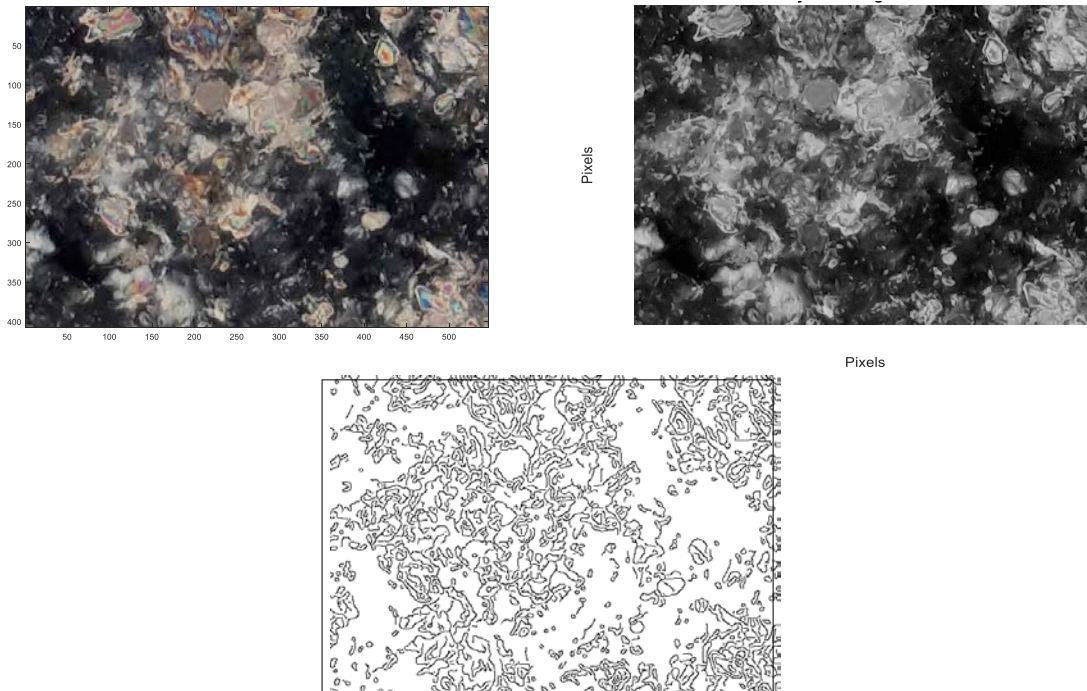


Figure 13.30 Colour image of frazil crystals from MIZ2 (top left), grayscale image (top right left), outlines of frazil crystal edges (bottom)

A full height thick section was cut from one of two ice cores at MIZ3, collected from a floe consisting of cemented pancake ice with a plane area of some 60.0 m by 40.0 m. The section was imaged and analysed on 27th July 2019, and cut sections of this core were stored together with the second core in a freezer at -20 deg C. for later thick and thin sectioning, imaging and analysis on campus at the University of Cape Town. Images of the thick section core are shown in Figure 13.30.

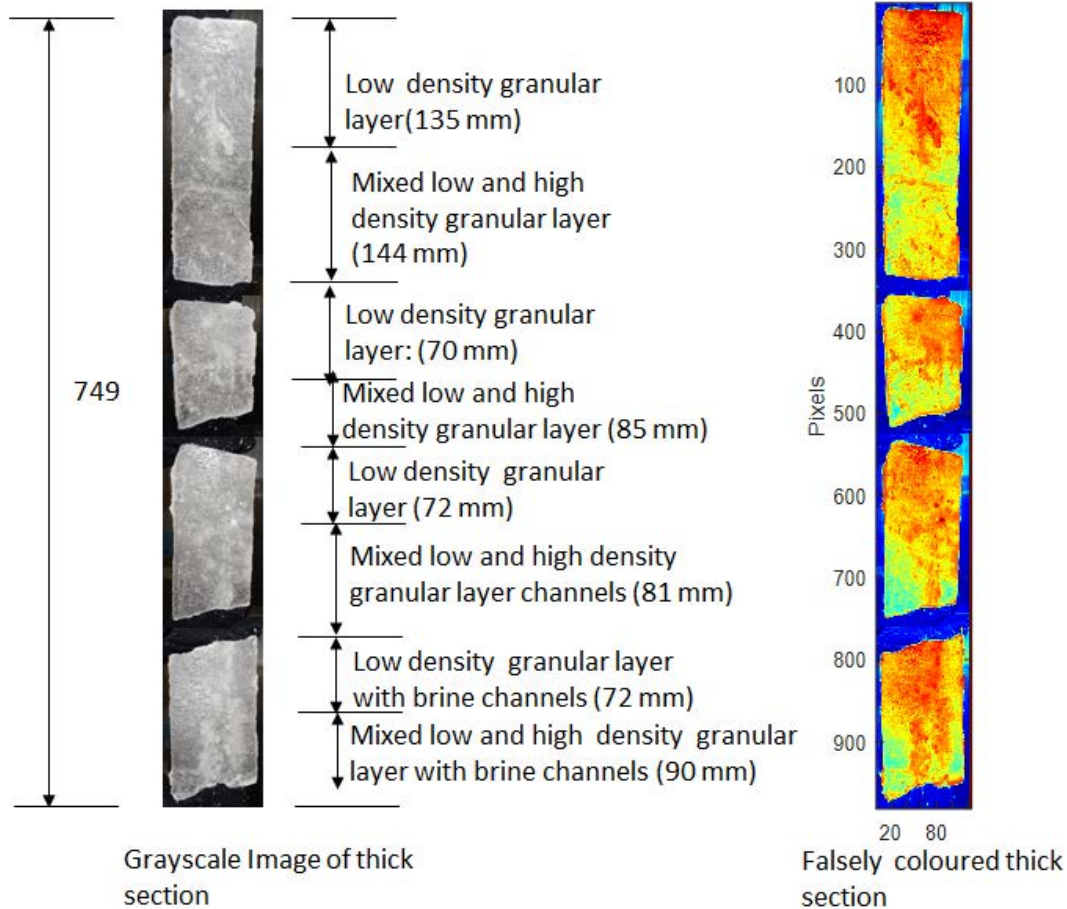


Figure 13.31 Images of thick section core analysed on the 27th July 2019,

MIZ 1):

Imaging and analysis of a full height thick section cores cut from pancake ice samples on deck. The pancakes were lifted from the sea by means purpose designed equipment developed in the Civil Engineering Department at University of Cape Town Full height thick section, cut from two of six ice cores collected from the individual pancake ice samples, were imaged and analysed on 28 and 31st July 2019. The cut sections of each core were stored together with the other four cores in a freezer at -20 deg C. for later thick and thin sectioning, imaging and analysis on campus at the University of Cape Town. Images of the thick section core that was analysed on are shown in figure 4.

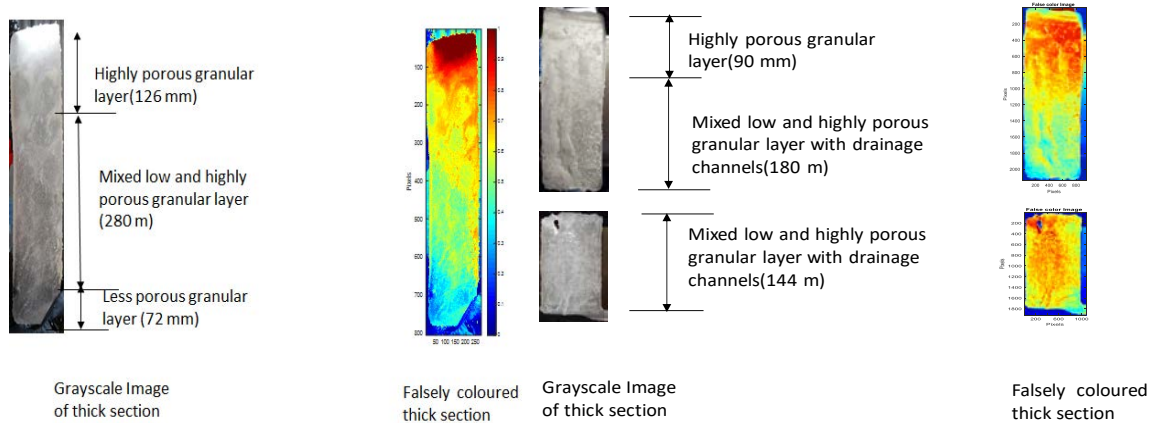


Figure 13.32 Images of thick section core analysed on the 28th July 2019 (left), and 31 July 2019 (right), showing fabric texture details

#### Summary:

- The frazil ice crystals and thick section samples that were processed were all imaged and analysed in the mobile polar laboratory at -10 deg C.
- The thick sections that were analysed were cut from the ice core samples with a stainless-steel circular saw.
- The frazil images were imaged between polarized paper
- The thick sections were imaged with either (i) normal laboratory lighting, or (ii) conventional undershelf strip lighting backgrounds.
- The visual features in the thick sections comprised a range on granular ice densities, brine concentrations, brine channels, clear ice and gas (air) bubbles.
- A light box, polarized paper and a tripod and digital camera was used for the imaging.
- Post processing of the images was carried out using MATLAB Software
- Ice fabric details as well as brine concentrations and channels were identified and analysed

#### Future improvements

The collection and analysing of the frazil went well, but it was difficult to spread the crystals in a thin enough section on the glass slides for optimal birefringence analysis. The slides are stored in the mobile polar laboratory and will continue to be analysed on campus.

The cutting and analysis of the full height thick sections of the cores went well with some meaningful results

The analysis of the proposed thin sections was postponed, and will be done on campus at University of Cape town when a microtome will be available for the preparation of the slides.

SCALE Winter cruise. Abridged ASPeCt datasheet															
time	date	Lat	Lon	TC	c1	ty1	z1	f1	c2	ty2	z2	f2	c3	ty3	z3
13	2019/07/26	56 22.125	000 13.259 E	0											
14	2019/07/26	56 36.309	000 08.391 E	10	6	30		100	2	90		300	2	12	
15	2019/07/26	56 49.849	000 03.684 E	3	3	30		100							
16	2019/07/26	57 00.004	000 00.189 W	10	8	30		100	1	10			1	90	
23	2019/07/26	56 59.915	000 00.907 E	10	1	30		100							
1	2019/07/27	57 06.340	000 00.824 W	10	9	30		100							
2	2019/07/27	57 09.615	000 00.272 E	0											
3	2019/07/27	57 15.776	000 00.173 E	10	9	30		100	1	10					
4	2019/07/27	57 21.885	000 00.156 E	10	9	30		100	1	10					
5	2019/07/27	57 27.540	000 00.219 E	9	9	30	30	100							
6	2019/07/27	57 33.539	000 00.057 E	1	60	30	40	500	9	30		400			
7	2019/07/27	57 39.692	000 00.058 W	10	10	30	25	400							
8	2019/07/27	57 47.005	000 00.171 W	9	9	30	35	400							
9	2019/07/27	57 57.840	000 00.517 W	10	9	60	50	600	1	40	0.1	200			
10	2019/07/27	58 07.140	000 00.218 W	10	10	60		700							
17	2019/07/27	57 55.645	000 01.077 W	10	10	60		700							
18	2019/07/27	57 51.207	000 00.884 W	10	10	60		500							
19	2019/07/27	57 44.230	000 00.260 W	8	7	60		500	1	30		400			
20	2019/07/27	57 35.149	000 00.096 W	6	5	60			1	30		400			
21	2019/07/27	57 23.760	000 00.016 E	10	10	30		400							
4	2019/07/28	57 16.431	000 00.526	6	6	30	40	400							
5	2019/07/28	57 10.365	000 00.295	9	8	30		400	1	90		300			
7	2019/07/28	57 03.838	000 04.606	10	10	30	30	400							
9	2019/07/28	56 48.344	000 15.513	8	8	30		400							
14	2019/07/28	56 40.289	000 25.125	10	9	30		400	1	10					
15	2019/07/28	56 40.641	000 27.093	10	9	30		400	1	10					
16	2019/07/28	56 40.491	000 26.958	0											

17	2019/07/28	56 39.755	000 27.044	10	8	30		400	1	10			1	90	
18	2019/07/28	56 36.550	000 26.007	10	1	30		400	7	40		400	2	10	
19	2019/07/28	56 29.546	000 33.285	0											
20	2019/07/28	56 20.901	000 39.657	0											

SCALE Spring cruise. Abridged ASPeCt datasheet

date	time	lat	long	TC	c1	ty1	z1	f1	sz1	bi1	c2	ty2	z2	f2
2019/10/22	8	55 49.421	000 00.138 E	0										
2019/10/22	9	55 59.539	000 00.361 E	0										
2019/10/22	10	55 59.711	000 02.797 E	0										
2019/10/22	11	55 59.099	000 04.940 E	1	1	90								
2019/10/22	12	55 59.389	000 03.759 E	1	1	10								
2019/10/22	13	56 05.821	000 00.841 E	0										
2019/10/22	14	56 14.477	000 00.585 E	3	2	30	20	100			1	90		300
2019/10/22	15	56 15.060	000 03.988 E	4	3	30	20	100			1	90		300
2019/10/22	16	56 13.069	000 05.651 E	0										
2019/10/22	17	56 17.085	000 04.671 E	0										
2019/10/22	18	56 27.217	000 00.628 E	0										
2019/10/22	19	56 36.648	000 00.147 E	10	9	30	30	100	20		1	90		300
2019/10/22	20	56 45.364	000 00.105 E	7	6	30	20	100	40		1	10		
2019/10/22	21	56 52.865	000 00.529 E	10	9	30	40	100	20		1	90		300
2019/10/22	22	57 00.536	000 01.228 E	10	9	30	30	100	20		1	10		
2019/10/22	23	57 07.589	000 00.752 E	10	9	30	30	100	20		1	10		
2019/10/23	0	57 16.129	000 01.113 E	10	9	30	40	100	10		1	10		
2019/10/23	1	57 24.128	000 00.247	10	9	30	40	100	10		1	10		
2019/10/23	2	57 32.834	000 01.422	10	9	90	20	100	10		1	10		
2019/10/23	3	57 36.837	000 00.849	9	8	60	50	400	20		1	90		300
2019/10/23	4	57 43.803	000 00.640	9	8	60	40	400	20		1	90		300
2019/10/23	5	57 51.776	000 00.508	9	8	60	50	400	30		1	90		300
2019/10/23	6	57 56.932	000 00.302	9	8	60	50	500	20		1	90		300
2019/10/23	7	57 59.315	000 00.477	10	10	60	50	500	20					
2019/10/23	8	57 58.221	000 00.532											
2019/10/23	9	57 57.087	000 00.649											
2019/10/23	10	57 55.929	000 00.736											
2019/10/23	11	57 54.735	000 00.784											

2019/10/23	12	57 53.524	000 00.838																
2019/10/23	13	57 58.042	000 00.708																
2019/10/23	14	58 04.252	000 01.352	10	10	60	100	600											
2019/10/23	15	58 09.103	000 00.438	10	10	60	50	500	15										
2019/10/23	16	58 17.552	000 00.049	10	10	60	40	500	20										
2019/10/23	17	58 26.036	000 00.318	10	10	60	40	500	30										
2019/10/23	18	58 34.492	000 01.598	10	10	60	50	500	20										
2019/10/23	19	58 41.567	000 00.208	10	10	60	40	700	30										
2019/10/23	20	58 48.804	000 00.047	10	10	60	40	700	10										
2019/10/23	21	58 52.464	000 00.297 W	6	5	60	30	700	10	1	90								300
2019/10/23	22	58 56.650	000 00.286	10	10	60	80	600	15										
2019/10/23	23	58 59.167	000 00.904 W	10	10	50	50	600	20										
2019/10/24	0	59 02.296	000 00.131 W	10	10	60	70	700	30										
2019/10/24	1	59 05.266	000 00.615	10	10	70	75	700	40										
2019/10/24	2	59 10.160	000 00.252 W	10	10	60	80	700	30										
2019/10/24	3	59 15.331	000 00.527	10	5	60	30	600	20	5	10								
2019/10/24	4	59 20.682	000 00.617	10	10	70	70	700	15										
2019/10/24	5	59 22.372	000 01.086	10	10	60	70	700	25										
2019/10/24	6	59 22.010	000 01.404																
2019/10/24	7	59 21.611	000 01.775																
2019/10/24	8	59 21.207	000 02.196																
2019/10/24	9	59 20.803	000 02.626																
2019/10/24	10	59 20.416	000 03.032																
2019/10/24	11	59 20.065	000 03.406																
2019/10/24	12	59 19.740	000 03.769																
2019/10/24	13	59 19.371	000 04.142																
2019/10/24	14	59 19.083	000 04.527																
2019/10/24	15	59 18.800	000 04.953																
2019/10/24	16	59 18.509	000 05.420																
2019/10/24	17	59 16.877	000 08.882																

2019/10/24	18	59 08.803	000 05.175	10	10	60	30	700						
2019/10/24	19	59 01.399	000 00.930	9	8	60	30	700			1	20		200
2019/10/24	20	58 58.914	000 00.821	9	8	60	60	800			1	20		200
2019/10/24	21	58 58.580	000 01.266											
2019/10/24	22	58 58.273	000 01.655											
2019/10/24	23	58 58.011	000 01.990											
2019/10/25	0	58 57.830	000 02.309											
2019/10/25	1	58 57.699	000 02.692											
2019/10/25	2	58 57.581	000 03.059											
2019/10/25	3	58 57.451	000 03.438											
2019/10/25	4	58 57.281	000 03.873											
2019/10/25	5	58 57.676	000 05.466											
2019/10/25	6	58 57.412	000 06.006											
2019/10/25	7	58 57.111	000 06.552											
2019/10/25	8	58 56.767	000 07.096											
2019/10/25	9	58 56.380	000 07.596											
2019/10/25	10	58 56.005	000 07.987											
2019/10/25	11	58 55.681	000 08.236											
2019/10/25	12	58 55.418	000 08.358											
2019/10/25	13	58 58.191	000 08.553											
2019/10/25	14	59 06.701	000 13.747	9	9	60	60	600	20					
2019/10/25	15	59 13.318	000 13.239	9	9	70	70	700	10					
2019/10/25	16	59 13.176	000 12.874											
2019/10/25	17	59 11.614	000 19.419											
2019/10/25	18	59 08.048	000 31.458	3	3	10	5		30					
2019/10/25	19	59 04.405	000 45.782	4	3	60	50	600	10					
2019/10/25	20	59 00.552	000 57.300	9	9	60	30	600	10					
2019/10/25	21	59 00.439	000 59.522	10	10	60	60	700	20					
2019/10/25	22	59 00.125	000 59.279											
2019/10/25	23	58 59.738	000 58.962											

2019/10/26	0	58 59.289	000 58.442																
2019/10/26	1	58 58.840	000 57.986																
2019/10/26	2	58 58.440	000 57.600																
2019/10/26	3	58 57.948	000 57.135																
2019/10/26	4	58 57.464	000 56.618																
2019/10/26	5	59 01.492	000 59.930																
2019/10/26	6	59 05.055	001 02.024	10	10	60	80	700	20										
2019/10/26	7	59 03.877	001 04.627	10	10	60	80	700	30										
2019/10/26	8	58 58.134	001 04.863	10	10	60	40	700	20										
2019/10/26	9	58 54.899	001 09.373	10	10	60	30	700	20										
2019/10/26	10	58 59.187	001 10.709	0															
2019/10/26	11	59 02.949	001 09.416	10	10	60	40	600	20										
2019/10/26	12	59 03.252	001 15.501	10	10	60	60	700	40										
2019/10/26	13	58 55.877	001 14.819	9	9	70	70	700	10										
2019/10/26	14	58 56.037	001 20.635	10	10	60	60	700	20										
2019/10/26	15	58 59.403	001 20.934	10	10	60	80	800	30										
2019/10/26	16	59 05.670	001 20.492	10	10	60	60	800	30										
2019/10/26	17	59 00.475	001 22.174	10	9	50	10	800	30	1	10								
2019/10/26	18	58 58.082	001 25.036	10	10	60	40	800	30										
2019/10/26	19	58 55.891	001 30.305	10	10	60	40	800	20										
2019/10/26	20	59 01.193	001 34.515	9	8	60	30	800	20	1	20								200
2019/10/26	21	59 00.624	001 43.184	9	9	60	40	800	30										
2019/10/26	22	58 59.730	001 47.668	0															
2019/10/26	23	59 00.689	002 02.702	6	5	60	40	800	20	1	10								
2019/10/27	0	59 00.286	002 09.843	10	10	60	50	800	30										
2019/10/27	1	59 01.115	002 27.489	10	10	60	40	600	20										
2019/10/27	2	59 00.051	002 47.100	4	4	60	30	600	10										
2019/10/27	3	59 00.040	003 00.990	10	10	60	40	700	10										
2019/10/27	4	58 59.501	003 01.259																
2019/10/27	5	58 58.927	003 01.420																

2019/10/27	6	58 58.395	003 01.484												
2019/10/27	7	58 59.127	002 58.839												
2019/10/27	8	58 59.361	002 58.685												
2019/10/27	9	58 57.352	003 00.758												
2019/10/27	10	59 00.268	003 10.565	10	10	60	40	500	25						
2019/10/27	11	58 59.025	003 21.481	10	10	60	90	700	30						
2019/10/27	12	58 58.786	003 39.331	8	7	70	10	600	10	1	12			200	
2019/10/27	13	58 59.587	003 54.524	10	7	60	20	700	20	2	40			400	
2019/10/27	14	59 03.639	004 07.707	10	8	60	30	500	30	1	40			400	
2019/10/27	15	59 09.202	004 20.608	9	9	60	20	600							
2019/10/27	16	59 09.055	004 39.180	9	9	50	20	600							
2019/10/27	17	59 13.342	004 55.273	7	7	40	10	600							
2019/10/27	18	59 16.521	005 11.942	7	7	60	20	700							
2019/10/27	19	59 15.899	005 12.645	8	8	60	30	600							
2019/10/27	20	59 17.004	005 19.231	8	8	60	30	600							
2019/10/27	21	59 19.827	005 30.147	9	9	60	40	800							
2019/10/27	22	59 19.193	005 38.074	10	10	60	90	800							
2019/10/27	23	59 17.499	005 47.357	9	9	60	50	800							
2019/10/28	0	59 20.789	006 02.905	10	10	60	100	800	40						
2019/10/28	1	59 22.020	006 12.908	10	10	60	300	100	20						
2019/10/28	2	59 22.740	006 28.920	10	10	60	60	500	25						
2019/10/28	3	59 23.907	006 34.298	10	10	60	50	500	30						
2019/10/28	4	59 23.671	006 34.245	0											
2019/10/28	5	59 23.392	006 34.167												
2019/10/28	6	59 23.054	006 34.100												
2019/10/28	7	59 22.649	006 33.957												
2019/10/28	8	59 22.277	006 34.329												
2019/10/28	9	59 21.753	006 34.373												
2019/10/28	10	59 21.175	006 34.436												
2019/10/28	11	59 20.559	006 37.167												

2019/10/28	12	59 19.870	006 37.089																
2019/10/28	13	59 19.195	006 37.122																
2019/10/28	14	59 18.565	006 37.085																
2019/10/28	15	59 17.951	006 36.945																
2019/10/28	16	59 17.383	006 36.783																
2019/10/28	17	59 16.849	006 36.649																
2019/10/28	18	59 16.317	006 36.516																
2019/10/28	19	59 15.806	006 36.416																
2019/10/28	20	59 15.286	006 36.385																
2019/10/28	21	59 16.582	006 41.425																
2019/10/28	22	59 16.886	006 50.351	10	10	60	30	700	20										
2019/10/28	23	59 19.485	006 59.530	10	10	60	50	700	20										
2019/10/29	0	59 21.702	007 14.834	10	10	60	80	700	20										
2019/10/29	1	59 23.840	007 31.659	10	10	60	50	700	30										
2019/10/29	2	59 26.591	007 47.132	0															
2019/10/29	3	59 27.260	008 05.698	0															
2019/10/29	4	59 26.994	008 08.456	8	7	60	40	700	25						1	90			300
2019/10/29	5	59 26.391	008 08.378	0															
2019/10/29	6	59 25.832	008 08.289	0															
2019/10/29	7	59 25.303	008 08.283	0															
2019/10/29	8	59 24.750	008 08.321	0															
2019/10/29	9	59 24.164	008 08.429	0															
2019/10/29	10	59 23.577	008 08.675	0															
2019/10/29	11	59 22.939	008 09.020	0															
2019/10/29	12	59 22.232	008 09.334	0															
2019/10/29	13	59 21.559	008 09.737	0															
2019/10/29	14	59 20.920	008 10.194	0															
2019/10/29	15	59 20.390	008 10.594	0															
2019/10/29	16	59 19.416	008 10.897	0															
2019/10/29	17	59 21.014	008 28.476	10	9	60	40	700	10						1	20			200

2019/10/29	18	59 23.658	008 42.446	8	7	60	30	600	40		1	20		200
2019/10/29	19	59 24.645	008 51.454	10	10	60	50	800	40					
2019/10/29	20	59 30.558	009 02.528	0										
2019/10/29	21	59 30.476	009 16.419	6	5	50	20	600	10		1	10		
2019/10/29	22	59 30.460	009 28.642	7	50	60	40	500	10		2	50		400
2019/10/29	23	59 30.455	009 38.405	10	10	60	30	700	10					
2019/10/30	0	59 29.888	009 55.850	0										
2019/10/30	1	59 30.098	010 10.373	10	10	60	40	700	30					
2019/10/30	2	59 30.181	010 26.386	0										
2019/10/30	3	59 30.078	010 45.561	8	7	60	30	700	20		1	10		
2019/10/30	4	59 29.757	010 49.242	9	7	60	40	700	30		1	90		300
2019/10/30	5	59 29.531	010 49.446											
2019/10/30	6	59 29.312	010 49.721											
2019/10/30	7	59 29.139	010 50.151											
2019/10/30	8	59 28.955	010 50.703											
2019/10/30	9	59 28.775	010 51.264											
2019/10/30	10	59 28.653	010 51.939											
2019/10/30	11	59 28.518	010 52.702											
2019/10/30	12	59 28.308	010 53.697											
2019/10/30	13	59 28.260	010 54.305											
2019/10/30	14	59 28.183	010 55.008											
2019/10/30	15	59 28.103	010 55.649											
2019/10/30	16	59 28.045	010 56.188											
2019/10/30	17	59 27.367	010 59.359											
2019/10/30	18	59 26.631	011 12.423	10	10	60	80	700	20					
2019/10/30	19	59 25.986	011 22.477	10	10	60	120	700	40					
2019/10/30	20	59 24.898	011 35.000	10	2	70	80	400	20		8	40		600
2019/10/30	21	59 21.360	011 50.295	0										
2019/10/30	22	59 17.373	012 04.588	8	7	60	50	600	10		1	90		300
2019/10/30	23	59 14.940	012 23.682	9	8	60	50	600	10		1	10		

2019/10/31	0	59 13.011	012 41.699	9	9	30	30	100	10					
2019/10/31	1	59 10.552	013 00.667	9	9	30	10	100	20					
2019/10/31	2	59 08.655	013 20.469	10	9	60	30	500	20		1	20		200
2019/10/31	3	59 06.120	013 39.784	10	9	50	30	500	10		1	20		200
2019/10/31	4	59 04.067	013 58.831	9	8	60	40	500	10		1	90		300
2019/10/31	5	59 00.596	014 17.986	7	2	30	20	100	10		5	50		500
2019/10/31	6			9	9	20			10					
2019/10/31	7			10	10	60	60	800	20					
2019/10/31	8			0										
2019/10/31	9	58 46.016	015 41.517	0										
2019/10/31	10	58 54.282	015 45.704	9	9	60	40	500	20					
2019/10/31	11	58 49.052	015 51.500	9	8	60	50	600	10		1	90		300
2019/10/31	12	58 50.195	015 56.539	8	8	30	20	100	10					
2019/10/31	13	58 52.895	016 01.508	9	9	30	20	100	5					
2019/10/31	14	58 46.017	016 06.781	8	7	30	30	100	5		1	10		
2019/10/31	15	58 55.606	016 07.467	10	10	60	35	500	20					
2019/10/31	16	58 47.322	016 11.490	5	5	60	45	500	5					
2019/10/31	17	58 51.957	016 16.620	9	9	60	40	500	10					
2019/10/31	18	58 52.702	016 21.396	9	9	30	30	100	20					
2019/10/31	19	58 45.446	016 27.925	9	9	30	40	100	10					
2019/10/31	20	58 43.555	016 42.517	9	8	30	40	100	20		1	20		200
2019/10/31	21	58 40.719	016 55.568	8	7	60	35	500	15		1	30		100
2019/10/31	22	58 38.524	017 09.203	9	3	60	30	500	10		3	30		100
2019/10/31	23	58 36.125	017 22.220	9	3	30	20	100	10		6	50		400
2019/11/01	0	58 34.155	017 35.133	9	9	30	40	100	20					
2019/11/01	1	58 32.515	017 45.167	10	10	30	40	100	10					
2019/11/01	2	58 32.602	017 45.442											
2019/11/01	3	58 32.694	017 45.890											
2019/11/01	4	58 32.820	017 46.453											
2019/11/01	5	58 32.850	017 47.728											

2019/11/01	6	58 33.037	017 48.616											
2019/11/01	7	58 33.237	017 49.563											
2019/11/01	8	58 33.410	017 50.612											
2019/11/01	9	58 33.605	017 51.771											
2019/11/01	10	58 33.514	017 53.167											
2019/11/01	11	58 33.441	017 54.153											
2019/11/01	12	58 33.264	017 55.273											
2019/11/01	13	58 32.988	017 56.061											
2019/11/01	14	58 32.734	017 56.788											
2019/11/01	15	58 32.539	017 57.330											
2019/11/01	16	58 32.444	017 57.745											
2019/11/01	17	58 32.430	017 58.043											
2019/11/01	18	58 32.530	017 58.305											
2019/11/01	19	58 32.931	018 02.312											
2019/11/01	20	58 33.695	018 13.982	9	9	60	40	400	20					
2019/11/01	21	58 34.132	018 24.584	10	10	60	40	400	20					
2019/11/01	22	58 33.594	018 35.969	9	8	60	40	400	15	1	90			300
2019/11/01	23	58 32.990	018 47.481	8	7	60	50	400	20	1	90			300
2019/11/02	0	58 32.877	019 00.645	9	8	60	30	400	20	1	90			300
2019/11/02	1	58 32.632	019 13.702	10	10	30	30	100	10					
2019/11/02	2	58 30.414	019 26.421	10	9	60	40	400	10	1	90			300
2019/11/02	3	58 30.046	019 39.693	9	9	60	40	400	10					
2019/11/02	4	58 30.100	019 52.856	9	8	60	40	400	20	1	90			300
2019/11/02	5	58 30.230	020 05.768	10	9	60	40	400	10	1	90			300
2019/11/02	6	58 30.033	020 17.606	9	9	30	30	100	20					
2019/11/02	7	58 30.117	020 30.421	9	9	60	40	400	20					
2019/11/02	8	58 29.463	020 43.319	9	9	30	40	100	10					
2019/11/02	9	58 28.968	020 59.256	9	9	30	45	100	10					
2019/11/02	10	58 34.915	020 59.002	10	10	30	50	100	20					
2019/11/02	11	58 41.803	020 59.294	9	7	60	50	400	20	1	90			300

2019/11/02	12	58 45.658	021 04.437	10	10	60	80	400	20					
2019/11/02	13	58 45.797	021 04.181											
2019/11/02	14	58 44.000	021 06.934											
2019/11/02	15	58 39.085	021 07.631	0										
2019/11/02	16	58 33.860	021 06.276	0										
2019/11/02	17	58 35.194	021 10.340	8	8	60	50	400	10					
2019/11/02	18	58 38.282	021 10.085	0										
2019/11/02	19	58 36.759	021 09.420	0										
2019/11/02	20	58 35.239	021 10.791	0										
2019/11/02	21	58 35.986	021 20.002	10	9	60	30	400	10	1	90		300	
2019/11/02	22	58 35.875	021 30.810	10	9	60	40	400	20	1	90		300	
2019/11/02	23	58 35.276	021 40.675	10	9	60	40	400	20					
2019/11/03	0	58 32.995	021 50.340	9	9	60	45	400						
2019/11/03	1	58 29.984	021 59.716	10	10	60	40	400						
2019/11/03	2	58 29.485	022 00.043	0										
2019/11/03	3	58 28.783	021 57.955	0										
2019/11/03	4	58 29.471	021 58.862	0										
2019/11/03	5	58 28.467	021 56.162	0										
2019/11/03	6	58 28.846	021 58.513	0										
2019/11/03	7	58 29.465	022 00.122	0										
2019/11/03	8	58 28.424	021 59.764	0										
2019/11/03	9	58 28.036	021 59.013	0										
2019/11/03	10	58 27.699	021 59.138	0										
2019/11/03	11	58 27.388	021 58.882	0										
2019/11/03	12	58 26.643	021 59.763	0										
2019/11/03	13	58 25.855	021 59.491	0										
2019/11/03	14	58 23.365	022 07.776	0										
2019/11/03	15	58 17.933	022 23.989	0										
2019/11/03	16	58 10.184	022 38.563	0										
2019/11/03	17	58 03.127	022 54.264	9	2	30		100	0	2	90		300	

2019/11/03	18	57 55.757	023 08.947	0										
2019/11/03	19	57 47.452	023 24.833	3	3	30	20	100	10					
2019/11/03	20	57 38.174	023 38.887	0										
2019/11/03	21	57 30.824	023 55.941	10	8	60	40	400	20		2	90		300
2019/11/03	22	57 20.586	023 59.424	10	9	30	50	100	20		1	90		300
2019/11/03	23	57 09.072	024 00.462	0										
2019/11/04	0	57 09.096	023 59.688	0										
2019/11/04	1	57 09.101	023 59.697	0										
2019/11/04	2	57 09.101	023 59.698	0										
2019/11/04	3	57 09.101	023 59.697	0										
2019/11/04	4	57 09.102	023 59.698	0										
2019/11/04	5	57 08.978	023 59.274	0										
2019/11/04	6	57 08.977	023 59.275	0										
2019/11/04	7	57 07.949	023 46.408	0										
2019/11/04	8	57 05.513	023 27.715	0										
2019/11/04	9	57 04.072	023 12.384	0										
2019/11/04	10	57 02.633	022 47.992	0										
2019/11/04	11	56 55.750	022 28.306	0										
2019/11/04	12	56 50.699	022 13.036	10	8	60	40	4	10		2	90		300
2019/11/04	13	56 50.507	022 14.586	0										
2019/11/04	14	56 48.541	021 54.804	0										
2019/11/04	15	56 47.711	021 36.682	10	10	90	60	300	20					
2019/11/04	16	56 46.346	021 17.144	10	10	90	40	300	10					
2019/11/04	17	56 43.275	020 55.103	0										
2019/11/04	18	56 41.628	020 35.401	0										
2019/11/04	19	56 41.010	020 16.168	0										
2019/11/04	20	56 40.145	019 59.461	0										
2019/11/04	21	56 38.305	019 42.503	0										
2019/11/04	22	56 36.481	019 26.015	0										
2019/11/04	23	56 35.457	019 09.750	0										



2019/11/08	6	56 18.613	002 15.559	10	10	60	55	600	8					
2019/11/08	7	56 14.493	002 04.873	10	10	60	45	600	8					
2019/11/08	8	56 12.358	001 51.570	10	10	60	40	600	5					
2019/11/08	9	56 11.406	001 38.467	9	9	60	40	600	5					
2019/11/08	10	56 09.297	001 28.545	8	8	90	40	300	15					
2019/11/08	11	56 07.916	001 14.902	7	4	60	35	600	10		3	90		300
2019/11/08	12	56 06.864	000 59.704	8	8	90	50	300	10					
2019/11/08	13	56 04.810	000 41.754	1	1	11								
2019/11/08	14	56 03.152	000 25.181	0										
2019/11/08	15	56 01.490	000 10.865	3	3	90		300						
2019/11/08	16	55 59.763	000 00.240 W	0										
2019/11/08	17	55 59.884	000 00.773											
2019/11/08	18	56 00.017	000 01.892											
2019/11/08	19	55 59.287	000 00.690											
2019/11/08	20	55 58.827	000 00.227											
2019/11/08	21	55 53.804	000 07.229 W											
2019/11/08	22	55 54.658	000 11.066 W											
2019/11/08	23	55 50.668	000 04.200 W											

## **14. TEAM SEALS**

The distribution, density and percentage contribution of pack-ice seals during ship-board censuses in the marginal sea ice zone of the Lazarev Sea in spring 2019 were investigated. Of the four true pack-ice phocid seal species, adult crabeater seals ( $n = 19$ ), leopard seals ( $n = 3$ ) and Ross seals ( $n = 9$ ) were sighted in the area bounded by  $00^{\circ}00'$  –  $22^{\circ}\text{E}$  and  $56^{\circ}$  –  $60^{\circ}\text{S}$ . Antarctic fur seals ( $n = 21$ ) were only encountered on the outer fringes of the pack-ice, and Weddell seals were absent, presumably due to their primary use of fast-ice and inner pack-ice habitats close to the coast. Five crabeater seal females and one leopard seal female attended pups. Only adult Ross seals were sighted at this early stage of their breeding season. Two Ross seals, both adult females, were restrained and instrumented with SPOT satellite-linked dataloggers (Wildlife Computers). Location data are continuously provided by CLS Argos and we are likely to have a detailed picture of the seals' movements by the time (January 2020) the trackers are lost during the Ross seal moulting season. These tracks will be analysed together with those ( $n = 11$ ) generated during the 2015/16 summer relief voyage of the *SA Agulhas II* and the 2018 deployments on Ross seals ( $n = 2$ ) off the *RV Polarstern* in the Eastern Weddell Sea. On three occasions we were allowed to manipulate the ship's cruise track to include 10 nm long north-south survey lines, spaced at 2.5 nm, during daylight hours. This we did firstly to cover the area in between longitudinally spaced, successive oceanographic stations as comprehensively as travel distance and speed allowed. Secondly, we aspired to an ideal survey design which would have multiple regularly spaced transects extending in a north-south direction across the ice gradient. However, since we could not operate south of  $60^{\circ}\text{S}$  latitude, the SCALE spring survey was of insufficient effort and scale, in both extent and duration, to locate Ross seals in particular during their austral spring breeding (pupping and mating) season in October/November.

*Acknowledgements:* The Officers and Crew of the MV SA Agulhas II extended every possible courtesy to us in support of our research objectives. Chief Scientist, Tommy Ryan-Keogh, creatively fitted our requirements into the overall logistical plan. Our work is an extension of the research of MNB and MW that was supported by the NRF (Grant Number 93088).

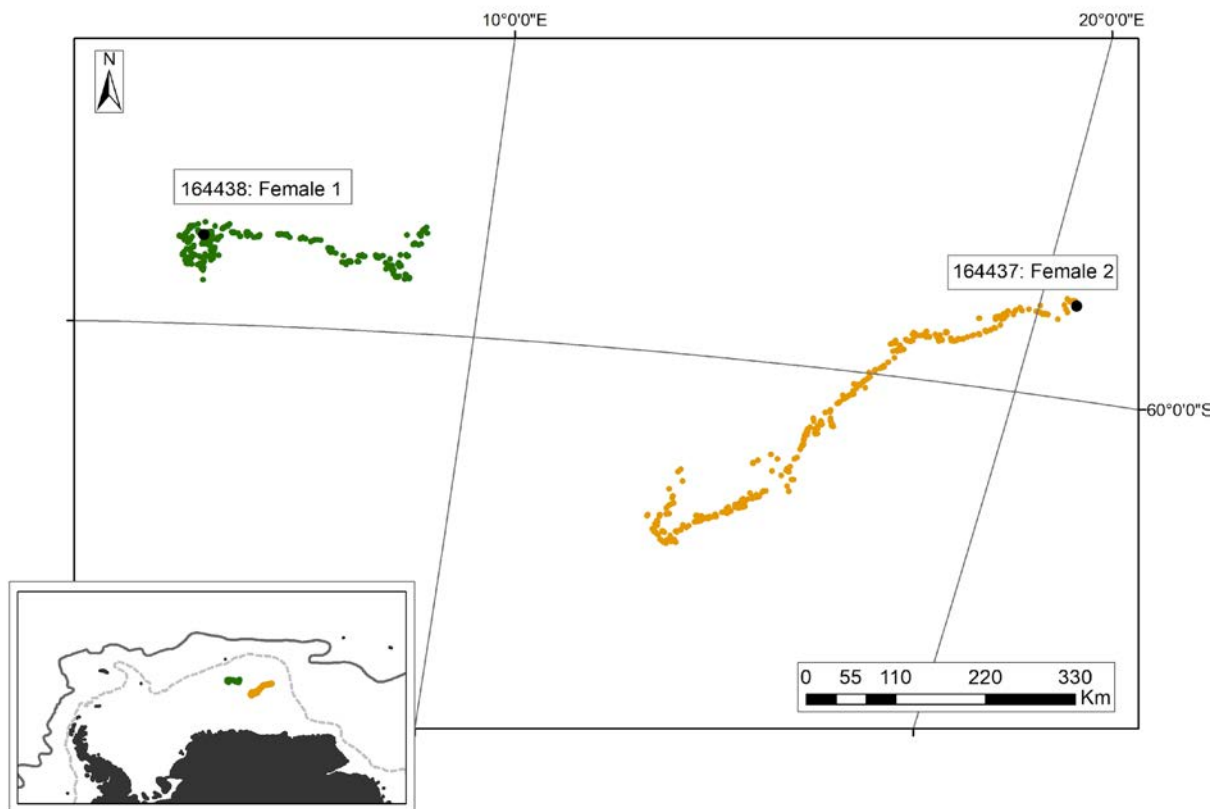


Figure 14.1: At-sea movement data of two Ross seals satellite trackers were deployed on during SCALE Spring voyage 2019. The black dots represent the deployment location for each of the animals respectively. The insert shows the position of the animals in relation to Antarctica, the Polar Front (solid grey line) and the southern boundary of the Antarctic Circumpolar Current (grey dashed line). Map: Dr Mia Wege.

## 15. TEAM TRACEX & IRON

### 15.1. Methodology and sampling strategy

#### 15.1.1. Trace metals, ligands and kinetics

Vertical samples were collected by a Seabird aluminium frame carousel, which was programmed to trip at predetermined depths, with the capacity to hold 24 Teflon-coated, acid cleaned, GO-FLO bottles on a rosette attached to a non-metallic line, simultaneously measuring parameters such as salinity, temperature, and fluorescence. Following collection, GO-FLOs were carefully packed into plastic liners and transferred into a class 100 (ISO) container for sampling. Prior to sample collection, each GO-FLO bottle was attached to an ultra-pure Nitrogen line to facilitate pressure difference experienced during sampling.

Seawater samples from 21 stations were sampled for unfiltered, filtered, and particulate samples. Unfiltered samples included nutrients, pigments, dissolved organic matter, and oxygen isotopes. Filtered samples included dissolved trace metals (dTM), dissolved iron (dFe), soluble iron (sFe), iron and copper ligands (FeL and CuL respectively), humic substances (HS) and Fe(II) kinetic (kFe). Each station consisted of two duplicate and two synchrotrons depths.

Filtered samples were filtered by a 0.2µm filter (Acropak 500 Supor Membrane) and dissolved Trace metals acidified to a pH of 1.7 with Merck Ultrapur® HCl (30%) and stored in 125ml LDPE bottles. Acidifying samples to a pH of 1.7 ensures a complete dissociation of organometallic complexes and solubilizes colloidal matter present in the seawater matrix, with samples acidified 24 hours after collection.

Particulate trace metals samples were collected on 0.45 µm acid cleaned PES membrane filters (Supor, Pall) mounted on swinnex filter holders. A volume ranging between 6 to 8 l of seawater was filtered for each sample. After filtration, filters were processed under a class 100 laminar flow bench and stored in acid cleaned petri dishes at -20 C until further processing back on land.

CuL, FeL, HS and kFe samples were frozen at -20°C after collection in 125 mL, 250 mL and 500 mL LDPE bottles (volume depending on the sample and the station). Following ship-board procedures, samples are stored until processing in a class-100 laboratory at Stellenbosch University, and at the other institutions mentioned in the table below. The following table also summarizes the different methods used to analyse the different parameters collected:

Trace metals	Method	Institution
dFe	FIA	CSIR
dAl	Mini-SIA	Stellenbosch University
dTM (Cu,Ni ,Zn ,REE etc )	SeAfast & ICP-MS	Stellenbosch University
Cu ligands	CLE-adCSV (Campos and van den Berg, 1994)	Universidad de Las Palmas de Gran Canaria
Fe ligands	CLE-adCSV; Mahieu et al., in prep)	University of Liverpool

Humic substances	Voltammetry (Whitby and van den Berg, 2015)	University of Liverpool
kFe	Quimioluminescence	Universidad de Las Palmas de Gran Canaria
pTM	ICP-MS (Planquette and Sherrel, 2012)	University of Brest

### 15.1.2. FeL, CuL and HS

Iron and copper are essential and toxic elements (function of their concentration) for terrestrial and marine life (Zhou et al., 2014). The poor solubility of these metals is enhanced in oxic waters by organic ligands which control at >99% the distribution and transport of Fe (Gledhill and van den Berg, 1994) and Cu (Moffett et al., 1990). An important pool of ligand, the humic substances (HS), is able to bind with both Fe and Cu (Abualhaija et al., 2015) and is therefore important to determine when measuring iron and copper ligands. The diversity of the ligand pool and the variability of its ability to bind with the different metals (not only Fe and Cu, and with potential competition between all concerned elements) is an important topic for the understanding of the fertilization process in areas of limited production such as the Southern Ocean.

During the SCALE Spring cruise, there are a total of 20 profile stations where FeL, CuL and HS samples have been collected. 10 of these stations concern the GEOTRACES transect, with 7 stations common to the SCALE Winter cruise for seasonal investigation. 7 profiles have been collected in the seasonal ice zone, completed by snow and ice core samples to provide a global picture of the sea-ice system, potentially specific in such specific areas. The last 3 profiles have been collected in the transition zone between ice zone and open waters, to complete and link these two specific systems.

### 15.1.3. Fe(II) Kinetics

The Fe(II) oxidation in seawater will provide valuable data in order to fully understand the iron biogeochemical cycles. The Fe(II) rate constant is related with the speciation, pH, temperature and organic ligands.

## 15.2. FISH activities

Surface seawater was collected using a torpedo FISH. This device can collect the surface seawater from 1-2 m depth, while the ship is steaming. Torpedo FISH was deployed off the side of the ship using a metal extension or core winch and the Kevlar rope, up to 5 m from the ship. Seawater was collected through a nozzle, made up of teflon, and was pumped to the class 100 trace metal clean container through an acid clean PVC tubes by a Teflon diaphragm pump, which was connected to an oil free air compressor. Using the torpedo fish, seawater was collected for measuring dissolved trace metals, dissolved Al, Pb isotopes and nutrients in every one/two hour. Once the fish was deployed, the entire connection, from the nozzle to diaphragm pump, was flushed with the ambient seawater for 2 hours prior to the sampling. The outlet of the diaphragm pump was connected to a

0.2 µm Sartobran acropak® filter to collect the dissolved samples, while the nutrients were collected unfiltered and stored in the freezer. The dissolved samples were acidified to pH~1.8 using Merck ultrapur® HCl immediately after the collection.

Table 15.2: List of samples collected by FISH

Sample Number	Date	Start time (UTC)	End time (UTC)	dT M1	dT M2	d Al	Pb isotopes	Nutrients
Fish 1	13.10.2019	14:04	14:05	√	√	√		
Fish 2	13.10.2019	16:02	16:06	√	√	√	√	
Fish 3	13.10.2019	18:00	18:02	√	√	√		
Fish 4	13.10.2019	22:00	22:03	√	√	√		
Fish 5	14.10.2019	00:01	00:01	√	√	√		
Fish 6	14.10.2019	02:00	02:03	√	√	√		
Fish 7	14.10.2019	03:00	03:54	Reference seawater collected (35 L)				
Fish 8	14.10.2019	04:00	04:04	√	√	√		
Fish 9	14.10.2019	06:00	06:03	√	√	√		
Fish 10	14.10.2019	08:00	08:02	√	√	√		

Fish 11	14.10.2 019	10:00	10:01	√	√	√		
Fish 13	17.10.2 019	15:00	15:09	√	√	√		
Fish 14	17.10.2 019	17:00	17:02	√	√	√		
Fish 15	17.10.2 019	17:19	17:32	Ref ere nce sea wat er coll ecte d (22 L)				
Fish 16	17.10.2 019	19:00	19:04	√	√	√		
Fish 17	17.10.2 019	21:10	21:13	√	√	√		
Fish 18	17.10.2 019	22:49	22:50	√	√	√		
Fish 19	18.10.2 019	01:04	01:16	√	√	√		
Fish 20	18.10.2 019	03:00	03:02	√	√	√		
Fish 21	18.10.2 019	05:00	05:04	√	√	√		
Fish 22	18.10.2 019	07:06	07:20	√	√	√		
Fish 23	18.11.2 019	18:01	18:03	√	√	√	√	
Fish 24	18.11.2 019	19:00	19:01	√	√	√	√	

Fish 25	18.11.2 019	19:59	20:01	√	√	√	√	√
Fish 26	18.11.2 019	21:00	21:02	√	√	√	√	
Fish 27	18.11.2 019	22:00	22:05	√	√	√	√	√
Fish 28	18.11.2 019	23:00	23:02	√	√	√	√	
Fish 29	18.11.2 019	00:00	00:05	√	√	√	√	√
Fish 30	19.11.2 019	01:01	01:03	√	√	√	√	
Fish 31	19.11.2 019	02:00	02:06	√	√	√	√	√
Fish 32	19.11.2 019	03:00	03:05	√	√	√	√	
Fish 33	19.11.2 019	04:00	04:10	√	√	√	√	√
Fish 34	19.11.2 019	05:00	05:05	√	√	√	√	
Fish 35	19.11.2 019	06:01	06:20	√	√	√	√	√
Fish 36	19.11.2 019	07:03	07:10	√	√	√	√	
Fish 37	19.11.2 019	07:58	08:05	√	√	√	√	√
Fish 38	19.11.2 019	09:01	09:02	√	√	√	√	
Fish 39	19.11.2 019	09:57	09:59	√	√	√	√	√
Fish 40	19.11.2 019	10:58	10:59	√	√	√	√	
Fish 41	19.11.2 019	11:56	11:58	√	√	√	√	√
Fish 42	19.11.2 019	12:43	12:45	√	√	√	√	√

dTM1: dissolved trace metal-1 (125 mL); dTM2: dissolved trace metal-2 (125 mL); dAl: dissolved Al (125 mL); Pb isotopes (1 L)

### 15.3. Trace metals in ice cores and snow

Sea ice winter formation and spring-summer melt is an important mechanism which accumulates and releases trace metals back into the system. However, the relative importance of this mechanism is still to be comprehensively determined (Lannuzel et al., 2011). The released metals play, potentially, a crucial role in the development of spring and summer phytoplankton blooms in the Southern Ocean (Grotti et al., 2005; Lannuzel et al., 2011, 2014). Hence seasonal sea-ice dynamics may play a significant role in the CO<sub>2</sub> uptake mechanisms of the Southern Ocean.

#### Sampling strategy:

Ice cores and snow samples were collected in the Antarctic marginal ice zone at 4 and 7 stations, respectively. A total of 24 ice cores and 150 snow samples were collected. All samples were collected upwind to avoid contamination from the ship stacks.

Ice cores were drilled using an electrical drill and a carbon fiber barrel. The barrel used for coring was cleaned with solvents and de-ionized water prior to each coring station. Prior to collecting any core for trace metal or isotope analysis, the barrel was conditioned by coring two ice cores. The third ice core retrieved was used for phytoplankton pigment analysis. In total six cores were taken at each coring location. One core for pigment, three cores for trace metals (particulate, dissolved, and soluble), and two cores for isotope analysis (Zn, Fe, Pb). Ice cores were transferred from the barrel directly into acid clean plastic liners and stored in the -20 °C freezer. Ice cores were stored horizontally to prevent brine water movements within the core.

Snow samples were collected using acid cleaned polypropylene sheets and transferred into acid cleaned zip lock bags. On each location and depending on the snow thickness we collected an upper, middle, and lower snow layer and a bulk sample comprising all layers. Samples were stored at -20 °C freezer prior to processing.

#### Sample processing

Ice core processing will take place back in the home laboratory at Stellenbosch University. Eighty snow samples were processed on board following trace metal clean protocols. Melting of snow samples was done in a class 100 laboratory. Snow samples were transferred into 5 L acid cleaned PP buckets and left to melt overnight. After each batch of processed samples, the PP buckets were rinsed 5 times with de-ionized water and filled with a 2 M HCl solution (Suprapur, Fisher) and left at least 24h prior to be used again.

Melted snow samples were then transferred into 1 L acid cleaned LDPE bottles. A subsample from the melted snow was collected in 125 mL acid cleaned LDPE bottles for determination of the total metal fraction. A second subsample was taken for salinity measurement. Filtration for dissolved trace metals was achieved simultaneously for 12 samples using a 12-channel peristaltic pump connected with 12 x Swinnex filter holders (25 mm ø, Millipore). The filter holders were loaded with acid cleaned 0.45 µm PES membrane filters (Supor, Pall). The dissolved fraction was collected in acid cleaned 125 mL LDPE bottles (Nalgene). After the dissolved fraction filtration finished, a second acid

cleaned Swinnex filter holder containing 0.02  $\mu\text{m}$  membrane filters was attached to the first one in order to sample for soluble trace metals in 60 mL acid cleaned LDPE bottles. Upon soluble filtration was finished the remaining melted snow was filtered through the 0.45  $\mu\text{m}$  filter and the filter was stored in acid cleaned petri dishes for the determination of particulate trace metals. Additionally, on each station a combined pool of layers was filtered for the determination of Pb isotopes in snow. Samples for total, dissolved, soluble, and isotopes were acidified to  $\text{pH} < 1.9$  using HCl (UpA, Fisher) and stored in double zip lock bags until analysis in the home laboratory.

Analysis of samples:

Samples for particulate trace metals will be analyzed in Brest (France) following Planquette and Sherrel, 2012. Samples for total, dissolved, and soluble trace metals will be preconcentrated using SeaFast (ESI) systems and analyzed on an ICPMS at Stellenbosch University. Isotope samples will be processed at Stellenbosch University and analyzed elsewhere.

#### **15.4. Pigments**

Our understanding of the biogeochemical dynamics in the Southern Ocean is limited due to the complexity of exploring such an isolated oceanic region via ship, most especially during the austral winter and spring months when water sampling can be most challenging. Consequently, there is still a data and knowledge gap for phytoplankton and trace metal distribution for the Atlantic Southern Ocean during spring. One potential driver, which we don't yet understand fully, is the availability of metals that often are found in limiting concentrations in the Southern Ocean (Morel and Price 2003). Within the Atlantic Southern Ocean, few studies have been done to assess the links between phytoplankton community compositions and trace metal distribution across different zones, depths and seasons. There are still some uncertainties of what effect trace metal availability, like Cu, Zn, Fe, Ni, Co, Mn and Cd (Twining and Baines 2013), and their co-limitation with light (Viljoen et al. 2018), will have on the phytoplankton productivity and overall community composition changes in relation with various other environmental factors (Moore et al. 2013; Viljoen et al. 2019). More data is needed from other seasons and additional sampling stations to better describe phytoplankton distribution in relation to trace metal distributions (Cloete et al. 2019). This will be in part constrained by the measurements of various phytoplankton pigments within high-resolution surface samples as well as vertical depth profiles within the open ocean.

Additionally, we have yet to comprehensively describe the distribution of phytoplankton within sea ice and the role of annual sea ice melt as an active source pool of both phytoplankton and trace nutrients to the Antarctic euphotic waters (Lannuzel et al. 2011). Sea-ice is populated by a range of microorganisms surviving in a diverse "pool" of micro and macro-nutrients, salinity and irradiance. This resident population, posited as a "seed population", and the entrained sea-ice nutrients may provide the crucial framework for seasonal blooms (Grotti et al. 2005), like a spring bloom. It is probable that trace metal fluxes from melting sea ice may be enhancing or sustaining photosynthetic micro-organism (phytoplankton) productivity in remote seasonally ice-covered regions. Whilst

seasonal sea-ice cover inhibits irradiance within the surface mixed layer – accordingly restricting productivity – annual melts play a crucial role in water mass stabilisation and bio-active trace metal inputs favouring the growth of phytoplankton (Grotti et al. 2005). Hence sea-ice may play a significant role in the CO<sub>2</sub> uptake mechanisms of the Southern Ocean and the elucidation of these mechanisms is imperative. Our effort to better understand the distribution of phytoplankton groups/species within sea-ice in relation to trace metal distribution will be done by the measurements of various phytoplankton pigments melted sea-ice cores (pancakes & consolidated) as well as vertical depth profiles from multiple CTD stations within the marginal ice zone.

#### Objective of Pigment project:

The main aim of the project is to understand the role the microbes, such as phytoplankton, play on the trace metal distribution along with the impact of the trace metal availability on the microbes and how this changes between various seasons. This includes the abundances as well as the community structure. For this purpose the measurements of photosynthetic pigments will be used to assess the phytoplankton community structure, abundance, photophysiological state and degradation/grazing.

Additionally, this project will investigate the relatively unknown phytoplankton dynamics in the Southern Ocean winter/spring sea ice from ice cores. The main objective of this study is to gather a high-quality dataset of phytoplankton pigment concentrations along multiple transects and depths within open ocean and ice covered areas.

The main objective was met during this cruise when the TracEx team successfully sampled for photosynthetic pigments, including accurate chlorophyll-a (chl<sub>a</sub>) via HPLC analysis, from the ship's underway surface water supply, Niskin (Classic) CTD casts and ice cores.

#### Underway pigment sampling & processing:

Along the southward transect (12/10/2019 to 22/10/2019) surface pigment samples were continuously taken from the ship's bow intake by TracEx members Andrea and Raya. Sampling was done 4-hourly on the hour to match every second macronutrient sample (taken 2-hourly by team NOCE) for easier data interpretation later. These samples were taken every four hours to also fit into the underway sampling schedule of the other teams (i.e. Fawcett, Altieri and Walker teams) on-board. During towfish sampling care was taken during pigment sampling to match with every 4th trace metal sample. Accompanying high resolution data on temperature and salinity will be retrieved from the ship's TSG system. However, TSG data was recorded on the pigment sampling log sheet for every sample as well. The appearance of pancake ice marked the end of the southbound underway sampling at 56°S.

Sub-Sampling strategy and Material: For phytoplankton pigments, 1-3 L water were directly filtered from an underway supply tap using an in-line filter holder through 25 mm diameter GF/F Whatman filters. Filters were removed from the filter holder, while taking care to block direct light, folded into a 2 mL cryovial and stored at -80°C.

Niskin CTD: Vertical Depth Profiles (Both open ocean and MIZ):

Pigment samples were taken to determine the phytoplankton community composition along the cruise transects, including vertical depth profiles, and how and why they changed and compare these to trace metal changes. Pigment data will be furthermore combined with the results from the genomic analysis (Team MICROBIO). Pigment samples for vertical depth profiles (6 depths) were taken from all Niskin CTD casts, both open ocean and within the MIZ (ice conditions), that totalled to 27 stations (162 filters collected).

Sampling strategy and methodology: Following a pre-determined water budget as per the needs of the different teams on board, ca. 2 L of water for each of the six depths (typically 5, 20, 50, 75, 125, 150 m) were collected (sub-sampled) for pigments. This was done by sub-sampling water from the different Niskin bottles, representing the various desired depths, into labelled dark PE bottles. Samples were filtered immediately after sub-sampling from Niskin bottles or samples were temporarily stored in a cold room. All 6 samples were filtered simultaneously as fast as possible through 25 mm Ø GF/F filters (nominal pore size 0.7 µm) using a filtration rack and a vacuum pump. Filters were folded, placed into their respective pre-labelled cryo vial and stored in the -80°C freezer in a cryovial box until analysis by HPLC.

Ice core sampling and subsampling:

Sampling of pancakes and sea ice cores is detailed in the “Sea Ice Team” section (XX). At each marginal ice zone station (pancake and consolidated ice) using a corer cleaned using the Geotraces cleaning protocols, the TracEx team received one core (always the 1st core taken) for determining phytoplankton abundance and community composition determination. The ice cores were placed in acid-cleaned plastic liners and stored frozen (-20°C) immediately. Ice cores were cut into sub-sections of Top, Middle and Bottom within 24 h, each segment placed in a separate ziplock bag and stored frozen for later melting and filtering (similar as for depth samples above) at SU.

### **15.5. Assessment of potential eolian input**

Dust represents a potentially major external source of trace metals for the Southern Ocean. In the open oceans the deposition of external nutrients can increase primary production. The extent of the role that dust plays for ocean primary productivity and thus CO<sub>2</sub> uptake along with dimethyl sulfate (DMS) emissions, depends on a variety of factors such as a) extent of nutrient limitation in the oceanic region, b) timing of the dust deposition in view of phytoplankton seasonal development, c) nutrient load in the deposited dust, and c) solubility of the nutrients, the latter especially considering the micro-nutrients (e.g., trace metals such as Fe, Co, Zn etc). Here we collected aeolian to analyse a) the macro- and micronutrient composition, and b) to conduct experiments to better understand the dust’s potential to fertilise the marine phytoplankton communities.

A TISCH Environmental high-volume dust sampler (Figure ) was set-up on Monkey Island (8<sup>th</sup> floor) to collect aerosols above the Southern Ocean during all the steaming transects.

The dust sampler was connected to a wind-direction controlled switch provided by Team NAIR (UCT) ensuring that the pump switched off when the wind direction was unfavourable to avoid contamination from the ship stack or any other risk of contamination, such as low head wind speeds. More details are provided in Section (Team NAIR (UCT)). A total of 14 air filters (acid-cleaned 8x10 inch Whatman 41 filter sheets) were collected. The filters will be subsampled to analyse for carbon and nitrogen in collaboration with Team NATM (UCT) as well as for trace metal composition and potential pollutants. Part of the filters will be used for SEM analysis and determination of particle characteristics. In addition, part of each filter were used for the dust dissolution and incubation experiments described below.



Figure 15.1. High-Volume air sampler on Monkey Island (SA Agulhas II). The TRACEX dust sampler was connected to a wind-direction control switch from the Team NAIR.

### **Flow-through leaching experiments to determine the dissolution rate of dust into seawater and assess eolian trace metal bio-availability**

Flow-through experiments to assess the leaching of trace nutrients were conducting on all the filters using seawater collected from the GoFlo bottles at various stations. Additionally, dust samples of anthropogenic origin collected previously in Saldanha Bay, South Africa, West Coast, were exposed to the same procedure to compare “natural” with “anthropogenic” dust characteristics.

The flow through experiments were conducted inside the on-board class 100 clean container by placing the dust filter in a plastic inline filter holder and using a low-volume peristaltic pump to continuously pump freshly collected seawater through the sampled dust filter over a time series (30 min, 1 hour, 90 min and 2 hours). Dust collected previously from Saldanha Bay was placed on a filter and subjected to the same procedure. Experiments were terminated after 2 hours as, based on past experiments, there is minimal dissolution after 2 hours. The solutions containing the leached metals were acidified and stored for analysis. Additionally, the dissolution from all the filters will be measured using ammonium acetate (pH 4.7, 1.1 M) leach procedure (Baker et al. 2006, 2007) in the laboratory on land. A fraction of the aerosol filter sample will be immersed in the ammonium acetate solution extraction solvent for 1 hour, with four intervals of manual shaking for one hour.

## Dust addition incubation experiments

In collaboration with Asmita Singh (Team Production), Ismael tested the impact of anthropogenic dust on the Southern Ocean phytoplankton community. Details on the incubation set-up are provided in Team Production's section. Briefly, seawater was collected using the torpedo FISH (**Error! Reference source not found.**) on the 23 July 2019 at 12:00pm, at 50°49S 002°40. Approximately 800mL of surface water was sub-sampled into a set of 1L acid-cleaned polycarbonate bottles. All bottles were incubated for 24h at light intensities and temperatures mimicking ambient seawater conditions. Three 1L bottles were dedicated for the testing of dust impacts, while similar sets of triplicates were used for controls, testing iron addition (Asmita Singh, see section Team Production) only and testing impact of multi-element addition (Johan Viljoen). At the beginning and end of the 24h incubation period, the Fv/Fm and chl<sub>a</sub> concentration were tested and compared to those measured in the initial seawater and in the control bottles.

### 15.6. Particulate trace metals (McLane pumps)

A major thrust of the proposed research is to gain a fundamental insight to chemical changes that occur on the mineral-water interface in the presence of organic ligands at nano-meter scales. Once this fundamental understanding is in place we can then expand the understanding in several applied avenues – oceanic productivity and CO<sub>2</sub> exchange being primary beneficiaries. We aim to do this by elucidating on the following controls:

- i) Via Scanning Electron Microscopy (SEM) generate textural and morphological data for Cu and Zn particulates in the Southern Ocean. Thereby determine the role that particle morphology plays in governing the trace metals of the biogeochemical system.
- ii) Employing the novel picoTrace acid digestion module (DAS) and Inductively Coupled Plasma Mass Spectroscopy (ICP-MS) to generate a chemical characterization of marine particles. This will be linked to an existing dissolved fraction dataset creating an exciting framework to interpret the interplay between fractions and the role this has on phytoplankton productivity.
- iii) Evaluate Cu and Zn chemical speciation in marine colloids and nano-particles using Synchrotron Spectroscopic Techniques (e.g. XANES, SXRF). Thereby investigate the spatial differences in Cu, Zn particle chemistry and link them to particle source regions, in situ processing and transformations; and provide insight into their relationship with the ambient marine biota.

*Sampling strategy and methodology:* Jean performed in-situ collection of trace metal particulates (pTM) at five stations in the Southern Ocean using two WTS-LV McLane pumps (4L/min and 8L/min, McLane Research Laboratories Inc., USA; Figure ) suspended on a steel cable general purpose winch. The pumps were fitted with the 142mm diameter vertical intake filter stacks – the 8L/min pump will hereon be referred to as the dual flow. The Whatman Nuclepore (142mm) polycarbonate membrane filters (0.2 $\mu$ m) were used for pTM collection and fitted on the lowest tier of the 4L and DF pump. The Nuclepore filters utilized for pTM collection were soaked in a 0.1M HCl Suprapur (Merck) solution for 20 hours followed by a Milli-Q rinse (3X) and bath (4 hours) prior to each station. An acid cleaned and Milli-Q stored 200 $\mu$ m pre-filter mesh was inserted in the top tier of the vertical stack of both pumps to remove any unwanted material on the pTM filter – such as zooplankton.

The filters were loaded 2 hrs prior to deployment, and immediately removal upon retrieval after pumping Milli-Q through the system to limit NaCl precipitation; all performed in the TracEx trace clean container (ISO class 5) under the laminar flow. Flow heads were kept covered with zip-locks during transport periods. The vertical intake stacks were filled to the top with Milli-Q water prior to deployment. Filters for trace metals were placed directly into acid cleaned petri dishes using PTFE forceps, sealed with nitrogen in acid clean Mylar pouches, double zip-locked, and stored in the -25°C freezer.



Figure 15.2. McLane pumps before deployment (left panel) and during the Open Day Science Show (right panel) on board RV SA Agulhas II.

### **15.7. Water sampling for trace metals, isotopes, macronutrients and phytoplankton community composition along vertical profiles in the MIZ**

A new, smaller trace metal clean sampling array was used for this year's water collection at the three MIZ stations (Table 15.1). This so-called "miniGoFlo" rosette has similar features as the routine GoFlo rosette described earlier. The closing mechanism of the sampling bottles also allow for trace metal clean sampling. The miniGoFlo bottles, with a

volume of 5L, are much smaller than the routine GoFlo bottles. The rosette was attached to the same Kevlar conductive cable as the routine GoFlo rosette and operated similarly as described above.

Table 15.1. Trace metal clean CTD casts within the MIZ

TracEx Activity	Date	Time (UTC)	Lat [S]	Long [E]	Station name
miniGoFlos	7/26/2019	18:45	57°00	00°00	MIZ1s
miniGoFlos	7/28/2019	0:10	57°19.15	00°01	MIZ2
miniGoFlos	7/28/2019	16:00	56°40.49	00°27.95	MIZ1n

*Sampling strategy and methodology:* Subsampling from the mini-GoFlo array was conducted in another class 100 certified trace metal clean container. The advantage of this new array was that individual bottles remain on the rosette from deployment in the ocean throughout sub-sampling in the container, which avoids manual carrying individual bottles as described for routine GoFlo arrays. Three stations were occupied within the MIZ at 57.00°S;0.00° (MIZ1A), 57.17°S;0.01E° (MIZ2B) and 56.67°S;0.45°E (MIZ1E). Subsampling followed similar protocols as described for routine GoFlos: dissolved and particulate trace metals, dissolved aluminium (for SIA - Sequential Injection - analysis), zinc and lead isotopes. Samples for macronutrients and phytoplankton pigments were taken as well from the mini-GoFlo casts.



Figure 15.3. Preparation (left panel) and deployment (right panel) of "mini-GoFlo" rosette for trace metal clean sampling in the marginal ice zone.

## 15.8. References

Grotti, M., Soggia, F., Ianni, C., & Frache, R. (2005). Trace metals distributions in coastal sea ice of Terra Nova Bay, Ross Sea, Antarctica. *Antarctic Science*, 17(2), 289-300.

Lannuzel, D. et al. (2011) 'Distribution of dissolved and particulate metals in Antarctic sea ice', *Marine Chemistry*. Elsevier B.V., 124(1–4), pp. 134–146. doi: 10.1016/j.marchem.2011.01.004.

Lannuzel, D. et al. (2014) 'Size fractionation of iron, manganese and aluminium in Antarctic fast ice reveals a lithogenic origin and low iron solubility', *Marine Chemistry*. Elsevier B.V., 161, pp. 47–56. doi: 10.1016/j.marchem.2014.02.006.

Planquette, H., & Sherrell, R. M. (2012). Sampling for particulate trace element determination using water sampling bottles: methodology and comparison to in situ pumps. *Limnology and Oceanography: methods*, 10(5), 367-388.

Cloete, R., J. C. Loock, T. Mtshali, S. Fietz, and A. N. Roychoudhury. 2019. Winter and summer distributions of Copper, Zinc and Nickel along the International GEOTRACES Section GIPY05: Insights into deep winter mixing. *Chem. Geol.* 511: 342–357. doi:10.1016/J.CHEMGEO.2018.10.023

Grotti, M., F. Soggia, C. Ianni, and R. Frache. 2005. Trace metals distributions in coastal sea ice of Terra Nova Bay, Ross Sea, Antarctica. *Antarct. Sci.* 17: 289–300. doi:10.1017/S0954102005002695

Lannuzel, D., A. R. Bowie, P. C. van der Merwe, A. T. Townsend, and V. Schoemann. 2011. Distribution of dissolved and particulate metals in Antarctic sea ice. *Mar. Chem.* 124: 134–146. doi:10.1016/j.marchem.2011.01.004

Moore, C. M., M. M. Mills, K. R. Arrigo, and others. 2013. Processes and patterns of oceanic nutrient limitation. *Nat. Geosci.* 6: 701–710. doi:10.1038/ngeo1765

Morel, F. M. M., and N. M. Price. 2003. The biogeochemical cycles of trace metals in the oceans. *Science* (80-. ). 300: 944–947. doi:10.1126/science.1083545

Twining, B. S., and S. B. Baines. 2013. The Trace Metal Composition of Marine Phytoplankton. *Ann. Rev. Mar. Sci.* 5: 191–215. doi:10.1146/annurev-marine-121211-172322

Viljoen, J. J., R. Philibert, N. Van Horsten, T. Mtshali, A. N. Roychoudhury, S. Thomalla, and S. Fietz. 2018. Phytoplankton response in growth, photophysiology and community structure to iron and light in the Polar Frontal Zone and Antarctic waters. *Deep. Res. Part I Oceanogr. Res. Pap.* 141: 118–129. doi:10.1016/j.dsr.2018.09.006

Viljoen, J. J., I. Weir, S. Fietz, R. Cloete, J. Loock, R. Philibert, and A. N. Roychoudhury. 2019. Links between the phytoplankton community composition and trace metal distribution in summer surface waters of the Atlantic

**16. TEAM VIBRATION**  
**16.1. Vibration Measurements**

The analysing the vibration data provides insight into the wave slamming experienced by the vessel, which may influence the fatigue life of the vessel. Operational Modal Analysis (OMA) is employed to investigate the vessel’s global structural dynamic response characteristics, namely the natural frequencies and mode shapes. The stern slamming experienced by the SAA II and the resulting vibration levels are also investigated in the context of human comfort.

The vibration team installed a total of 28 accelerometers throughout the vessel to measure the vibration response of the vessel structure throughout the voyage during different operational conditions. Vibration measurements were conducted in accordance with guidelines as specified in ISO 2631-1:1997 and BS ISO 20283-2:2018. An LMS SCADAS Mobile SMO03 master-slave system was employed, in conjunction with LMS Turbine Testing acquisition software, to record data recorded by the 10 DC and 18 ICP accelerometers. Vibration was predominantly recorded in the +Z direction, however, some sensors were also orientated to measure in the +Y and +X directions.

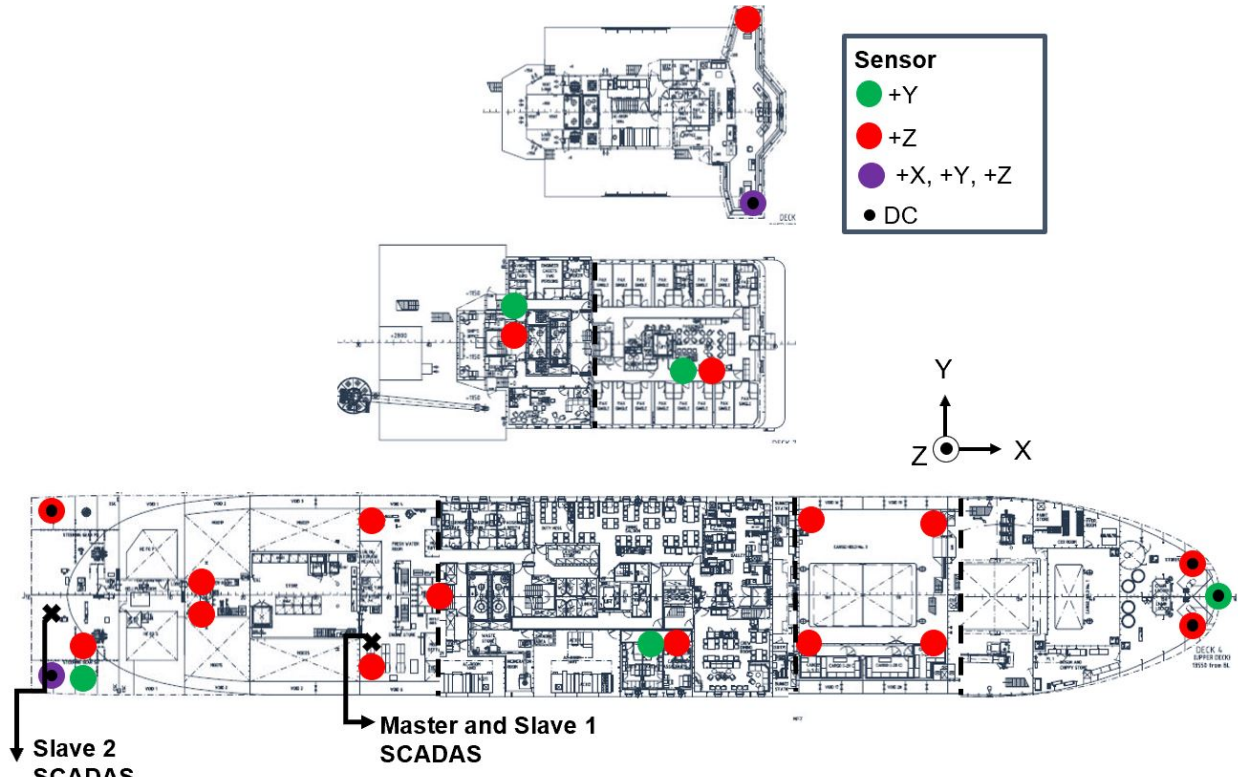


**Figure 16.1:** Sensor Layout

**Table 16.1:** Sensor layout and specifications for the winter cruise (for the spring cruise point 25 and 26 were excluded)

<i>Point #</i>	<i>Deck</i>	<i>Location name</i>	<i>Sensor Type</i>	<i>Serial number</i>	<i>Sensitivity (mV/g)</i>
----------------	-------------	----------------------	--------------------	----------------------	---------------------------

1	9	<i>Bridge</i>	<i>DC</i>	<i>LW9811</i>	<i>199.7</i>
2	9	<i>Bridge</i>	<i>DC</i>	<i>LW6300</i>	<i>199.4</i>
3	9	<i>Bridge</i>	<i>DC</i>	<i>LW8388</i>	<i>200.1</i>
4	9	<i>Bridge</i>	<i>ICP</i>	<i>34757</i>	<i>99.8</i>
5	8	<i>Deck 8</i>	<i>ICP</i>	<i>18869</i>	<i>104.0</i>
6	8	<i>Deck 8</i>	<i>ICP</i>	<i>38403</i>	<i>98.3</i>
7	7	<i>Deck 7</i>	<i>ICP</i>	<i>34758</i>	<i>98.2</i>
8	7	<i>Deck 7</i>	<i>ICP</i>	<i>62626</i>	<i>102.5</i>
9	4	<i>Bow</i>	<i>DC</i>	<i>LW11070</i>	<i>199.6</i>
10	4	<i>Bow</i>	<i>DC</i>	<i>LW6309</i>	<i>196.1</i>
11	4	<i>Bow</i>	<i>DC</i>	<i>LW11069</i>	<i>198.4</i>
12	4	<i>Chef's room</i>	<i>ICP</i>	<i>50900</i>	<i>102.3</i>
13	4	<i>Chef's room</i>	<i>ICP</i>	<i>34759</i>	<i>103.6</i>
14	4	<i>Ceiling</i>	<i>ICP</i>	<i>62623</i>	<i>102.2</i>
15	3	<i>Cargo-hold</i>	<i>ICP</i>	<i>62178</i>	<i>102.6</i>
16	3	<i>Cargo-hold</i>	<i>ICP</i>	<i>49501</i>	<i>102.3</i>
17	3	<i>Cargo-hold</i>	<i>ICP</i>	<i>18863</i>	<i>105.2</i>
18	3	<i>Cargo-hold</i>	<i>ICP</i>	<i>49498</i>	<i>100.6</i>
19	2	<i>Engine store</i>	<i>ICP</i>	<i>62624</i>	<i>101.4</i>
20	2	<i>Fresh water</i>	<i>ICP</i>	<i>62625</i>	<i>101.6</i>
21	2	<i>Stern thruster</i>	<i>ICP</i>	<i>49500</i>	<i>100.3</i>
22	2	<i>Stern thruster</i>	<i>ICP</i>	<i>49493</i>	<i>97.6</i>
23	2	<i>Steering gear</i>	<i>ICP</i>	<i>49495</i>	<i>98.5</i>

24	2	<i>Steering gear</i>	<i>ICP</i>	<i>62627</i>	<i>101.9</i>
25	2	<i>Steering gear</i>	<i>DC</i>	<i>LW6302</i>	<i>198.6</i>
26	2	<i>Steering gear</i>	<i>DC</i>	<i>LW6310</i>	<i>197.8</i>
27	2	<i>Steering gear</i>	<i>DC</i>	<i>LW6308</i>	<i>198.3</i>
28	2	<i>Steering gear</i>	<i>DC</i>	<i>LW11071</i>	<i>199.2</i>

## **16.2. Wave observations**

During open water transit, the ocean conditions were recorded by the vibration team from the bridge. The wave direction, wave height, wave period, encounter frequency and the Beaufort number were all determined through visual observation. The wind speed, wind direction, ship velocity and ship heading were also recorded from the navigational equipment located in the bridge. Observers noted an estimate of the frequency of slamming encountered. These parameters were recorded every ten minutes for the winter cruise during daylight hours, however the observation intervals were reduced to hourly observations for the spring cruise. We completed a total of 369 hourly wave observations during the spring cruise.

## **16.3. Ice observations**

During transit in the marginal ice zone, the ice conditions were recorded by the vibration team and members of the UCT team from the bridge. Observations included one minute assessments of changes in the ice conditions, which are used to generate averages for ten minute intervals. The concentration of ice, type of ice, floe size and the thickness of ice were recorded. The thickness of the snow layer on top of the ice was also estimated. The level of vibrations and the amount of ramming encountered were also noted. Twenty-four hour observations were conducted in the marginal ice zone for both the winter and spring cruise. Therefore, a total of 15600 minute by minute ice observations were completed in the spring cruise.

## **16.4. Cabin sound and vibration measurements**

Structural vibration measurements were conducted near the accommodation and working areas of the passengers and crew which were applied to aid the study of human comfort. These measurements on their own were not enough to measure human comfort due to the locations at which it is installed. Therefore, the vibration team installed two triaxial accelerometers, one on the floor (see figure 16.2) and the other on the bed (see figure 16.2) in one of the cabins in which our team members resided. The head and torso simulator (HATS - Acoustic dummy) named Mike was used to conduct sound measurements (see figure 16.2). Both tri-axial accelerometers and headphones were connected to the Squadriga II that was used as a mobile data acquisition system. Mike was allocated a berth in order to make these measurements possible on both SCALE cruises.

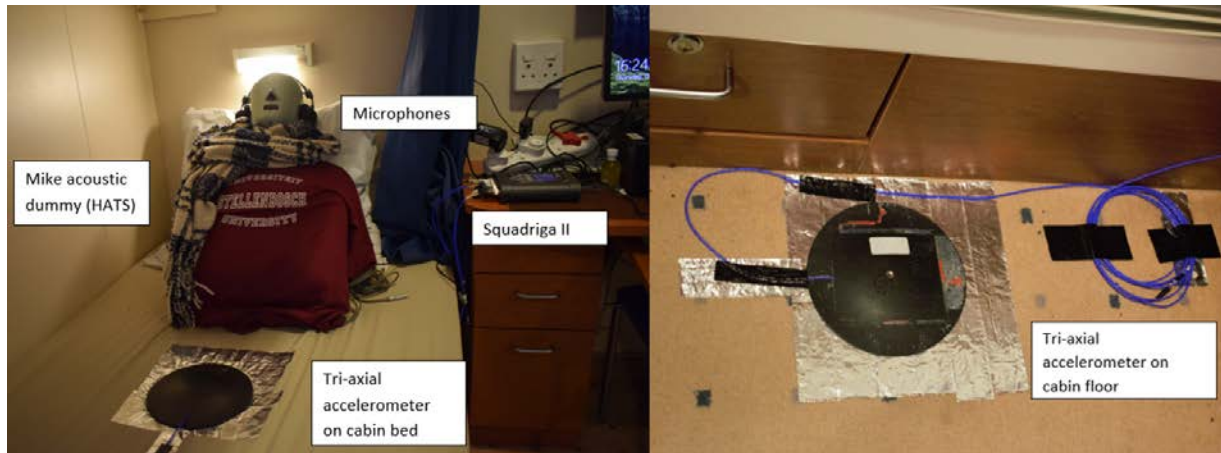


**Figure 16.2:** Cabin sound and vibration measurement setup.

### 16.5. Human comfort survey

At the start of both SCALE voyages passengers receive a presentation where the value of the survey to the study of human comfort was explained. Passengers were then asked to willingly participate in answering these surveys daily. The surveys were checked at the end of every week and participants that have completed their surveys to that date received an incentive in the form of a beverage of their choice. At the end of each voyage a lucky draw was held from the participant numbers of all completed surveys and the winner received a R500. Figure 16.3 represents the total number of passengers that completed their surveys during the weekly checks over the duration of Winter cruise. Figure 16.4 shows the percentage of passengers that participated over specific periods during the Spring cruise. The data from the survey are the subjective data while the full-scale vibration measurements the objective data. The subjective and objective data were used to determine correlations in an effort to quantify comfort. Figure 16.7 and figure 16.8 indicate the survey questions that were distributed on Winter and Spring cruise respectively. Figure 16.5 and figure 16.6 represent the peak vibration acceleration levels from a human point of view that was experienced in the bridge over the duration of the Winter and Spring respectively.

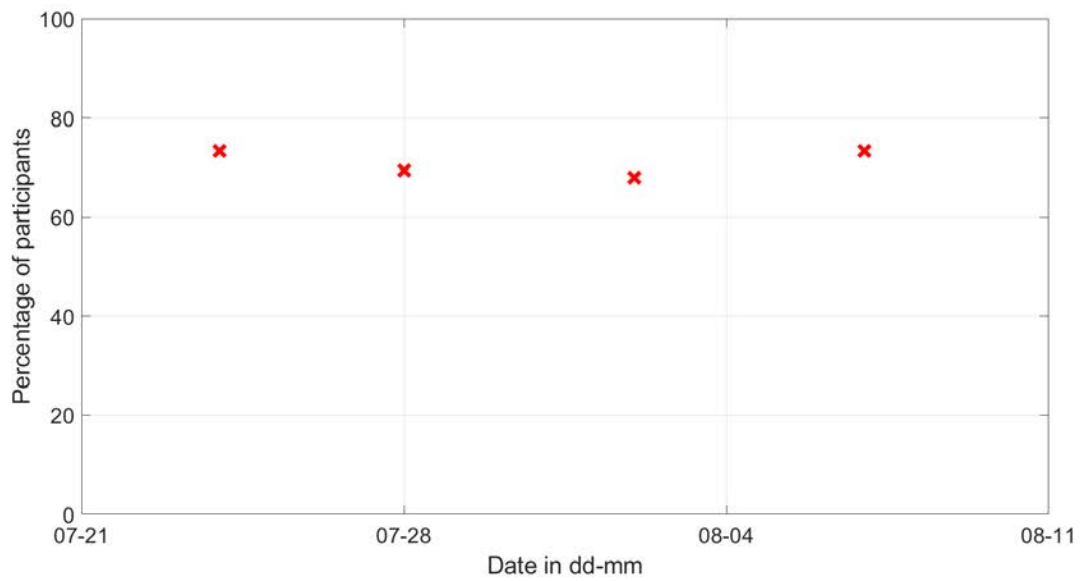


**Figure 16.3:** Percentage of participants that completed the survey during Winter cruise

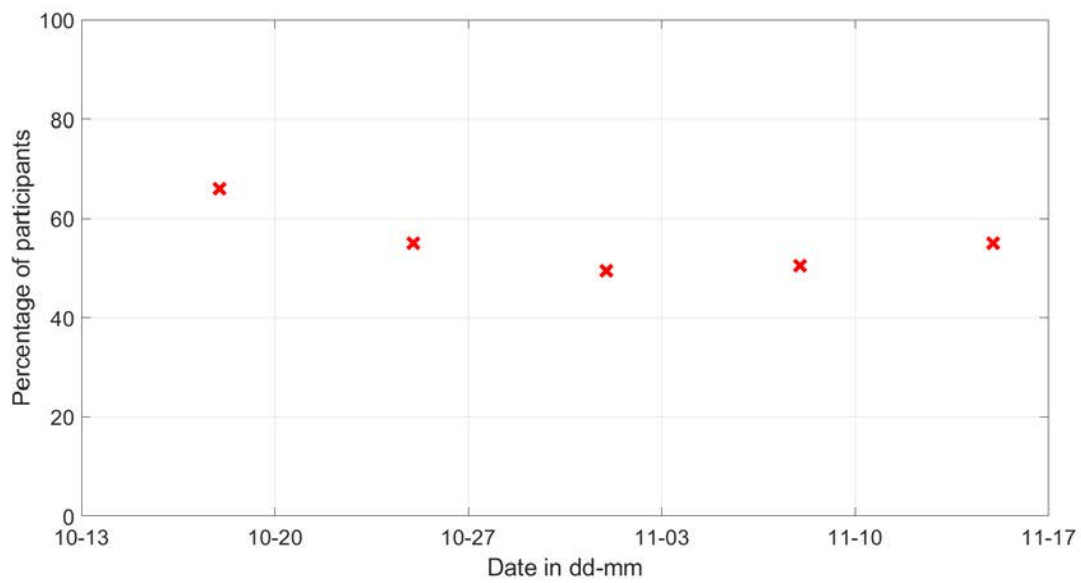


**Figure 16.4:** Human response survey participation rate during Spring cruise

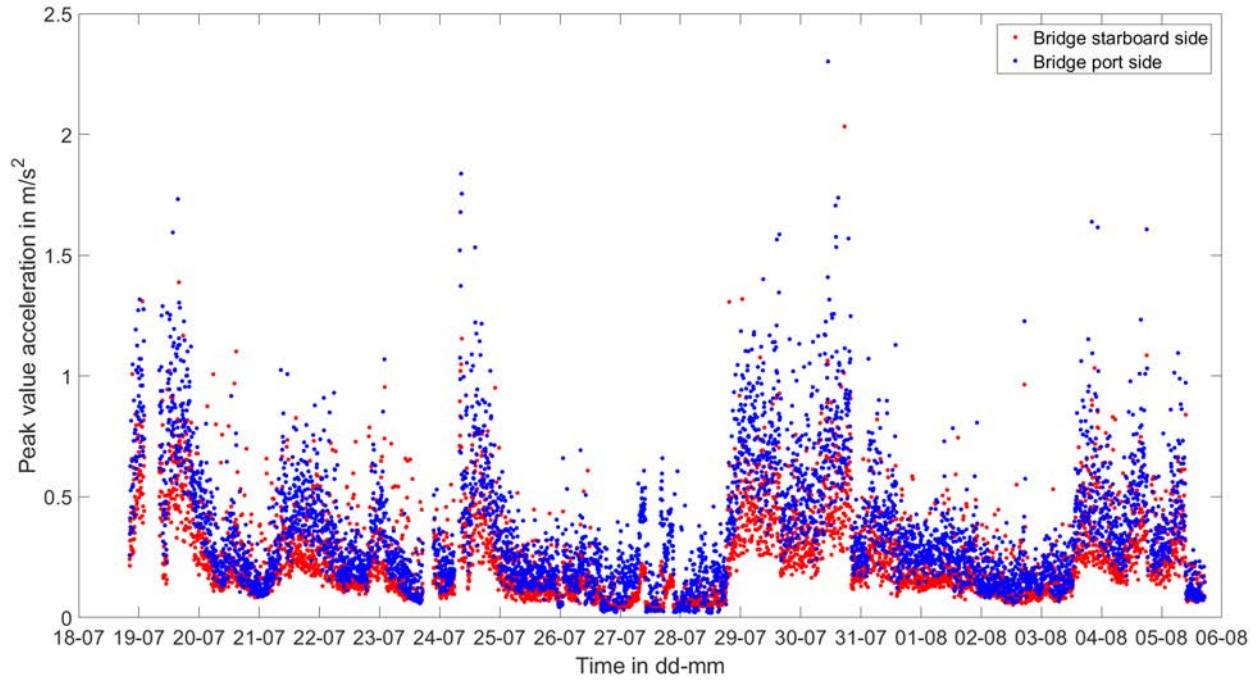


**Figure 16.5:** Frequency weighted peak value acceleration in the Bridge on Winter Cruise 2019

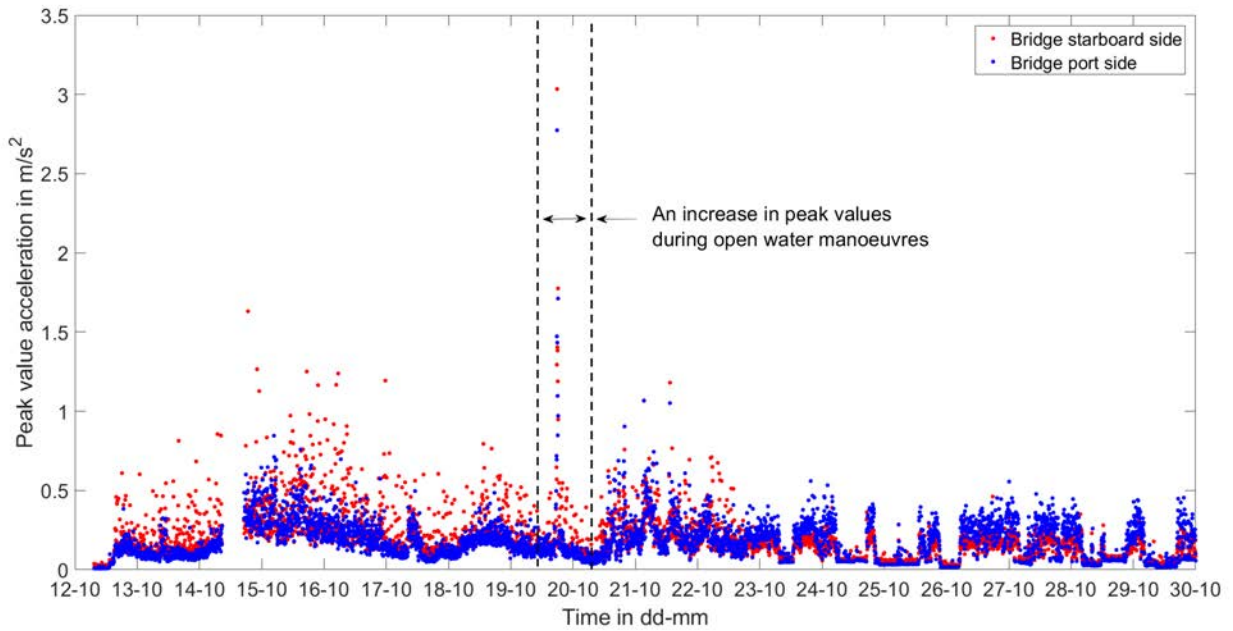


**Figure 16.6:** Frequency weighted peak value acceleration in the Bridge on Spring Cruise 2019

Day 1: Thursday, (18/07/19 08:00) – Friday, (19/07/19 08:00)

1. **Encountered slamming:**  No  Occasionally  Regularly

2. **If you consider slamming on what scale do you experience:**

2.1. 24 – Hour *average* slamming rating

2.2. Rating for slamming induced *vibration*

2.3. Rating for slamming induced *noise*

3. **Which is the main source of your discomfort and/or activity disturbance?**

3.1. **Activities affected by slamming**

4.1. Reason for activity disturbance:

5. **In case of sleep disturbance indicate:**

5.1. Disturbance *rating*:

5.2. How often did slamming *wake* you up?

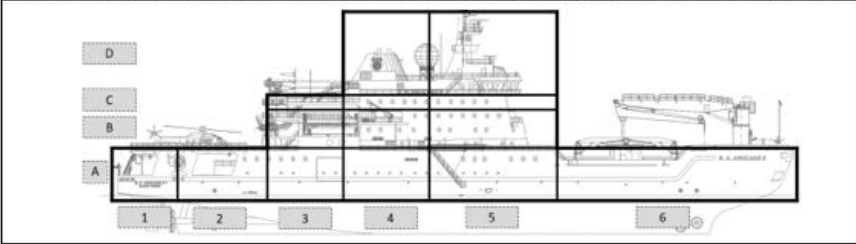
5.3. **Why** did slamming *wake* you?

5.4. Shift *worked*:

5.5. **Time** of disturbance:

5.6. **Comment**:

6. **Indicate three locations where you encountered the most slamming in order of most (1) to the least (3):**



7. **Motion Sickness**

Did you get motion sick?		Did you vomit?		What is your illness rating on a scale of 0-3?			
Yes	No	Yes	No	0 - Nothing	1 - Slight	2 - Moderate	3 - Dreadful
<input type="radio"/>	<input type="radio"/>	<input type="radio"/>	<input type="radio"/>	<input type="radio"/>	<input type="radio"/>	<input type="radio"/>	<input type="radio"/>

Figure 16.7: SCALE Winter Cruise 2019 daily survey

Day 1: Friday, (11/10/19 08:00) – Saturday, (12/10/19 08:00)

1. **Encountered slamming:**  No  Occasionally  Regularly

2. **If you consider slamming on what scale do you experience:**

2.1. 24-Hour *average* slamming rating:  0 - Comfortable  1  2  3 - Uncomfortable  4  5  6  7 - Extremely Uncomfortable  8  9  10

2.2. Rating for slamming induced *vibration*:  0 - Comfortable  1  2  3 - Uncomfortable  4  5  6  7 - Extremely Uncomfortable  8  9  10

2.3. Rating for slamming induced *noise*:  0 - Comfortable  1  2  3 - Uncomfortable  4  5  6  7 - Extremely Uncomfortable  8  9  10

3. **Which is the main source of your discomfort and/or activity disturbance?**

Slamming (vibration and sound when ship hits waves)  Rigid body motion (roll, pitch or yaw of the ship)  Both  N/A

4. **Activities affected:**

	Sleeping	Typing/Writing	Visual Tasks	Equipment Use	Equipment Damage
Slamming	<input type="radio"/>				
Rigid Body Motion	<input type="radio"/>				
Both	<input type="radio"/>				
None	<input type="radio"/>				

4.1. **Reason for activity disturbance:**

	Rate (Frequency) of slams	Magnitude of slams
Yes	<input type="radio"/>	<input type="radio"/>
No	<input type="radio"/>	<input type="radio"/>

5. **In case of sleep disturbance indicate:**

5.1. Disturbance *rating*:  0 - Comfortable  1  2  3 - Uncomfortable  4  5  6  7 - Extremely Uncomfortable  8  9  10

5.2. How often did slamming *wake* you up?  None  Once  More than once

5.3. **Why** did slamming *wake* you?  Yes  No

	Noise due to slamming	Vibration due to slamming
Yes	<input type="radio"/>	<input type="radio"/>
No	<input type="radio"/>	<input type="radio"/>

5.4. Shift *worked*:  08:00 - 12:00  12:00 - 18:00  18:00 - 00:00  00:00 - 08:00

5.5. **Time** of disturbance:

<input type="radio"/>																			
<input type="radio"/>																			

5.6. **Comment:**

6. **Indicate three locations where you encountered the most slamming in order of most (1) to the least (3):**

7. **Motion Sickness**

Did you get motion sick?		Did you vomit?		What is your illness rating on a scale of 0-3?			
Yes <input type="radio"/>	No <input type="radio"/>	Yes <input type="radio"/>	No <input type="radio"/>	0 - Nothing <input type="radio"/>	1 - Slight <input type="radio"/>	2 - Moderate <input type="radio"/>	3 - Dreadful <input type="radio"/>

Figure 16.8: SCALE Spring Cruise 2019 daily survey

## 16.6. Slam observation GUI (Graphical User Interface)

Slam observations were conducted on both SCALE voyages to increase the pool and resolution of the subjective human comfort data. This was performed simultaneously with the ship manoeuvres as described in the Winter and Spring Cruise sections separately. On Winter Cruise the vibration team went to the CTD control room, Deck 7 lounge and Bridge during the ship manoeuvres and used the GUI from Figure 16.9, during Spring Cruise only the bridge was used for the slam observations. The GUI was designed to record the instantaneous time when observers felt a slam and the other questions that went along with it. This data was then saved in separate excel sheets to compare it with the full-scale measurements in the bridge.

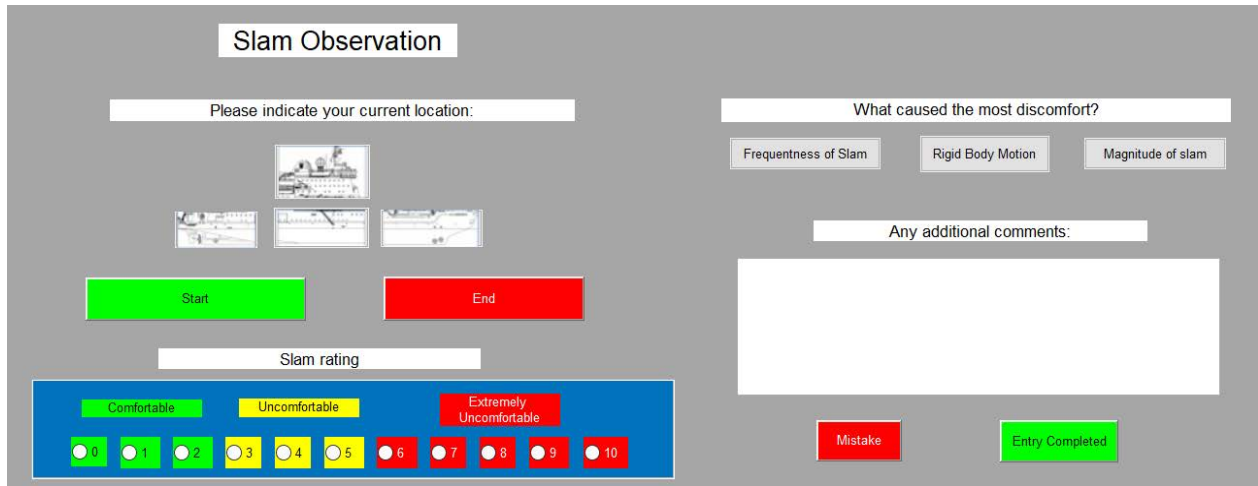


**Figure 16.9:** Slam observation GUI used during both SCALE cruises

### 16.7. Shaft-line

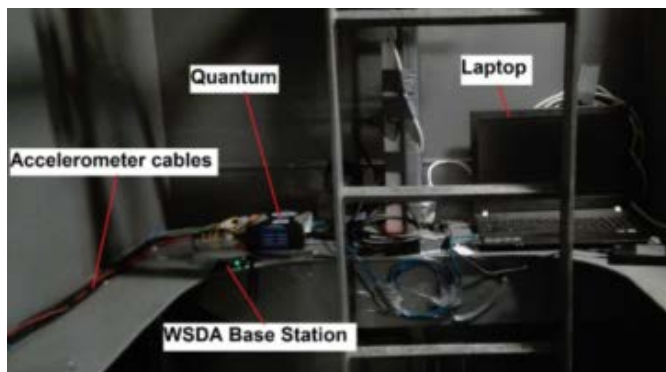


**Figure 16.10:** Shaft-line measurement setup for the SCALE cruises

Accelerometers and strain gauges were used to measure the response of the shaft-line (see figure 16.10). ICP accelerometers were installed to measure the vibration on the bearing housings in all three directions. Pre-installed strain gauges were used to measure the torque and thrust. An HBM QuantumX was used as a data acquisition system and the CatmanEasy software as interface between the laptop and quantum. A V-Link wireless measurement system was used to transmit strain gauge data from the rotating shaft to

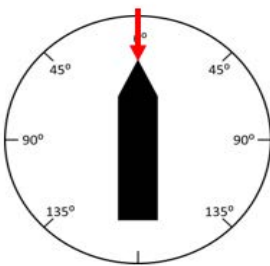
the Quantum for recording. For the Spring Cruise, a tachometer and zebra zape were also installed on the shaft-line in order to record the angular velocity.

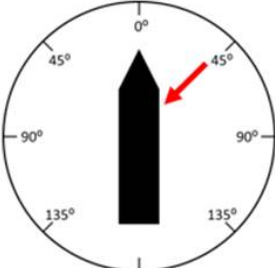
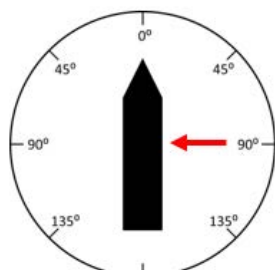
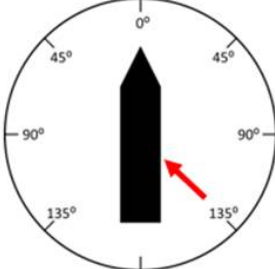
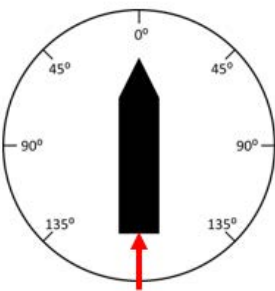
## 16.8. Winter Cruise

During the SCALE Voyage CTD stations, when the ship was stationary (moving at approximately 0 kn) the ship was positioning itself in certain directions. In most cases, the Captain would angle the ship so that the wave angle (heading relative to the ship) was 45° or 135° or 225° or 315°. It was reported that these manoeuvres prevent slamming at the stern during CTD operations. However, these manoeuvres increase the rolling motion of the ship which leads to discomfort for the crew and passengers on board. The Sound and Vibration Research Group (SRVG) has requested that some of these manoeuvres be tested. This was done to determine at which wave angle stern (or bow) slamming occurs. Wave observations were conducted to determine the average wave height, the maximum wave height, the encounter frequency and the ratio of the wavelength to the ship length. The following section summarises the manoeuvres that were conducted.

### 16.8.1. A systematic study of slamming vs relative heading

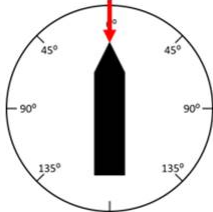
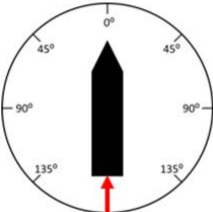
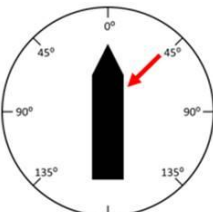
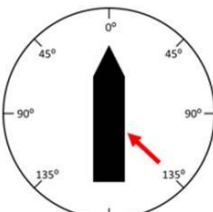
The following manoeuvres were conducted while the ship was stationary  
Ship speed: 0 kn

Manoeuvre	Date and time (UTC)	Wave and slamming observations location
Head on waves 	1/07/2019 08:47	GUI - Bridge Wave observations
	25/07/2019 10:00	GUI - Bridge Wave observations
	29/07/2019 20:00	GUI - Bridge Wave observations
	29/07/2019 16:00	GUI - Stern Wave observations
	22/07/2019 23:30	GUI - Bridge Wave observations
	29/07/2019 20:00 (35°)	GUI - Bridge Wave observations
	30/07/2019 19:30	GUI - Bridge

	02/08/2019 09:00	Wave observations GT6
	02/08/2019 16:49	GUI Wave observations
	22/07/2019 23:00	GUI - Bridge Wave observations
	24/07/2019 08:20	GUI - Bridge Wave observations
<p>Following waves</p> 	24/07/2019 08:00	GUI - Bridge Wave observations

### 16.8.2. A systematic study of slamming vs encounter frequency

The following manoeuvres were conducted while the ship was moving.

Manoeuvre	Ship Speed (kn)	Date and time (UTC)	Wave slamming and observations location
<b>Head on waves</b> 	6	31/07/2019 13:29	GUI - Bridge Wave observations
	8	31/07/2019 13:45	GUI - Bridge Wave observations
	10	31/07/2019 13:30	GUI - Bridge Wave observations
<b>Following waves</b> 	6	02/08/2019 17:20	GUI - Bridge Wave observations
	8	02/08/2019 17:36	GUI - Bridge Wave observations
	10	02/08/2019 17:53	GUI - Bridge Wave observations
	7-9	29/07/2019 09:00 (30°)	GUI – Bridge Wave observations
	6-8	29/07/2019 12:00 (30°)	GUI - Deck 7 lounge Wave observations
	16	03/08/2019 13:00 (0 – 45°)	GUI – Bridge Wave observations
	11.4	21/07/2019 11:40	GUI-Bridge and Stern Wave observations

### 16.9. Spring Cruise

#### 16.9.1. Achieved open water ship manoeuvres

A study of the ship response to well-developed wave states is required to understand the effect that relative heading and the encounter frequency of waves have on wave slamming. To this end, four types of ship manoeuvre tests were performed while the ship was navigating in open water and as described in the subsequent sections. For the manoeuvres, the relative angle at which waves approached the vessel was controlled. The angles predominantly considered are illustrated in figure 16.11, these include angles from  $0^\circ$  for head on waves, to  $180^\circ$  for following waves, in intervals of  $45^\circ$ . A more detailed description of each test is presented below, with reference to table 16.2.

The open water manoeuvres conducted on 18 November 2019 correspond to the time initially allocated to the vibration team for dedicated ship manoeuvres. The vibration team was also grateful to receive additional time for dedicated ship manoeuvres during the glider transect stations.

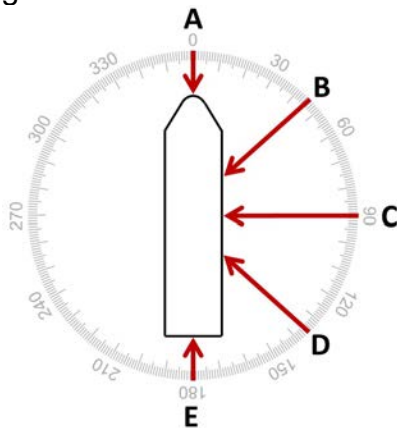


**Figure 16.11:** Relative angle at which waves approach the vessel (A)  $0^\circ$ , (B)  $45^\circ$ , (C)  $90^\circ$ , (D)  $135^\circ$ , (E)  $180^\circ$

**Table 16.2:** Spring cruise operational manoeuvres

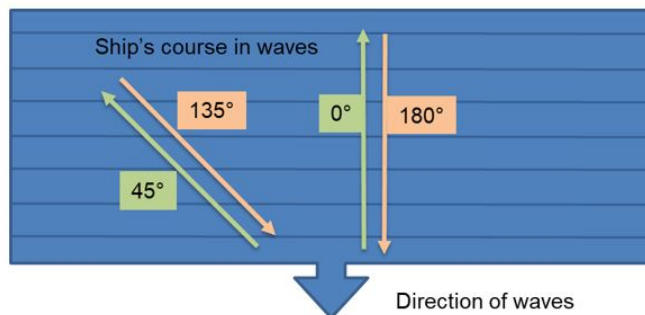
#	Manoeuvre	Date (2019)	Start time	End time	Total time	Relative angle of waves
1	Change in direction (0 knots)	19 October	15:45	17:17	1 hr 32 min	0, 45, 90, 135 and 180°
		20 October	00:13	02:25	2 hr 12 min	
		18 November	11:13	12:43	1 hr 30 min	
2	Change in speed (3,6 and 9 knots)	20 October	15:43	19:32	3 hr 49 min	0, 45, 135 and 180°
		18 November	12:47	16:34	3 hr 47 min	
3	Stop test	21 October	06:22	07:13	51 min	0 and 180°
4	Rudder angle test	21 October	07:19	07:42	23 min	N/A

### Change in direction

The ship is held in a stationary position and the relative angle of the approaching waves is adjusted to each of the relative angles, namely; 0, 45, 90, 135 and 180°. The position is held for a total of 15 minutes at each angle.

This test was repeated three times to be able to analyse whether the results obtained are consistent. On 19 October, after the first glider transect, the first experiment was conducted. On 20 October after the third glider transect the experiment was repeated, using angle intervals of 15°. Therefore relative wave angles of 0, 15, 30, 45, 60, 75, 90, and 105° were considered, which is different to the other tests. Finally, on 18 November the test was conducted for a third time.

### Change in speed



The relative angle of the approaching waves is adjusted to 0, 45, 135 and 180°. At each relative angle the ship travels at a constant speed of 3, 6 and 9 knots consecutively, maintaining the angle relative to approaching waves. The operating conditions are maintained for a total of 15 minutes at each speed and angle. This experiment was repeated twice, one of which took place after the second glider team transect.

### Stop test

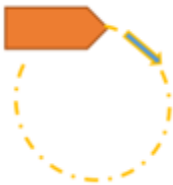


The stop test consisted of two separate tests of a similar nature as described below. Both were conducted after the fourth glider team transect.

3.1. The ship travelled at a constant speed of 8 knots, then the power of the ship was stopped and the time taken for the vessel to slow down and completely stop was recorded. This test was repeated twice, once with the vessel travelling head on into the waves and once with the vessel going back with the waves approaching from behind.

3.2. The ship travelled at a constant speed of 8 knots, then the ship was reversed at full power and the time taken for the vessel to slow down and completely stop was recorded. This test was repeated twice, once with head on waves and once with following waves.

### Rudder angle test



The ship maintained a constant speed of 8 knots and the rudder angle was set to 10°. The time taken for the vessel to turn one full revolution was recorded. This test was recorded for comparison with the rudder angle turning tests conducted in the marginal ice zone. This test was also conducted after the fourth glider team transect.

#### 16.8.2. Achieved ship manoeuvres in the marginal ice zone

To better understand ship-ice interaction events, ship manoeuvres were performed while the ship was navigating between stations in the marginal ice zone (MIZ). Three types of tests were requested and are described in the following sections. All ice manoeuvres were conducted on 2 November 2019.

### Constant speed ice passage

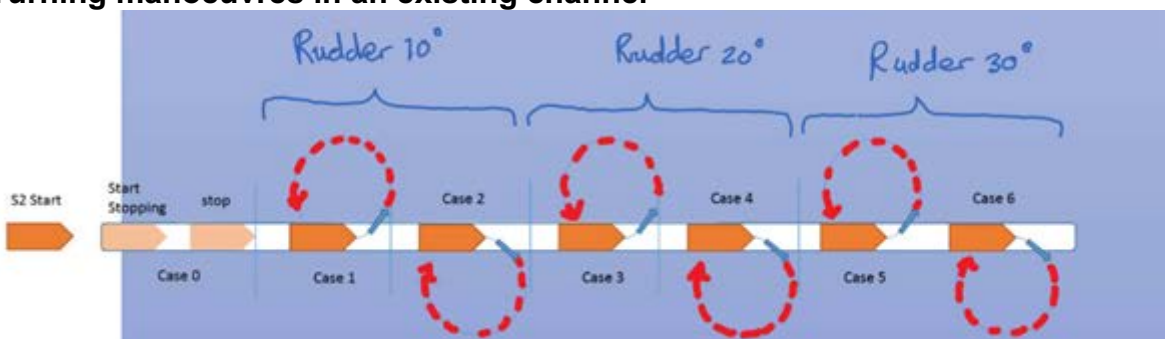


The ship breaks through ice at a constant speed in a straight path. During the manoeuvre, the draught of the vessel, distance travelled and temperature were recorded. The starting and end times as well as the time taken for the vessel to travel three ship lengths was recorded. The speeds were chosen to be 4, 6, and 8 knots.

Case study	Speed (kn)	Time (UTC)
------------	------------	------------

1	4	t0 = 13:51:59 t1 = 14:07:15
2	6	t0 = 14:10:03 t1 = 14:25:18
3	8	t0 = 14:28:24 t1 = 14:43:30

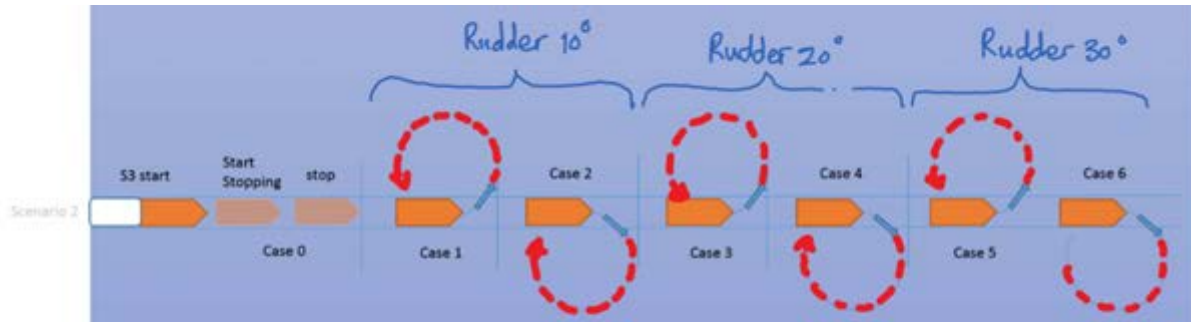
### Turning manoeuvres in an existing channel



The rudder angle was adjusted and the vessel speed was maintained at a constant 6-8 knots. The time taken to complete each quarter of the circular path was recorded. The vessel was set to break out of an existing channel in the ice.

Case study	Speed (kn)	Rudder angle and Direction of turn	Time (UTC)
1	6 - 8	10° Portside	t0 = 17:54:57 t1 = 18:14:20
2	6 - 8	10° Starboard side	t0 = 18:16:04 t1 = 18:36:04
3	6 - 8	20° Portside	t0 = 18:43:22 t1 = 18:55:09
4	6 - 8	20° Starboard side	t0 = 19:02:08 t1 = 19:14:06
5	6 - 8	30° Portside	t0 = 19:20:05 t1 = 19:29:30
6	6 - 8	30° Starboard side	t0 = 19:31:20 t1 = 19:40:57

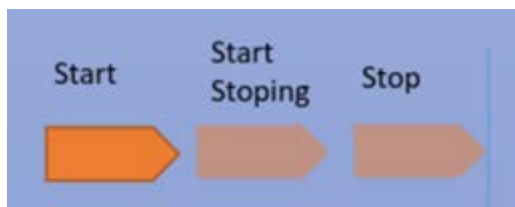
### Turing manoeuvres without an existing channel



The rudder angle was adjusted, and the vessel speed was maintained at a constant 6-8 knots. The time taken to complete each quarter of the circular path was recorded. The vessel was set to turn without any existing channel in the ice.

Case study	Speed (kn)	Rudder angle and Direction of turn	Time (UTC)
1	6 - 8	10° Portside	t0 = 15:23:29 t1 = 15:43:00
2	6 - 8	10° Starboard side	t0 = 14:46:08 t1 = 15:03:35
3	6 - 8	20° Portside	t0 = 16:36:27 t1 = 16:48:49
4	6 - 8	20° Starboard side	t0 = 16:22:01 t1 = 16:34:33
5	6 - 8	30° Portside	t0 = 17:02:51 t1 = 17:11:47
6	6 - 8	30° Starboard side	t0 = 16:50:56 t1 = 17:00:19

### Bringing the ship to a complete stop in the ice



The rudder angle is maintained at 0° and the vessel travels at a constant speed of 6 knots. Two similar tests were then conducted. First, the power of the ship is stopped and the time for the ship to come to a complete stop is recorded. Secondly, the ship reaches a

constant speed of 6 knots, then the ship is reversed at full power and the time for the ship to come to a complete stop is recorded. During the manoeuvre, the draught of the vessel, distance travelled and temperature were recorded. The starting and end times were also recorded.

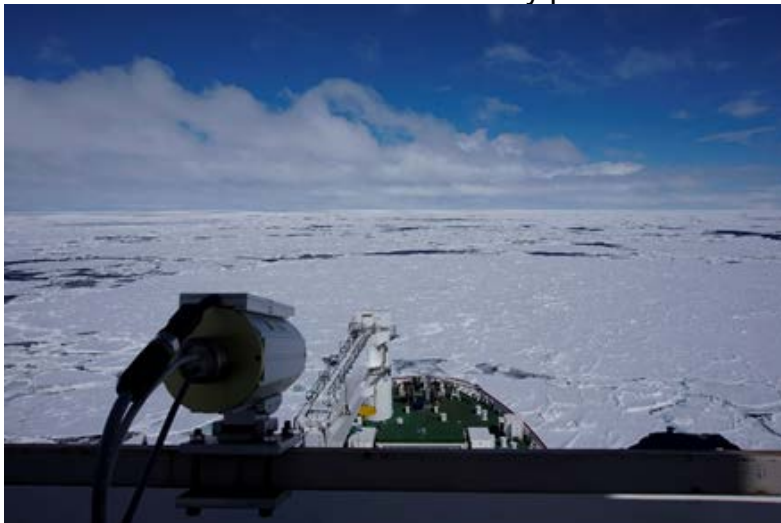
Case study	Time (UTC)
1 - Come to stop by itself	t0 = 17:15:53 t1 = 17:21:06 - 0.5 kn t2 = 17:21:37 - 0.3 kn t3 = 17:21:50 - 0.2 kn
2 - Reverse the ship at full power	t0 = 17:25:19 t1 = 17:27:00

### 16.10. Installation of sea-ice field analysis equipment

In order to continue the development of an automatic sea-ice field analysis tool, a number of cameras and sensors have been installed on decks 9 and 10. Such a tool can provide instantaneous and high rate information of the ice conditions in which the ship is/has been travelling, such as the ice concentration, sea-ice floes sizes and thickness.

#### 16.10.1. Crow's nest observatory deck (Deck 10)

A machine vision camera, IMU and GNSS sensors were installed and set up for recording while navigating in icy waters, as well as in open water. The camera and other sensors were installed outside the observatory platform in deck 10, on a self-made frame:



#### 16.10.2. Monkey deck (Deck 9)

Two additional GoPro cameras and LIDAR were installed on deck 9, in order to determine sea-ice thickness:



**Figure 16.12** depicts new types of sea-ice conditions encountered, providing additional data for making the algorithm more robust.



**Figure 16.13:** Left, pancake ice conditions; right, night conditions with searchlights on.

### **16.11. Acknowledgements**

The Vibration team would like to thank the South African Department of Environmental Affairs (DEA), the crew, officers and Captain Knowledge of the SA Agulhas II represented by African Marine Solutions (AMSOL) for their support, hospitality, interest in our research goals and allowing us to perform measurements and manoeuvres. Furthermore, we would like to thank the National Research Foundation and the Department of Science and Technology under the South African National Antarctic Programme for their support in this research. For providing the opportunity to build relationships with other fellow scientists from all over the world and to exchange valuable insight. We are grateful to the Wave and Sea Ice team for their assistance with regards to making our wave and ice observations more effective. The Stellenbosch University vibration team would also like to thank our collaborators at Norwegian University of Science and Technology (NTNU) and Aalto University. We would like to give gratitude to all the scientists that willingly participated in our human comfort surveys for their interest, time and effort to help conduct our research when they had their own research to do, we truly appreciate it. Chief scientists, Marcello Vichi and last but not least Thomas Ryan-Keogh, even though it was his first cruise as Chief scientist, he managed to do a first class job. We appreciate the

effort both of you put into the planning, organizing and leading of the SCALE voyages. These SCALE voyages were a privilege to be part of and we hope that there will be many more to come.

### **16.12. References**

BS ISO 20283-2:2016 (2016) 'Mechanical vibration - Measurement of vibration on ships Part 2: Measurement of structural vibration'.

BS ISO 2631-1:1997 (1997) 'Mechanical vibration and shock - Evaluation of human exposure to whole body vibration Part 1: General Requirements', BS ISO 2631-1:1997.

## **17. TEAM WAVE**

### **17.1. Scientific background**

The Southern Ocean is warming more rapidly than the rest of the global ocean, as confirmed by the Intergovernmental Panel on Climate Change (IPCC) in its Fourth Assessment Report (Solomon et al. 2007). Recent changes in Antarctic sea ice are a major indicator and driver of warming such as the shrinking sea ice cover observed since 2016, which is the largest anomaly in existing records (Meehl et al. 2019). The Southern Ocean and Antarctic are critical to the global climate, so that understanding the changes they are experiencing and anticipating future changes is of urgent importance. In this regard, improving the performance of Earth System models is a top research priority as it will underpin more robust analysis and diagnosis of climate change and guide international efforts for protecting and conserving Antarctica, the Southern Ocean and neighbouring nations. Current model capabilities, however, are impaired by a lack of direct observations and uncertainties in satellite remote sensing technology, which are critical constraints for fundamental understanding of atmosphere–sea ice–ocean coupled processes and model accuracy.

A sophisticated sea ice model is a key component for contemporary Earth System models, as sea ice plays a crucial role in the climate system by (i) reflecting up to 90% of the solar energy incident on it, which would otherwise be absorbed by the dark ocean it covers, (ii) modulating momentum transfer between the atmosphere and ocean, and (iii) driving thermohaline circulation, which transports cold water towards the equator. Antarctic sea ice is made up of welded and loose floes—discrete chunks of sea ice, with diameters ranging from metres to kilometres—and its large-scale dynamic and thermodynamic behaviours are intimately linked to floe-scale processes. In this respect, the next generation of sea ice models are being developed with the primary goal to incorporate floe-size effects (e.g. Notz, 2012; Bateson et al., 2019; Roach et al. 2018).

At floe scale, the interaction between ocean waves and sea ice floes is crucial. As waves penetrate deep into the ice-covered ocean, the pack ice is forced to break into smaller floes during spring and summer and loose floes are prevented to weld during autumn and winter. Thus, ocean waves have a notable impact on sea ice dynamics, regulating the seasonal sea ice expansion and retreat (the sea ice cycle, e.g. Liu and Mollo-Christensen, 1988; Alberello et al. 2019a; Vichi et al., 2019). Recent southward shifts in storm tracks (Hartmann et al., 2013) has redirected larger waves towards the sea ice edge (Dobrynin et al., 2012), exacerbating effects of wave action on sea ice (e.g. Turner et al., 2017).

Theoretical, numerical and experimental models exist to describe this interaction process. Fundamental physics, however, still remain uncertain due to approximations of current knowledge and lack of direct (in-situ) observations. To fill the gap, joint research by the University of Cape Town, the University of Melbourne (Australia) and the University of Adelaide (Australia) has leveraged on past winter cruises of the SA Agulhas II to conduct unique Antarctic field campaigns to measure floe scale processes such as the propagation of waves in ice, floe size distributions, sea ice concentration and sea ice drift in the marginal ice zone (MIZ), i.e. the outer region of sea ice characterised by loose floes of different size and concentration (Alberello et al., 2019b; Vichi et al., 2019). Although previous campaigns have cast some new light on the ocean physics at high latitude,

additional observations are still needed to achieve a more comprehensive understanding of these floe scale processes. In this regard, a new set of observations of waves, sea ice and their mutual interaction has been gathered during the SCALE 2019 winter and spring cruises to extend the previously collected data bases and form a more robust tool for the investigation of fundamental physics. This new database is complemented with concurrent measurements from the newly launched CFOSAT satellites. Combination of field and satellite data will allow first the calibration and validation of the satellite technology in the marginal ice zone and subsequently support new science to enhance understanding of sea ice-ocean interaction processes.

## 17.2. Activity report

Two main activities were undertaken by the Wave group during the SCALE 2019 cruises: (1) continuous wave and ice measurements with stereographic techniques; (2) observation of ocean surface (skin) temperature with thermal imaging. The latter activity was intended as a trial for the development of an underway autonomous measurement system for sea surface and sea ice temperature.

## 17.3. Stereo vision camera system for wave and sea ice monitoring

### 17.3.1. Equipment

A stereo video technique originally developed by Benetazzo (2006) was applied to measure waves, waves-in-ice and sea ice properties during the entire cruise. The method is based on a pair of industrial cameras that records a video sequence of synchronised and largely overlapping video images of the ocean surface (an example of an image pair in the marginal ice zone is presented in Figure 17.1). By applying binocular photogrammetry techniques, post processing of the image pair allows the reconstruction of the three-dimensional features of a footprint of the ocean surface. Note that the method differs from the traditional stereo-photogrammetric analysis of a single stereo-pair, because the use of video allows a continuous sequence of stereo-images to be digitally sampled and analysed, providing a spatio-temporal description of the sea surface.

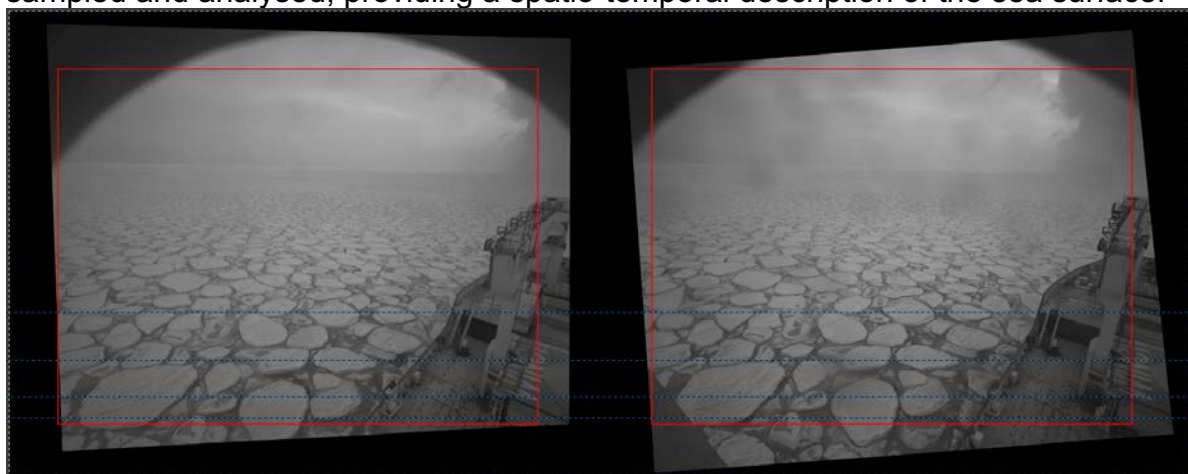


**Figure 17.1:** Example of synchronised image pair in the MIZ. Acquisition system

The camera system comprises of two GigE Monochrome Industrial Camera (2/3" CMOS Global Shutter, 2448 x 2048, 5MP, 3.45um pixels, 38fps, Sony IMX264LLR, 8/12 bits) equipped with 5mm F1.8, Cmount, 10MP, 2/3" lens Goyo. The cameras were installed on the port side of the monkey bridge of the SA Agulhas II (Figure 17.2, panels a and b). The cameras were mounted at a distance of about 4m from each other (see Figure 17.2, panel b). Their longitudinal axes were kept parallel. Both cameras were angled ~25 degrees below the horizon. Considering that the height of the monkey bridge is about 35m from the waterline, this particular configuration allowed observations of a footprint of the ocean extending up to 140m from the ship. This was enough to capture waves outside the area of disturbance of the ship (an example of reconstructed three-dimensional ocean surface is presented in Figure 18.3).

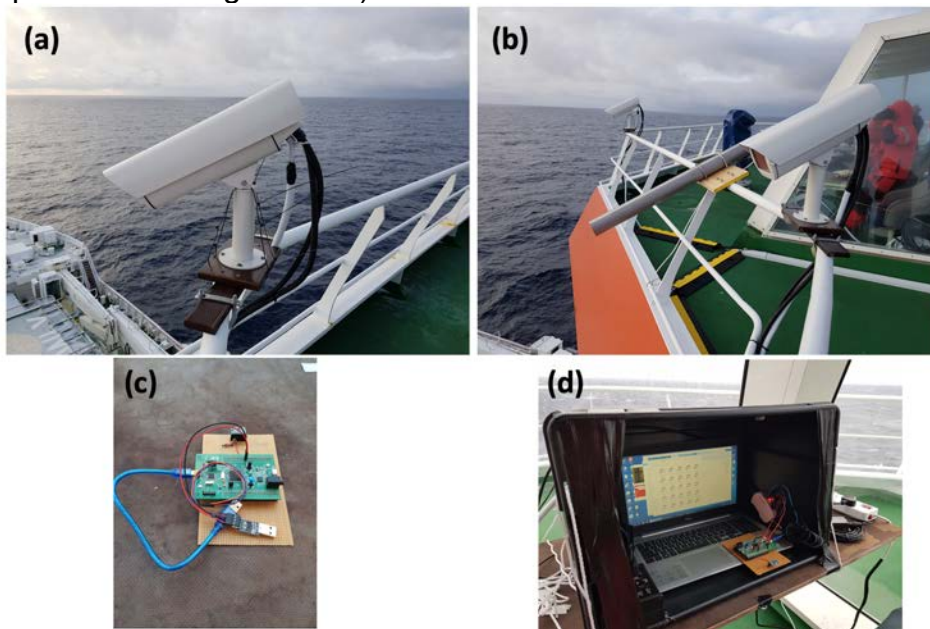


**Figure 17.2:** Industrial cameras installed on the SA Agulhas II (panels a and b); motion sensor unit (IMU, panel c); computer unit for data acquisition (panel d)

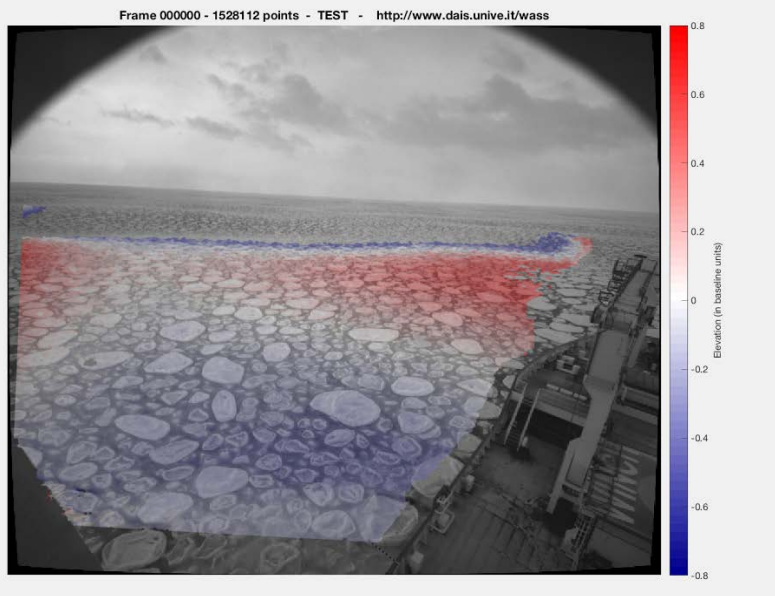


**Figure 17.3:** Example of reconstructed three-dimensional wave field in the marginal ice zone.

A prototype of the stereo camera system was tested during a previous winter cruise in 2017 (e.g. Alberello et al. 2019b). During the SCALE winter cruise 2019, an automated acquisition system was introduced. The cameras were controlled by a laptop computer wired to the cameras (Figure 17.2, panel d). Synchronised pairs of images were acquired at a sampling frequency of 1Hz (1 frame per second). In standard operating conditions, sequences of 20 minutes were recorded continuously during daytime (roughly from 0900 to 1600 UTC in winter and 0800 to 1900 in spring– night recording is not possible with available technology). The particular time length of the sequence allows enough data for the reconstruction of average metocean parameters such as the wave spectrum, the significant wave height, mean periods, etc... (note that the lengths of 20 minutes is a standard requirement from the World Meteorological Organisation, WMO, for metocean observations).

The cameras were operated via a script (MatLab in winter, Python in spring) that controlled the acquisition, the trigger and the frame rate. The spring cruise setup improves on the reliability of the acquisition system. In addition, the script automatically stored the 20 minutes sequences on external hard drives. Two backups of the original acquisition were produced.

Post processing of the images is sensitive to the motion of the ship. In order to eliminate the ship motion, a motion sensor unit (IMU) was installed nearby the cameras (Figure 17.2, panel c and d), and synchronized with the camera acquisition. The IMU was operated at a sampling frequency of 10Hz. This sampling frequency minimises the error in the computation of ship displacements and rotations from the IMU observations (i.e. accelerations and rotational velocities), which are then used to correct the image (i.e. project the image to the original horizontal plane).

### 17.3.2. Image processing and preliminary analysis

Synchronized images are post-processed to reconstruct spatio-temporal information of the sea surface. This is achieved using the Wave Acquisition Stereo System (WASS) freeware software, which is an optimised stereo processing pipeline for sea waves three dimensional reconstruction (<https://www.dais.unive.it/wass/index.html>).

WASS reconstructs the three-dimensional ocean surface. Further post processing based on the Fast Fourier Transformation is applied to extract the energy wave spectrum, from which basic wave parameters can be inferred. An example of the reconstructed ocean surface is presented in Figure 17.3, while directional wave spectra are shown in Figure 17.4.

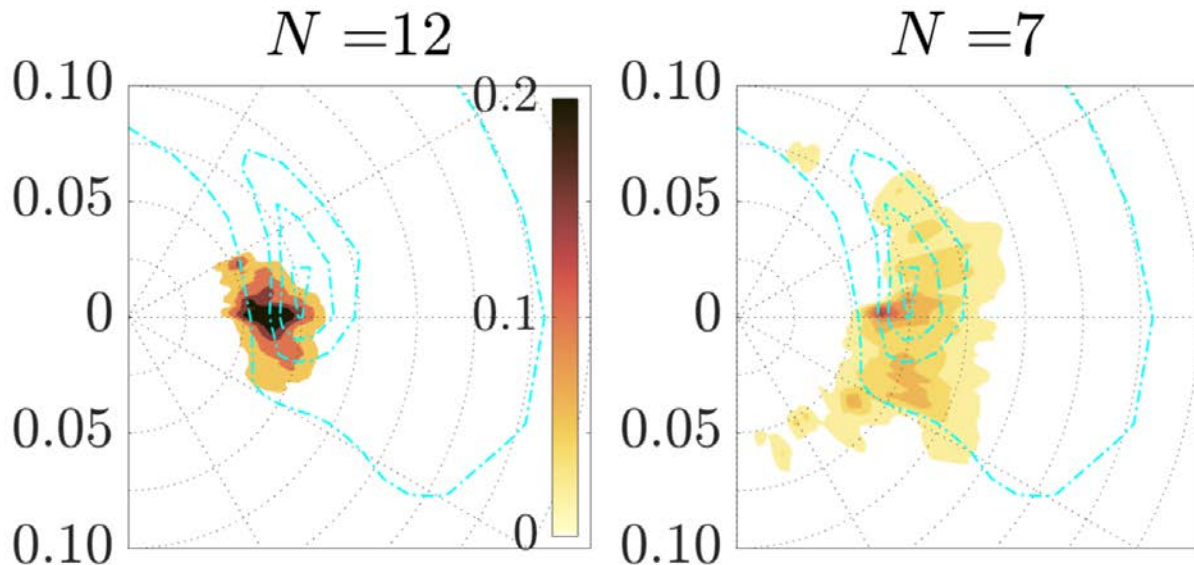


**Figure 17.4:** Examples of reconstructed directional wave spectra in the marginal ice zone (filled contour plot). The blue overlying contours – dashed lines – represent wave spectral condition in the open ocean (i.e., incident wave field).

The aforementioned technique allows the identification of wave motion regardless the presence of sea ice, i.e. allows the ocean surface reconstruction both in the open ocean and in the marginal ice zone. Videos of the ocean surface in the marginal ice zone are also used to identify geometrical characteristics of ice floes, namely the floe size distribution. To this end, an automated algorithm was developed using MatLab Image Processing Toolbox to extract sea ice metrics from the recorded images, by isolating floes from the background frazil ice and water (an example is presented in Figure 18.5, see also Alberello et al., 2019b, for more details).

## 17.4. Thermal camera system for detection of ocean surface and sea ice temperature

### 17.4.1. Equipment

Open ocean and sea-ice skin temperature were recorded using a high-speed infrared camera (FAST M350 TEL-5115), equipped with 13 mm lens. This instrument allowed acquisition of high-speed thermal imaging at a temporal resolution up to 44Hz, enabling

the detection of challenging targets such as breaking wave events in the open ocean and pancake-like floes in the marginal ice zone. Accuracy of sea surface temperature is 0.01 K. The camera was mounted on a tripod and operated from deck 7 (~28 m above the ship's bow line) at port side (figure 6).

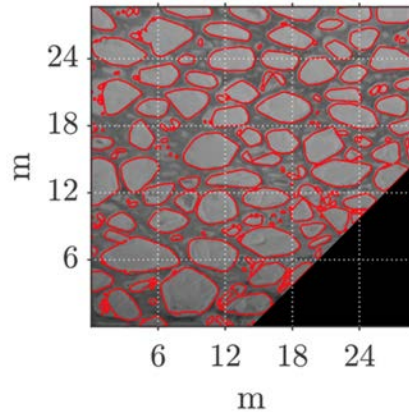


**Figure 17.5:** Detection of ice floes from acquired image (Alberello et al. 2019b)



**Figure 17.6:** High-speed infrared camera for thermal imaging

As the camera lens cannot be obscured by any protective screen (plastic, glass or similar) to avoid biases in temperature measures, the use of conventional protecting enclosures was not possible, preventing automatic underway acquisitions. To protect the camera from the harsh Southern Ocean winter conditions, it was mounted and unmounted at regular intervals and manually operated (Figure 17.6).

In the marginal ice zone, the infrared imaging was applied to retrieve the thermal structure and geometry of the water-frazil-pancake ice continuum (see Figure 17.7, panel a). To this end, the camera was operated continuously (at 2 Hz) during the transient from the entrance into the marginal ice zone and compact ice.

In the open ocean, the aim was to identify the thermal signature of whitecaps and breaking waves. A portion of the sky was captured to infer air temperature and enable estimation of air-sea boundary layer stability (see Figure 17.7, panel b). Measurements of open ocean was carried out twice a day (morning and afternoon) for the acquisition of 10 minutes sequences.

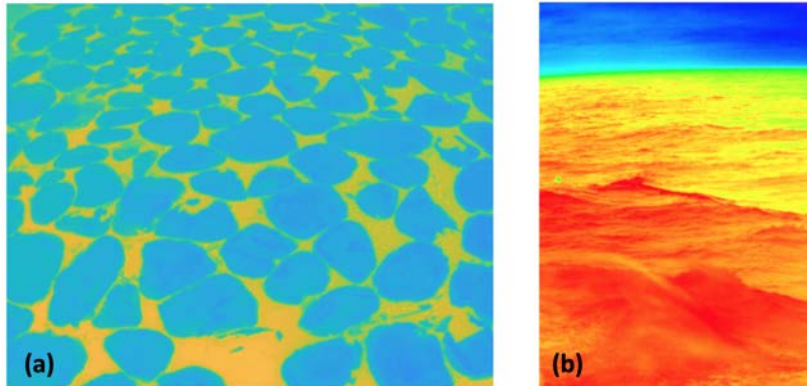


**Figure 17.7:** Examples of thermal imaging: marginal ice zone (panel a); and open ocean (panel b).

#### 17.4.2. Preliminary analysis

Infrared images are post-processed using MatLab and specific functions capable of reading \*.hcc files. Such functions return a matrix of pixels, the value of which is the sea surface temperature (the unit of temperature is Kelvin).

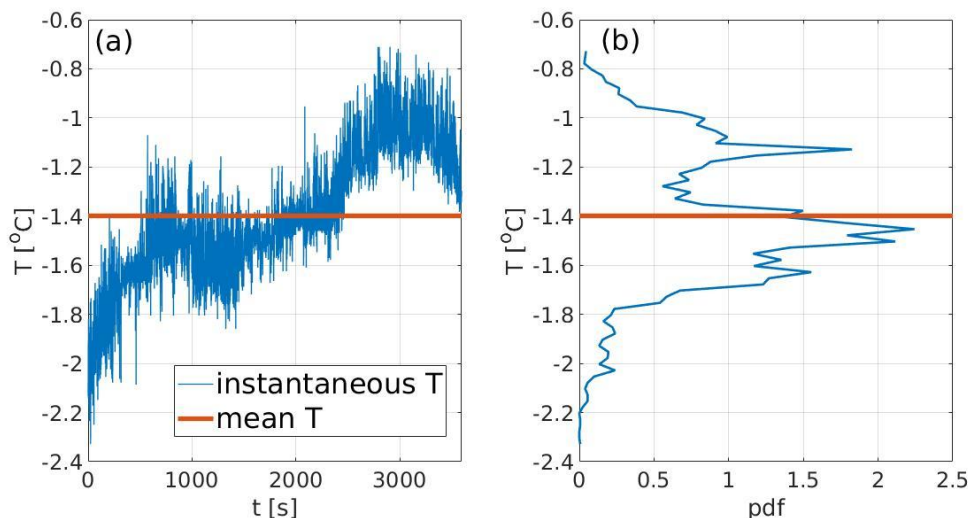


**Figure 17.8:** Example of temperature measured over 1 hour in the marginal ice zone (panel a) and corresponding probability density function (panel b) which highlights the bimodal structure of the surface temperature (the peak at higher temperature is representative of water, the one at lower temperature of ice floes).

#### 17.5. Satellite observations from the CFOSAT mission

The University of Cape Town, the University of Melbourne and the University of Adelaide are part of the calibration and validation team of the newly launched satellite mission CFOSAT. This is a joint mission of the Chinese (CNSA) and French (CNES) space agencies with the goal to monitor the ocean surface winds and waves and to provide information on related ocean and atmospheric science and applications.

Satellite observations – wave spectra, integrated parameters such as significant wave height and peak wave period, ice concentration and ice thickness – have been downloaded for coordinates (latitude, longitude and time) matching ship-borne measurements. An example of an energy wave spectrum recorded from CFOSAT is presented in figure 17.8.

In the post-processing phase satellite and field (ship borne) data will be combined to validate the former. After validation, we will leverage on the global availability of satellite observations to complement field data and extend the investigation of sea ice dynamics to global scale. Combination of satellite and field data will therefore allow interconnection between small- and large-scale processes.

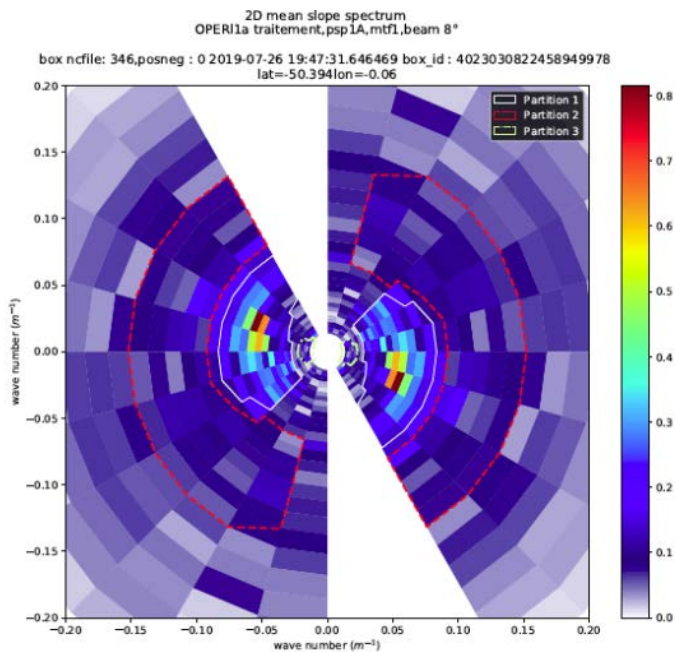


**Figure 17.9:** Example of directional wave energy spectrum detected nearby the SA Agulhas II on July 26<sup>th</sup>, 2019, at 19:47 UTC.

## 17.6. Conclusions

A system of stereo cameras was installed on the SA Agulhas II and operated during the SCALE 2019 winter and spring cruises. Instrumentation monitored continuously the ocean surface to infer information on surface waves (particularly the energy wave spectrum) in both the open ocean and the marginal ice zone. Stereo images were also used to detect geometrical properties of ice floes to infer floe size distribution.

An infrared camera was used to measure sea surface temperature from the ship. In the open ocean, measurements consisted in the skip temperature of surface water and heat exchange during wave breaking. In the marginal ice zone, measurements provided

information on the thermal properties of pancake ice, interstitial frazil ice and water between ice floes.

Finally, the database has been complemented by satellite measurements from the newly launched satellite mission CFOSAT. Observations consist of basic wave parameters (wave spectrum and average parameters) and sea ice properties such as the concentration and thickness.

## 17.7. References

Alberello, A., Bennetts, L., Heil, P., Eayrs, C., Vichi, M., MacHutchon, K., Onorato, M., and Toffoli, A. (2019a) Drift of pancake ice floes in the winter Antarctic marginal ice zone during polar cyclones. Submitted to *J. Geophys. Res. Oceans.* – available at <https://arxiv.org/abs/1906.10839>

Alberello, A., Onorato, M., Bennetts, L., Vichi, M., Eayrs, C., MacHutchon, K., and Toffoli (2019b). Pancake ice-floe size distribution during the winter expansion of the Antarctic marginal ice zone. *The Cryosphere*, 13(1):41–48. doi: 10.5194/tc-13-41-2019.

Bateson, A. W., Feltham, D. L., Schröder, D., Hosekova, L., Ridley, J. K., & Aksenov, Y. (2019), Impact of floe size distribution on seasonal fragmentation and melt of Arctic sea ice. *The Cryosphere Discuss.*, <https://doi.org/10.5194/tc-2019-44>.

Dobrynin, M, Murawski, J. and Yang, S. (2012), Evolution of the global wind wave climate in CMIP5 experiments. *Geophysical Research Letters* 39, L18606.

Hartmann, D. L. et al. (2013), The Physical Science Basis, in *Climate Change 2013*, eds Stocker, F. F. et al., 159 – 254, Cambridge University Press..

Liu, A. K. and E. Mollo-Christensen (1988), Wave propagation in a solid ice pack, *J. Phys. Oceanogr.*, 18(11), 1702-1712.

Meehl G.A. et al. (2019), Sustained ocean changes contributed to sudden Antarctic sea ice retreat in late 2016. *Nat. Commun.*, 10(1), p.14.

Notz D. (2012), Challenges in simulating sea ice in Earth System Models. Wiley *Interdisciplinary Reviews: Climate Change*, 3(6), 509-526.

Roach L.A., Dean S.M., and Renwick J.A. (2018), Consistent biases in Antarctic sea ice concentration simulated by climate models. *The Cryosphere*, 12(1):365–383, doi: 10.5194/tc-12-365-2018.

Solomon S. et al. (2007), *Fourth Assessment Report of the Intergovernmental Panel on Climate Change*, <https://www.ipcc.ch/assessment-report/ar4/>.

Turner, J., Phillips, T., Marshall, G. J., Hosking, J. S., Pope, J. O., Bracegirdle, T. J. and Deb, P. (2017), Unprecedented springtime retreat of Antarctic sea ice in 2016. *Geophysical Research Letters*, 44(13), 6868-6875

Vichi, M., Eayrs, C., Alberello, A., Bekker, A., Bennetts, L., Holland, D., de Jong, E., Joubert, W., MacHutchon, K., Messori, G. and Mojica, J., (2019), Effects of an explosive polar cyclone crossing the Antarctic marginal ice zone. *Geophysical Research Letters*, 46(11), 5948-5958.

## **18. TEAM WHALES**

### **18.1. Abstract**

Between the 12th of October and the 19th of November in 2019, the SCALE (Southern Ocean Seasonal Experiment) spring cruise was performed. A line-transect cetacean survey in the ice-edge area between 024°E to 000° of longitude was proposed as part of the experiment, given the little knowledge of the cetaceans occurrence and distribution in the area during this time of the year. In addition, observations were performed during the transit to and from the proposed area, making maximum use of the opportunity of covering such a considerable area that can include part of migration areas for baleen whale species that perform seasonal migrations. In the Southern Hemisphere, these migrations occur between breeding grounds in low and medium latitudes, where individuals stay mainly during winter months, and feeding grounds in high latitudes, where they are found during summer time. A total of 165.65 hours of observations were performed during the cruise. 84 sightings of an estimated 272 individuals were recorded by the research team. Eight different species of cetacean could be identified. The most common species in number of sightings (groups) was humpback whale (n=29), followed by minke (n=8) and long-finned pilot whales (*Globicephala melas*) (n=5). It was not possible to identify the species of 32 of the sightings. Weather conditions were impeditive for a better data collection, as they were not favorable for observations in a considerable number of days during the cruise. However, cetacean data collection during SCALE was successful and data will be analyzed in the near future.

### **18.2. Introduction**

The majority of baleen whales species undertake long and seasonal migrations between summer feeding grounds in high latitudes and winter breeding grounds in tropical and subtropical regions (Cummings, 1985). These are the blue (*Balaenoptera musculus*), sei (*Balaenoptera borealis*), fin (*Balaenoptera physalus*), minke (*Balaenoptera acutorostrata*), humpback (*Megaptera novaeanglie*) and southern right (*Eubalaena australis*) whales. Given such migrations, the number of whales found in the Southern Ocean fluctuates considerably along the year, even though some other cetaceans' species can be in the area all year-round, as the killer whale (*Orcinus orca*). Peak numbers of baleen whales in Antarctic waters tend to happen annually from January to April. Blue whales generally arrive earlier, followed by fin whales, humpback whales then sei whales (Shirihai & Kirwan, 2007).

The timing and distribution of annual whale migrations between northern breeding grounds and southern feeding grounds in the Southern Hemisphere is influenced by a number of factors, including sea surface temperature (SST), depth, sea ice extent, predation risk, and productivity and food abundance (e.g. Avgar *et al.*, 2013; Cherry *et al.*, 2013).

In general, cetacean species in Antarctica are believed to be impacted by climate change mainly indirectly, as a consequence of alterations in sea ice patterns and in the availability of Antarctic krill *Euphausia superba* (Nicol *et al.*, 2008). This occurs because most baleen whales (including blue, fin, sei, humpback, and minke) in the area forage almost

exclusively on Antarctic krill (Mackintosh, 1965; Gaskin, 1982; Kawamura, 1994), which is considered a key species in the Southern Ocean ecosystem (Atkinson *et al.*, 2009). In the last decades, the availability of this food resource might have been affected by climate variability such as the warming that is observed mainly in the western Antarctic Peninsula (WAP) (Atkinson *et al.*, 2004; Moline *et al.*, 2004).

Although different research projects have been investigating cetaceans in the Southern Ocean, there are still many gaps of knowledge regarding these animals. Few research cruises dedicated to cetacean monitoring have been done in the Southern Ocean during spring season, so little is known about the species in the area at this time of the year, and also their distribution and abundance in the region. In addition, knowledge of species distribution and abundance in the Southern Ocean generally is limited as dedicated cetacean surveys consume significant amounts of ship time, are personnel intensive and hence rather costly (Burkhardt & Lanfredi, 2012).

Among information about cetaceans in Antarctic, that are the results from the IWC IDCR/SOWER cruises (e.g. Ensor *et al.*, 2008) that identified the region between 020°E–000°E as a whale ‘hotspot’ during the austral summer months. The same stretch of longitude area was investigated in summer 2014 (Findlay *et al.*, 2014). Considering this, it was planned that the same area would be included in the SCALE spring cruise so it could be investigated at a different time of the year than previously done.

Habitat modelling can be used for the investigation of cetaceans’ distribution and habitat use (Bailey & Thompson, 2009; Silber *et al.*, 2017). Previous studies have investigate the influence of environmental variables on the distribution and habitat use of baleen whales in the Southern Ocean (e.g., Friedlaender *et al.*, 2006; Beekmans *et al.*, 2010; Santora *et al.*, 2010; Bombosh *et al.*, 2014). Some of them found that physical features such as fronts, eddies and bathymetry, that are known to influence krill distribution and density in NAP, as Bransfield Strait (Wilson *et al.*, 1999; Thompson *et al.*, 2009), are influencing whale distribution. Bathymetry features may provide krill retention in certain regions, making it possible to predict feeding areas used by these animals (Croll *et al.*, 2005).

The Whales and Climate Research Program has been developed since 2018 as a partnership between Australia and South Africa with the main aim of establishing a fundamental understanding of the relationships between ocean temperatures, ocean circulation, ocean biogeochemistry, and recovering whale populations. An investigation on whales occurrence and distribution in the ice margin and also on the way from South Africa to and from this area in then aligned to the scope of the project and can potentially provide information on the migration of humpback whales and other baleen species that can be found in the area planned for the SCALE spring cruise.

The SCALE represented then a great opportunity for contributing to this issue. In doing this during the spring cruise, we are covering a time of year that has been poorly investigated regarding cetaceans occurrence and distribution. For the winter cruise there was no Whale Team participating on the SCALE given the low number of whales in Antarctic waters in this time of the year and due to the very short days (few daylight hours), preventing cetaceans observations.

### **18.3. Cruise Plan**

The SCALE voyage was performed by the ice breaker *SA Agulhas II* and was divided into four legs:

1. A southwest journey conducted from Cape Town to the 000°E of longitude and to consolidated area ice around the 60°S (with oceanographic stations on the way);
2. An ice research and seal tagging leg (including oceanographic stations), conducted in the ice at around 60°S from 000° to 024°E of longitude;
3. A whale survey, conducted 5nm away from the ice-edge from 024°E to 000° of longitude (with three oceanographic stations); and
4. A northeast journey (also with oceanographic stations) from the 000°E of longitude to Cape Town.

Although the name of one of the legs is referred to a 'whale survey', observation the cetacean monitoring were planned for the whole trip, whenever conditions allowed to, as described in the Research Methodology session later in this report.

#### **18.4. Research Methodology**

The research conducted during the SCALE expedition involved a visual line-transect aimed to get data to the investigation of the cetaceans in the ice-edge area from 024°E–000°E and in the area navigated to and from the ice-edge (i.e. in all cruise legs previously described in this report) during spring season and to the estimation of the abundance of most common species. The survey design was planned to perform a whale transect in a distance roughly 5nm from ice-edge. For this study the ice-edge was defined as conditions that caused the ship to decrease speed or change course for any length of time.

Observation effort was done whenever the conditions allowed to, regardless of the area in which the vessel was sailing. Favorable conditions included daylight, sea state from 0-5 in the Beaufort scale, ice coverage lower than 70% in the monitored area, and adequate sightability (please see 'Environmental Data' session below for further details). In addition, the ship would need to be navigating at a speed of at least 6knots.

Survey activities were classified as on-effort and off-effort. On-effort activities occurred when full search effort was executed on track line and under acceptable environmental conditions. Off-effort activities were activities that occur at all other times, for example when the vessel was not underway or when weather conditions were unfavorable (e.g. sea state higher than 5 in the Beaufort scale). Independent of the effort type, the observations were always performed in the passing mode, i.e., no closure was attempted to approach the whales.

The sighting survey was carried out from two platforms. The platform classified as on-effort was located in the crow's nest of the vessel at a position of 27 m above sea level. This observation platform was used for the majority of the survey. A secondary observation platform, classified as off-effort, was located on the monkey island, directly above the bridge, located 23.55 m above sea level.

There were three observers on board (Fig. 18.1). For on-effort observations, two observers were on watch at all times, one seated in a starboard and other in a portboard position. Each one monitored a 90° area for the bow of the vessel to its respective port. The third observer was in a resting position, and could help in data record and species identification in some cases. Rotations between the observers positions were done every

1:30h following the order portboard, starboard and resting positions. For off-effort observations, one to three observers were at the observation point seating in a position that allowed the visualization of an 180° area around the vessels' bow.



Figure 18.1: Observers that composed the Whale Team on board *SA Agulhas II* for the SCALE spring cruise while performing observations from the crows' nest in an area close to the ice-edge (a). They were, namely, from left to right, Sanne Paarman, Jeffrey Slater and Elisa Seyboth (b).

Searching was carried out using reticulated binoculars and naked eye. Observers searched for cues such as a splash, blow or body of a cetacean. All search effort and all cetaceans spotted were logged.

Data collected was divided into four types, namely environmental data, effort data and sighting data. Each type of data was recorded in a separate form.

### *Environmental Data*

Environmental conditions were recorded in the Weather Record forms using a consistent methodology. This record was completed on a daily basis every hour from 7:00AM to 7:00PM or from before/to after that if the conditions were favorable for observation out of this general standard period.

The recorded information included the time, position of the vessel, weather general condition, wind speed and direction, SST, visibility, sea state (Beaufort scale), swell and sightability.

Weather conditions were chosen among blue sky (0-20% cloud coverage - 01), partly cloudy (21-80% cloud coverage - 02), cloudy (81-99% cloud coverage - 03), overcast (100% cloud coverage - 04), rain (05), mist (06), fog (07), fog patches (08) and drizzle (09).

Visibility was recorded as how good was the condition to monitor the area from the ship to the horizon, being classified as 1 (poor), 2 (moderate), 3 (good) or 4 (excellent).

Sea state was recorded in the Beaufort scale. This scale accounts for conditions of the waves and wind. Observers selected codes from 0 (calm) to 9 (high breaking waves).

Swell was recorded in the International Scale where observers noted the general swell, wavelength and height of waves as a rating from 0 to 9.

Sightability was recorded as a subjective impression of the conditions for spotting whales, taking into account all factors that affect it, including all the previous described (weather condition, visibility, sea state and swell). Observers selected codes ranging from 1 (very poor) to 5 (excellent).

### *Effort Data*

All data relevant to the observation activities (on and off-effort) were recorded in the Effort Record forms.

Codes included beginning on-effort observations (BP), beginning off-effort observations (OE), transit without full search effort (TD), drifting (DR), ST (ship stopped for an activity). The end of the research for the day (ED) was the last code on a daily effort record. The Effort Record forms also included the date and time as well as the position, course and speed of the vessel. These data allowed the computation of time, distances covered and the location of all activities.

### *Sightings Data*

For each sighting the observer recorded a variety of data. The cruise serial number was recorded as well as the vessel's code from where the sighting was made. The date of the sighting was recorded as YYMMDD. Every day, each sighting was allocated a chronological sighting number starting with 001.

The sighting type in relation to search effort was recorded as on-effort or off-effort. The local ship time at which the sighting was first made was recorded as the sighting time. The sighting in relation to the vessel's trackline was recorded as dead ahead (A), dead astern (B), port (P) or starboard (S).

An angle board was used to determine the estimated angle from the bow of the vessel to the sighting. The angle is estimated at the moment of the first sighting and recorded as degrees port or starboard from the bow. Where sightings are observed again later, a second estimated angle is recorded. The estimated distance from the observer to the sighting at the sighting time was recorded using reticulated binoculars. Both angle and distance are essential information for the analyses of the data for abundance estimation. The sighting cue (blow, jump or splash, animal, slick or ring, blow and animal, color under water or associated fauna) that alerted the observer to the sighting was recorded using a variety of codes.

A numeric code was used to identify cetacean species (see Table 1 in the appendix). If it was not possible to identify the species, but the sightings displayed characteristics of a specific species, it was registered as "Like" a species, for example species code 71 "Like humpback whale". Some sightings could not be identified and were thus listed according to size, for example species code 64 "Unidentified large baleen whale". Where no sign of size or other characteristic could be identified, the sighting was recorded as species code 9 "Whale".

The group size (lower, best, higher) as estimated for each sighting.

The observer who made the sightings records where the sighting was made as well as his or her initial. OT (other) were used as the initials of the observer in case it was done opportunistically by a member of another team on board – all sightings made in this

circumstance was considered as off-effort. Whenever possible, sightings were photographed for photo-id purposes.

## 18.5. Results

### *Research Effort*

A total of 165.65 hours of observations were performed during the cruise. From this total, 83.17h were on on-effort mode while the other 58.58h occurred on off-effort mode. The breakdown of research time is shown in Table 18.1.

Table 18.1: Breakdown of time spent on survey activities. A reason is indicated for the days when it was not possible to perform observations.

<b>Date</b>	<b>On Effort (min)</b>	<b>Off Effort (min)</b>	<b>Total time (min)</b>	<b>Comment</b>
13-Oct	481	0	481	
14-Oct	0	0	0	Weather too poor to survey
15-Oct	0	0	0	Weather too poor to survey
16-Oct	197	0	197	Vessel stopped
17-Oct	414	46	460	Vessel stopped
18-Oct	118	0	118	Weather became too poor to survey
19-Oct	0	0	0	Weather too poor to survey
20-Oct	51	0	51	Weather became too poor to survey
21-Oct	0	0	0	Weather too poor to survey
22-Oct	0	0	0	Weather too poor to survey
23-Oct	0	0	0	Consolidated ice cover >70%
24-Oct	0	0	0	Consolidated ice cover >70%
25-Oct	0	305	305	

26-Oct	0	750	750	
27-Oct	0	420	420	
28-Oct	0	0	0	Consolidated ice cover >70%
29-Oct	0	0	0	Consolidated ice cover >70%
30-Oct	0	0	0	Consolidated ice cover >70%
31-Oct	234	403	637	Off effort/Casual observations (Ice cover >70%)
1-Nov	0	0	0	Vessel stopped
2-Nov	0	423	423	Vessel stopped for seal tagging
3-Nov	276	0	276	Vessel stopped
4-Nov	593	0	593	Vessel stopped for frazil ice collection
5-Nov	644	108	752	Vessel stopped for safety drill
6-Nov	694	125	819	Vessel stopped for safety drill
7-Nov	0	521	521	
8-Nov	0	346	346	
9-Nov	0	0	0	Weather too poor to survey
10-Nov	0	338	338	Vessel stopped
11-Nov	0	371	371	
12-Nov	152	159	311	Vessel stopped
13-Nov	0	0	0	Weather too poor to survey

The distribution of survey effort during the survey is shown in Figure 18.2 below.

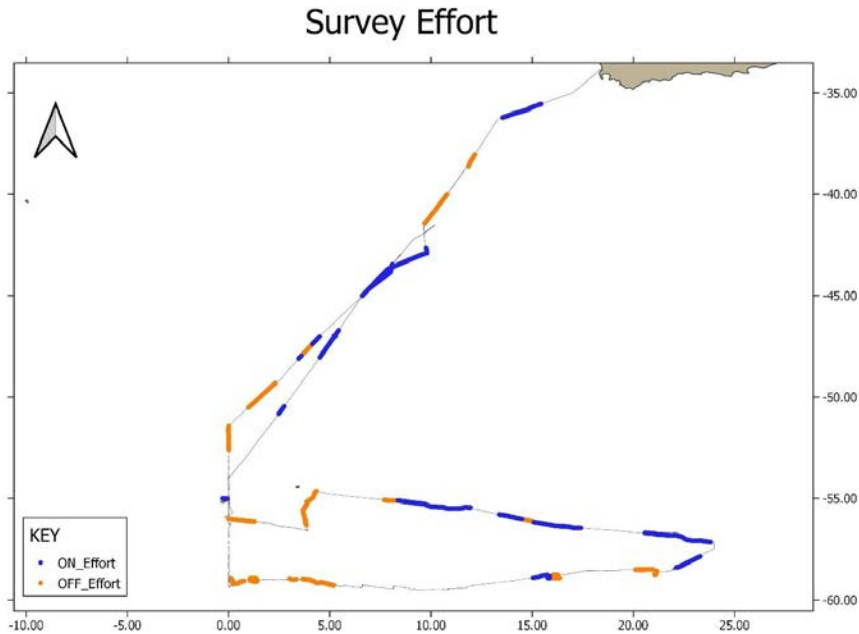


Figure 18.2: Map with the trajectory of the ship during the SCALE spring cruise, with the indication of on (in blue) and off-effort (in orange) observations for cetaceans monitoring.

### *Weather Conditions*

An assessment of the weather conditions was conducted and recorded every hour, including times when survey effort was not carried out.

Figures 18.3 to 18.7 show the frequency of the occurrence of the different conditions that are related to detectability of the whales, including weather, wind speed, visibility, sightability and sea state. As can be seen, overcast and cloudy conditions accounted for most general weather conditions. Moderate visibility was the most common during the whole cruise. Beaufort scale 6 was the most common sea state condition registered. Low swell (less than 2m high) with short-average wave length was another frequent condition found during the cruise. Given these limited conditions for observations, sightability was considered as very poor in most of the evaluations, but it was rated as good or excellent in some occasions. There is a disparity in the total number of records among the mentioned environmental conditions because during the period in the ice area, we couldn't evaluate some of them, as sea state and swell.

Wind speed and direction are not being presented as the values recorded in the SDS system of the vessel are not correct. We will wait for the corrected version of the data to then include in the data base and in the results.

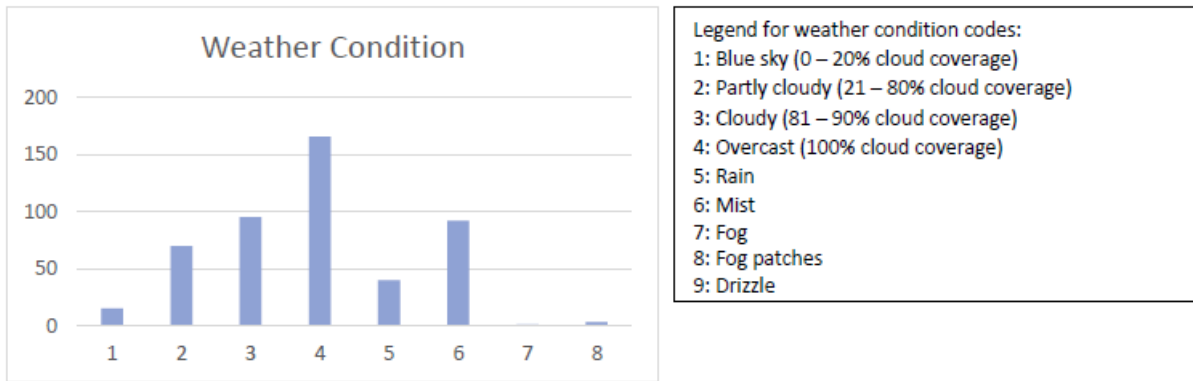


Figure 18.3: Frequency of occurrence of weather conditions during the SCALE spring cruise.

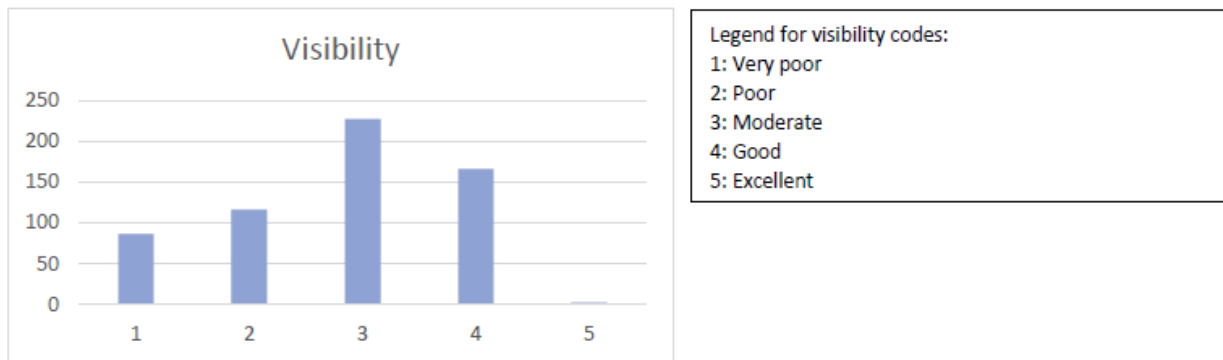


Figure 18.4: The frequency of each rating of visibility during the SCALE spring cruise.

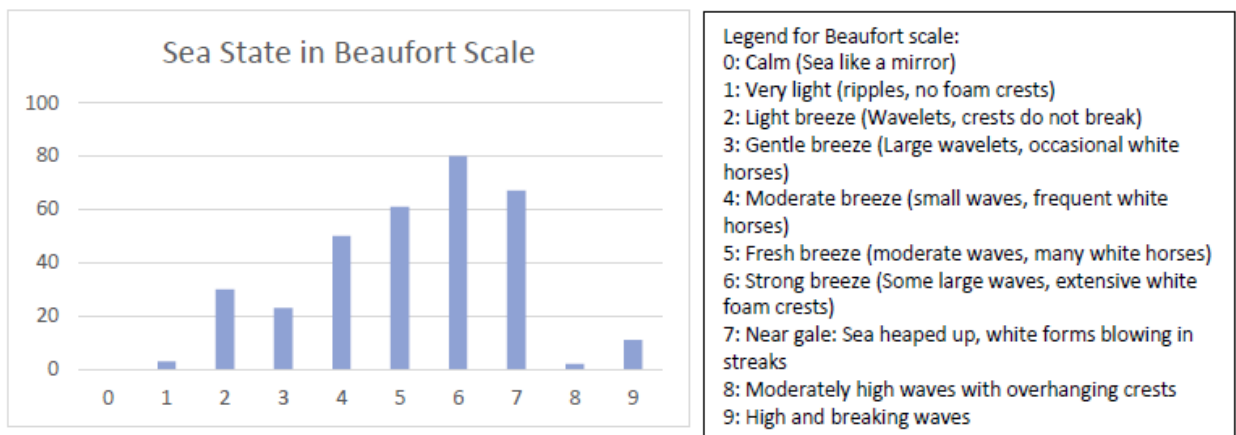


Figure 18.5: Frequency of occurrence of different sea state conditions following the Beaufort scale during the SCALE spring cruise.

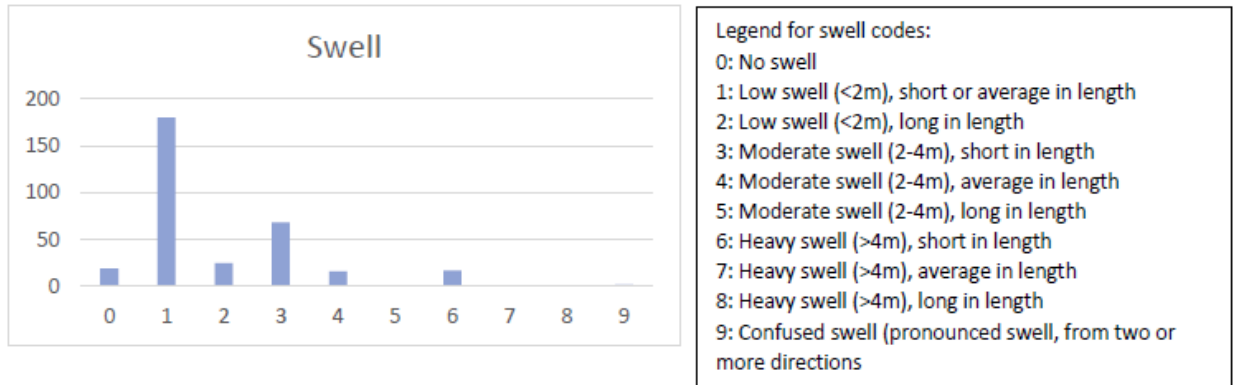


Figure 18.6: Frequency of occurrence of each swell condition registered during the SCALE spring cruise.

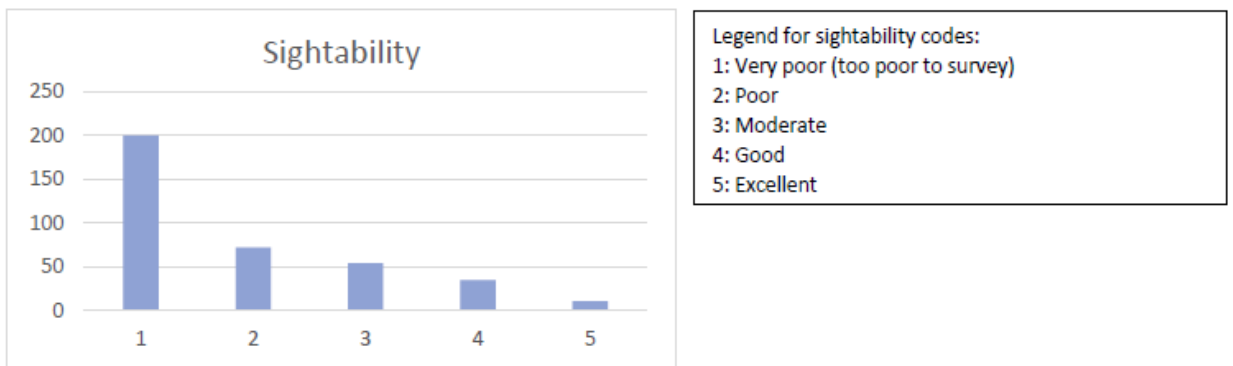


Figure 18.7: The frequency of each rating of sightability during the SCALE spring cruise.

### Cetacean Sightings

A total of 84 sightings of an estimated 272 individuals were recorded by the research team during the cruise. From that, 54 were done in on-effort, while 30 were during off-effort observation (Table 18.2). Eight different species of cetacean could be identified. The most common species in number of sightings (groups) was humpback whale (n=29), followed by minke (n=8) and long-finned pilot whales (*Globicephala melas*) (n=5) (Table 2). It was not possible to identify the species of 32 of the sightings.

Table 18.2: Whale sightings from the SA *Agulhas II* during the SCALE spring cruise.

ID code	Species name or description	Sightings during on-effort	Sightings during off-effort		
<b>Number of groups</b>	<b>Number of individuals</b>	<b>Number of groups</b>	<b>Number of individuals</b>		
1	Blue whale ( <i>Balaneoptera musculus</i> )	2	2	2	3

3	Sei whale ( <i>Balaenoptera borealis</i> )	0	0	1	3
60	"Like sei whale"	0	0	1	1
4	Minke whale ( <i>Balaenoptera acustorostrata</i> )	5	6	3	4
7	Humpback whale ( <i>Megaptera novaeangliae</i> )	14	19	1	1
71	"Like Humpback whale"	4	6	0	0
10	Killer whale ( <i>Orcinus orca</i> )	1	7	0	0
14	Southern rightwhale dolphin ( <i>Lissodelphis peronei</i> )	1	50	1	4
24	S. Bottlenose whale ( <i>Hyperoodon planifrons</i> )	1	10	0	0
41	Long-finned pilot whale ( <i>Globicephala melaena</i> )	4	59	1	5
9	Unidentified whale	11	12	0	0
16	Unidentified whale or dolphin	1	2	0	0
64	Unidentified large baleen whale	8	9	9	1
76	Unidentified small cetacean	2	3	1	2
<b>Total</b>	<b>54</b>	<b>185</b>	<b>30</b>	<b>8</b>	<b>7</b>

Only on one occasion it was possible to get a picture for photo-id - it was from a humpback whale.

The position of all cetaceans sighted during the cruise are presented in the map below (Fig. 18.8).

## Cetacean Distribution

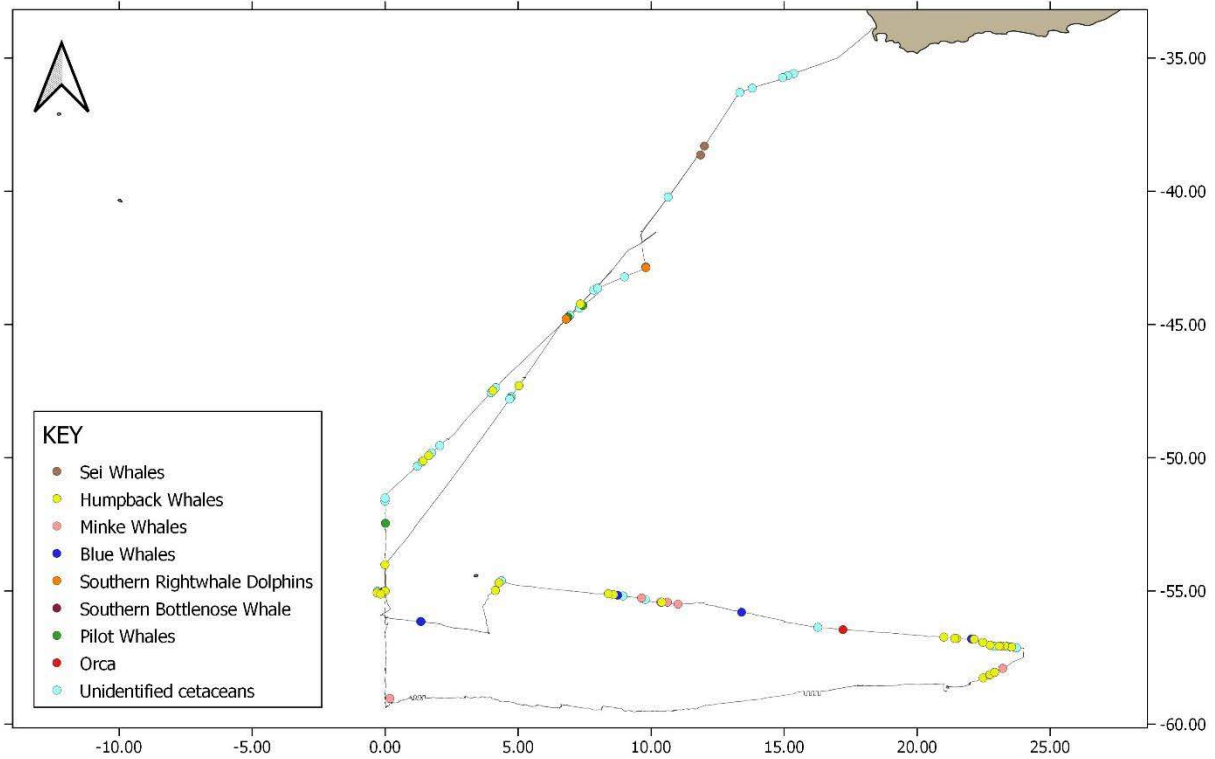


Figure 18.8: Map with the position of all cetaceans sighted during the SCALE spring cruise. Different colors represent different species, as indicated in the legend.

### 18.6. Considerations on the Data Collected

The cruise represented an opportunity for the investigation of the occurrence and distribution of cetacean species in an area important for a number of species that could potentially be encountered in the area.

Weather conditions were impeditive for a better data collection, as in a considerable number of days only opportunistic (off effort) observations could be performed. Wind speed (resulting in a sea state higher than 5 in the Beaufort scale) and fog accounted for the poor sighting conditions. However, a good area could be covered and a valuable cetacean data set was built during the SCALE spring cruise.

The cetacean data obtained will be investigated in relation to environmental conditions such as SST, bathymetry, distance from the ice margin, distance from oceanic currents) to contribute to the habitat use and distribution of the species observed in the monitored area. In addition, the data obtained can be investigated in relation to data from other teams on board (e.g. on chlorophyll-a concentration, trace metals, microplastics, zooplankton, sea ice type and concentration) in the near future, as one example of the multidisciplinary of SCALE.

Although the whale survey planned between the latitudes 024°E - 000° couldn't happen in a transect 5nm away from the sea ice margin (for a reason that is still not clear), we

succeed in data collection regarding cetaceans both in the whale survey area and in the way to and from this area. It is then very likely that the goals for the cetaceans component of the cruise will be achieved in the near future.

### **18.7. Acknowledgements**

We are grateful to the captain and all crew of the *SA Agulhas II* on board the cruise and to all researchers that supported our work. Thanks to Derek Engelbrecht for sharing images that helped in the identification of some of the individuals sighted. All funding from the Department of Environmental Affairs (DEA) and National Research Funding (NRF) to support SCALE is very much appreciated. Loan of gears from the DEA and loan of equipment from the Marine Research Institute Whale Unit/University of Pretoria are gratefully acknowledged. The Whales and Climate Research Program is funded by a generous donation from an anonymous charitable trust.

### **18.8. References**

Atkinson, A., Siegel, V., Pakhomov, E., Rothery, P., 2004. Long-term decline in krill stock and increase in salps within the Southern Ocean. *Nature* 432, 100-103.

Atkinson, A., Siegel, V., Pakhomov, E. A., Jessopp, M. J. & Loeb, V. 2009. A re-appraisal of the total biomass and annual production of Antarctic krill. *Deep-Sea Res. Pt. I* 56, 727–740.

Avgar, T., Street, G., & Fryxell, J. 2013. On the adaptive benefits of mammal migration. *Canadian Journal of Zoology*, 92(6), 481-490.

Bailey, H., & Thompson, P. M. 2009. Using marine mammal habitat modelling to identify priority conservation zones within a marine protected area. *Marine Ecology Progress Series*, 378:279-287.

Beekmans, B. W. P. M., Forcada, J., Murphy, E. J., Baar, de, H. J. W., Bathmann, U. V., & Fleming, A. H. 2010. Generalised additive models to investigate environmental drivers of Antarctic minke whale (*Balaenoptera bonaerensis*) spatial density in austral summer. *Journal of Cetacean Research and Management*, 11:115-129.

Bombosch, A., Zitterbart, D. P., Van Opzeeland, I., Frickenhaus, S., Burkhardt, E., Wisz, M. S., & Boebel, O. 2014. Predictive habitat modelling of humpback (*Megaptera novaeangliae*) and Antarctic minke (*Balaenoptera bonaerensis*) whales in the Southern Ocean as a planning tool for seismic surveys. *Deep-Sea Research Part I: Oceanographic Research Papers*, 91:101-114.

Burkhardt, E., & Lanfredi, C. 2012. Fall feeding aggregations of fin whales off Elephant Island (Antarctica). International Whaling Commission paper SC/64/SH9.

- Cherry, S. G., Derocher, A. E., Thiemann, G. W., & Lunn, N. J. 2013. Migration phenology and seasonal fidelity of an Arctic marine predator in relation to sea ice dynamics. *Journal of Animal Ecology*, 82(4), 912-921.
- Croll, D. A., Marinovic, B., Benson, S., Chavez, F. P., Black, N., Ternullo, R., & Tershy, B. R. 2005. From wind to whales: trophic links in a coastal upwelling system. *Marine Ecology Progress Series*, 289:117–130.
- Cummings, W.C. 1985. Right whales, *Eubalaena glacialis* (Müller, 1776) and *Eubalaena australis* (Desmoulins, 1822). In: RIDWAY, SH & SR HARRISON (eds.). Handbook of Marine Mammals. Volume 3: The Sirenians and Baleen Whales. Academic Press, London. p. 275-304.
- Findlay, K., Thornton, M., Shabangu, F., Venter, K., Thompson, I. & Fabriciussen, O. 2014. Report of the 2013/14 South African rAntarctic Blue Whale Survey, 000° - 020°E. International Whaling Commission paper SC/65b/SH01.
- Friedlaender, A. S., Halpin, P. N., Qian, S. S., Lawson, G. L., Wiebe, P. H., Thiele, D., & Read, A. J. 2006a. Whale distribution in relation to prey abundance and oceanographic processes in shelf waters of the Western Antarctic Peninsula. *Marine Ecology Progress Series*, 317:297-310.
- Gaskin, D. E. 1982. *The ecology of whales and dolphins*. Heinemann, London.
- Kawamura, A. 1994. A review of baleen whale feeding in the Southern Ocean. *Reports of the International Whaling Commission*, 44:261-271.
- Nicol, S., Worby, A., Leaper, R., 2008. Changes in the Antarctic sea ice ecosystem: potential effects on krill and baleen whales. *Mar. Freshwater Res.* 59, 361-382.
- Mackintosh, N. A. 1965. *The stocks of whales*. Fishing News Books, London.
- Moline, M.A., Claustre, H., Frazer, T.K., Schofield, O., Vernet, M., 2004. Alternation of the food web along the Antarctic Peninsula in response to a regional warming trend. *Global Change Biol.* 10, 1973-1980.
- Santora, J. A., Reiss, C. S., Loeb, V. J., & Veit, R. R. 2010. Spatial association between hotspots of baleen whales and demographic patterns of Antarctic krill *Euphausia superba* suggest size dependent predation. *Marine Ecology Progress Series*, 405:255–269.
- Shirihai, H., & Kirwan, G. M. 2008. *Complete guide to Antarctic wildlife*. Princeton University Press.
- Silber, G. K., *et al.* 2017. Projecting Marine Mammal Distribution in a Changing Climate. *Frontiers in Marine Science*, 4:1-14.
- Thompson AF, Heywood KJ, Thorpe SE, Renner AHH, Trasviña A. 2009. Surface circulation at the tip of the Antarctic Peninsula from drifters. *J Phys Oceanogr* 39:3–26.

Wilson, C., Klinkhammer, G. P., & Chin, C. S. 1999. Hydrography within the central and east basins of the Bransfield Strait, Antarctica. *Journal of Physical Oceanography*, 29:465–479.

## Washup Notes

### Winter Cruise

This scientific cruise was sponsored by DSI through NRF/SANAP and facilitated by DEAFF

- No major technical problems to report during the voyage. About 80% of the science was achieved. The reduction was necessary to accommodate the trip to East London for the Open Day.
- The ship equipment was functional besides the ADCP that could not be fixed on time after the Seamester cruise. Winches in order and no intervention on cable lengths. A bias in the anemometer was noticed before departure when compared with the calibrated SAWS sensor. To contact Marc de Vos for more info.
- Vichi requested clarity regarding how procedures should be properly managed for scientific voyages. The contract between the governmental departments is not specific to each voyage and therefore some steps are not clear and left to the scientists. These costs are not always included in scientific projects and therefore an extended discussion with DSI is needed. This is particularly relevant regarding the management of detachable modules that are not permanent (containers).
- How to handle the customs issues for containers –clearance of containers, certificates and safety requirements. During this voyage there was an expectation that the ship management was handling this as part of the contract. However, the contract between governmental departments just involve the additional costs for ship operations when not in port.
- For the next spring cruise cargo clearance (including handling of radioactive material) will be handled by the science groups in agreement with the funder DSI. DEAFF will ultimately make sure that all documents are in order
- A similar issue pertains the presence of technicians on board to operate winches and assist science activities. It has been clarified that DEAFF technicians are required on board when equipment belongs to the department. In the case of scientific voyages, the technicians will have to be hired by the chartering party and approved by DEAFF.
- The best long-term solution to the issues above is to follow the charter route – charter contract to be developed around a template to be provided by Jawahir. The charter contract will clarify all these aspects.
- Underway pumps need to be flushed – Marcello to provide more information to AMSOL regarding what kind of chemicals to use
- A complex cruise like this requires better external and internal communication channels with land and between teams. Network connection – WiFi not working ideally especially during glider deployments. Increasing the BW is however not an option. Better regulation of access during deployment by selecting devices that can have access. Use of dedicated IP and MAC address. The same for dedicated social media and advertising.
- To communicate between teams, we can explore a VOIP solution for internal comms. Mathibela to follow up on existing apps. Quick solution is to use HF radios so many channels are possible
- Several electrical equipment installed on Monkey Island that only has 16 Amps

power point. This caused tripping and heaters could not be used – specs are required before voyage to make plans for increasing power supply.

- Scientific storage - Ideally all equipment should be removed after the voyage. Include in the sailing orders that equipment will have be removed at the end of the voyage
- Points raised by Captain
  1. Clearing and shifting of the vessel – ship’s crew and delays possible missing of flights
  2. Containers arrived the last day
  3. Five sprinkler heads were burst because of the low temperature
  4. Frostbite and safety issues on ice operations. Chief scientist and team leaders must ensure participants respect the duration of shifts.
  5. People’s behaviours need to be disciplined through their team leaders for not following vessel procedures

## Spring Cruise

This scientific cruise was sponsored by DSI through NRF/SANAP and facilitated by DEAFF

- Containers to be overhauled to ensure compliance with ships systems going forward
- Water supply pipes for the containers need to be updated - either the installation of pressure regulators or thicker pipes
- Future cruises will use the ships preferred clearing agent, with associated costs to be covered by the scientific parties involved
- No electrical technician provided by DEFF - they will ensure this does not happen on future cruises
- The MilliQ supply in the lab needs to be serviced on a regular basis - DEFF will cover the maintenance of this
- The cleaning of the scientific seawater supply, including both pumps, will now be carried out as standard at the end of all cruises
- The scientific storeroom needs to be emptied before future cruises - this requires members of the scientific community to remove their gear or it will be disposed of
- The faulty ADCP is being repaired by DEFF

## Cruise Participants

### Winter Cruise

Team	Name	Affiliation	Country	Gender	Demography	Role
OCE	Marcello Vichi	UCT	South Africa	M	White	<b>Chief Scientist</b>
	Tahlia Henry	NMU	South Africa	F	Coloured	<b>Team Leader</b>
BIRDS	Vincent Ward	DEFF/BirdLife South Africa	South Africa	M	White	<b>Bird observer/ Team Leader</b>
	Vanessa Stephen	DEFF/BirdLife South Africa	South Africa	F	White	Bird observer
	Kim Stevens	DEFF/BirdLife South Africa	South Africa	F	White	Bird observer
CO2	Warren Joubert	SAWS	South Africa	M	Coloured	<b>Team Leader</b>
	Margret Ogundare	Stellenbosch University, Earth Sciences	Nigeria	F	Black	PhD Student
	Jossias Duvane	UEM, Maputo, Mozambique (SOCCO)	Mozambique	M	Black	PhD Student
DMS	Dennis Booge	GEOMAR Helmholtz Centre for Ocean Research Kiel	Germany	M	White	<b>Team Leader/ Postdoc</b>
	Li Zhou	GEOMAR Helmholtz Centre for Ocean Research Kiel	Germany	F	White	PhD Student
	Miming Zhang	Third Institute of Oceanography , Xiamen	China	M	White	Postdoc
GLIDERS	Josh Huysamen	SA-RobOTIC	South Africa	M	White	<b>Team Leader - (SAZ &amp; PUZ) - Glider and CTD</b>
	Hendrik Otto	SA-RobOTIC	South Africa	M	White	Electronics - Glider and CTD
	Louise Biddle	UGot	Sweden	F	White	<b>Team Leader -</b>

						<b>(SIZ) - Gliders</b>
	Kevin Thielen	UGot	Sweden	M	White	PhD Student
IRON	Thato Mtshali	CSIR	South Africa	M	Black	<b>PI/ Team Leader</b>
	Houda Beghoura	UBO	France	F	White	PhD Student
	Léo Mahieu	University of Liverpool	UK	M	White	PhD Student
	Fortunate Shingange	CSIR	South Africa	F	Black	MSc Student
	Tumelo Moalusi	CSIR	South Africa	M	Black	Student assistant
	Marc de Vos	SAWS	South Africa	M	White	<b>Team leader</b>
METEO	Mardene de Villiers	SAWS	South Africa	F	White	Met & sea ice observations
	Carla-Louise Ramjukadh	SAWS	South Africa	F	Coloured	Met & sea ice observations
	Casey Lyttle	SAWS	South Africa	F	White	Met & sea ice observations
	Christina Liesker	SAWS	South Africa	F	White	Forecast support & met obs
	Jarishma Gokul	UP - CMEG	South Africa	F	Indian	<b>Team leader</b>
MICROBIO	Jessica Koopman	UP - CMEG	South Africa	F	White	Postdoc
	Mancha Mabaso	UP - CMEG	South Africa	F	Black	MSc Student
	Percy Mutseka Lunga	UP - CMEG	South Africa	M	Black	PhD Student
	Diego Castillo Vaca	UP - CMEG	South Africa	M	White	PhD Student
	Kurt Spence	UCT	South Africa	M	White	<b>Team leader (MSc student)</b>
NATM	Shantelle Smith	UCT	South Africa	F	White	PhD student

	Eleonora Puccinelli	UCT	South Africa	F	White	Postdoc
	Jessica Burger	UCT	South Africa	F	White	PhD student
NOCE	Raquel Flynn	UCT	South Africa	F	White	<b>Team leader (PhD student)</b>
	Luca Stirnimann	UCT	South Africa	M	White	PhD student
	Ruan Parrott	UCT	South Africa	M	White	PhD student
	Lumi Haraguchi	Aarhus University	Denmark	F	Asian	Postdoc - int. collaborator
	Sina Wallschuss	UCT	South Africa	F	White	MSc student
PLANK TON	David Walker	CPUT	South Africa	M	White	<b>PI/Team Leader</b>
	Simone Louw	CPUT	South Africa	F	White	Btech Student
	Nadine Ellis	CPUT	South Africa	F	Coloured	Btech Student
	Megan Shipton	CPUT	South Africa	F	White	Btech Student
	Sonya de Waardt	CPUT	South Africa	F	White	Btech Student
PLASTIC	Vonica Perold	UCT	South Africa	F	White	<b>Team leader</b>
	Eleanor Weideman	UCT	South Africa	F	White	MSc Student
PRODU CTION	Thomas Ryan-Keogh	CSIR	South Africa	M	White	<b>PI/Team leader</b>
	Asmita Singh	CSIR	South Africa	F	Indian	PhD student
	Choaro Dithugoe	CSIR	South Africa	M	Black	PhD student
	Frieda Geldenhuys	CSIR	South Africa	F	White	PhD student
	Emma Bone	CSIR	South Africa	F	White	PhD student
	Mpho Lefatle	CSIR	South Africa	F	Black	PhD student
	Catherine Mitchell	Bigelow	US	F	White	Postdoc - int. collaborator
SEAICE	Sebastian Skatulla	UCT	South Africa	M	White	<b>PI/Team leader</b>

	Keith MacHutchon	UCT	South Africa	M	White	<b>PI</b>
	Tokoloho Rampai	UCT	South Africa	F	Black	<b>PI</b>
	Rutger Marquart	UCT	South Africa	M	White	PhD student
	Emmanuel Omatuku Ngongo	UCT	South Africa	M	Black	PhD student
	Benjamin Hall	UCT	South Africa	M	White	MSc student
	Mark Hambrock	UCT	South Africa	M	White	MSc student
	Andrea Cook	UCT	South Africa	F	White	MSc student
	Siobhan Johnson	UCT	South Africa	F	White	MSc student
	Joerg Schroeder	Univ. of Duisburg-Essen	Germany	M	White	<b>PI</b>
	Carina Nisters	Univ. of Duisburg-Essen	Germany	F	White	Postdoc
	Tommy Mielke	Univ. of Duisburg-Essen	Germany	M	White	Postdoc
	Felix Paul	Univ. of Duisburg-Essen	Germany	M	White	MSc student
	Ehlke de Jong	UCT	South Africa	F	White	PhD student
	Riesna R Audh	UCT	South Africa	F	Indian	PhD student
	Ashleigh Womack	UCT	South Africa	F	White	MSc student
	Robyn Verrinder	UCT	South Africa	F	White	<b>PI</b>
	Jamie Jacobson	UCT	South Africa	M	White	MSc student
TRACEX	Susanne Fietz	Stellenbosch University, Earth Sciences	South Africa	F	White	<b>PI/Team Leader</b>
	Jan-Lukas Menzel	Stellenbosch University, Earth Sciences	SA	M	White	Postdoc
	Saumik Samanta	Stellenbosch University, Earth Sciences	SA	M	White	postdoc

	Jean Look	Stellenbosch University, Earth Sciences	SA	M	White	PhD student
	Ryan Cloete	Stellenbosch University, Earth Sciences	SA	M	White	PhD student
	Ismael Kangueehi	Stellenbosch University, Earth Sciences	SA	M	Black	PhD student
	Johan Viljoen	Stellenbosch University, Earth Sciences	SA	M	White	PhD student
	Tara de Jongh	Stellenbosch University, Earth Sciences	SA	F	White	MSc student
	Zandria Jordaan	Stellenbosch University, Earth Sciences	SA	F	White	MSc student
	Herman Boock	Stellenbosch University, Earth Sciences	SA	M	White	MSc student
	Raya Stavreva	Stellenbosch University, Earth Sciences	SA	F	White	MSc student
	Bernhard Wenzel	Technichal University Braunschweig	GE	M	White	MSc student
TRACEX/ IRON	Jennifer Mary Ivanoff	University Las Palmas de Gran Canaria	ES	F	White	MSc student
VIBRATION	Jesslyn Bossau	Stellenbosch University, Engineering	South Africa	F	White	M.Eng student
	Nicole Taylor	Stellenbosch University, Engineering	South Africa	F	White	M.Eng student
	Martinique Engelbrecht	Stellenbosch University, Engineering	South Africa	F	Coloured	M.Eng student
	Armand van Zuydam	Stellenbosch University, Engineering	South Africa	M	White	<b>Team leader</b> M.Eng student
	Tor Magnus Aarskog	Norwegian University of Science and Technology (NTNU)	Norway	M	White	M.Eng / international student collaborator
WAVE	Alessandro Toffoli	The University of Melbourne	Australia	M	White	<b>PI/Team Leader</b>

	Alberto Alberello	University of Adelaide	Australia	M	White	Postdoc
	Gabriele Messori	University of Uppsala	Sweden	M	White	Assoc. Professor/Int. collaborator

## Spring Cruise

Team	Name	Affiliation	Country	Gender	Demography	Role
BIRDS	Derek Engelbrecht	BirdLife South Africa	South Africa	M	White	<b>Team Leader</b>
	Sally-Anne Sivewright	BirdLife South Africa	South Africa	F	White	Bird observer
CO2	Mutshutshu Tsanwani	DEA	South Africa	M	Black	<b>Team Leader</b>
	Baxolele Mdokwana	DEA	South Africa	M	Black	Team member
	Zanele Binase	CSIR/UCT	South Africa	F	Black	MSc student
	Joseph Matong	CSIR	South Africa	M	Black	Intern
	Nhlakanipho Fakude	CSIR	South Africa	M	Black	Intern
	Christopher Jabulani	CPUT	South Africa	M	Black	Team member
DMS	George Manville	PML	UK	M	White	<b>Team Leader</b>
	Tebatso Martin Moloto	CSIR/NWU	South Africa	M	Black	PhD Student
GLIDERS	Joshua Huysamen	STS	South Africa	M	White	<b>Team Leader</b>
	Heino Els	STS	South Africa	M	White	Team member
	Louise Biddle	UGOT	Sweden	F	White	<b>Team Leader</b>
	Isabelle Giddy	UGOT/UCT/C SIR	South Africa	F	White	PhD student
	Johan Edholm	UGOT	Sweden	M	White	MSc Student
	Hanna Rosenthal	UGOT	Sweden	F	White	MSc Student
IRON	Thato Mtshali	CSIR	South Africa	M	Black	<b>Team Leader</b>
	Fortunate Shingange	CSIR/UCT	South Africa	F	Black	MSc student
	Leo Mahieu	University of Liverpool	UK	M	White	PhD Student
	Jennifer Ivanoff	ULPGC-IOCAG	Spain	F	White	PhD Student
	Stephan Krisch	GEOMAR	Germany	M	White	Team member
METEO	Mardene de Villiers	SAWS	South Africa	F	White	<b>Team Leader</b>

	Prince Mlongwana	SAWS	South Africa	M	Black	Meteo technician
	Rebecca Hoffman	SAWS	South Africa	F	White	<b>Forecaster</b>
MICROBIO	Jarishma Gokul	University of Pretoria	South Africa	F	Indian	<b>Team Leader</b>
	Jessica Koopman	University of Pretoria	Netherlands	F	White	PostDoc
	Percy Mutseka Lunga	University of Pretoria	Zimbabwe	M	Black	PhD Student
	Diego Castillo Vaca	University of Pretoria	Ecuador	M	White	PhD Student
	Oluwatayo Makinde	University of Pretoria	Nigeria	M	Black	PhD Student
	Yvonne Marvellous Akpudo	University of Pretoria	Nigeria	F	Black	PhD Student
	NATM	Kurt Spence	UCT	South Africa	M	White
Shantelle Smith		UCT	South Africa	F	White	PhD student
Jessica Burger		UCT	South Africa	F	White	PhD student
Sive Xokashe		UCT	South Africa	M	Black	Honours student
Ruan Parrott		UCT	South Africa	M	White	PhD student
Lumi Haraguchi		Syke Finland	German	F	White	Researcher
NOCE	Raquel Flynn	UCT	South Africa	F	White	<b>Team Leader</b> PhD student
	Heather Forrer	UCT	South Africa	F	White	MSc student
	Sina Wallschuss	UCT	South Africa	F	White	MSc student
	Eesaa Harris	UCT	South Africa	M	Coloured	Honours student
	Luca Stirnmann	UCT	Italian	M	White	PhD student
	Sven Kranz	UCT	German	M	White	Team member
	Rachel Thomas	UCT	American	F	White	PhD Student

	Sveinn Einarsson	UCT	American	M	White	PhD Student
PLANK TON	Simone Louw	CPUT	South Africa	F	White	<b>Team Leader</b> BTech student
	Megan Shipton	CPUT	South Africa	F	White	BTech student
	Nadine Ellis	CPUT	South Africa	F	Coloured	Btech student
	Stian Louw	CPUT	South Africa	M	White	Btech student
	Nasreen Burgher	CPUT	South Africa	F	Coloured	Btech student
	Steve Tebele	CPUT	South Africa	M	Black	Btech student
	Bianca Jooste	CPUT	South Africa	F	Coloured	Btech student
PLASTIC	Eleanor Weideman	UCT	South Africa	F	White	<b>Team Leader</b> MSc student
	Michael Daniel	UCT	South Africa	M	White	MSc student
PRODUCTI ON	Tommy Ryan-Keogh	CSIR	South Africa	M	White	<b>Chief Scientist / Team Leader</b>
	Asmita Singh	CSIR/SU	South Africa	F	Indian	PhD student
	Choaro Dithugoe	CSIR/RU	South Africa	M	Black	PhD student
	Mpho Lefatle	CSIR	South Africa	F	Black	Intern
	Jeff McQuaid	AWI	Germany	M	White	Researcher
	Bongiwe Jojo	CSIR/UCT	South Africa	F	Black	MSc student
	Maximilian Unterberger	Ifremer	France	M	White	Team member
SEAICE	Justin Pead	UCT	South Africa	M	White	<b>Team Leader</b>
	Rutger Marquart	UCT	South Africa	M	White	PhD student
	Riesna Audh	UCT	South Africa	F	Indian	PhD student
	Felix Paul	Univ. of Duisburg-Essen	Germany	M	White	MSc student

	Siobhan Johnson	UCT	South Africa	F	White	MSc student
	Mark Hambrock	UCT	South Africa	M	White	MSc student
	Kelsey Kaplan	UCT	South Africa	F	White	Honours student
	Boitumelo Matlakala	UCT	South Africa	F	Black	Honours student
	Tshepang Khoboko	UCT	South Africa	F	Black	Honours student
	Hasham Taujoo	UCT	South Africa	M	Indian	Honours student
	Sejal Pramlall	UCT	South Africa	F	Indian	Honours student
	Wayne de Jager	UCT	South Africa	M	White	Honours student
	Jonathan Rogerson	UCT	South Africa	M	White	MSc student
SEALS	Marthán Nieuwoudt Bester	University of Pretoria	South Africa	M	White	<b>Team Leader</b>
	Horst Bornemann	Alfred Wegener Institute	Germany	M	White	Team member
	Nico Lübcker	University of Pretoria	South Africa	M	White	PhD Student
	William Albert (Wiam) Haddad	University of Pretoria	South Africa	M	White	Team member
TRACEX	Jan-Lukas Menzel	Stellenbosch University	South Africa	M	White	<b>Team Leader</b>
	Andrea Baker	Stellenbosch University	South Africa	F	White	Postdoc
	Saumik Samanta	Stellenbosch University	South Africa	M	Indian	Postdoc
	Tara de Jong	Stellenbosch University	South Africa	F	White	MSc Student
	Raya Stavreva	Stellenbosch University	Bulgaria	F	White	MSc Student
VIBRATION	Jesslyn Bossau	Stellenbosch University, Engineering	South Africa	F	White	M.Eng student
	Martinique Engelbrecht	Stellenbosch University, Engineering	South Africa	F	Coloured	<b>Team Leader</b> M.Eng student
	Andrei Sandru	Aalto University	Finland	M	White	PhD student

WAVE	Alberto Alberello	University of Melbourne / University of Adelaide	Australia	M	White	<b>Team Leader</b>
	Ippolita Tersigni	University of Melbourne	Australia	F	White	PhD student
FLUX	Clare Eayrs	NYU Abu Dhabi	United Arab Emirates	F	White	<b>Team Leader</b>
	Daiane Faller	NYU Abu Dhabi	United Arab Emirates	F	White	Researcher
WHALES	Elisa Seyboth	Cape Peninsula University of Tehnology (CPUT)	South Africa	F	White	<b>Team Leader</b>
	Jeffrey Slater	Cape Peninsula University of Tehnology (CPUT)	South Africa	M	White	Team member
	Sanne Paarman	Cape Peninsula University of Tehnology (CPUT)	South Africa	F	White	Team member